

University of Nottingham
UK | CHINA | MALAYSIA

The response of survivin to hypoxia and the functional roles of its subcellular pools.

Alexander J. Fezovich, BSc, MSc

Thesis submitted to the University of Nottingham for the degree of Doctor of Philosophy

April 2022

Abstract

Survivin is a highly conserved and multifaceted protein with well characterised roles in mitosis and inhibition of apoptosis. Largely absent from normal adult tissue, survivin is highly expressed in most cancers and is an attractive target for cancer therapeutics. Further evidence has implicated survivin in a number of additional pathways, including cell metabolism, DNA repair and autophagy. These functions are associated with distinct subcellular pools of survivin, located in the cytoplasm, nucleus and mitochondria.

To date, research on survivin has focused on its activity under normoxia. However, solid tumours often establish adverse microenvironmental conditions, characterised by reduced oxygen and nutrient availability. Such conditions are thought to initiate a series of cellular adaptations resulting in altered cell metabolism, elevated treatment resistance and greater tumour aggression. As a protein upregulated by hypoxia and in cancers generally, the contributions of survivin to these adaptations is of great interest. This thesis aims to investigate the potential roles of survivin in hypoxia and further characterise the functional significance of its subcellular pools.

Subcellular fractionation and imaging techniques identified a clear repositioning of survivin from the cell cytoplasm to the mitochondria and nucleus under hypoxia. As these organelles are associated with altered mitochondrial metabolism and increased treatment sensitivity respectively, metabolic and cell survival assays were performed to assess their significance. The specific roles of the subcellular populations were supported by the generation of cell lines expressing survivin constructs targeted to these regions.

Survivin expression in the mitochondria correlated with an increase reliance on glycolysis for ATP production both in normoxia and hypoxia. This appeared to be mediated by upregulation of proteins involved in the glycolytic pathway and inhibition of oxidative phosphorylation, achieved in part by reduced mitochondrial membrane polarisation. A number of potential survivin interactors were identified, establishing various prospective intersections in metabolic pathways through which survivin may operate in cancerous cells.

Forced localisation of survivin to the nucleus has been associated with a loss of apoptosis inhibition and treatment sensitisation. Nuclear survivin has also been associated with DNA damage and may facilitate DNA repair. In contrast to these findings, this thesis reports can inhibit apoptosis under both hypoxia and when forcibly expressed in the nucleus, in a manner independent of DNA repair. This may be mediated by the altered stabilisation of survivin binding partners involved in the regulation of apoptosis and together suggest the utilisation of novel mechanisms to promote survival of cancer cells under hypoxia.

Table of Contents

Plagiarism Statement *8*

Abbreviations *9*

Chapter 1 – Literature Review *19*

1.1 Cancer and the tumour microenvironment 19

1.2 Survivin 21

1.3 Hypoxia and Cancer 27

1.4 Challenges in studying normoxia and hypoxia in vitro 33

1.5 Cell Division and Regulation 35

1.5.1 Cell cycle stages 36

1.5.2 Prophase 38

1.5.3 Prometaphase 39

1.5.4 Metaphase 41

1.5.5 Anaphase 45

1.5.6 Telophase and cytokinesis 46

1.6 Tumour Metabolism 47

1.7 Mitochondrial functions and their regulation 51

1.7.1 The Electron Transport Chain (ETC) 52

1.7.2 Cristae Regulation 55

1.7.3 Mitochondrial Dynamics 56

1.7.4 Proton Leakage 59

1.8 DNA Damage 60

1.8.1 Internal sources of DNA damage 61

1.8.2 Ionizing radiation 62

1.8.3 Ultraviolet radiation 62

1.8.4 Topoisomerase inhibitors 63

1.8.5 Bleomycin antibiotics 64

1.9 DNA Damage Repair 65

1.9.1 Base excision repair (BER) 66

1.9.2 Nucleotide excision repair (NER) 66
1.9.3 Mismatch repair (MMR) 67
1.9.4 Single stranded break repair (SSBR) 68
1.9.5 Double stranded break repair (DSBR) 69
1.10 Regulated Cell Death 73
1.10.1 Apoptosis 73
1.10.2 Pathanatos 78
1.11 Rationale 79
1.12 Hypothesis and Aims 79
Chapter 2 – Materials and Methods 81
2.1 Cell Culture 81
2.1.1 Monolayer cultures 81
2.1.2 Spheroid cultures 81
2.1.3 Decellularised Matrices 82
2.1.4 Resazurin Assay 82
2.1.5 IC50 Drug and UVC Dose Response 82
2.1.6 siRNA 82
2.2 Biomaterials 83
2.2.1 Tissue Decellularisation 83
2.3 Flow Cytometry 83
2.3.1 Caspase 3/7 Assay 83
2.3.2 Cell Cycle Assay 84
2.4 Molecular Biology 84
2.4.1 Preparation of RNA Extracts 84
2.4.2 cDNA Synthesis 85
2.4.3 Primer Design 85
2.4.4 Primer Optimisation 86
2.4.5 Reaction Efficiency 88
2.4.6 RT-PCR 89
2.4.7 Plasmid Constructs 90
2.5 Protein Analysis 90

2.5.1 Preparation of Whole Cell Extracts 90
2.5.2 Preparation of Subcellular Fractions 91
2.5.3 Bradford Assay 92
2.5.4 SDS PAGE 92
2.5.5 Immunoblotting 92
2.5.6 Protein Purification 93
2.5.7 GST-Pulldown 94
2.6 Histology 94
2.6.1 Embedding 94
2.6.2 Sectioning 95
2.6.3 Immunohistochemistry 95
2.7 Microscopy 96
2.7.1 Live Imaging 96
2.7.2 Fixed Sample Preparation 96
2.7.3 Image Processing 97
2.8 Statistical Analyses 98
Chapter 3 – Survivin localisation in response to hypoxic and genotoxic stress 99
3.1 Overview 99
3.1.1 Spatial regulation of survivin during interphase 99
3.1.2 Cell Culture Techniques 101
3.1.3 Aims 107
3.2 Results 108
3.2.1 Survivin Localisation under conditions within the TME 108
3.2.2 Survivin Localisation under hypoxia 115
3.2.3 Survivin Localisation in response to genotoxic stress 119
3.2.4 Survivin localisation by post-translational modifications and protein interactions 128
3.2.5 Geldanamycin as a cell synchronisation tool 137
3.2.6 Development of 3D culture techniques 147
3.3 Discussion 153
3.3.1 Hypoxia induces translocation of survivin to the cell nucleus and mitochondria. 153
3.3.2 Nuclear translocation is not reliant on K129, S20 or T34 modifications. 156
3.3.3 Geldanamycin as a tool for cell synchronisation 158

3.3.4 Spheroid cultures and decellularized matrices reveal unique cell phenotypes 160
3.3.5 Summary 162

Chapter 4 – Nuclear survivin is cytoprotective..... 163

4.1 Overview..... 163
4.1.1 Survivin inhibits apoptosis within the cytoplasm 163
4.1.2 Survivin influences DNA repair and genotoxic resistance. 165
4.1.3 Aims 167

4.2 Results..... 168
4.2.1 Survivin is cytoprotective under normoxic and hypoxic conditions 168
4.2.2 Survivin regulates expression of cell survival proteins..... 170
4.2.3 Nuclear and mitochondrial targeted survivin is cytoprotective 175
4.2.4 Identification of putative binding partners involved in DNA repair and apoptosis 180
4.2.5 Cytoprotection by nuclear survivin is not conferred through DNA repair. 181

4.3 Discussion..... 188
4.3.1 Nuclear and mitochondrial survivin promote cell survival under hypoxia 188
4.3.2 Cytoprotection by nuclear survivin is not contingent on DNA repair 189
4.3.3 Survivin differentially regulates the expression of cell survival proteins under hypoxia 190
4.3.4 Summary 193

Chapter 5 – Survivin Mediates Cell Metabolism..... 194

5.1 Overview..... 194
5.1.1 Proposed roles for survivin in cellular metabolism..... 194
5.1.2 Regulation of mitochondrial respiration..... 197
5.1.3 Cell Metabolism 198
5.1.4 Aims 199

5.2 Results..... 200
5.2.1 Survivin promotes aerobic glycolysis..... 200
5.2.2 Survivin inhibits OXPHOS 203
5.2.3 Development of a mitochondrial analysis workflow and software 204
5.2.4 Survivin influences mitochondrial mass but not fission/fusion..... 211
5.2.5 Survivin reduces mitochondrial membrane potential in cancer cells 214
5.2.6 Survivin may interact with numerous metabolic proteins 217

5.3 Discussion 219
5.3.1 Survivin promotes glycolysis in cancer cell lines 219
5.3.2 Survivin inhibits OXPHOS and mitochondrial membrane polarisation. 221
5.3.2 Identification of putative mitochondrial partners of survivin in cancer cells. 222
5.3.3 Development of mitochondrial and image analysis software 224
5.3.4 Summary 224
Chapter 6 – General Discussion *225*
6.1 Overview 225
6.2 Survivin localisation within the TME 226
6.3 Nuclear survivin and links to the DNA damage response 227
6.4 Nuclear and mitochondrial-localised survivin is cytoprotective 228
6.5 Survivin promotes the Warburg effect 231
6.6 Cross-talk in cell survival mechanisms 233
Bibliography *235*
Appendix *295*

Plagiarism Statement

I certify that all work in this thesis is my own and I take full responsibility for it. Any materials, published or unpublished, not resulting from my own experimentation have been recognised in the text or in the acknowledgments.



Alexander Fezovich

Abbreviations

2PG	2-Phosphoglyceric acid
3PG	3-Phosphoglyceric acid
53BP1	p53-binding protein 1
ACAA2	Acetyl-CoA acyltransferase 2
ADM	Adrenomedullin
ADP	Adenosine diphosphate
AIF	Apoptosis inducing factor
AIFM1	Apoptosis inducing factor mitochondria associated 1
AIP	Aryl hydrocarbon receptor-interactive protein
AMP	Adenosine monophosphate
AMPK	AMP-activated protein kinase
ANOVA	Analysis of variance
ANT	Adenine nucleotide translocase
APAF1	Apoptotic protease activating factor
APC/C	Anaphase-promoting complex or cyclosome
APE1	AP endonuclease 1
APLF	Aprataxin-and-PNK-like factor
APTX	Aprataxin
ARNT	Aryl hydro-carbon receptor nuclear translocator
ATP	Adenosine triphosphate
ATP5F1C	ATP synthase F1 subunit gamma
ATR	Ataxia-telangiesctasia and Rad3-related
ATRIP	ATR-interacting protein
α-KG	α-Ketoglutaric acid
BAD	BCL2 associated agonist of cell death

BAK	BLC2 antagonist/killer 1
BAX	BL2 associated X, apoptosis regulator
BCL-W	Apoptosis regulator BCL-W
BCL-XL	BCL-2-like protein long isoform
BCL2	B-cell lymphoma-2 protein
BER	Base excision repair
BFL-1	BCL2-related protein expressed in foetal liver 1
BID	BH3 interaction domain death agonist
BIM	BCL2-interacting mediator of cell death
BIR	Baculovirus inhibitor of apoptosis protein repeat
BLM	Bloom syndrome protein
BMF	Bcl2 modifying factor
BOK	BL2 family apoptosis regulator
BPG	2,3-Biphosphoglycerate
BRCA1	Breast cancer type 1 susceptibility protein
c-FLIP	Cellular FADD-like IL-1β-converting enzyme-inhibitory protein
CAIX	Carbonic anhydrase IX
CASP	Caspase
CBP	CREB-binding protein
CBP	CAMP response element-binding protein
CCAN	Constitutive centromere associated network
CCL5	Chemokine (C-C motif) 5
CDK	Cyclin-dependent kinase
CDK	Cell-cycle-dependent kinase
CDKN2AIP	CDKN2A interacting protein
cDNA	Complementary DNA
CENP	Centromere protein
CENT2	Centrin 2

CHIP	Carboxyl terminus of HSP-interaction protein
CLAP	Chymostatin : leupeptin : antipain : pepstatin A
CPC	Chromosomal passenger complex
CPD	Cyclobutene pyrimidine dimer
CPT1A	Carnitine palmitoyltransferase 1A
CRM1	Chromosome maintenance 1
CSA	Cockayne syndrome WV repeat protein A
CSB	Cockayne syndrome protein B
CSC	Cancer stem cell
C_T	Threshold breaking cycle
CtIP	CtBP-interacting protein
CXCL11	Chemokine (C-X-C motif) 11
CYCS	Cytochrome c, somatic
Cyto	Cytoplasmic
DAMP	Damage associated molecular pattern
DD	Death domain
DDR	DNA damage response
DEPC	Diethylpyrocarbonate
DISC	Death-inducing signalling complex
DMEM	Dulbecco's Modified Eagle's medium
DNA	Deoxyribonucleic acid
DNA-PKcs	DNA dependent protein kinase catalytic subunit
DNA2	DNA replication helicase/nuclease 2
DNAJA1	DnaJ homolog subfamily A member 1
DRP1	Dynamin-related protein 1
DSB	Double-strand break
dsDNA	Double-strand DNA
DTT	Dithiothreitol
ECL	Enhanced chemiluminescence

ECM	Extracellular matrix
EDTA	Ethylenediaminetetraacetic acid
EGTA	Ethylene glycol-bis(β-aminoethyl ether)-N,N,N′,N′-tetraacetic acid
EME1	Essential meiotic structure-specific endonuclease 1
EMT	Epithelial-mesenchymal transition
ER	Endoplasmic reticulum
ERCC1	Excision repair cross complementation group 1
ETC	Electron transport chain
EXO1	Exonulease 1
F6P	Fructose 6-phosphate
FADD	FAS associated via death domain
FADH	Reduced flavin adenine dinucleotide
FAS	Fas cell surface death receptor
FASLG	FAS ligand
FBP	Fructose 1,6-biphosphate
FCS	Foetal calf serum
FDA	Food and Drug Administration
FEN1	Flap structure-specific endonuclease 1
FIH	Factor inhibiting HIF
FIS1	Mitochondrial fission 1 protein
FN1	Fibronectin 1
FOXP3	Forkhead box P3
g-H2AX	Gamma H2AX
G3P	Glyceraldehyde 3-phophate
G6P	Glucose 6-phosphate
G6PD	Glucose-6-phosphate dehydrogenase
GAPDH	Glyceraldehude-3-P-dehydrogenase
GDP	Guanosine diphosphate

GEN1	GEN1 Holliday junction 5' flap endonuclease
GFP	Green fluorescent protein
GG-NER	Global genome NER
GLUT	Glucose transporter
GST	Glutathione S-transferase
GTP	Guanosine triphosphate
H2AX	H2A histone family member X
HADHA	Hydroxyacyl-CoA Dehydrogenase Trifunctional Multienzyme Complex Subunit Alpha
HBXIP	Hepatitis B X-interacting protein
HDAC6	Histone deacetylase 6
HEPES	N-2-Hydroxyethylpiperazine-N'-2-Ethanesulfonic Acid
HIF	Hypoxia-inducible factors
HLA-G	Human leukocyte antigen G
HMGA2	High-mobility group AT-hook 2
HR	Homologous recombination
HRE	HIF-binding response elements
HRK	BCL2 interacting protein
HSP	Heat shock protein
IAP	Inhibitor of apoptosis protein
IDL	Insertion-deletion loop
IGF2	Insulin like growth factor 2
IMM	Inner mitochondrial membrane
IMMT	Inner membrane mitochondrial protein
IMS	Intermembrane space
INCENP	Inner centromere protein
INF2	Inverted formin 2
IR	Ionizing radiation
LDHA	Lactate dehydrogenase

LET	Linear energy transfer
LIG	Ligase
LMB	Leptomycin B
LOX	Lysyl oxidase
MCC	Mitotic checkpoint complex
MCL1	Induced myeloid leukaemia cell differentiation protein 1
MCTS	Multicellular tumour spheroids
MDC1	Mediator of DNA damage checkpoint protein 1
MDM2	Mouse double minute 2 homolog
MDR1	Multidrug resistance 1
MERC	Mitochondria-ER contact site
MFF	Mitochondrial fission factor
MFN1	Mitofusin 1
MICOS	Mitochondrial contact site and cristae organisation system
MID	Mitochondrial dynamics protein
Mito	Mitochondrial
MLH1	MutL homolog
MMP	Matrix metalloproteinase
MMR	Mismatch repair
MOMP	Mitochondrial outer membrane permeabilization
MRE11	Meiotic recombination 11 homolog 1
MRN	MRE11, RAD50, NBS1 complex
MSH	MutS homolog
MT	Microtubule
mtDNA	Mitochondrial DNA
NA	Numerical aperture
NADPH	Reduced nicotinamide adenine dinucleotide phosphate
NBS1	Nijmegen breakage syndrome 1
NER	Nucleotide excision repair

NES	Nuclear export sequence
NES	Nuclear export sequence
NF-κB	Nuclear factor kappa-light-chain-enhancer of activated B cells
NHEJ	Non-homologous end joining
Nuc	Nuclear
OCT4	Octamer-binding transcription factor 4
ODD	Oxygen dependent degradation domain
OMM	Outer mitochondrial membrane
OPA1	Optic atrophy-1
OXPHOS	Oxidative phosphorylation
P4HA	Prolyl 4-hydroxylase
PALB2	Partner and localiser of BRCA2
PARP	Poly(ADP-Ribose)Polymerase
PBS	Phosphate buffered saline
PCC	Pearson's correlation coefficient
PCD	Programmed cell death
PCNA	Proliferating cell nuclear antigen
PCR	Polymerase chain reaction
PD-L1	Programmed death-ligand 1
PDK1	Pyruvate dehydrogenase kinase 1
PEP	Phosphoenolpyruvic acid
PFK	Phosphofructokinase
PFKBF3	6-phosphofructo-2-kinase/fructose-2,6-biphosphatase-3
PFKL	6-phosphofructokinase
PGK1	Phosphoglycerate kinase 1
PHD	Prolyl hydroxylase domain-containing proteins
PI3K	Phosphatidylinositol 3'-kiniase
PKA	Protein kinase A

PKM	Pyruvate kinase
PMS2	PMS1 homolog 2
PMSF	Phenylmethylsulphonyl fluoride
PNKP	Polynucleotide kinase 3′-phosphate
POL	Polymerase
PP	Pyrimidone photoproducts
PPP	Pentose phosphate pathway
PRKAA1	AMP-activated catalytic subunit alpha 1
PS	Phosphatidylserine
PUMA	P53-upregulated modulator of apoptosis
pVHL	Von Hippel-Lindau tumour suppressor
RACK1	Receptor of activated protein kinase C 1
RAD23B	Radiation sensitive 23B
Rb	Retinoblastoma
Rbl5P	Ribose 5-phosphate
RC-SSBR	Replication-coupled SSBR
RMI1	RecQ-mediated genome instability protein 1
RNA	Ribonucleic acid
RNF	Ring finger protein
ROS	Reactive oxygen species
RPA	Replication protein A
RPE	Retinal pigment epithelium
RT-PCR	Real time PCR
SAC	Spindle assembly checkpoint
SCO2	Synthesis of cytochrome *c* oxidase 2
SDHA	Succinate dehydrogenase
SDS	Sodium dodecyl sulphate
SDS PAGE	SDS polyacrylamide gel electrophoresis
SDW	Sterile distilled water

siRNA	Small interfering RNA
SMAC	Second mitochondrial-derived activator of caspase
SSB	Single-strand break
SSBR	Single-strand break repair
ssDNA	Single-strand DNA
SVN	Survivin
tBID	Truncated BID
TBP	TATA-box binding protein
TBS	Tris-buffered saline
TBST	TBS with Tween-20
TC-NER	Transcription coupled NER
TCA	Tricarboxylic acid cycle
TDP1	Tyrosyl-DNA phosphodiesterase 1
TEMED	Tetramethylethylenediamine
TFIIH	Transcription initiation factor II H
TGF	Transforming growth factor
TIGAR	TP53-induced glycolysis regulator
TLS	Translesion synthesis
TME	Tumour microenvironment
TMRE	Tetramethlrhodamine ethy ester perchlorate
TNFR1	Tumour necrosis factor receptor 1
TOP	Topoisomerase
TRAIL	Tumour necrosis-related apoptosis inducing ligand
TRAILR	TRAIL receptor
TSA	Trichostatin-A
UCP	Uncoupling protein
USP7	Ubiquitin-specific-processing protease 7
UV	Ultraviolet
UV-DDB	Ultraviolet-damaged DNA damage-binding protein

UVSSA	UV-stimulated scaffold protein A
VDAC	Voltage dependent anion channel
VEGF	Vascular endothelial growth factor
VEGFR	VEGF receptor
WCE	Whole cell extract
WRN	Werner syndrome protein
XIAP	X-linked inhibitor of apoptosis protein
XLF	XRCC4 like factor
XPB	Xeroderma pigmentosum type B
XPC	Xeroderma Pigmentosum, complementation group C
XPD	Xeroderma Pigmentosum Protein
XPF	Xeroderma pigmentosum, complementation group F
XPG	Xeroderma pigmentosum, complementation group G
XRCC	X-ray cross-complementation
YBX1	Y-box binding protein 1

Chapter 1 – Literature Review

1.1 Cancer and the tumour microenvironment

Cancer refers to a range of linked diseases characterized by dysregulated cellular division that may culminate in the invasion and obstruction of vital organs, killing the host organism. Indeed, cancer is the second leading cause of mortality globally with an increasing prevalence (Siegel et al. 2018). The malignant transformation of normal cells manifests as a result of serial genetic and epigenetic alterations, enabling them to circumvent the homeostatic controls that ordinarily restrict aberrant cellular behaviour. Mutations may arise as the result of DNA damage incurred through the action of carcinogens or by errors produced during replication, imparting a selective advantage and promoting tumour growth and progression (Hassanpour, Dehghani 2017). Whilst unregulated proliferation serves as a defining feature of cancerous cells, tumour malignancy necessitates the development of additional characteristics to support their expansion and escape from tumour-suppressive host responses. These may include evasion of apoptosis and the immune system, metabolic deregulation, induction of angiogenesis and increased migratory capacity (Hanahan, Weinberg 2011).

However, the generation of tumours characteristically involves components of normal organs in addition to neoplastic cells. Cancer progression and metastasis therefore develops as a result of both autonomous defects in tumour cells and the concerted response of the host organism (Yuan et al. 2016). It is with this understanding that a greater emphasis has been placed on the functional and physical relationships developed between cancer cells and normal host tissues, known as the "desmoplastic reaction", "tumour stroma" or "tumour microenvironment" (TME) (Kalluri 2016). Within this environment, many neoplastic

and stromal cells exist and maintain cell-cell and cell-extracellular matrix (ECM) interactions within a three-dimensional space. The nature of these adhesive interactions, such as the spatial distribution of ligands (Thery 2010), influences a range of cellular behaviours including proliferation, survival, differentiation and migration (Orr et al. 2006; Wozniak et al. 2004). In replicating cellular responses in an artificial environment, it is therefore important to consider how these relationships are re-established.

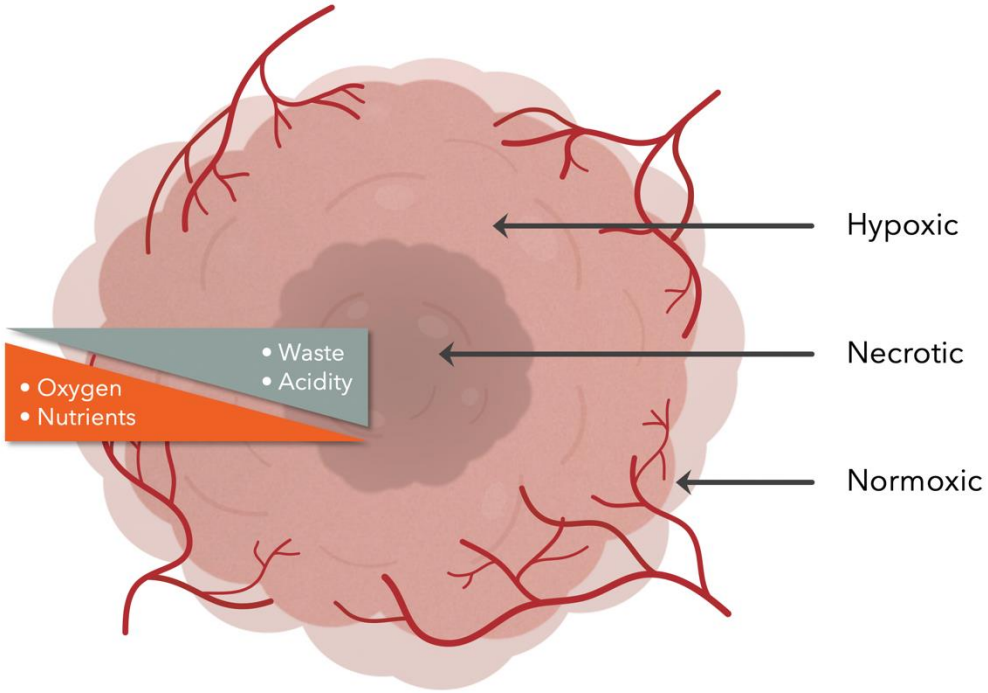


Figure 1.1 – Schematic of the tumour microenvironment (TME). As tumour cells are positioned at greater distances from surrounding blood vessels, factors such as oxygen tension and nutrients become limited and decrease with distance, developing regions with distinct microenvironmental characteristics. Created by author.

The TME is primarily composed of blood and lymphatic vessels, fibroblasts, immune cells and the ECM (Petrova et al. 2018). Both the initiation of tumours (Desmoulière et al. 2004) and their subsequent development may be supported by components

of the TME (Balkwill et al. n.d.). Stromal cell types, such as macrophages and fibroblasts, form bidirectional and dynamic relationships with both tumour cells and each other, creating a complex and continually developing signalling network that plays a salient role in the malignant conversion of host tissue and may dictate disease progression (Yuan et al. 2016). Moreover, as cancerous lesions increase, gradients are established across the tumour in factors such as nutrients, oxygen, signalling molecules, pH and waste products, as depicted in Fig. 1.1. As a result, tumours may be comprised of regions experiencing drastically different conditions and consequently see the development of distinct subpopulations, both in their stromal and neoplastic cell types. The establishment of adverse conditions, such as hypoxia, initiates a series of cellular responses that have been linked with increased malignancy, greater therapeutic resistance and diminished clinical outcome (Muz, de la Puente, Azab, Azab 2015; Wilson, Hay 2011). It is therefore important to consider the heterogeneity of both the cell types involved in the TME and the conditions that give rise to their distinct subpopulations.

1.2 Survivin

Since its discovery over two decades ago (Ambrosini et al. 1997), survivin has garnered considerable attention from oncologists and cell biologists alike, taking it from a simple neoplastic marker to a complex regulator of numerous cellular networks with far reaching implications for cellular homeostasis and human pathology. Its universal overexpression in human tumours and relative absence in terminally differentiated adult tissues has established survivin as an attractive target for cancer therapeutics (Velculescu et al. 1999). Meanwhile, research into its cellular functions has implicated survivin in various pathways including apoptosis inhibition, mitosis, autophagy, DNA repair and mitochondrial dynamics (Wheatley, Altieri 2019; Garg et al. 2016). Whilst our understanding of the diverse and multifaceted

role survivin plays in cell biology has developed significantly over recent years, much uncertainty and contention remains over the precise mechanisms by which survivin exerts its regulatory influences.

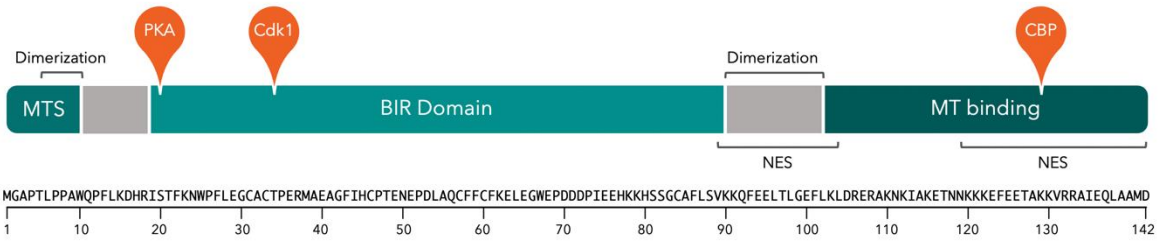


Figure 1.2 – Summary of the two-dimensional structure and functions of survivin. Survivin is targeted for phosphorylation by PKA at S20, regulating XIAP binding; phosphorylation by Cdk1 at T34, regulating metaphase stabilisation; and acetylation at K129 by CBP, promoting dimerization and inhibiting CRM1-mediated nuclear export. Created by author.

Containing a single baculovirus inhibitor of apoptosis protein repeat (BIR) domain, survivin is defined as an inhibitor of apoptosis protein (IAP), as shown in Fig. 1.2. Other IAP family members include NAIP, cIAP1/2 and XIAP, of which survivin is the smallest member [142 amino acids (aa); 16.5 kDa] (Li et al. 1999). Unlike other members, survivin has no intrinsic enzymatic functions and may instead function as an adaptor protein, reliant on other proteins to realise its downstream effects (Wheatley, Altieri 2019; Garg et al. 2016). Consequently, an understanding of its interactome may be essential to elucidating its precise role in cellular pathways. Indeed, survivin exist in distinct subcellular pools during interphase that are associated with specific cellular functions, potentially as a result of the prospective binding partners available within these compartments. These include the nucleus, cytoplasm and mitochondria (Fortugno et al. 2002; Dohi, Beltrami, et al. 2004; Li et al. 2005).

1.2.1 Subcellular localisation

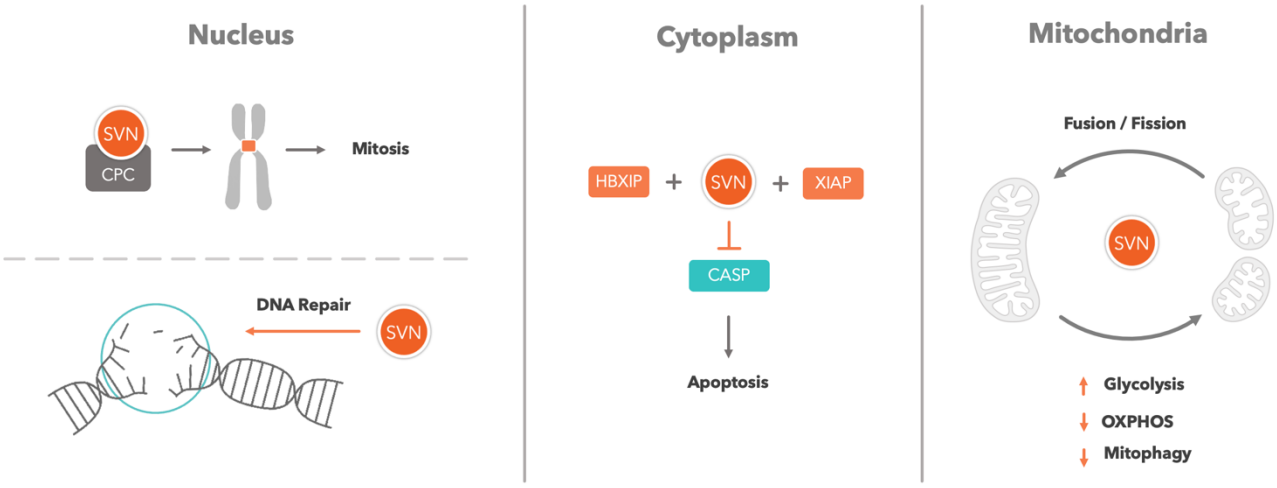


Figure 1.3 – Key functions of survivin within different cellular compartments. Within the nucleus, survivin operates as a member of the chromosomal passenger complex (CPC) to mediate chromosome segregation and facilitate mitosis. In response to DNA damage, survivin may support DNA repair through a number of proposed mechanisms. Cytoplasmic survivin inhibits apoptosis either through direct interaction with pro-apoptotic proteins or in tandem with other pro-survival proteins. Whilst the precise role of survivin within the mitochondria is unclear, survivin expression has been linked with altered mitochondrial morphology, increased glycolysis and decreased oxidative phosphorylation (OXPHOS) and mitophagy. Created by author.

1.2.1.1 Cytoplasm

During interphase, survivin predominantly resides in the cytoplasm (Colnaghi et al. 2006; Stauber et al. 2007) as a result of a nuclear export sequence (NES) present within the dimerization interface and a bipartite NES in the C-terminus (Stauber et al. 2006). Additionally, survivin is preferentially degraded in the nucleus following ubiquitination by the 26S proteasome with a half-life of 30-120 min (Connell et al. 2008). Together these exclude the protein from the nucleus and potentially serve as a spatial regulation of survivin activity. Cytoplasmic residence is thought to be

associated with the anti-apoptotic functions of survivin. Indeed, forced nuclear localisation correlated with heighten sensitivity to chemotherapy and radiotherapy (Knauer et al. 2007; Connell et al. 2008). How this cytoprotective activity is achieved however is a point of contention. Whilst survivin overexpression is undoubtedly associated with diminished caspase activity, survivin is not thought to bind to caspase enzymes at physiologically relevant concentrations (Tamm I et al. 1998). Early research implicated a binding interaction between XIAP and survivin (Altieri 2010; Dohi, Okada, et al. 2004), facilitating the anti-apoptotic effects of XIAP. In addition, survivin may prevent the release of pro-apoptotic factors, such as apoptotic protease-activating factor (APAF1), or prevent the binding of second mitochondrial-derived activator of caspase (Smac; also known as DIABLO) to other IAP family members, prohibiting their anti-apoptotic function (Sun et al. 2005). However, recent studies have failed to replicate direct interactions with XIAP and challenge an indirect influence on the XIAP pathway (Zumbrägel et al. 2017). Whilst numerous studies have demonstrated a correlation between survivin expression and apoptosis resistance, it therefore remains unclear how this achieved mechanistically.

1.2.1.2 Nuclear

Nuclear survivin has been further linked with autophagy, a process associated with healthy turnover of cellular components but with implications for both pro- and anti-apoptotic responses. Survivin has been shown to negatively regulate autophagy via HSPB1/Hsp27 downregulation, resulting in increased ubiquitination of ATG7, as well as direct inhibition of the ATG12-ATG5-ATG16L1 complex formation (Lin et al. 2020). However, despite the association of autophagy with cell survival, survivin knockdown was shown to increase autophagy-mediated ROS-dependent DNA damage and compromise viability (Cheng et al. 2021). Strict regulation of autophagy is therefore important to cell survival and the role of survivin as a negative regulator may thereby act to promote genomic stability. Other research

has suggested survivin expression may conversely act to promote genetic heterogeneity and DNA damage (Conde et al. 2017a), possibly suggesting a nuanced relationship in which survivin levels must be carefully managed.

Although actively excluded from the nucleus during interphase, it enters the nucleus in late G2 and is associated with the chromosomes during mitosis. Specifically, survivin coordinates with Aurora B, Borealin and inner centromere protein (INCENP) to form the chromosomal passenger complex (CPC) (Honda et al. 2003; Stauber et al. 2006). This complex oversees correct chromosomal alignment and segregation and subsequent cytokinesis.

Nuclear localisation is also observed in response to genotoxic stimuli (Capalbo et al. 2010). DNA damage induces a rapid accumulation of survivin within the nucleus with implications for DNA damage repair. Maintenance of the genetic material of the cell is vital to the continued function and survival of the cell and wider host organism. Genomic integrity and faithful replication are essential to avoid mutations that might lead to aberrant cell function and further pathological developments. A failure to repair this damage may result in cell senescence or induce cell death. Even in neoplastic cells, in which genomic instability serves as a hallmark of cancer(Hanahan, Weinberg 2011), excessive DNA damage can induce apoptosis, forming the basis for many anti-cancer treatment strategies. In mammalian cells, multiple DNA repair pathways exist depending on the form of DNA damage that has taken place. In the case of double stranded DNA breaks, two primary pathways are responsible their repair: homologous recombination (HR) and non-homologous end joining (NHEJ) (Valerie, Povirk 2003; Shiloh 2003). HR represents the preferred repair pathway for accurate repair of DNA lesions and utilises sister chromatids to provide template DNA strand for repair. As such, HR is limited to late S and G2 phases of the cell cycle and is actuated by numerous proteins, including RAD54, RAD54L and MRE11 (Sung, Klein 2006). Survivin expression has been linked with

the expression of these proteins and downregulation of survivin is associated with compromised DNA repair capabilities (Cheng et al. 2021). NHEJ serves as the predominant repair mechanism throughout most of the cell cycle as it is not contingent on sister template strands. This flexible repair mechanism sees the binding of a Ku70/Ku80 heterodimer to both ends of the DNA break and subsequent recruitment of the catalytic subunit of the DNA dependent protein kinase catalytic subunit (DNA-PKcs). Nucleases and DNA polymerases may process these ends before the DNA strands are finally ligated by a complex comprised of DNA ligase IV, X-ray cross-complementation group 4 (XRCC4) and XRCC4 like factor (XLF) (Valerie, Povirk 2003; Chatterjee, Walker 2017a). While survivin expression levels have not been linked with expression levels of NHEJ proteins, recent research has demonstrated an interaction between these proteins, (Capalbo et al. 2010; Güllülü et al. 2021) and indicated a potential role for survivin in NHEJ. Indeed, survivin puncta were observed to colocalise with g-H2AX and DNA-PKcs/MDC1/Ku70 complexes (Capalbo et al. 2010). However, in both HR and NHEJ, the precise role survivin plays in potentially facilitating and/or regulating these processes remains to be clarified. The mechanisms underpinning survivin's nuclear localisation in these contexts are also unclear. Survivin contains no clear nuclear localisation signal (NLS) (Villapol et al. 2008) and may be dependent on cofactors for nuclear shuttling. Indeed, large survivin constructs thought to be too large to pass through the nuclear membrane via passive diffusion have demonstrated nuclear localisation (Connell et al. 2008) with some evidence they are actively imported (Colnaghi et al. 2006).

1.2.1.3 Mitochondria

Unique to cancer cells appears to be a mitochondrial pool of survivin (Dohi, Beltrami, et al. 2004; Wheatley, Altieri 2019; Garg et al. 2016). Although obscured by cytoplasmic survivin when imaging, mitochondrial survivin has been demonstrated by subcellular fractionation (Beghein et al. 2016) and is targeted to

the mitochondria by a short mitochondrial targeting sequence present in the N-terminus (Dunajová et al. 2016), where it resides in the inner mitochondrial membrane and matrix (Rivadeneira et al. 2015). Mitochondria localisation may be additionally facilitated by heat shock protein 90 (HSP90) and aryl hydrocarbon receptor-interactive protein (AIP) (Byoung, Altieri 2006). This population has itself been linked with multiple cellular processes including altered apoptosis inhibition, cell metabolism and mitochondrial dynamics. Genotoxic stress was shown to increase this mitochondrial pool (Asumen et al. 2010) before being released upon apoptotic stimulation with enhanced cytoprotective activity relative to cytoplasmic survivin (Dohi, Beltrami, et al. 2004). The mechanisms and mitochondrial functions underlying this mitochondrial accumulation of survivin, its release and its enhanced efficacy all remain to be elucidated.

Whilst our understanding of the functional roles survivin plays in cellular homeostasis and neoplasia has developed substantially over the last two decades, much remains to be elucidated including fundamental questions surrounding the mechanism of its anti-apoptotic activity. The diverse and complex range of processes linked with this multifaceted protein complicate interpretations of its downstream impacts and present methodological challenges in delineating its direct effects.

1.3 Hypoxia and Cancer

As a result of solid tumour development, inadequate vascularisation generates regions of limited blood supply and consequent hypoxia. For tumours developed in many organs, such as the cervix, breast and liver, oxygen concentration averages approximately 1% (Brooks et al. 2004; Vaupel et al. 2007a). These hypoxic tumour regions have generated significant clinical interest due to their correlation with

increased tumour malignancy, treatment resistance, and likelihood of metastasis (Höckel, Vaupel 2001).

Hypoxia is typically established at a distance of ~100 μm from functional blood vessels (Helmlinger et al. 1997) as a result of limited oxygen diffusion, whilst greater distances (approx. 150 μm) may lead to an anoxic environment, incompatible with sustained survival and give rise to regions of necrosis. Indeed, hypoxia typically leads to cell death in normal cells. However, this region may also induce genomic changes that facilitate survival through cellular adaptations, enabling the local tissue to tolerate reduced nutrition and the hostile conditions imposed by this aberrant microenvironment (Hall, Giaccia 2011). As such, solid tumour development establishes a selective pressure that promotes survival of cell subpopulations with the necessary genetic and metabolic alterations to endure these conditions and consequently potentiate tumour malignancy.

The cellular response to diminished oxygen availability is primarily ascribed to the family of hypoxia-inducible factors (HIF), which plays a critical role in tumour malignancy both in neoplastic and stromal cells (Muz, de la Puente, Azab, Azab 2015). However, it should be noted the NF-κB, MAPK and PI3K/AKT/mTOR pathways are also associated with hypoxia and regulate cellular functions such as proliferation, survival, inflammation and migration and may also result in activation of the HIF pathway (Muz, de la Puente, Azab, Azab 2015). The HIF family is comprised of the transcription factors HIF-1, HIF-2 and HIF-3, which are composed of an alpha subunit and a constitutively expressed aryl hydro-carbon receptor nuclear translocator (ARNT) beta subunit. Discrete HIF-binding response elements (HRE) within the genome serve as downstream HIF targets and lead to increased expression of genes involved in genomic instability, angiogenesis, metastasis, invasion, autophagy, metabolism and therapeutic resistance (Petrova et al. 2018). These responses have been largely attributed to HIF-1 and HIF-2 and are the most widely studied HIF family members. Despite similarities in the structural

characteristics of these proteins, HIF-1 and HIF-2 generate divergent transcriptional responses and overall biological actions (Loboda et al. 2010), possibly due to differences in their transactivation domains (Mole et al. 2009). For example, late stage colon cancer tumours presented with strong HIF-1a expression and reduced HIF-2a staining whilst the reverse trend was observed in early stage tumours (Imamura et al. 2009), suggesting differing roles for these proteins in tumour activity.

In the presence of oxygen, these transcription factors are inactivated through the action of prolyl hydroxylase domain-containing proteins (PHDs). The HIF-α subunits harbour oxygen dependent degradation domains (ODDs) and more specifically proline residues at positions 402/564 in HIF-1α and 405/531 in HIF-2α, which are targeted by PHD-mediated hydroxylation (Smirnova et al. 2012). As a consequence, the HIF transcription factors are rendered vulnerable to ubiquitination by the von Hippel-Lindau tumour suppressor (pVHL) E3 ligase complex and subsequent degradation by the proteasome. In addition to oxygen, PHD activity may be further modulated by mitochondrial derived ROS, Kreb cycle intermediates (e.g. succinate), iron, and ascorbate (Snell et al. 2014). HIF-1α activity is also subject to additional regulatory controls. Factor inhibiting HIF (FIH) reduces HIF transcriptional activity through hydroxylation of asparagine residues, which are necessary for binding with the HIF cofactors p300 and CREB-binding protein (CBP). Heat shock protein 70 (Hsp70) and carboxyl terminus of HSP-interaction protein (CHIP) may function as alternative routes of protein degradation whilst the mTOR signalling pathway may conversely increase HIF-1a production.

The HIF pathway regulates hundreds of genes (Muz et al. 2014) and a diverse range of cellular responses, summarised in table 1(Yu et al. 2017; Karakashev, Reginato 2015). The increased migratory capacity of tumour cells in response to hypoxic conditions is well documented (Muz, de la Puente, Azab, Ghobrial, et al. 2015; Cairns, Hill 2004; Cairns et al. 2001). This is partly achieved through the promotion

of epithelial-mesenchymal transition (EMT), a process in which cells undergo altered gene expression in the acquisition of increased mobility and plasticity.(Singh, Settleman 2010) EMT is a key feature of invasive cells and is characterised by loss of epithelial-associated gene expression, such as adhesion-associated molecules E-cadherin and β-catenin (Kim et al. 2002), and production of mesenchymal-associated proteins, such as N-cadherin and vimentin(Hsu et al. 2000; Manotham et al. 2004). Hypoxia-induced transforming growth factor beta (TGF-β) upregulation results in the activation of numerous transcription factors, including Smads, Slug and Snail (Azab et al. 2012), which facilitate this process.

Role	HIF Target Genes
Proliferation and Survival	Cyclin D1, Cyclin G2, TGF-α, NOS2, ADM, C-MYC, IGF2, CAIX
Metabolism	GLUT1, GLUT3, GAPDH, Leptin, PGK1, PFKL, LDHA, PKM, PFKBF3
Metastasis	Vimentin, TGF-α, Collagen V, MMP2, MMP9, FN1, c-Met, Keratin, CAIX, P4HA, LOX
Angiogenesis	VEGF, VEGFR, NOS, LEP, TGF-β3, ADM, LEP
CSCs Development	Notch, OCT4, C-MYC, Telomerase
Inflammation and Immunosuppression	FOXP3, PD-L1, CCL5, CXCL11, HLA-G, CD137, VEGF, NF-κB
Therapeutic Resistance	Bcl-2, Beclin1, Survivin, p53, MDR1

Table 1.1 - Summary of HIF target genes and their role in tumour malignancy.

ADM, adrenomedullin; CAIX, carbonic anhydrase IX; CCL5, chemokine (C-C motif) 5; CXCL11, Chemokine (C-X-C motif) 11; FN1, fibronectin 1; FOXP3, forkhead box P3; GAPDH, glyceraldehude-3-P-dehydrogenase; GLUT, glucose transporter; HLA-G, human leukocyte antigen G; IGF2, insulin like growth factor 2; LDHA, lactate dehydrogenase; LOX, lysyl oxidase; MDR1, multidrug resistance 1; MMP, matrix metalloproteinase; NF-κB, nuclear factor kappa-light-chain-enhancer of activated B cells; OCT4, octamer-binding transcription factor 4; P4HA, prolyl 4-hydroxylase; PD-L1, programmed death-ligand 1; PFKBF3, 6-phosphofructo-2-kinase/fructose-2,6-biphosphatase-3; PFKL, 6-phosphofructokinase; PGK1, phosphoglycerate kinase 1; PKM, pyruvate kinase; TGF, transforming growth factor; VEGF, vascular endothelial growth factor; VEGFR, VEGF receptor. Created by author.

Additionally, HIF promotes the generation of permeable, aberrant vascularisation through the recruitment and induced differentiation of endothelial cells via VEGF regulation (de la Puente et al. 2013), subsequently aiding tumour cell extravasation and circulation. Following relocation, downstream HIF targets promote the invasion of new tissue. ECM modification and degradation are key processes in metastatic dissemination and are actuated by the expression of proteins such as matrix metalloproteinases (MMPs). MMP2 and MMP9 have been implicated in hypoxic breast and colon cancer (Choi et al. 2011; Krishnamachary et al. 2003) and serve to disrupt cell-cell and cell-ECM interactions and breakdown components of the ECM, assisting tumour cell infiltration.

Paradoxically, neovascularisation may fail to alleviate oxygen deficiency as the resultant vasculature is characterised by an abnormal and functionally compromised structure and composition (Helmlinger et al. 1997). Featuring dilated and elongated blood vessels with endothelium lacking functional cell receptors and blood flow regulation, the vasculature is prone to stasis and limited oxygen delivery. Termed "ischemic hypoxia", these conditions are typically transient and give rise to

acute conditions of low oxygen levels (Vaupel, Harrison 2004; Vaupel et al. 2001) whilst chronic hypoxia may occur as solid tumour growth distances cancerous tissue from patent blood vessels (Bayer, Vaupel 2012). Furthermore, anaemic hypoxia may develop through impairment of oxygen transport by the circulatory system, often as a result of iron deficiency or myelosuppression induced by chemotherapy treatment (Busti et al. 2018). Further adaptations include initiation of cell cycle arrest, differentiation, necrosis and apoptosis (al Tameemi et al. 2019).

Hypoxia has received much attention for its role in generating highly resistant subpopulations of tumour cells and poses a major obstacle in the treatment of cancer (Wilson, Hay 2011). Many patients experience recurring tumours and relapse as a result of residual tumour cells that survive the initial treatment course (Munshi, Anderson 2013). This therapeutic resistance is established through a range of alterations in cellular activity. Namely, induced quiescence in which cellular proliferation is arrested, granting increased protection to external stress and particularly therapies that aim to exploit the traditionally high proliferation rate of cancer cells; apoptosis resistance through impairment of apoptotic pathways (Dong et al. 2003) and upregulation of anti-apoptotic proteins (Rohwer, Cramer 2011), such as survivin (Zhang et al. 2014); and metabolic reprogramming, resulting in reduced mitochondrial oxidative metabolism and selective mitochondrial autophagy (Karakashev, Reginato 2015). Radioresistance is rapidly elevated as oxygen levels are reduced to less than 3.3-3.9% (al Tameemi et al. 2019), achieved in part by the reliance of radiotherapy on oxygen to generate radicals, such as hydroxyl radiation and superoxide, and realise its genotoxic effects. Furthermore, radiation treatment can nearly double HIF1a activity ~24 h following exposure, although this effect is dependent on interactions with the TME and thus restricted to in vivo models (Moeller et al. 2007).

Hypoxia therefore not only facilitates the generation of aggressive tumour cells but also plays a crucial role in the development of resistance to treatment. Indeed, a number of HIF inhibitors have been developed over the past two decades and research into their potential as novel cancer treatments is ongoing (Yu et al. 2017).

1.4 Challenges in studying normoxia and hypoxia in vitro

Whilst conditions within standard cell culture incubators, which control for humidity and CO_2 levels, are often described as normoxic or physoxic, this is an inaccurate representation of oxygen availability under normal physiological conditions. Oxygen levels within the body exist in a continuum, ranging from the high levels seen in the arterial blood (~13%) to low levels in the dermis (~1%) (Carreau et al. 2011). The oxygen concentration for cells within incubators – commonly referenced as 20.9%, i.e. atmospheric oxygen level, but which more accurately resides at approximately 18.6% within culture dishes (Wenger et al. 2015) – therefore describe an abnormally elevated oxygen state.

However, oxygen levels within the media immediately surrounding cultured cells are subject to a range of dynamic factors. Oxygen diffusion becomes limited at a distance of approximately 100 - 200 μm in culture medium (Olive et al. 1992). For cells grown in a 10 mm culture dish this is an order of magnitude smaller than the typical depth created by the addition of growth media for example, creating a system where an oxygen equilibrium between cells and the air within culture flasks is unsustainable. Intracellular oxygen is consumed through a number of reactions, although its role as the terminal electron acceptor during glucose metabolism serves as the primary source of O_2 depletion (Zhang et al. 2012). As oxygen is exhausted, intracellular O_2 levels decline, potentially creating hypoxic conditions even at the high O_2 levels seen within standard incubators. As such, the oxygen

availability experienced by cells is the product of numerous factors including cell confluency and metabolic activity, incubation time without media change, incubator oxygen concentration and media depth. Without specialised equipment to determine pericellular O_2 levels or use of oxygen permeable cell culture dishes, which have proven unsuitable for many cell lines, accurate determination of oxygen availability is often difficult. Moreover, the physiological and biological relevance of specific oxygen concentrations will differ between cells types; neuronal cells are highly intolerant of hypoxic conditions (Cervós-Navarro, Diemer 1991) whilst oxygen levels are naturally very low for dermal cells (~1%) (Carreau et al. 2011) for example.

As a consequence of the challenges to accurate O_2 measurements, experimental protocols typically ignore these complexities and simply describe the culture conditions used. Their capacity to create a normoxic or hypoxic environment is validated through their ability to elicit different biological responses, e.g. if cells incubated at 20% O_2 garner no detectable HIF-1α expression whilst a significant increase is demonstrated when lowered to 1% O_2, these conditions might be described as "normoxic" and "hypoxic" respectively. However, in neither case is the true oxygen concentration experienced by the cultured cells known nor how these relate to physiological or pathophysiological norms. Furthermore, tumour cell lines may respond differently to hypoxic conditions, with cell death or cell survival partially determined by the time of exposure to low oxygen levels. Acute and chronic hypoxia are similarly ill-defined amongst oncogenic experiments and require additional consideration when interpreting such data (Bayer, Vaupel 2012) . While these approaches may suffice in exploring the potential roles of hypoxia, care should be taken in generalizing these results to *in* vivo models.

Tissue	Normal O_2 Level	Tumour O_2 Level	Reference
Ambient Air	20.9%	-	(Wenger et al. 2015)
Culture Flask	18.6%	-	(Wenger et al. 2015)
Brain	3.4%	1.7%	(Vaupel et al. 2007b)
Lung	5.6%	1.9%	(Falk et al. 1992)
Liver	5.4%	0.8%	(McKeown 2014)
Arterial Blood	13.2%	-	(Carreau et al. 2011)
Prostate	6.7%	0.6%	(Parker et al. 2004)
Breast	6.8%	1.3%	(McKeown 2014)

Table 1.2 - Median oxygen levels within different regions of the body under physiological conditions and in tumours.

1.5 Cell Division and Regulation

Cell division is a complex and tightly orchestrated process which sees the replication and division of a cell's genetic information and contents, culminating in the generation of two daughter cells and expansion of the original tissue. This process is fundamental to the survival and function of multicellular organisms, playing an essential role in homeostasis, embryonic development (Siefert et al. 2015) and tissue regeneration (Krafts 2010). However, dysregulation of these events

may additionally promote genetic mutations, compromising normal cell function and activity, and is the cornerstone of aberrant tumour growth (Liu et al. 2019). Numerous regulatory elements are consequently tasked with ensuring the controlled proliferation of healthy tissue and faithful replication of their genomic material (Vermeulen et al. 2003). Factors influencing cell proliferation may derive from either intracellular or extracellular signals and support both physiological and pathophysiological development. External environment conditions, such as nutrient and oxygen supply, can stimulate both entry into the cell cycle or abstinence from it (Douglas, Haddad 2003) and play a role in tumour development.

1.5.1 Cell cycle stages

Cell division may be broadly divided into two stages: mitosis, which involves division of the DNA/genetic material and separation of organelles into two distinct cells, and interphase, the interlude between these mitotic events, summarised in Fig. 1.4. Whilst mitosis (Fig. 1.5) is the physical separation of cellular content and generation of daughter cells, interphase is responsible for the preparation and initiation of cell division. Interphase may itself be divided into the G_1, S, and G_2 phases (Norbury, Nurse 1992). G_1 serves as an intermediary step immediately following cell division in which the cell may either enter a resting state termed G_0, which accounts for the majority of non-proliferating cells in the human body, or commit to further proliferation and proceed to S phase. To determine which of these pathways is undertaken, the first regulatory checkpoint, referred to as the 'restriction point', directs subsequent cell activity. This checkpoint functions as a fundamental obstacle to pathological cell growth and an important safeguard of tissue homeostasis. Few cells retain the necessary capacity to overcome the restriction point, rendering them mitotically inert. This is achieved through the binding and concomitant inhibition of retinoblastoma (Rb) protein fragments p107 and p130 to the E2F family of transcription factors, whose downstream targets are necessary for S-phase activity and cell cycle progression.

Advancing past the restriction point requires stimulation of the cell by external growth factors, which subsequently invoke signalling pathways leading to the translation of cyclin D proteins. Cyclin D activity in turn leads to activation of cyclin-dependent kinase (CDK) 4, which phosphorylates Rb and relieves E2F repression, restoring its transcriptional activity. Gene targets of E2F proteins include cyclin E. In tandem with CDK2, cyclin E establishes a positive feedback loop of cyclin E upregulation in addition to transcription of the necessary machinery for DNA synthesis which characterises S-phase activity. Following the transition to S-phase, passing through cell cycle checkpoints is no longer contingent on external growth factor signalling and the cell is thus committed to cell cycle progression.

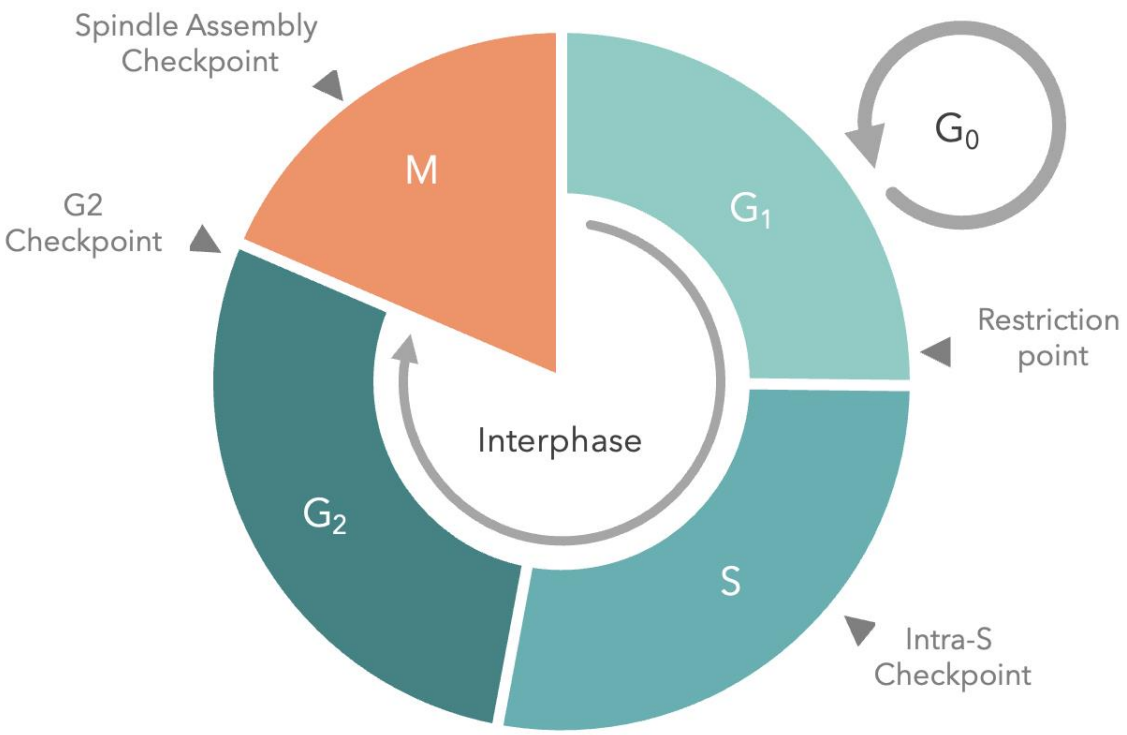


Figure 1.4 – Summary of cell cycle stages and checkpoints. Created by author.

Replication of the genome is an energetically demanding process which sees the complete and single duplication of the cell's genomic material, providing the basis for chromosome separation during mitosis. Instigation of DNA synthesis occurs at replication origins, as defined by a number of proteins which ensure the initiation of DNA replication at these sites only once per cell cycle (Nishitani, Lygerou 2004). During this time, the cell is acutely vulnerable to DNA damage as lesions additionally act as physical obstructions to the replicative process. The intra-S-phase checkpoint is tasked with stabilizing the replisome should active polymerases encounter DNA lesions that block their progress. Stalling of DNA replication leads to replisome component Mrc1 phosphorylation by the sensor kinase ataxia-telangiesctasia and Rad3-related (ATR), facilitating the binding of the intra-S-phase effector kinase Chk2. Following its incorporation with the replisome, Chk2 is also phosphorylated by ATR before becoming fully activated by autophosphorylation (Xu et al. 2006). Activated Chk2 then phosphorylates several replisome subunits, including MCM helicase, to stabilize it (Stead et al. 2012). The replisome may then remain in place until the obstruction is removed and the replicative process can proceed. Alternatively, DNA lesions may be resolved through post-replication repair pathways or the cell may utilise the nascent strand as a template to continue (Lee, Myung 2008). Completion of DNA replication is a key checkpoint in safeguarding genomic integrity. Attempting to undergo mitosis before obstructions have been resolved and the replicative process has concluded may result in reduced ploidy of daughter cells.

1.5.2 Prophase

During replication, cohesins tie each DNA duplex to its sister, creating compact chromatids that enable the accurate separation and distribution of the genome to daughter cells (Peters et al. 2008). Such DNA condensation occurs during the first mitotic phase, termed prophase, and serves to individualise DNA strands into

distinct and separable elements. DNA compaction is likely facilitated by chromatin modifications, such as phosphorylation and acetylation, as well as the activity of condensins, a protein family involved in ds-DNA folding (Richard Mcintosh 2016; Thadani et al. 2012). Prophase further coordinates the brake down of numerous cellular components during this preparatory mitotic phase, including the nuclear envelope, Golgi complex and cytoskeleton (Steinhardt, Alderton 1988; Richard Mcintosh 2016). Extensive cytoskeletal restructuring subsequently facilitates equipartitioning of cellular components and cell division. Solubilisation of many interphase polymers reduce the viscosity of the cytoplasm and aids in the diffusive redistribution of cytoplasmic elements such as ribosomes and enzymes complexes. A breakdown of the cytoskeleton additionally precipitates cell rounding, imparting a symmetry to cell structure that supports the equal dispersal of cell contents while additionally aiding spindle reorientation in response to external cues that govern correct positioning of daughter cells (Fink et al. 2011). Although MTs and microfilaments largely dissolve during this period, some stress fibres remain at cell cortex to facilitate later contractile ring formation (Mitsushima et al. 2010) whilst centrosomes initiate the generation of new MTs in the assembly of the spindle (Ma, Poon 2011). Indeed, cytoskeletal breakdown liberates many of the necessary molecules necessary in the construction of cytokinetic machinery.

1.5.3 Prometaphase

The mitotic spindle, formed during prometaphase, is tasked with segregation of chromatids to evenly distribute the cell genome to its daughter cells. This is achieved through the positioning of centrosomes at opposing sides of the nucleus to form distinct asters. Here, highly dynamic MTs grow radially and interact with different cellular components to coordinate the correct spatial distribution of chromatids, giving rise to MTs with distinct functional roles: astral MTs bind with the cell membrane and anchor the spindle poles within distinct regions of the cell; polar

MTs facilitate the spatial distancing of spindle poles through interdigitation within the midzone region, providing a structural foundation for motor proteins to subsequently push the poles apart; and kinetochore MTs crucially interact with the chromatids to instigate their repositioning and regulate subsequent mitotic activity (Cheeseman 2014). Specialised protein complexes comprised of approximately 100 different polypeptides assemble on chromatin to form kinetochores, which in turn bind with the kinetochore MTs. Kinetochore components include the Ndc80 complex, KNL1 and CENPF, which bind to MT walls. Additionally motor enzymes bind to MTs with either a minus end-directed motor (dynein), at least one plus end-directed motor (kinesin-8 proteins and CENP-E) and a disassembly-promoting kinesin (kinesin-13) (Richard Mcintosh 2016; Cheeseman 2014). Together these proteins provide the bidirectional motor force and the regulatory capacity to govern MT dynamics, conferring kinetochore MTs the necessary flexibility to mediate tightly controlled chromosome segregation. Moreover, spindle MTs exhibit notable instability and may shrink as a result, providing MTs the opportunity to either be rescued and resume growth, or be dismantled and allow their gamma-tubulin ring complex to generate a new MT (Goodson, Jonasson 2018). In combination with revolving movements (Mitsushima et al. 2010), the dynamic growth and shrinkage of kinetochore MTs enable repeated probing of the nuclear space to bind with target chromatids (Kirschner, Mitchison 1986). This imprecise method of chromosome capture may often result in undesired interactions however. Successful chromosome segregation requires sister chromatids to be bound to the ends of MTs originating from opposing centrosomes (amphitelic attachments), necessitating additional regulatory mechanisms to avoid or resolve inappropriate complexes (Magidson et al. 2011).

Numerous regulatory mechanisms exist to mediate this critical mitotic step. As bound chromatids are pulled towards one of the centrosomes, their sister chromatids are oriented away and towards the opposing centrosome to facilitate its

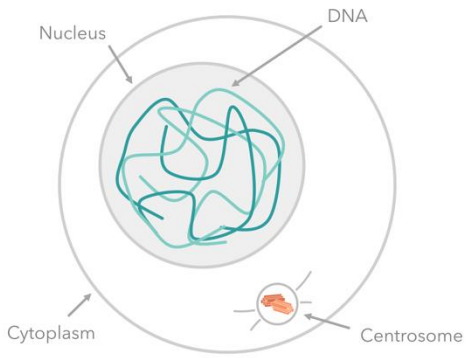
counter attachment (Foley, Kapoor 2013). Were monotelic attachments (where only one chromatid is bound to a kinetochore MT) or syntelic attachments (where both sister chromatids are bound to MTs from the same centrosome) to occur, subsequent progression through mitosis would result in genomic disparity and abnormal ploidy of the daughter cells (Nicholson, Cimini 2011). Such attachments are in part dissuaded by the regulation dynein activity, which is required for the pulling of attached chromatids towards the centrosomes. Dynein activity is reliant on the presence of tension within the MTs to stabilise its attachment (Bruce Nicklas et al. 1998). This tension is elegantly established when sister chromatids are correctly bound to opposing centrosomes but notably absent when both chromatids are pulled to the same point. Asymmetric kinetochore attachments thus fail to stabilise dynein and thereby disrupt chromatid translocation. The resolution of dysfunctional attachments additionally requires complex disassembly. Aurora B regulates the activity of several kinetochore components including the NDC80 complex involved in MT binding (DeLuca et al. 2011). Aurora B-mediated phosphorylation then promotes MT detachment and MT-kinetochore instability as a result. Dissolution of incorrect MT attachments subsequently provide kinetochores further opportunities to form the desired MT-kinetochore arrangement. In a similar fashion to dynein activity, tension at the kinetochore decreases Aurora B activity, thus correct amphitelic attachments preserve kinetochore-MT complexes (Lampson, Cheeseman 2011).

1.5.4 Metaphase

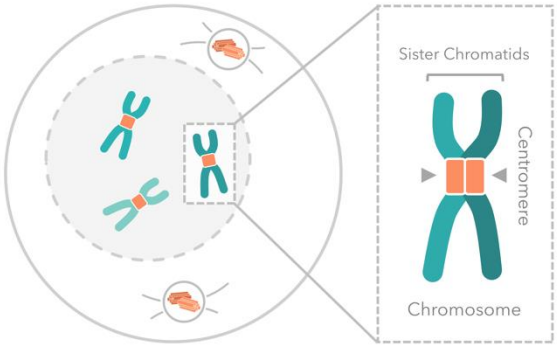
Metaphase is characterised by the congression of chromosomes at the equatorial plane of the spindle. This is thought to occur as a result of a polar ejection force in which spindle poles appear to exert of a repulsive force on the chromosomes during prometaphase, likely mediated by kinesin activity or unstable MTs that grow into condensed chromatin (Richard Mcintosh 2016; Brouhard, Hunt 2005). In

moving to the equatorial plane, chromosomes are positioned at equal distances from the polar regions, thereby reducing the probability that some chromosome may be left behind during their separation in anaphase. Maintenance of this metaphase state is notably reliant on GTP hydrolysis to sustain the dynamic instability of MTs (Matos et al. 2009; Saxton et al. 1984). Indeed, rather than staying at the equator, chromosomes typically oscillate along the spindle axis during metaphase.

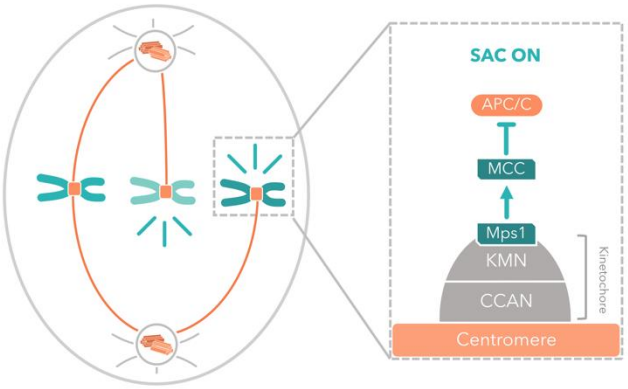
Interphase



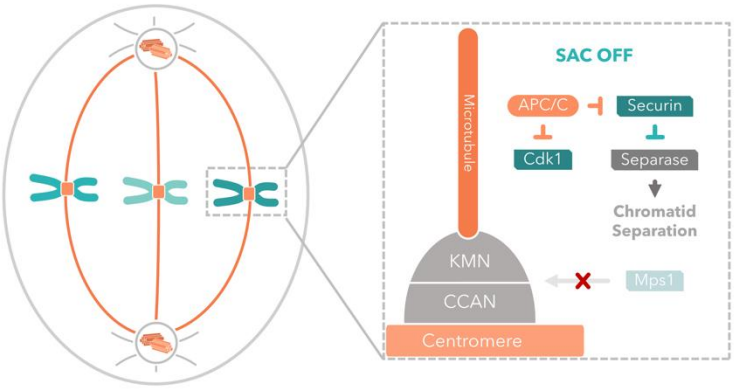
Prophase



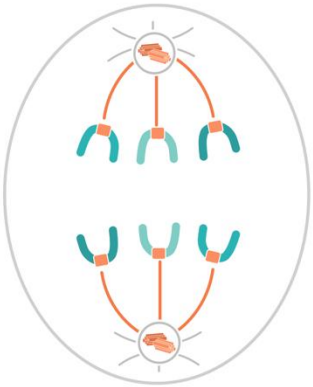
Prometaphase



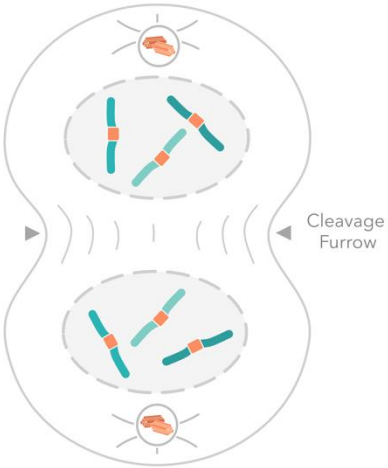
Metaphase



Anaphase



Telophase



Cytokinesis

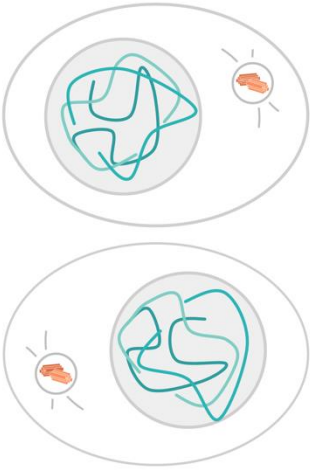


Figure 1.5 – Summary of mitosis stages. **Prophase:** DNA condenses into chromosomes with two chromatids held together at the kinetochore. The nuclear envelop begins to breakdown. Centrosomes duplicate and begin developing bipolar spindles. **Prometaphase:** The nuclear envelope has fragmented. Spindle poles have formed and kinetochore microtubules bind to chromosomes. The spindle assembly checkpoint (SAC) remains in operation while unbound kinetochores remain, inhibiting the APC/C via recruitment of Mps1 and prevents further cell cycle progression. **Metaphase:** Chromosomes are aligned at the equator of the spindle and all kinetochores are bound, preventing Mps1 activity. This relinquishes APC/C inhibition, enabling downstream chromatid separation through separase-mediated cleavage of cohesion molecules. **Anaphase:** Kinetochore microtubules shorten, separating sister chromatids and pulling them towards the poles. **Telophase:** The nuclear envelope begins to reform around the separated chromatids as the cleavage furrow starts to form. **Cytokinesis:** Nuclear envelope reformation is completed and contraction of the cleavage furrow generates two identical daughter cells as the DNA decondenses. Created by author.

A regulatory checkpoint, termed the spindle assembly checkpoint (SAC), serves to delay the onset of anaphase until the spindle has correctly attached to all chromosomes. Protein complexes formed on the kinetochore involve the binding of the constitutive centromere associated network (CCAN) to centromeric chromatin containing histone H3 variant CENP-A. CCAN in turn connects the chromosomes to the outer KMN network, which is itself a complex of the Knl1, Mis12 and Ndc80 sub-complexes. Aurora B, as part of the chromosomal passenger complex (CPC), is targeted to unattached kinetochores by the regulatory CPC subunits INCENP, Survivin and Borealin (Musacchio 2015). The CPC then mediates phosphorylation of various kinetochore substrates, such as CENP-A in the inner kinetochore and KMN network subunits in the outer kinetochore, to facilitate recruitment of the SAC kinase Mps1, which subsequently phosphorylates MELT repeats in Knl1 (London, Biggins 2014). Downstream consequences of these phosphorylation events include the recruitment of BubR1:Bub3, Cdc20 and C-Mad2, together referred to as the mitotic checkpoint complex (MCC) (London,

Biggins 2014). MCC functions as the SAC effector and targets and inhibits the anaphase-promoting complex or cyclosome (APC/C), whose ubiquitin ligase activity would normally promote proteasome-mediated degradation of Cyclin B and Securin. Consequently, MCC activity prohibits further progression through mitosis. Once kinetochores are bound, it is thought MTs serve as competitive inhibitors of Mps1 sites and subsequently prevent MCC activation. Alternatively, it has been proposed that MT binding may instead impede Mps1 activity by increasing the distance between the Mps1 and its SAC signalling substrate (Aravamudhan et al. 2015). In either case, elevated APC/C activity leads to downstream Cdk1 inactivation via Cyclin B degradation, and Seperase-mediated chromatid separation, enabled by Securin degradation. Cessation of metaphase and the commencement of anaphase is clearly demarcated by the separation of sister chromatids. With the dissolution of Securin by APC/C activity, concomitant inhibition of Seperase is relinquished, facilitating chromatid segregation by Seperase-mediated hydrolysis of the cohesion molecules that previously bound sister chromatids (Kumar 2017).

1.5.5 Anaphase

The transition of complexed sister chromatids to individualised chromosomes and movement towards the spindle poles constitutes the first component of anaphase (anaphase A). This is followed by the spatial distancing of the spindle poles away from one another in preparation of cell division (anaphase B). In both cases, MT dynamics and kinesin activity keenly contribute to these processes.

With the degradation of the second APC/C target, Cyclin B, CDK1 is inactivated and significant shifts in the landscape of mitotic kinases are instigated to prepare for the transition back to interphase. Chromosomes begin to condense next to the spindle poles with the contraction of chromosomes arms (Renshaw et al. 2010) and the

nuclear envelope starts to reassemble with the fusion of envelope fragments and reconstitution of nuclear proteins, including the nuclear pore complexes (Güttinger et al. 2009). The newly reprised nuclear membrane enables the cell to re-establish a functional relationship between the nuclear and cytoplasmic spaces as transcription begins to restart and the nucleoli is reformed. Together, these processes begin to reconstruct the necessary cellular components for functional cell activity following cell division (Richard Mcintosh 2016). During the closing stages of the division process, the cell must finally partition itself into two distinct daughter cells.

1.5.6 Telophase and cytokinesis

This physical separation is mediated by the development of a cleavage furrow. Diffusive signals from the spindle midzone are focused by astral MTs and initiate the assembly of contractile rings, composed of actin filaments and membrane-associated myosin-II, to form around the equator of the cell (Su et al. 2014). These filaments provide the necessary force to generate contraction of the cell membrane at the midzone, forming the cleavage furrow that ultimately divides the mother cell. Cytokinesis is further supported by the mitotic spindle, which establishes antiparallel, interdigitating MTs in the formation of the central spindle and is involved in the segregation of the chromosomes, positioning of the cleavage furrow and distancing of the daughter cells (Nguyen, Robinson 2020). Two master regulatory complexes oversee this process: the CPC and centralspindlin complex. The CPC dynamically relocates during different stages of mitosis and regulates a diverse range of processes to ensure successful cell division and mitotic exit. These include the stabilisation of the spindle midzone, ingression of the cleavage furrow, DNA condensation near the cleavage furrow, timing of nuclear envelope reformation and control over the timing of abscission in the midbody (Kitagawa, Lee 2015). Following the metaphase-to-anaphase transition, the CPC repositions from

the chromosomes to the spindle midzone. Aurora B activity subsequently promotes the recruitment of centralspindlin. The centralspindlin complex is comprised of kinesin-like protein MKLP1 and a Rho GTPase activating protein, CYK-4. Together, these proteins mediate GTPase activity, positioning of the division plane, assembly of the midbody and abscission (White, Glotzer 2012). Stabilisation of the spindle midzone is realised through MT bundling and centralspindlin further recruits factors such as RhoGEF Ect2 for late telophase/cytokinesis. Ect2 initiates the activation of Rho activity to promote actin polymerisation and the formation of the contractile ring. A small pool of CPC additionally relocates to the cell cortex to mediate furrow ingression. Here, Aurora B phosphorylates Septin filaments, thought to aid contractile ring formation, and disassembly of intermediate filaments that may impede furrow constriction (Carmena et al. 2012). Notably, Aurora B may act independently of the CPC to regulate the abscission checkpoint, which stalls further division in response to lagging chromatin (Mackay et al. 2010).

1.6 Tumour Metabolism

The elevated growth, survival and proliferation of tumour cells is thought to be supported by a systemic rewiring of their metabolic pathways. Whilst normal tissues efficiently generate ATP through the breakdown of glucose into pyruvate to serve as a metabolite in the citric acid cycle and downstream oxidative phosphorylation (OXPHOS), cancer cells curiously exhibit a proclivity for glycolysis, even in conditions conducive of aerobic respiration. Despite its documentation over 100 years ago and the keen interest of the scientific community, the precise nature and function of this unusual metabolic profile remains unclear. However, numerous studies have proposed potential explanations and unique advantages to 'aerobic glycolysis' in tumour development, also known as the 'Warburg Effect' (Liberti, Locasale 2016).

For normal tissues, oxygen serves as an inhibitor of glycolysis (Pasteur effect), with the high ATP levels produced by the mitochondria functioning as allosteric inhibitors of the glycolytic enzyme phosphofructokinase (PFK) (Alfarouk et al. 2014). Subsequent pyruvate processing favours entry into aerobic respiration and the efficient generation of ATP in an oxygen dependent manner. However, eukaryotic cells may also support ATP production under hypoxic conditions, albeit less efficiently. Whilst aerobic respiration generates 32 ATP molecules per glucose molecule, glycolysis nets only 2 (Melkonian, Schury 2021). Additionally, these cells must contend with the production of lactic acid as a waste product, which may raise intracellular pH with implications for various cell pathways such as apoptosis, cell division and glycolysis itself (Ward et al. 2020). Activation of HIF1a under hypoxia leads to the upregulation of numerous glycolytic protein isoforms, including pyruvate dehydrogenase kinase 1 (PDK1), carbonic anhydrase-9 (CA-IX), glucose transporters 1-3 (Glut1-3), glyceraldehyde phosphate dehydrogenase (GAPDH) and lactate dehydrogenase-A (LDHA) (Semenza 2010). This enzymatic repertoire supports a metabolic shift away from OXPHOS and towards glycolysis and it has been proposed HIF-1a may drive the Warburg Effect in malignant cells. Whilst HIF1a is optimally stabilised at ~1% O_2, respiration only becomes proportional to oxygen levels at ~0.4-0.7% O_2 (Wilson et al. 1988; Kennedy, Jones 1986), suggesting a premature metabolic response to lowered oxygen levels. This may serve a cytoprotective function, however, and mitigate oncogene-induced senescence resulting from pyruvate dehydrogenase-mediated oxygen consumption and redox stress (Kaplon et al. 2013). HIF1a stabilisation has been demonstrated under normoxic conditions for numerous cell lines with a ~50% incidence (Robey et al. 2005). Expression of metabolic genes, including Glut-1, LDHA, PKM2 and VDAC1 significantly correlated with metastatic tissue, establishing a clear link between cell metabolism and tumour aggression (Graziano et al. 2016). The use of inhibitors targeting enzymes involved in cell glycolysis, such as LDHA (Le et al. 2010), has been the target of novel therapeutic strategies to reduce tumour aggression (Ganapathy-

Kanniappan, Geschwind 2013). Further, HIF1a endows cells with the necessary transmembrane transport proteins to regulate lactic acid levels and thus mediate intracellular pH at the consequence of acidifying the extracellular space (Weidemann, Johnson 2008), although this too may support an aggression tumour phenotype. Matrix acidity is associated with suppression of the anti-cancer immune response (Locasale, Cantley 2010), enhanced motility and modified cellular and intercellular signalling that precipitates tissue malignancy (Boedtkjer, Pedersen 2020). Extracellular lactate may additionally be taken up by tumour-associated fibroblasts through monocarboxylate co-transporters MCT1 and MCT4. As part of the lactic acid cycle, these stromal cells may then regenerate pyruvate and refuel tumour cells (Koukourakis et al. 2006). It should be noted that despite a demonstrable correlation between aerobic glycolysis and tumour aggression in vitro, it is not necessarily universal; various tumour types exhibit both malignancy and partial or complete utilisation of traditional OXPHOS for ATP production (Zheng 2012).

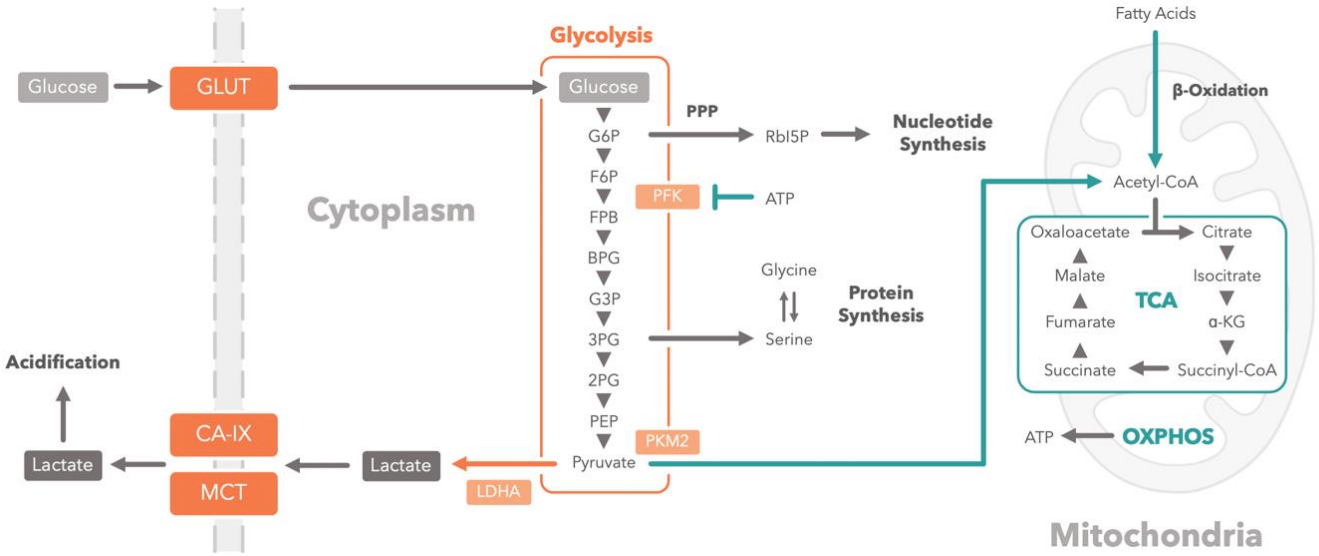


Figure 1.6 – Overview of cellular ATP production pathways.

2PG, 2-phosphoglyceric acid; 3PG, 3-phosphoglyceric acid; ATP, adenosine triphosphate; α-KG, - α-ketoglutaric acid; BPG, 2,3-biphosphoglyerate; CAIX, carbonic anhydrase IX; F6P,

fructose 6-phosphate; FBP, fructose 1,6-biphosphate; G3P, Glyceraldehyde 3-phosphate; G6P, glucose 6-phosphate; LDHA, lactate dehydrogenase; MCT, monocarboxylate transporter; PEP, phosphoenolpyruvic acid; PKM2, pyruvate kinase 2; PPP, pentose phosphate pathway; RbI5P, Ribose 5-phosphate. Created by author.

Cell metabolism is intrinsically linked the structure and activity of its mitochondrial components (Chandra, Singh 2011). The mitochondria serve as the key site of OXPHOS and arbiters of aerobic respiration. However, these organelles respond dynamically to the wider metabolic context of the cell. Eschewing pathways of aerobic respiration deprives the mitochondria of substrates such as acetyl-CoA and oxygen, inducing dramatic structural and functional changes with a resultant loss of membrane potential, reduced OXPHOS activity and uneven cellular distribution (Ježek, Plecitá-Hlavatá 2009). Whilst glycolysis is a highly inefficient means of ATP production in terms of relative glucose consumption, the quantity synthesised remains comparable regardless of the pathway utilised (Liberti, Locasale 2016). Although HIF activity leads to p21 upregulation and concomitant cell cycle arrest, some cancers continue to maintain cell proliferation under hypoxic conditions through sustained Notch and mTOR activity (Zou et al. 2013). In processing glucose in this manner, the cell additionally generates secondary metabolites to be utilised in the generation of lipids, proteins and nucleic acids to support further proliferation and cancer cell development (Graziano et al. 2016).

The elevated demand for glucose to maintain ATP synthesis through glycolysis, either due to hypoxia or aerobic glycolysis, necessities increased expression of glucose transport proteins (Zhou et al. 2016). This transport is mediated by the 13 facilitative glucose transporter family (Glut/SLC2A) members, with differing tissue expression profiles. Glut-1 is expressed in virtually all tissues and its overexpression correlates with increased glucose uptake, distance from stromal blood supply and ultimately HIF-1a driven glycolysis (al Tameemi et al. 2019). Indeed, numerous

hypoxia-related components are associated with Glut-1 expression, including calcium channel and VEGF receptor activation (Suh, Han 2013). Glucose also serves as a vital substrate for triglyceride, glycoprotein and glycogen synthesis to support tumour development (Martinez-Outschoorn et al. 2016). Levels of Glut1 expression are associated with tumour aggressiveness, treatment resistance and diminished clinical outcome (Trendowski et al. 2015; Kunkel et al. 2003).

Glycolysis therefore supports a number of tumour behaviours, ranging from simply satisfying its energy demand within a hypoxic tumour environment to the generation of important secondary metabolites and regulation of ROS production. Cell metabolism thus interacts and coordinates with other cellular pathways with the potential to support cell proliferation, treatment resistance and tumour development.

1.7 Mitochondrial functions and their regulation

Following the discovery of the Krebs cycle, mitochondria have been positioned at the heart of cellular metabolism and an essential component of eukaryotic life. Their ability to efficiently generate ATP has principally associated them with bioenergetics. However, research has further unveiled a diverse and indispensable repertoire of cellular functions, ranging from cell pluripotency and senescence to differentiation and apoptosis. As such, they are uniquely positioned as mediators of both cell life and death. Their regulation is therefore critical to the management of normal cell activity.

The transition of early Earth to a highly oxidising atmosphere favoured organisms with the metabolic capacity to prosper in this new environment (Lyons et al. 2014). Endosymbiotic theory proposes the eukaryotic life of today is owed to the incorporation of protomitochondria by early proto-eukaryotes, which conferred a

selective advantage based chiefly on their respiratory capacity (Sagan 1967). Indeed, the function of modern mitochondria was first ascribed to, and remains primarily associated with, their central role in the production of ATP through oxidative reactions. Following the breakdown of glucose to pyruvate in the cytosol, mitochondrial proteins facilitate the conversion of pyruvate to acetyl CoA, where it subsequently enters the citric acid cycle. Here, electrons are stored in the carrier molecules NADH and $FADH_2$ through iterative processes of oxidation (Walsh et al. 2018). The electron transport chain (ETC) utilises these electrons to establish a proton gradient that ultimately facilitates the generation of ATP by ATP synthase.

1.7.1 The Electron Transport Chain (ETC)

Positioned within folds of the inner mitochondrial membrane (IMM), termed cristae, the ETC is comprised of the transmembrane protein complexes (I-IV) and the electron transfer carriers cytochrome c and ubiquinone. These complexes assemble together with F_1F_0ATP synthase (also termed complex V) to give rise to super complexes that form the basis of ATP production during oxidative phosphorylation (OXPHOS). NADH-ubiquinone oxidoreductase (complex I) is the largest enzyme complex and oversees the transfer of electrons from NADH in the matrix to ubiqinone (also termed coenzyme Q) (Efremov, Sazanov 2011). Here electrons pass through a series of redox centres of increasing affinity within the complex, lowering electron energy state, and thereby freeing energy for complex I to enable the transfer of protons from the matrix to the intermembrane space (IMS). This initial step provides ~40% of the proton flux necessary for the synthesis of ATP by F_1F_0ATP synthase (Efremov, Sazanov 2011). Succinate dehydrogenase (complex II) serves as both a component of the Krebs cycle as well as the ETC, establishing a link between metabolism and OXPHOS (Cecchini 2003). Whilst complex II does not directly pump protons across the IMM, this protein similarly transfers electrons to ubiqinone to be utilised by complex III, although electrons are instead supplied by the carrier

molecule $FADH_2$ (R. Z. Zhao, Jiang, Zhang, Z. Bin Yu 2019). Also known as cytochrome c oxidase or CoQ-cytochrome c reductase, complex III coordinates the transfer of electrons from ubiquinone to cytochrome c, transporting protons in the process. Finally, complex IV (also known as cytochrome c oxidase) transfers electrons to the final electron acceptor O_2 to generate H_2O in a similar fashion. Together, these complexes establish a strong proton gradient across at the IMM in which movement towards mitochondrial matrix is energetically favourable. F_1F_0ATP synthase utilises this stored electrochemical energy to induce conformational changes that enable the phosphorylation of ADP to form ATP molecules (Jonckheere et al. 2012). Under normal physiological conditions, OXPHOS provides approximately 70% of the energy consumed by cell metabolism (Zheng 2012) and is the primary source of energy production within the cell (R. Z. Zhao, Jiang, Zhang, Z. Bin Yu 2019).

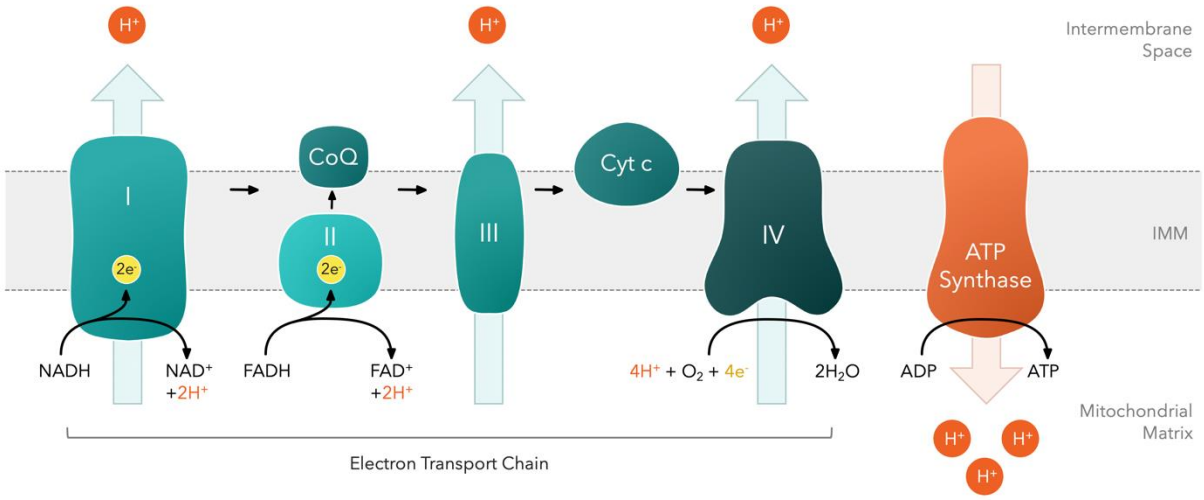


Figure 1.7 – Overview of the electron transport chain. Molecules of NADH and FADH deliver high energy electrons to complexes I and II of the electron transport chain (ECT) respectively. As these electrons are passed through the ECT, they provide the necessary energy for the movement of protons to the intermembrane space and establish an electrochemical gradient. This potential energy is harnessed by ATP synthase to generate ATP molecules that fuel cell metabolism. Created by author.

However, the transfer of electrons is an incompletely controlled process, with 0.2-2% of electrons instead leading out of the ETC and interacting with oxygen to produce superoxide or hydrogen peroxide radicals (Cadenas, Davies 2000; Turrens 2003). Complex I and, to a lesser extent, complex III are considered the main sources of mitochondrial reactive oxygen species (ROS) production (Brand 2010; Kowaltowski et al. 2009). Whilst contribution by complex II is thought to be negligible under normal conditions, complex II mutations are associated with increase ROS production in related diseases (Hoekstra, Bayley 2013). Moreover, acute hypoxia initiates a superoxide burst during the first few minutes, primarily as a result of complex I activity (Hernansanz-Agustín et al. 2017). Excessive ROS production is associated with DNA damage, protein oxidation, impaired mitochondrial function and ultimately cell death (Orrenius et al. 2007). ROS generation is thought to play a key role in ischemia-reperfusion injury (Robin et al. 2007), chronic inflammatory diseases and the development of cancer (Song, Zou 2015). Regulation of OXPHOS and wider mitochondrial activity is therefore key in safeguarding cells from pathological developments as well as the mediation of cellular adaptations to hypoxic conditions, both in the management of ROS production and in the effective production of energy under conditions of low oxygen availability. While ROS production is generally associated with pathological consequences, recent studies have demonstrated a significant role for ROS as secondary messengers that mediate intracellular pathways (De Giusti et al. 2013). Protein oxidation serves as an important regulator of protein activity, particularly for receptors, caspases, kinases, ion channels and transcription factors (De Giusti et al. 2013). HIF-1a stabilization may be dependent on the presence of ROS and therefore vital to the adaptation of cells to low oxygen conditions and the proliferation of cells including endothelial cells and vascular smooth muscle cells (Diebold, Chandel 2016), although this assertion has been disputed (Chua et al. 2010). ROS may also activate AMPK under hypoxia and upregulate cytoprotective autophagy (Emerling

et al. 2009) as well as other signalling pathways including protein kinase B (AKT) and mitogen-activated protein kinase (Kaminskyy, Zhivotovsky 2014). Indeed, elevated ROS production under hypoxia may induce the redox adaptation response, facilitating cancer cell survival via upregulation of survival molecules and enhanced drug inactivation (Page et al. 2008). The downstream impacts of ROS generation are therefore nuanced and must be carefully maintained to facilitate cell function and survival. Management of mitochondrial OXPHOS, and therefore mitochondrial ROS generation, may occur through three key pathways: alteration of cristae structure, mitochondrial morphology, and regulation of proton leakage.

1.7.2 Cristae Regulation

Cristae form key sites of mitochondrial activity, both in ATP production and regulation of apoptosis. These invaginations of the IMM expand the respiratory capacity of mitochondria by increasing the available membrane area within which components of the ETC are positioned. This in turn facilitates the generation of a proton gradient and subsequent phosphorylation of ADP by ATP synthase. Biogenesis of cristae is regulated chiefly by the mitochondrial contact site and cristae organizing system (MICOS) (Giacomello et al. 2020). This large protein structure is composed of two protein assemblies: MIC27-MIC10-MIC12 together with MIC60-MIC19 via a MIC19 linker (Friedman et al. 2015). Located in the IMM, each MICOS component exercises a specific effect on the shape of the mitochondrial membranes, generating the required curvature for cristae formation. It has also been proposed that ATP synthase itself exerts a crucial force involved in the bending of lipid bilayers (Strauss et al. 2008). Formation and maintenance of cristae junctions are additionally overseen by OPA1. Notably OPA1 occurs in two distinct forms: an unprocessed version of OPA1 (termed long OPA1 or L-OPA1), which is positioned in within the IMM, and a soluble protease-cleaved OPA1 (termed short OPA1 or S-OPA1), which resides in the intermembrane space and

serves as a linker for L-OPA1. Together these OPA1 molecules operate to generate cristae junctions and determine lumen width (Meeusen et al. 2006).

1.7.3 Mitochondrial Dynamics

The multifaceted arbitration of cell activity by mitochondria is achieved in part by the dynamic modulation of their ultrastructural architecture. Changes in cellular conditions, such as nutrient and oxygen availability, may induce morphological changes to adapt to these environmental vicissitudes and promote cell survival. Conversely, initiation of apoptosis may similarly produce drastic alterations to mitochondrial structure. Ultrastructural changes fall under two categories: mitochondrial fusion, which sees the fusion of distinct mitochondria and formation of complex tubular networks, and mitochondrial fission, which involves the segregation of one mitochondrion into two distinct organelles (Westermann 2010).

Mitochondrial fusion operates at both the outer mitochondrial membrane (OMM) and the IMM with the fusion of their respective lipid bilayers (Giacomello et al. 2020) through a hemi-fusion intermediate structure (Chernomordik, Kozlov 2008), summarised in Fig. 1.8. This union first requires fusing mitochondria to position themselves within close proximity to one another. Whilst the mechanisms underlying mitochondrial fusion remain to be elucidated, it is thought the transmembrane protein mitofusin 1 (MFN1) facilitates this process via a GTPase domain that governs protein conformation (Tolosa-Díaz et al. 2020). Anchored within the OMM, an extramitochondrial segment of MFN1 protrudes into the cytoplasmic space where it may interact with and tether the outer membranes of other mitochondria. Subsequent GTP hydrolysis then converts the protein from a four-helix bundle arrangement to a closed fold-knife like conformation, securing and pulling the membranes to each other to potentiate fusion of the lipid bilayers (Yan et al. 2018). MFN2 is thought to share some functional overlap with MFN1and similarly participates in mitochondrion-mitochondrion interactions as well as their

positioning with other organelles, such as the endoplasmic reticulum (ER) (Giacomello et al. 2020), although it appears to play a lesser role (Chen et al. 2005). Complete fusion, however, requires fusing of the IMMs as well. Just as OPA1 is thought to connect opposing sides of the IMM within cristae junctions and regulate lumen width, convergence of IMM lipid bilayers during fusion is thought to connect IMMs of distinct mitochondria and mediate their fusion. Again, the balance and interaction of the processed (S-OPA1) and unprocessed (L-OPA1) forms are key to the regulation of IMM fusion (Baker et al. 2014). Multiple enzymes are responsible for S-OPA1 generation, although YME1L1 plays a key role (Griparic et al. 2007). OMA1 peptidase similarly processes the L-OPA1 form and may regulate mitochondria fission and fragmentation as a result (Baker et al. 2014).

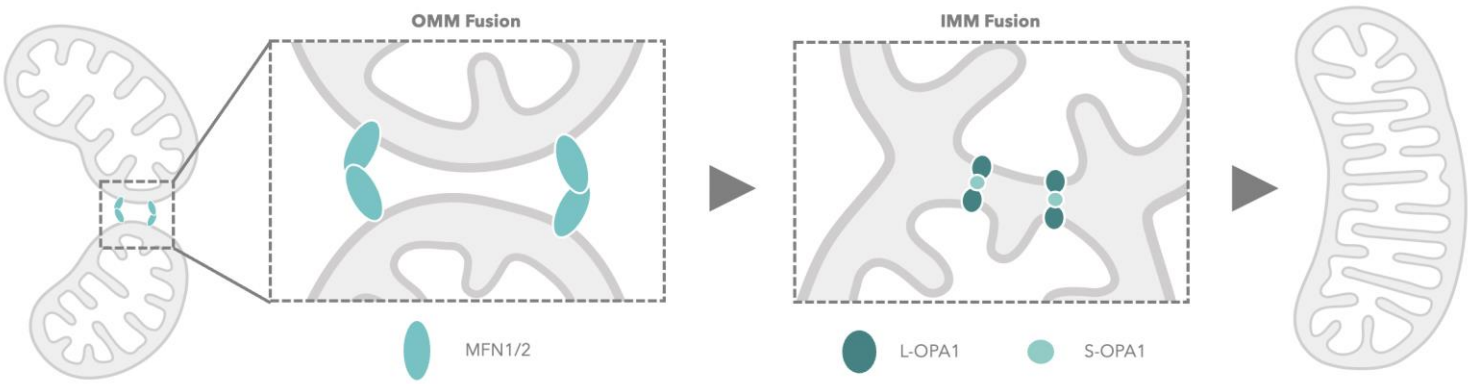


Figure 1.8 – Overview of mitochondrial fusion. Created by author.

Fission is primarily performed by dynamin-related protein 1 (DRP1) and regulates the segmentation of a mitochondrion into smaller distinct mitochondria, summarised in Fig. 1.9. Phosphorylation of serine 637 by protein kinase A (PKA) renders DRP1 inactive, where it resides in the cytoplasm (Cereghetti et al. 2008). Dephosphorylation by calcineurin initiates translocation of DRP1 to the mitochondria (Cereghetti et al. 2008b) where it binds with receptors expressed on the OMM, namely mitochondrial fission factor (MFF), mitochondrial fission 1 protein

(FIS1), mitochondrial dynamics protein of 49 kDa (MID49) and MID51 (Losó n et al. 2013). Much of our understanding of mitochondrial fission comes from studies in yeast, focusing primarily on interactions between DRP1 and FIS1. Curiously, whilst FIS1 overexpression leads to fragmentation (James et al. 2003), its depletion is not associated with an aberrant mitochondrial phenotype in mammalian cells (Otera et al. 2010). Fragmentation may instead be secondary to other FIS1 functions, such as regulation of Ca^{2+} influx (Alirol et al. 2006) and inhibition of mitochondrial fusion machinery (R. Yu et al. 2019). Rather, MFF appears to act as the prevailing DRP1 receptor in mammals (Giacomello et al. 2020). Scission of the mitochondria is driven by oligomerisation of DRP1, which forms linear polymers upon GTP binding. Subsequent hydrolysis of GTP leads to polymer shortening and formation of closed rings that may trigger mitochondrial constriction (Kalia et al. 2018). This process occurs at sites proximal to smooth ER, which surround the mitochondria and facilitate the cooperation of DRP1 with inverted formin 2 (INF2) and formin-binding protein spire 1C, which may induce accumulation of actin filaments and myosin II to support DRP1 polymerisation (Korobova et al. 2014). Mitochondria-ER contact sites (MERCs) further support the delivery of Ca^{2+} to mitochondria from the ER and subsequent activation of IMM constriction, independent of DRP1, to complete the fission process (Korobova et al. 2013).

These processes have been linked to the development of tumours and their progression to metastasis (Boulton, Caino 2022). Expression of proteins involved in mitochondrial fission, such as FIS1 (Karimi et al. 2022), DRP1 (Zhao et al. 2013) and MFF (Seo et al. 2019) are associated with neoplastic tissue and correlate with cancer aggression and enhanced metastatic potential (Sun et al. 2018; Zhao et al. 2013). The downstream consequences of these mitochondrial changes may lead to

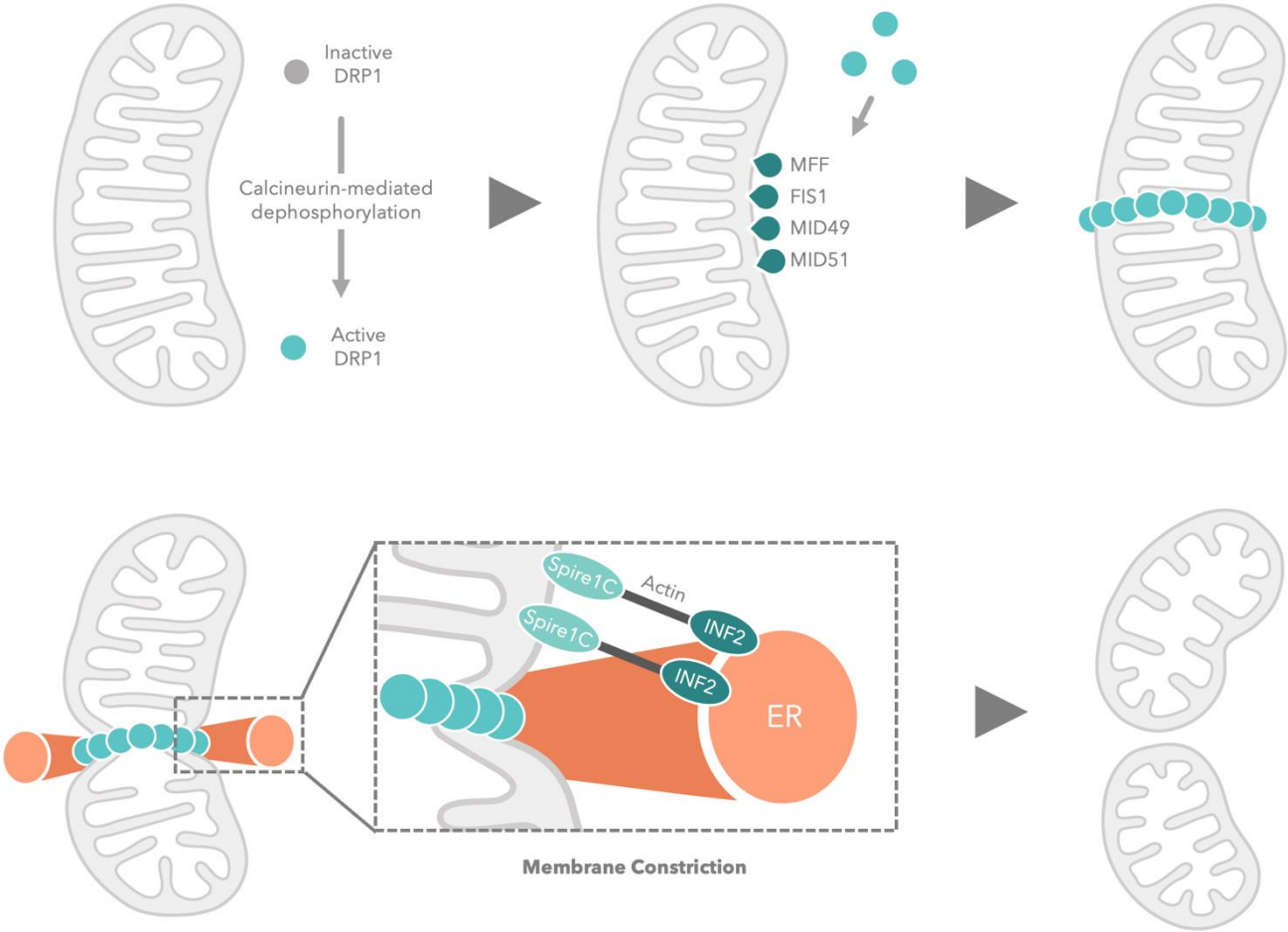


Figure 1.9 – Overview of mitochondrial fission. Created by author.

increased Ca^{2+} promoted motility (Sun et al. 2018), formation of lamellipodia (Zhao et al. 2013) and wider metabolic changes that support an aggressive tumour phenotype (Liang et al. 2020).

1.7.4 Proton Leakage

Proton leakage describes the movement of protons across the IMM in a manner independent of ATP synthase and undermines the electrochemical potential of the mitochondria (R. Z. Zhao, Jiang, Zhang, Z. Bin Yu 2019). A basal level of proton leakage occurs as a result of incomplete proton sequestration offered by the lipid bilayer as well as the activity of adenine nucleotide translocase (ANT), a

mitochondrial carrier protein responsible for the exchange of ATP and ADP between the mitochondria and cytoplasm. Proton leakage may also be utilised as a regulatory tool of membrane potential and consequent OXPHOS activity through the expression of ANT and a family of mitochondrial anion carrier proteins termed uncoupling proteins (UCPs) (Giacomello et al. 2020). Five UCPs have been identified in mammals (UCP1, 2, 3, 4 and 5) which form dimers in the IMM to facilitate proton reflux into the matrix (Krauss et al. 2005), leading to reduced oxidative phosphorylation and concomitant ROS generation (Nègre-Salvayre et al. 1997). In reducing membrane potential, electron movement during the ETC is accelerated and the probability of direct electron transfer to O^2 molecules is reduced (R. Z. Zhao, Jiang, Zhang, Z. Bin Yu 2019), termed 'uncoupling to survive' (Brand 2000). UCP2 demonstrates near ubiquitous expression in human cell types and its expression has been associated with increased resistance to apoptosis induced by gemcitabine (Dalla Pozza et al. 2012), hypoxia/reoxygenation (Collins et al. 2005) and UV radiation (Derdak et al. 2008). Their activity may be further modulated by the presence of cellular metabolites, with purine nucleotides (ATP, ADP, GTP and GDP) inhibiting UCP function while fatty acids and ROS function as activators (Ramsden et al. 2012; Xia et al. 2008; Shabalina et al. 2004). Mitochondrial membrane potential may therefore support and be supported by the wider metabolic profile of the cell. Indeed, several cancer types demonstrate elevated rates of fatty acid oxidation (Harper et al. 2002), which may in turn support the Warburg effect, reduce oxidative stress and facilitate therapeutic resistance through UCP activity.

1.8 DNA Damage

DNA breaks or mutations may incur severe biological alterations that result in diminished cell viability and potentiate neoplastic behaviours. The maintenance of genomic integrity is therefore vital to its continued function and the wider survival

of multicellular organisms as a whole. However, DNA is continually assailed by genotoxic stimuli and concomitant DNA damage, which must be managed to maintain genetic integrity. As a consequence, numerous cell response pathways have been identified, tasked with repairing the afflicted damage or initiating cell death pathways (Hoeijmakers 2009).

1.8.1 Internal sources of DNA damage

Sources of genomic damage may be both internal and external in origin. During DNA replication, spontaneous base deamination and oxidative damage are all endogenous sources of potential DNA alterations the cell must contend with in the preservation of genomic integrity. Despite the high fidelity of replicative polymerases (δ and ε), single base insertions, deletion errors and substitutions occur at a rate of 10^{-6} – 10^{-8} per cell per generation (Kunkel 2009), whilst the spontaneous transformation of cytosine, adenine, and guanine may produce uracil, hypoxanthine, and xanthine upon loss of their exocyclic amine respectively. Reactive oxygen species (ROS), such as hydrogen peroxide, superoxide radicals and hydroxyl radicals, are a normal by-product of the electron transport chain (ETC), catabolic oxidases, peroxisomal metabolism, and anabolic processes (Henle, Linn 1997; Burton E. Tropp 2012) and play important roles in redox signalling and antimicrobial responses. The isolation of respiration to the mitochondria serves to confine ROS production to this specialised compartment whilst antioxidants may quench excess ROS. However, their high reactivity additionally poses a threat to nucleic material and dysregulation of ROS production and management may consequently incur genomic damage. Electrophilic radicals produced by a Fenton's reaction are the most reactive and damage DNA bases by attacking the sugar residue, hydrogen atom abstraction, or adding to their double bonds (Winterbourn 2008). Indeed, ROS radicals cause an estimated 2,300 single strand breaks per cell per hour through damage to the DNA backbone (Chatterjee, Walker 2017a).

1.8.2 Ionizing radiation

Exogenous sources of damage may occur naturally or be utilised as a targeted therapy strategy and include ionizing radiation (IR), ultraviolet (UV) radiation and alkylating agents. Sources of IR are diverse and range from radioactive material found naturally in the environment to specialised medical equipment. Types of IR include alpha, beta, gamma, neutrons, and X-rays, and may be classified by either producing direct or indirect effects in addition to their ionizing density (linear energy transfer (LET)). IR is capable of producing both single and double strand breaks as well as loss of sugar bases resulting in single stranded gaps. This spectrum of chemically different DNA lesions gives rise to sites of complex DNA alterations that pose a particular challenge for the cellular DNA repair machinery. Indeed, IR may produce closely located single-strand breaks (SSBs) on opposite strands and may themselves generate DSBs as the cell attempts to repair the damage (Pfeiffer et al. 2000). Indirect means of DNA damage include the production of hydroxyl radicals through water radiolysis (Desouky et al. 2015), which accounts for approximately 65% of IR induced DNA damage (Vignard et al. 2013). Consequently, IR produces a range of DNA lesions with a similar profile to ROS-mediated DNA damage (Chatterjee, Walker 2017a).

1.8.3 Ultraviolet radiation

UV radiation may be classified into three categories based on their wavelength: UV-C (190-290 nm), UV-B (290-320), and UV-A (320-400 nm). Of these, UV-C poses the greatest threat to DNA, which demonstrates maximal absorption of UV radiation in this range (260 nm). Whilst the quantum energies of UV radiation are insufficient to cause ionization, UV radiation may be either directly absorbed by matter, resulting in their photochemical alteration, or energy may be indirectly transferred by nearby

photosensitizers. DNA damage is primarily mediated by covalent links formed between adjacent pyrimidines, resulting in cyclobutene pyrimidine dimers (CPDs), pyrimidine (6 - 4) pyrimidone photoproducts ((6 – 4) PPs) and, to a lesser extent, pyrimidine hydrate, thymine glycols, and dipurine adducts (Chatterjee, Walker 2017a). Formation of CPDs and (6 – 4) PPs alter the DNA helix and require specialised polymerases to replicate past DNA lesions. Known as translesion synthesis (TLS), polymerases, such as REV1, can replicate opposite aberrant DNA structures, albeit with a lower fidelity, and give rise to genomic mutations. Although the ozone layer filters out most UV-C radiation (Davies 1995), this form of radiation is commonly used in a laboratory setting. However, UV-B and UV-A wavelengths are also physiologically relevant and more abundant in the environment, similarly producing DNA lesions through pyrimidine dimers, DNA adducts, DNA cross-links and strand breakages, although less efficiently (Chatterjee, Walker 2017a).

1.8.4 Topoisomerase inhibitors

Topoisomerase inhibitors aim to cripple the cellular mechanisms responsible for relieving superhelical tensions that form as a result of DNA replication and transcription. DNA supercoils, knots and interwound duplexes require DNA strands to be unlinked through strand cleavage performed by a class of proteins called topoisomerases (Schoeffler, Berger 2008). These proteins create transient DNA breaks, relinquishing the strict spatial confinements imposed by the double-helical structure and enabling greater reorganisation of the DNA strands to resolve wider topological tensions. DNA breaks are generated through nucleophilic attack of tyrosine residues within the phosphodiester backbone and occur either on a single strand, as generated by type I topoisomerases, or on both strands to create a double-strand break, as generated by type II topoisomerases (Schoeffler, Berger 2008). DNA topoisomerase II (TOP2) is capable of resolving larger topological issues by allowing for the complete passage of an unbroken DNA strand through

this transient double-strand break. Notably, TOP2 also facilitates the re-ligation of this break to reinstate DNA integrity and function(Nitiss 2009a). The generation and subsequent repair of double-strand breaks and the important role of TOP2 activity in the maintenance of genomic integrity has highlighted this enzyme as an attractive target in the development of cancer therapeutics. Indeed, a range of TOP2 inhibitors have been generated with potent anti-cancer activity. These may be broadly divided into two classes: catalytic inhibitors, which specifically function by repressing the catalytic activity of TOP2 without influencing the level of TOP2 covalent complexes, and TOP2 poisons, which conversely generate DNA lesions and inhibit TOP2 disassociation (Nitiss 2009b). Etoposide, a commonly used TOP2 poison and chemotherapeutic, inhibits the ligation of DNA strands following double-strand cleavage, thereby generating highly toxic DNA lesions. Etoposide is also thought to trap TOP2 as a complex covalently bound to DNA (Nitiss 2009a), which further its cytotoxicity by impeding transcription. Doxorubicin functions as a TOP2 poison in a similar fashion but exhibits the additional effect of inflicting chromatin damage via histone eviction (Pang, Qiao, Janssen, Velds, Groothuis, Kerkhoven, Nieuwland, Ovaa, Rottenberg, van Tellingen, et al. 2013). As a consequence, doxorubicin demonstrates downstream epigenomic and transcriptional alterations as well as significant attenuation of DNA repair (Qiao et al. 2020), resulting from H2AX eviction that precludes ATM-mediated phosphorylation as an early DDR step (Pang, Qiao, Janssen, Velds, Groothuis, Kerkhoven, Nieuwland, Ovaa, Rottenberg, van Tellingen, et al. 2013).

1.8.5 Bleomycin antibiotics

The bleomycin family of antibiotics, of which zeocin is a member, has been approved for the treatment of numerous cancer types since its FDA approval in 1975(JM, SD 1979), including squamous cell carcinomas, malignant lymphomas and germinal cell tumours (Brandt, Gerriets 2022). It has since fallen out of favour

for its high risk of adverse effects and has been replaced increasingly with newer chemotherapy regimens. However, bleomycin agents still utilised in biological research for their ability to mimic the genotoxic effects of radiation treatment (Povirk, Finley Austin 1991). Bleomycin primarily induces oxidative DNA damage through the formation of metallobleomycin complexes with redox-active metal ions such as iron and copper (Petering et al. 1990). These complexes subsequently generate ROS and consequent SSBs and DSBs between 3'-4' deoxyribose bonds (Brandt, Gerriets 2022). Bleomycin further induces G2 cell cycle arrest as a result of free base propenals, particularly thymine, generated from DNA damage, as well as downstream chromosomal aberrations, chromatid breaks and translocations (Murray et al. 2018; Brandt, Gerriets 2022). In addition to DNA repair pathways, bleomycin resistance may be mediated by the expression of bleomycin hydrolase, a cysteine proteinase that compromises the affinity of bleomycin for metal ions.

1.9 DNA Damage Repair

Before repair of DNA damage can occur, lesions must first be recognised. This is a challenging undertaking as DNA lesions typically exist in condensed complexes with proteins and chromatin in a vast pool of otherwise undamaged DNA (Sancar et al. 2004). More subtle aberrations may go unnoticed and only be recognised during the comprehensive assessment of base-pairs performed during replication (Tercero et al. 2003). Indeed, studies using low level UV irradiation and MMS to induce DNA damage have demonstrated a reliance on S-phase for checkpoint activation(Stokes et al. 2002; Callegari et al. 2010; Ward et al. 2004), evidencing replication forks as an important and highly sensitive detector of DNA lesions. However, high level UV and MMS treatments may activate the DNA damage checkpoint outside of S phase through nucleotide excision repair (NER) and base excision repair (BER) repair pathways respectively.

1.9.1 Base excision repair (BER)

Repair of single base damage without significant distortion of the alpha helix structure is carried out by BER (Dianov, Hü Bscher n.d.). Principally conducted during the G_1 phase, BER relies on chromatin remodelling at the site of damage before recognition by a DNA glycosylase (Odell et al. 2013), which serves to remove damaged nitrogenous bases whilst leaving the DNA backbone intact. Creation of abasic sites by monofunctional DNA glycosylases leads to short-patch-repair. This involves the creation of a nick in the phosphodiester backbone by AP endonuclease APE1 in preparation of gap tailoring and complementary base insertion by DNA polymerase POL β. Finally, the backbone nick is sealed and repair is completed by the action of DNA ligase LIG1 or a complex of LIG3 and XRCC1 (Almeida, Sobol 2007). In the case of bifunctional glycosylases, which also demonstrate β-lyase activity, long patch repair mechanisms are employed. This similarly involves excision of the base by the glycosylase before tailoring of the repair gap by APE1. In proliferating cells, POL δ or ε synthesize in a strand-displacement manner whilst POL β mediates this role in non-proliferating cells. The resultant flap is removed by flap endonuclease before ligation of the backbone by LIG1 (Almeida, Sobol 2007).

1.9.2 Nucleotide excision repair (NER)

Bulky lesions, such as cyclobutene pyrimidine dimers (CPDs) and (6 – 4) PPs induced by UV-C irradiation, produce distortions in the DNA helix that are recognised and repaired by NER machinery. Global genome NER (GG-NER) occurs in both transcribed and untranscribed DNA strands and involves recognition of transient ssDNA produced as a result of failed base pairing at the site of DNA damage by a complex of Xeroderma Pigmentosum, complementation group C (XPC), Centrin 2 (CENT2), and UV excision repair protein Radiation sensitive 23B (RAD23B) (Nishi et al. 2005). For UV-mediated CPDs, the ultraviolet-damaged DNA damage-binding protein (UV-DDB) complex binds to the DNA lesion and provide a platform for XPC binding followed by the transcription initiation factor II H (TFIIH) complex (Scrima et

al. 2008). TFIIH, a bifunctional enzyme with roles in both transcription and NER, opens the DNA double helix through the helicase activity of XPD and XPB subunits and facilitates subsequent nucleotide excision (Compe, Egly 2012). XPF-ERCC1 and XPG coordinate to perform dual excision of the DNA strand at short distances away from the DNA lesion. Gap filling and synthesis is carried out by proliferating cell nuclear antigen (PCNA) and XPG with concomitant polymerase activity provided by either POL ε in non-proliferating cells or POL δ and κ in replicating cells. Finally, DNA ligase LIG1 or the XRCC1-LIG3 complex repairs nicks in the DNA backbone (Ogi et al. 2010).

A second NER pathway, termed transcription coupled NER (TC-NER), occurs exclusively in transcriptionally active regions of DNA and demonstrates quicker lesion repair. TC-NER differs from GG-NER in its initiating step, in which stalling of RNA polymerase by DNA distortions function as a recognition signal. This precipitates recruitment of TC-NER-specific proteins Cockayne syndrome WV repeat protein A (CSA) and Cockayne syndrome protein B (CSB) (Fousteri et al. 2006). Together these serve as a platform for assembly of TC-NER associated factors, such as TC-NER-specific protein UV-stimulated scaffold protein A (UVSSA) and ubiquitin-specific-processing protease 7 (USP7) (Fousteri, Mullenders 2008). The CSA-CSB complex reverse translocates the RNA polymerase to enable TFIIH recruitment and subsequent repair of the DNA lesion in a similar fashion to GG-NER (Fousteri, Mullenders 2008).

1.9.3 Mismatch repair (MMR)

Following DNA replication, the MMR pathway repairs mismatched base pairs and insertion-deletion loops (IDLs) to increase the replicative fidelity of the synthesised DNA 100-fold (Arana, Kunkel 2010). MMR has been additionally implicated in numerous biological processes, including mitotic recombination, DNA-damage signalling, and apoptosis. MutSα heterodimer (MutS homolog (MSH) 6/MSH6)

recognises base mismatches and short nucleotide IDLs, with the MutSβ heterodimer (MSH2/MSH3) recognising large IDLs. Subsequently, the MutLα heterodimer (MLH1/PMS2) is recruited to the lesion and has the necessary endonuclease capabilities for 3′-nick directed excision. During 3′-nick directed MMR, PCNA is loaded onto the heteroduplex DNA through RFC and, together with MutSα, activates MutLα to produce a 3′ incision necessary for exonulease 1 (EXO1) activity and subsequent removal of a DNA section containing the lesion. POL δ, RFC, HMGB1, and LIG1 may finalise the synthesis of complementary DNA and ligation of the corrected DNA strand(Kadyrova, Kadyrov 2016). Inherent 3′ to 5′ exonuclease activity of POL δ may additionally be utilised for 5′-nick directed excision where the MutLa heterodimer is not able(Kadyrova, Kadyrov 2016).

1.9.4 Single stranded break repair (SSBR)

Single strand breaks (SSBs) are the most common DNA lesion and describe discontinuities in a single strand on the DNA double helix. Commonly accompanied by a loss of nucleotides and termini damage, SSBs may develop as a result of oxidative damage, abasic sites, or TOP1 dysfunction (Chatterjee, Walker 2017). Failure to resolve these breaks may prevent DNA replication and transcription and lead to excessive PARP activation, resulting in ATP, NAD^+, and apoptosis inducing factor (AIF) release and consequent death. Depending on the cause of SSB, three potential pathways are thought to mediate SSBR. Termed long patch SSBR, PARP1 rapidly detects and binds to SSBs where it undergoes cyclical poly (ADP) ribosylation, resulting in protein activation. PARP1 then aids in the recruitment and stabilization of numerous SSBR components at the site of damage, such as XRCC1 (Ray Chaudhuri, Nussenzweig 2017). Subsequently, end-processing is carried out by APE1, polynucleotide kinase 3′-phosphate (PNKP), and aprataxin (APTX) (McKinnon, Caldecott 2007a). Damaged termini are removed by FEN1 with the aid of PARP1 and PCNA, exposing a short ssDNA section for complementary base insertion by a combination of POL β, δ, and ε. Subsequent DNA ligation is then

conducted by LIG1 or LIG3α. Short-patch SSBR similarly involves APE1-mediated recognition and end-processing of SSBs created during BER. Subsequent gap-filling and ligation is carried out by POL β and LIG3 respectively (McKinnon, Caldecott 2007. Finally, repair of TOP1-induced SSBs are performed by the TOP1-SSB pathway. This differs from long patch repair in the actuation of end-processing by tyrosyl-DNA phosphodiesterase 1 (TDP1), which also facilitates removal of TOP1 from the DNA strand (Caldecott 2008). Similar to TC-NER, replication-coupled SSBR (RC-SSBR) operates in tandem with homologous recombination.

1.9.5 Double stranded break repair (DSBR)

Two major pathways maintain the integrity of cellular genomic material in the face of double strand breaks (DSBs): homologous recombination (HR) and non-homologous end joining (NHEJ). Both of these pathways are initiated by the registering of DSBs by chromatin modifications and the concomitant cascade of DSBR events, including ATM activation, H2AX phosphorylation, PARylation, and recruitment of MDC1, 53BP1 and BRCA1 (Liu et al. 2014). Whilst ATR responds to a multitude of genotoxins, including UV (Ünsal-Kaçmaz et al. 2002), etoposide (Zhao, Piwnica-Worms 2001) and hydroxyurea (Lin et al. 2017), Ataxia Telangiectasia Mutated (ATM) is primarily activated in response to double strand breaks (Iyer, Rhind 2017). It has been proposed that ATR activation results from the generation of a common intermediate, with replication protein A (RPA)–single-stranded DNA (ssDNA) complex suggested as a potential candidate (Iyer, Rhind 2017). Whilst polymerases typically stall upon meeting DNA lesions, helicases continue to unwind the proceeding DNA, generating lengths of ssDNA (Byun et al. 2005). RPA proteins then complex with the resultant ssDNA and interact with ATR-interacting protein (ATRIP), necessary for ATR activation (Zou, Elledge 2003). Similarly, double strand breaks and inter-strand crosslinks may produce ssDNA indirectly as a result of lesion processing by the cell. However, subsequent DSB resolution is variable and, in part, determined by the presence of template DNA strands.

1.9.5.1 Homologous recombination

Homologous recombination (HR) facilitates the accurate repair of DSBs through use of homologous DNA sequences present on sister chromatids. However, this requisite restricts HR to stages of the cell cycle in which duplicate chromosomes are present, namely late G2 and S phases. Rather than a tightly prescribed pathway, HR instead refers to a range of related sub-pathways, linked in their utilisation of DNA strand invasion and template-directed DNA repair synthesis. A complex of MRE11, RAD50 and NBS1 (MRN complex) recognises DSBs and recruit ATM and TIP60, leading to ATM and subsequent MDC1 activation(Chatterjee, Walker 2017b). MDC1 functions as a scaffold and mediates recruitment of E3 ligases RNF8 and RNF168 (Altmeyer, Lukas 2013), activity of which ubiquitinates H2AX with the ability to further recruit both BRCA1 and 53BP1. Downstream DSB repair is determined by the prevailing activity of either BRCA1 or 53BP1, leading to either HR or NHEJ mediated repair respectively (Chapman et al. 2012). In the context of S/G2 phases, BRCA1 antagonises and counteracts 53BP1 to instigate CtIP activity and initiate HR (Yu et al. 2006). Strand invasion first requires end resection in a process effected by CtIP facilitated MRN endonuclease activity and further EXO1 or BLM and DNA2 mediated resection, generating 3' overhangs through nucleolytic degradation (Chen et al. 2008; Nimonkar et al. 2011). With the exposure of ssDNA regions, RPA molecules attach to the overhangs and generate nucleoporin filaments with the aid of BRCA2 and PALB2, establishing the necessary protein complexes for strand invasion. Together with RAD54 and RAD54B, the DNA strand invades the template strand, establishing a Holliday junction and priming polymerase-directed synthesis (Mazin et al. 2010). Following reconstitution of the DNA sequence, the Holliday junction is resolved by GEN1 endonuclease and the BLM-TOPOIII-RMI1-RMI2, MUS81-EME1 and SLX1-SLX4 complexes(Chatterjee, Walker 2017c).

1.9.5.2 Non-homologous end joining

Conversely, nonhomologous end joining (NHEJ) is a repair mechanism that functions through-out the cell cycle without a reliance on sister chromatids. Whilst this process restores the structural integrity of the DNA duplex, it fails to replace the DNA sequence with the same fidelity as homogenous recombination (summarised in Fig 1.10). Instead, DNA sensing factors, Ku70 and Ku80, respond to DNA damage within seconds to prevent end resection and recruit other NHEJ members in a process mediated by p53BP1 (Panier, Boulton 2014). These include NHEJ components DNA-PKcs, XRCC4, LIG4, Aprataxin-and-PNK-like factor (APLF) and XRCC4-like factor (XLF) (Chatterjee, Walker 2017c). Rather than a defined pathway that responds to DSBs with the same downstream mechanism, recruitment of NHEJ factors may be graduated and determined by the complexity of damage (Yano, Chen 2008). However, upon its incorporation, DNA-PKcs both autophosphorylates, and phosphorylates proximal factors (Weterings, Chen 2008) and XRCC4 serves as a stabilising scaffold to facilitate recruitment of further components (Andres et al. 2012). Subsequently, DNA end processing leads to resection of naked DNA strands via Artemis, Ku, Aprataxin, APLF, WRN and PNKP activity (Chatterjee, Walker 2017b), leaving DNA gaps to be filled by either POL μ or POL γ in a template-dependent or -independent manner respectively (Roberts et al. 2010; Ramadan et al. 2004). Finally, NHEJ is completed with the ligation of DNA ends by LIG4 (Grawunder et al. 1997).

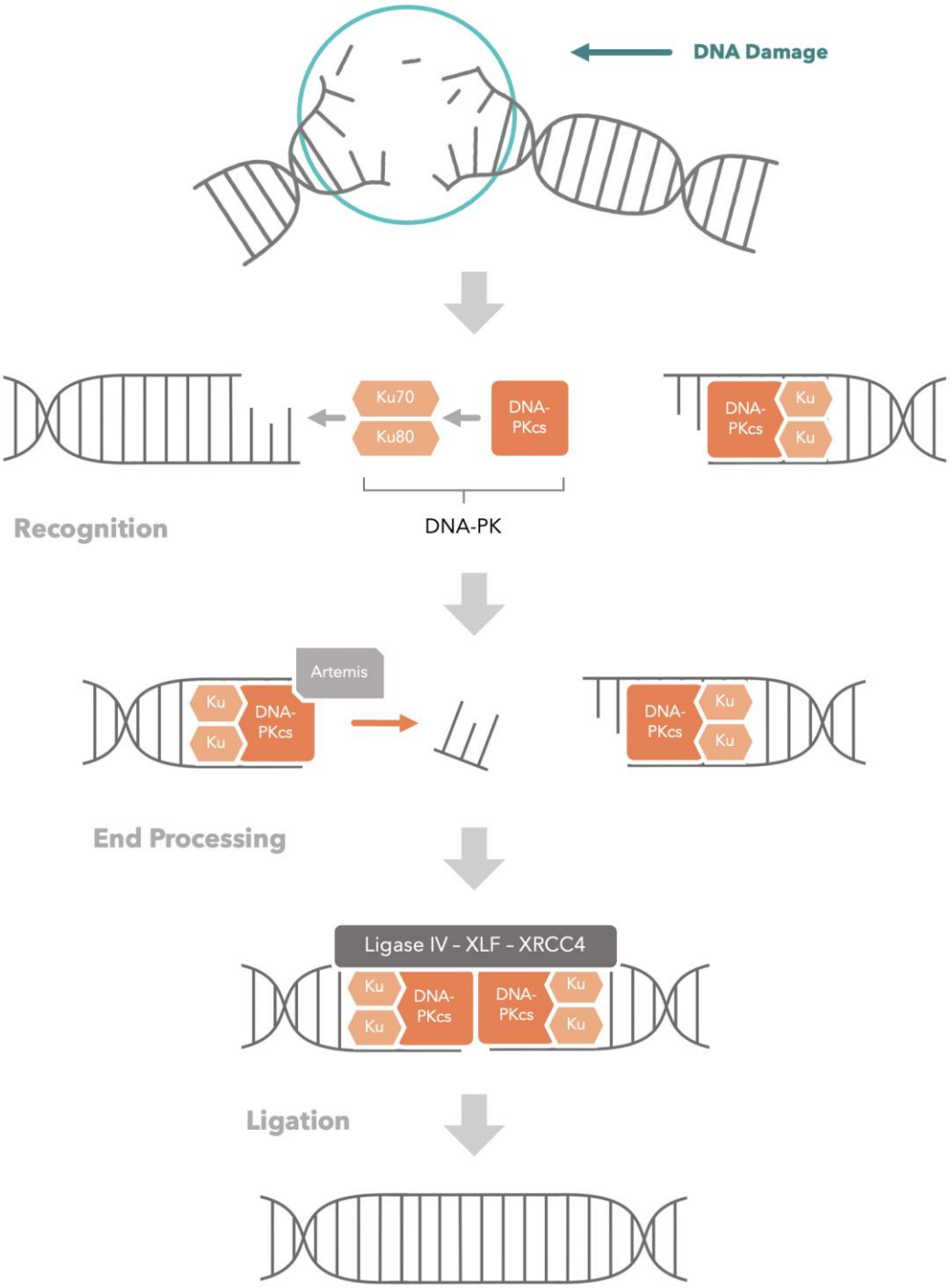


Figure 1.10 – Summary of the Non-homologous end joining repair (NHEJ) pathway.

Double-strand breaks are recognised by the DNA-PK complex with subsequent recruitment of Artemis to mediate end processing. DNA-PK complexes at exposed dsDNA ends further

coordinate with a ligase-XLF-XRCC4 complex to perform ligation, completing DNA repair. Created by author.

1.10 Regulated Cell Death

Excessive or dysregulated cell death is associated with negative survival outcomes. The controlled termination of cells is also a key tool in the development and maintenance of healthy multi-cellular organisms. Unicellular organisms have similarly controlled forms of autonomous cell death, but in this case they facilitate the wider survival of the species (Büttner et al. 2006; Green, Fitzgerald 2016). Regulation of cell-turnover and the removal of abnormal tissue (Soengas et al. 1999) as well as the development of complex biological structures, such as the creation of fingers and toes (Zakeri, Ahuja 1997), is reliant on the induction of cell death pathways. As a consequence, subversion of these processes is crucial to the persistence of aberrant and potentially malignant cell behaviours, as demonstrated in the pathological expansion of cancerous tissue (Hanahan, Weinberg 2011). The survival of multi-cellular organisms is therefore dependent on their capacity to regulate the controlled demise of their cellular constituents.

1.10.1 Apoptosis

Apoptosis describes a morphologically distinct form of cell death, in which controlled and energy-dependent biochemical mechanisms underpin the contained destruction of cellular components (Elmore 2007). This process represents the most well characterised form of programmed cell death (PCD) and differs from the uncontrolled form termed necrosis. By contrast, necrosis is defined as an energy independent process that occurs in response to severe insults, such as radiation, hypoxia and heat, and leads to membrane rupture and consequent expulsion of cellular contents, leading to instigation of inflammatory responses (D'Arcy 2019). Although simplistic, this categorisation of cell death prevailed during

early research, it belies the nuanced complexity of the numerous cell death subroutines understood today. Since the coining of apoptosis in 1972 (Kerr et al. 1972), the field of cell death has developed dramatically and has delineated a range of regulated cell death pathways, including classical apoptotic pathways to the more recent advent of alternative subroutines, such as ferroptosis and parthanatos (Galluzzi et al. 2018a).

1.10.1.1 The Intrinsic Apoptotic Pathway

Intrinsic apoptosis constitutes a central form of PCD in which exposure to microenvironmental perturbations induce profound alterations to mitochondrial ultrastructure and membrane permeability, resulting in the release of apoptogenic factors that precipitate cell demise, as depicted in Fig. 1.11. Such perturbations may include DNA damage, excessive ROS production, ER stress, replication stress and mitotic defects (Galluzzi et al. 2018a). Following induction of the intrinsic pathway, BL2 associated X, apoptosis regulator (BAX) and/or BLC2 antagonist/killer 1 (BAK) function together with BL2 family apoptosis regulator (BOK) to initiate mitochondrial outer membrane permeabilization (MOMP) (Llambi et al. 2016; Luna-Vargas, Chipuk 2016). BAK is constitutively situated within the OMM through interactions with voltage dependent anion channel 2 (VDAC2) (Ma et al. 2014), whereas BAX activity is restricted through its continuous cycling between the OMM and the cytosol, in which it exists in an inactive monomeric or dimeric conformation under physiological conditions (Garner et al. 2016). Cessation of this regulatory shuttling occurs in response to apoptotic stimuli, leading to the accumulation and activation of mitochondrial BAX and BAK pools by pro-apoptotic BH3-only proteins. These include p53-upregulated modulator of apoptosis (PUMA), BCL2-interacting mediator of cell death (BIM) and NOXA, whose activity is tied to transcriptional upregulation or, in the case of BH3 interaction domain death agonist (BID), post-translational activation (Galluzzi et al. 2018a). Transient interactions between these activator proteins and BAK and BAK subsequently initiate a series of conformations

changes that culminate in the assembly of a toroidal lipidic pore that compromises membrane permeability and induces severe mitochondrial segmentation (Aluvila et al. 2014; Salvador-Gallego et al. 2016; Kim et al. 2009). Anti-apoptotic members of the BCL2 family (BCL2, BCL-X_L, MCL1, BCL-W and BFL-1) antagonize this process, primarily through direct binding and concomitant inhibition of the activator proteins (Moldoveanu et al. 2014). Additionally, these pro-survival family members may facilitate cell survival through promotion of bioenergetic metabolism via F_1F_0ATP synthase activity (Alavian et al. 2011), regulation of ER Ca^{2+} levels (Vervliet et al. 2016) and modulation of redox homeostasis (Chen, Pervaiz 2007). Notably, some BH3-only proteins exert pro-apoptotic activity independent of BAK/BAX interaction, namely BCL2 associated agonist of cell death (BAD), Bcl2 modifying factor (BMF) and BCL2 interacting protein (HRK). The crucial role of this apoptotic system has been demonstrated by the profound resistance exhibited by the co-deletion of Bax, Bak1 and Bok in numerous cell types in addition to severe developmental defects (Wei et al. 2001; Ke et al. 2015; Lindsten et al. 2000).

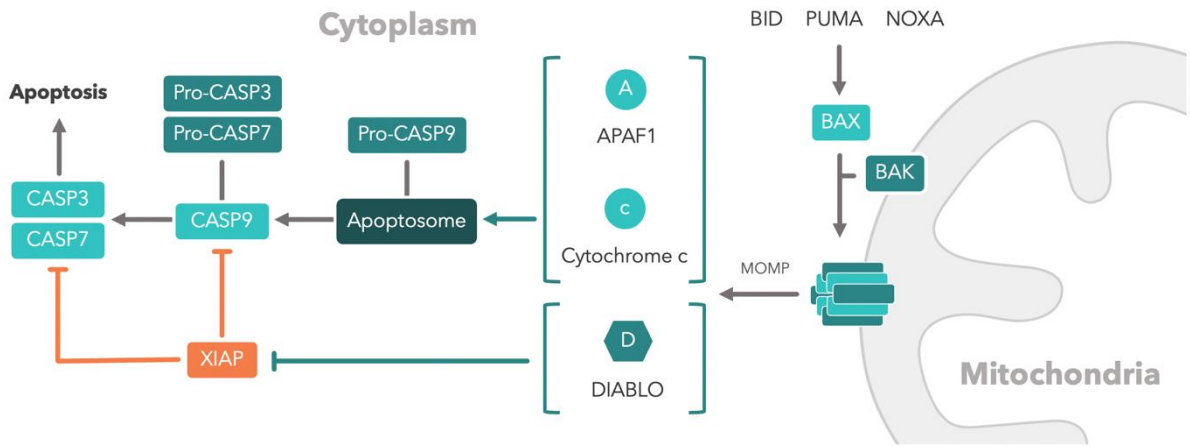


Figure 1.11 – The intrinsic apoptotic pathway. Activation of BAK and BAX leads to the formation of a lipidic pore in the mitochondrial membrane, releasing the pro-apoptotic factors APAF1, cytochrome c and DIABLO. DIABLO inhibits XIAP to prevent its anti-apoptotic activity. PAF1 and cytochrome c assemble with pro-caspase-9 to form the

apoptosome and generate active caspase-9. Caspase-9 mediates the activation of both caspase-3 and -7 and leads to cell destruction via apoptosis. Created by author.

Mitochondrial outer membrane permeabilization (MOMP) serves as the principle step in the intrinsic pathway and irreversibly coordinates the release of apoptogenic factors held within the mitochondrial intermembrane space, including cytochrome c, somatic (CYCS) and diablo IAP-binding mitochondrial protein (DIABLO, also termed second mitochondrial activator of caspases, SMAC). The release of CYCS and SMAC are further facilitated by cristae remodelling (Scorrano et al. 2002). SMAC facilitates apoptosis by relinquishing the inhibitory effects of the inhibitor of apoptosis (IAP) protein family, such as XIAP and c-IAP2 (Du et al. 2000; Salvesen, Duckett 2002). Notably, XIAP is the only identified IAP to demonstrate direct and stable binding with caspase enzymes (Eckelman et al. 2006). C-IAP1 and c-IAP2 actuate caspase inhibition indirectly through upregulation of c-FLIP or downstream activation of TAK1, both serving as potent inhibitors of FADD and CASP8 activity respectively (Silke, Meier 2013; Galluzzi et al. 2018b). Cytosolic CYCS, apoptotic factor activator factor 1 (APAF1) and pro-caspase 9 (CASP9) assemble to form a supramolecular complex that modulates CASP9 autocatalytic activation, termed the "apoptosome" (Li et al. 1997). Activated CASP9 is as an initiator caspase, capable of catalysing the proteolytic cleavage and consequent activation of the executioner caspases, CASP3 and CASP7. In contrast to CASP9, executioner caspases are responsible for the downstream demolition of cellular content(Julien, Wells 2017). Caspase activity is associated with many of the cellular features characteristic of apoptotic cells, including formation of apoptotic bodies (Sebbagh et al. 2001), DNA fragmentation (Nagata 2005) and phosphatidylserine (PS) externalisation (Martin et al. 1996). However, significant evidence suggests their activity is not essential for PCD and that the blocking of post-mitochondrial caspase activity may delay, but not necessarily preclude, cell death (Galluzzi et al. 2015). Rather, alternative cell death pathways may be initiated (Galluzzi et al. 2015; Galluzzi et al. 2018b). It has also

been proposed that MOMP may not universally lead to cell death and that this progression may be reversed in a process termed "anastasis" (Sun et al. 2017).

1.10.1.2 The Extrinsic Apoptotic Pathway

Extrinsic apoptosis (summarised in Fig. 1.12) responds to extracellular factors, leading to activation of death receptors upon cognate ligand binding (Wajant 2002), or in the absence of sufficient ligand interaction in the case of dependence receptors (Gibert, Mehlen 2015). Death receptors include Fas cell surface death receptor (FAS), tumour necrosis factor receptor 1 (TNFR1), TRAIL receptor 1 (TRAILR1) and TRAILR2 with concomitant ligands such as FAS ligand (FASLG) and TRAIL in the case the TRAILRs and FAS receptors respectively. Ligand binding results in stabilisation of the adapter FAS associated via death domain (FADD) interaction with the intracellular death domain (DD) of the receptor. Here, FADD serves as a bridge to promote assembly of the death-inducing signalling complex (DISC), which subsequently operates as a molecular platform to regulate downstream CASP8 and CASP10 activity (Dickens et al. 2012). In this context, FADD facilitates the homodimerisation of CASP8 and its resultant autoproteolytic cleavage and activation. Extrinsic apoptosis can then follow two pathways: in type I cells, such as thymocytes and lymphocytes, CASP8-mediated activation of CASP3 and CASP7 is sufficient to induce PCD and is not contingent on BAX, BAK or BID activity; in type II cells, such as hepatocytes and most cancer cells, PCD additionally require proteolytic cleavage of BID (Barnhart et al. 2003), potentially as a result of XIAP-mediated inhibition of CASP3 and CASP7 activity in these cells (Jost et al. 2009). This truncated form of BID (tBID) translocates to the OMM and serves as an activator of BAX/BAK-dependent MOMP and consequent CASP9-directed PCD (Tan et al. 2016). Following CASP3 and CASP7 activation, extrinsic apoptosis follows the same process of cellular demolition as the intrinsic pathway.

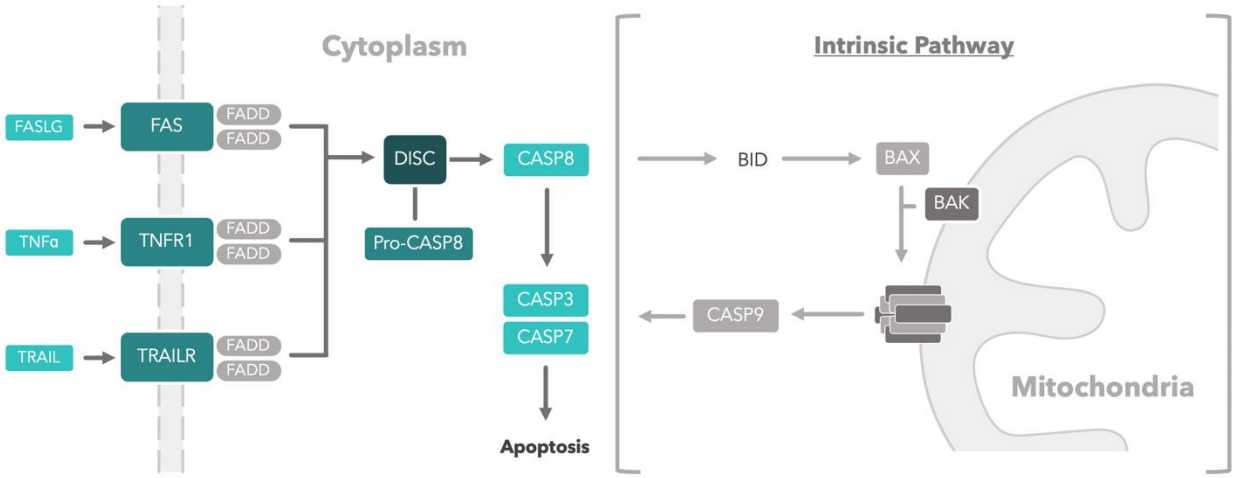


Figure 1.12 – The extrinsic apoptotic pathway. Activation of death receptors (FAS, TNFR1 and TRAILR) leads to assemble of the death-inducing signalling complex (DISC) and activation of caspase-8. Caspase-8 may directly activate the executioner caspases -3 and -7. Additionally, capsase-8 cleaves BID, activating the features of the intrinsic apoptotic pathway to form active caspase-9, which may further process pro-caspase -3 and -7 to their active form to induce apoptosis. Created by author.

1.10.2 Pathanatos

Parthanatos describes a form of RCD in which poly (ADP-ribose) polymerase 1 (PARP1) hyperactivation precipitates cell death as a result of bioenergetic and mitochondrial collapse. Whilst PARP1 functions as an important component of the DDR, parthanatos occurs in response to a range of cell stresses including hypoxia, oxidative stress, and hypoglycaemia in addition to prolonged DNA damage (Fatokun et al. 2014). Bioenergetic deprivation occurs through the inhibitory PARylation of hexokinase 1, a key enzyme involved in cellular glycolysis, and cripples cellular ATP production (Andrabi et al. 2014). Additionally, PARylation of AIFM1 serves as a critical step in pathanatotic cell death by promoting AIFM1 mitochondrial release and subsequent translocation to the nucleus where it regulates DNA fragmentation and chromatin condensation (Wang et al. 2011). Pathanatos may therefore function independently of apoptotic caspases. However,

PARP1 hyperactivation is also associated with poly (ADP-ribose) polymerisation and poly (ADP-risoyl)ation of proteins at the mitochondria, culminating in the collapse of mitochondrial membrane potential and MOMP (Galluzzi et al. 2018a). PARP1 activity may additionally utilise aspects of the intrinsic apoptotic pathway to realise its cytotoxic effects.

1.11 Rationale

Hypoxia constitutes a key aspect of the tumour microenvironment and initiates a broad range of cellular adaptations to facilitate cell survival. These are associated with increased rates of glycolysis, therapeutic resistance and reduced patient outcomes. Likewise, survivin expression has previously been linked to altered cell metabolism and greater resistance to cytotoxic agents. Survivin is thought to be upregulated by hypoxia and demonstrates increased expression in many cancers. However, the role of survivin in mediating hypoxic adaptations and its contribution to the hypoxic tumour phenotype has largely been unexplored.

1.12 Hypothesis and Aims

This study sets out to test the hypothesis that survivin expression increases cancer cell resistance to cytotoxic agents and promotes glycolysis under hypoxic conditions.

In testing this hypothesis, it aims to further explore:

- How survivin positioning within the cell is affected by exposure to low oxygen levels and genotoxic stress.
- The mechanisms mediating its subcellular localisation, in particular nuclear entry.

- The ability of nuclear survivin to promote cell survival (inhibit apoptosis) and whether DNA repair pathways are involved.
- How mitochondrial survivin influences cell metabolism and other mitochondrial activities.

Chapter 2 – Materials and Methods

2.1 Cell Culture

2.1.1 Monolayer cultures

HeLa (cervical cancer), U2OS (osteosarcoma), MCF7 (breast cancer), MRC5 (fibroblasts) and RPE (retinal pigment epithelium) cell cultures were derived from ATCC lines. Cells were cultured in tissue culture flasks at 37°C, 5% CO_2 in a humidified environment, hereon referred to as 'standard conditions'. For exposure to hypoxic conditions, cells were cultured at 37°C, 5% CO_2, 1% O_2 (atmospheric gas was displaced using nitrogen gas) in a humidified O_2 control glove box (COY Lab Products). Culture medium consisted of Dulbecco's Modified Eagle's medium with 4500 mg/L glucose, L-glutamine, sodium pyruvate and sodium bicarbonate (DMEM, D6429) supplemented with 10% foetal calf serum (Sigma, F7524), hereon referred to as 'complete media'. Cell lines stably expressing transfected constructs were maintained in complete media supplemented with 1mM G418 (ACROS organics) to maintain selective pressure.

Cells were passaged at ~90% confluency and harvested with trypsin-EDTA solution (Sigma, T4174) in Dulbecco's phosphate buffered saline (PBS; Sigma, D8537). Cells were diluted 1:10 with fresh complete media and cultured as described.

2.1.2 Spheroid cultures

MRC5 and MCF7 cells were seeded at a density of $2.5x10^6$ cells per 40 ml of complete media supplemented with 20 mM HEPES (pH 7.5) in sealed 50 ml Falcon tubes (Sarstedt). Cultures were incubated at 37°C in an orbital incubator (Sanyo) and rotated at 200 rpm without humidity or CO_2.

2.1.3 Decellularised Matrices

MCF7 cells were seeded at a density of $2.5x10^6$ cells per 6mm diameter matrix disk before incubation in standard conditions.

2.1.4 Resazurin Assay

Medium was aspirated and replaced with 1 volume of 40 μM resazurin in complete media and incubated under standard conditions for 1h, or every 30 min for 4h during metabolic assays. Fluorescence was measured on a spectrophotometer (BMG Labtech, FLUOstar Galaxy) at excitation 530 nm and emission 590 nm to determine the conversion of non-fluorescent resazurin to fluorescent resorufin.

2.1.5 IC50 Drug and UVC Dose Response

Cells were seeded at a density of $1.0x10^4$ cells per well in a CELLSTAR black 96-well polystyrene μClear plate (Greinder, #655090) and left overnight to adhere. Media was aspirated and replaced with fresh medium before relevant drug concentrations were serially diluted in triplicate alongside vehicle controls. For UVC treated cells, triplicate wells were treated with increasing dosages of 254 nm UVC (Vilber Lourmat; BLX254). Cells were incubated in standard conditions for 24h before a resazurin assay was performed (2.1.3). For zeocin treated cells, media was instead aspirated after a 4h incubation period before three 5 min washes were performed in complete media and then a 20h incubation in complete media before a resazurin assay was performed. Blank control samples were subtracted and expressed as a percentage of vehicle only treated samples.

2.1.6 siRNA

Cells were transfected using HiPerFect transfection reagent (Qiagen) according to the manufacturer's instructions. Survivin siRNA (Ambion) or negative control siRNA (Ambion) was diluted in PBS and added to cells at a final concentration of 30 nM.

The transfected cells were grown in antibiotic-free medium for a minimum of 48 hours.

2.2 Biomaterials

2.2.1 Tissue Decellularisation

Resected tissue was harvested immediately post-sacrifice. Tissue was decellularized using an immersion method (Atala A 2002). Briefly, resected tissues were immersed in sterile distilled water (SDW) for 48 h, with the water replaced every 24 h. Cellular debris was removed by 24 h incubation in decellularization buffer [0.05% NH_3OH (v/v), 0.5% Triton X-100 (v/v) dissolved in SDW]. Tissues were then washed in SDW for 24 h at 4°C with stirring. The resultant decellularized tissue was cut into 6mm diameter discs with a steel borer and inserted into 24-well plate inserts featuring 3 µm pores (Greiner Bio One). Tissues were equilibrated in PBS supplemented with 244 µM penicillin and 172 µm streptomycin for 24 h in standard conditions. Subsequently, PBS was replaced with complete media and incubated for 24 h to determine sterility and facilitate media equilibration.

2.3 Flow Cytometry

2.3.1 Caspase 3/7 Assay

Cell media was collected and replaced with PBS to remove residual media. PBS was subsequently collected and attached cells were with harvested with trypsin-EDTA solution in PBS and collected. Collected samples were centrifuged at 300 x g for 5 mins to pellet cells. The supernatant was discarded and cells were resuspended in PBS before being centrifuged again to pellet cells. The supernatant was discarded and cells were resuspended in 1x Assay buffer BA (Merck, #4700-1360) at a final concentration of $0.1x10^5$ – $5x10^5$ cells in 50 µl. Muse Caspase-3/7 Reagent (Merk,

#4700-1505) was dilute 1:8 with 1x PBS (Merk, #4700-1515) before being added to the prepared cell suspension (2.2.1). Samples were incubated at 37°C for 30 mins in a water bath (VWR). Muse 7-AAD Reagent (Merck, #4700-1510) was prepared by adding 2 µl of reagent to 148 µl of 1x Assay Buffer BA. 150 µl of prepared 7-AAD solution was added to each cell suspension sample and mixed thoroughly before being analysed by a Guava Muse Cell Analyzer (Merck, #0500-3115). 2000 events were measured and detection thresholds were set as recommended by the manufacturer.

2.3.2 Cell Cycle Assay

Cell media was aspirated and cell were washed with PBS before being harvested with trypsin-EDTA solution in PBS. Samples were centrifuged at 300 x g for 5 mins at 4°C to pellet cells. Pellets were washed in PBS and resuspended in 200 µl of PBS. The cell suspension was slowly mixed with 1 ml of ice cold 70% ethanol and stored at -20°C overnight. Subsequently, samples were centrifuged at 300 x g for 5min and washed once with PBS. Samples were resuspended in 200 µl Muse Cell Cycle reagent and incubated for 30 min at room temperature in the dark. Samples were thoroughly mixed before being analysed by a Guava Muse Cell Analyzer (Merck, #0500-3115). 2000 events were measured and detection thresholds were set as recommended by the manufacturer.

2.4 Molecular Biology

During all stages, filtered pipette tips (Sarstedt) and diethylpyrocarbonate (DEPC) treated buffers were used.

2.4.1 Preparation of RNA Extracts

$7x10^6$ cells at 80% confluency were scraped into 500ul of media before being lysed through a 5 min incubation at room temperature with 1 ml of TRI-reagent. 200 µl of

1-bromo-3-chloropropane [BCP; 11.76% (v/v) in TRI-reagent and complete media] was added to samples and mixed by inversion before a 3 min incubation at room temperature to separate RNA from DNA and protein/lipids. Phase separation was performed by centrifugation at 10,000 x g for 15 min at 4°C. The upper aqueous phase was collected and incubated at -20°C overnight in an isopropanol solution [256 mM sodium acetate pH 4, 36% isopropanol (v/v)]. Extracted RNA was precipitated by centrifugation at 17,000 x g for 15 min at 4°C and washed in 70% ethanol before further centrifugation at 17,000 x g for 15 min at 4°C. Residual DNA was removed by treatment with RNase-free DNase I (Qiagen, Cat No. 79254) as per the manufacturer's instructions. RNA was isolated by a 3 min incubation at room temperature with phenol-chloroform-isoamyl-alcohol [50% pheno-chloroform-isoamy-alcohol (v/v) 125:24:1] in dH_2O. Samples were centrifuged at 11,000 x g for 9 min at 12°C and the upper aqueous phase was collected. Extracted RNA was precipitated in ethanol solution [323 mM sodium acetate pH 5.2, 65% ethanol (v/v)] before being centrifuged at 17,000 x g for 15 min at 4°C to pellet RNA. Pellets were washed in 70% ethanol, centrifuged at 17,000 x g for 15 min at 4°C and dissolved in dH_2O before the final RNA concentration was determined by spectrophotometry (Nanodrop 2000, Thermo Scientific).

2.4.2 cDNA Synthesis

Reverse transcription of 1 µg of RNA was performed using iScript cDNA Synthesis Kit (Bio-Rad) according the manufacturer's instructions. Samples were run in duplicate with one reaction containing the complete reaction mixture (RT+) and the second lacking the reverse transcription enzyme (RT-). The resultant cDNA was stored at -20°C.

2.4.3 Primer Design

Primers were designed using the Primer-BLAST (Ye et al. 2012) online resource for the relevant genes listed in Table 2.1C. Primer-Blast default settings were modified

to require primer pairs to span at least one intron with an optimal T_m of 60°C and for primer to be situated on a exon-exon junction.

2.4.4 Primer Optimisation

Optimisation of RT-PCR-primer annealing temperature was performed using REDTaq polymerase (Table 2.1). All primers were designed with an optimum annealing temperature of 60°C and were tested at 2°C intervals between 56 and 64°C (Bio-Rad, T100 Thermal Cycler).

A

Constituent	Volume (µl)	Final Concentration
10X REDTaq buffer	2	1X
REDTaq Polymerase	1	0.05 U/µl
Forward Primer	0.5	250 nM
Reverse Primer	0.5	250 nM
dNTPs	0.5	250 µM
Template	1	500 pg/µl
ddH_2O	14.5	N/A

B

Step	1	2	3	4	5	6	7
Temperature (°C)	95	95	Tm	72	Return to 2	72	12
Time (s)	180	30	30	60	X39	300	-

C

Gene		Sequence	Designed by:
TBP	Forward	GTGGGGAGCTGTGATGTGAA	James F.E. Grey
	Reverse	ACGTCGTCTTCCTGAATCCC	

ACTB	Forward	GCAGAAAACAAGATGAGATTGGC	James F.E. Grey
	Reverse	TGTGAACTTTGGGGGATGCT	
TUBB	Forward	ACTTTGTATTTGGTCAGTCT	James F.E. Grey
	Reverse	TTGCTGATAAGGAGAGTGCCC	
BIRC5	Forward	AGGACCACCGCATCTCTACA	James F.E. Grey
	Reverse	TATGTTCCTCTATGGGGTCGT	
HIF1a	Forward	CATAAAGTCTGCAACATGGAAGGT	(Han et al. 2019)
	Reverse	ATTTGATGGGTGAGGAATGGGTT	
VEGF	Forward	CGAAGTGGTGAAGTTCATGG	(Mak et al. 2010)
	Reverse	GTACTCGATCTCATCAGGGT	
XIAP	Forward	TGCTTTAGGTGAAGGTGATAAAG	Isaac Atakpa
	Reverse	CAGATATTTGCACCCTGGATAC	
P53	Forward	GGGATGTTTGGGAGATGTAAG	(Yuan et al. 2014)
	Reverse	CAGATATGGGCCTTGAAGTTAG	
AIFM1	Forward	GTCTGCGTAATGTGCGTGTG	Amelia R. Townley
	Reverse	TGGAACAAGTTGCCTGGGAG	
GLUT1	Forward	CCTTCACTGTCGTGTCGCTGT	Alexander J. Fezovich
	Reverse	AGGACCCACTTCAAAGAAGGC	
CA-IX	Forward	CTGGTGACTCTCGGCTACAGCT	(Loong et al. 2021)
	Reverse	CTAGGATGTCACCAGCAGCCAGG	
LDHA	Forward	GCCCGACGTGCATTCCC	(Liu et al. 2003)
	Reverse	CAAGTTCATCTGCCAAGTCCTTC	
PRKAA1	Forward	TGAAACCTGAAAATGTCCTGCTTGA	Alexander J. Fezovich
	Reverse	TGGGCCTGCATACAATCTTCCT	
UCP2	Forward	CCCAGCTCAAGGTCAGGAATGT	Alexander J. Fezovich
	Reverse	TCTGCCGGAATAGGCACCA	
UCP3	Forward	AGCATACACCTCGGGCCATC	Alexander J. Fezovich
	Reverse	TGGCAGGGGAAGTTGTCAGT	

FIS1	Forward	GGAACAGCGGGATTACGTCT	Amelia R. Townley
	Reverse	TGCCCACGAGTCCATCTTTC	
DMN1L	Forward	AGAAAATGGGGTGGAAGCAGA	Amelia R. Townley
	Reverse	AGGCACCTTGGTCATTCCTG	
OPA1	Forward	CGACCCCAATTAAGGACATCC	Amelia R. Townley
	Reverse	TTCCCACACAATGTCAGGCA	
MFN2	Forward	CAGGACTGGTGGAGTCAACA	Amelia R. Townley
	Reverse	AGAGCAGGGACATTGCGTTT	

Table 2.1 – Summary of RT-PCR primer optimisation. **(A)** Stoichiometry of reaction mixture. **(B)** PCR programme used to assess optimisation. **(C)** Primer sequences tested.

2.4.5 Reaction Efficiency

The efficiency of RT-PCR reactions was by calculated through quantitative analysis of the threshold breaking cycle (C_T) for six, threefold serial dilution of template using the same primers with starting concentration 1.25 ng/µl. Samples were run in duplicate alongside water and RT- controls on a RT-PCR thermocycler (7500 Fast Real-Time PCR, Applied Biosciences). The parameters of this reaction are summarised in Table 2.2. A semi-log plot of C_T values against log DNA copy number was used generate a linear standard curve with gradient *m,* in line with the MIQE guidelines (Bustin et al. 2009). Reaction efficiency was calculated with the following equation:

$$Reaction\ Efficiency = 10^{\frac{-1}{m}} - 1$$

A

Constituent	Volume (µl)	Final Concentration
2X iTaq Universal SYBR Green Supermix	10	1X
Forward Primer	0.5	250 nM
Reverse Primer	0.5	250 nM
Template	1	-
ddH_2O	7.5	N/A

B

Step	1	2	3	4	5	6
Temperature (°C)	50	95	95	60	Return to 3	Default melt curve programme
Time (s)	120	60	15	60	X39	300

Table 2.2 – Summary of RT-PCR reaction efficiency. **(A)** Stoichiometry of the reaction mixture. **(B)** Thermocycler programme used to assess reaction efficiency.

2.4.6 RT-PCR

RT-PCR was carried out using iTaq Universal SYBR Green Supermix (Bio-Rad) as per the manufacturer's instructions on a RT-PCR thermocycler (7500 Fast Real-Time PCR, Applied Biosciences). cDNA was used at final concentration of 166.66 pg/µl and data were analysed by the Pfaffl method (Pfaffl 2001) using REST 2009 software (QIAGEN, bootstrap: 10000).

2.4.7 Plasmid Constructs

Construct	Vector	Created by:
GFP	pcDNA3.1(+)	C. Starck
SVN-GFP	pcDNA3.1(+)	S.P. Wheatley
MTS-SVN-GFP	pcDNA3.1(+)	L. Dunajova
SVN-NLS-GFP	pcDNA3.1(+)	R. Tewari
SVN^{1-120}-GFP	pcDNA3.1(+)	R. Tewari
SVN^{S20A}-GFP	pcDNA3.1(+)	R. Tewari
SVN^{S20D}-GFP	pcDNA3.1(+)	R. Tewari
SVN^{T34A}-GFP	pcDNA3.1(+)	R. Tewari
SVN^{T34E}-GFP	pcDNA3.1(+)	R. Tewari
GST	GEX4T1	Amersham
GST-SVN	GEX4T1	S.P. Wheatley
GST-BIR	GEX4T1	S.P. Wheatley

Table 2.3 – Summary of plasmid constructs used.

2.5 Protein Analysis

2.5.1 Preparation of Whole Cell Extracts

Cells were grown to ~80% confluency and harvested by scraping in ice cold PBS. Samples were subsequently centrifuged at 500 x g for 5 min at 4°C and resuspended in Tris-Triton buffer [100 mM NaCl, 10 mM Trisma, 1mM EDTA, 1 mM EGTA, 10% Glycerol (w/v), 1% Triton X-100 (v/v), 0.5% sodium deoxycholate (w/v), 0.1% SDS (W/V)] supplemented with an inhibitor cocktail [2 mM β-glycerophosphate, 1 µg/ml 1:1:1:1 chymostatin : leupeptin : antipain : pepstatin A (CLAP), 100 µm phenylmethylsulphonyl fluoride (PMSF), 20 mM Na_3VO_3, 2 mM $MgCl_2$ and 4 units/ml DNase (Quanta Biosciences)]. Samples were left to lyse for 30

min on ice with agitation before being sonicated at 50 Hz for 10 sec. Final protein concentration was determined by Bradford assay. Samples were then reduced in sample buffer [100 mM β-mercaptoethanol, 50 mM Trisma pH 6.8 with HCl, 10% glycerol (w/v), 2% SDS (w/v), 0.01% bromophenol blue (w/v)] at 95°C for 10 min.

2.5.2 Preparation of Subcellular Fractions

Cells were grown to ~80% confluency and harvested by scraping in ice cold PBS. Cells were pelleted at 500 x g for 5 min at 4°C and the supernatant was discarded. Pellets were resuspended in 1 ml extraction buffer [1.5 mM mannitol, 0.5 mM Sucrose, 10 mM ethylene glycol-bis(β-aminoethyl ether)-N,N,N',N'-tetraacetic acid, 10 mM 4-(2-hydroxythyl)-1-piperanzineethanesulfonic acid (HEPES), pH 7.5] supplemented with inhibitor cocktail [2 mM β-glycerophosphate, 1 µg/ml 1:1:1:1 chymostatin : leupeptin : antipain : pepstatin A (CLAP), 100 µm phenylmethylsulphonyl fluoride (PMSF), 20 mM Na_3VO_3, 2 mM $MgCl_2$ and 4 units/ml DNase (Quanta Biosciences)]. The cell suspension was lysed in a glass homogeniser (Teflon) and a small aliquot was collected, constituting the whole cell extract. The remaining sample was centrifuged at 1000 x g for 5 min at 4°C. The supernatant was collected and contained the cytoplasmic fraction. The pellet constituted the nuclear fraction and was resuspended in wash buffer [1.5 mM $MgCl_2$, 10 mM KCl, 0.5 mM dithiothreitol (DTT), 0.3% NP40 (v/v) and 10 mM HEPES] supplemented with the same inhibitor cocktail and centrifuged at 1,000 x g for 5 min at 4°C. This was step was repeated twice to remove cytoplasmic contamination of the nuclear fraction. Samples were centrifuged at 1,000 x g for 5 min at 4°C and pellets were resuspended in extraction buffer before being sonicated at 50 Hz for 10 sec. Finally, nuclear samples were centrifuged at 18,000g for 15 min at 4°C and the supernatant was collected. The cytoplasmic supernatant collected previously was subsequently centrifuged at 1,000 x g for 5 min at 4°C to remove nuclear contamination and subsequently centrifuged at 10,000 x g to pellet the mitochondria. The supernatant was collected and used as the cytoplasmic fraction. The mitochondrial pellet was

resuspended and centrifuged as before increase fraction purity and finally resuspended in extraction buffer. Final protein concentration was determined by Bradford assay. Samples were then reduced in sample buffer [100 mM β-mercaptoethanol, 50 mM Trisma pH 6.8 with HCl, 10% glycerol (w/v), 2% SDS (w/v), 0.01% bromophenol blue (w/v)] at 95°C for 10 min.

2.5.3 Bradford Assay

2 µl of protein samples were diluted in Bradford reagent (20% v/v) and the Bradford assay was performed as per the manufacturer's instructions, using BSA standards of 1-25 µg/ml to generate a standard curve.

2.5.4 SDS PAGE

Separation of proteins was performed by sodium dodecyl sulphate polyacrylamide gel electrophoresis (SDS PAGE) using 12% polyacrylamide gels [390 mM Trizma pH 8.8 with HCl, 12% acrylamide:bisacrylamide (37.5:1) (v/v), 3.5 mM SDS, 3.4 mM TEMED, 0.42 mM ammonium persulphate]. Prepared samples were loaded into the gel at a typical protein mass of 20 µg per well and run at 200 V in runner buffer [192 mM glycine, 25 mM Trizma, 3.5 mM SDS].

2.5.5 Immunoblotting

Tris-HCl gels were transferred onto nitrocellulose membrane (Amersham Biosciences) at 350 mA for 90 min in transfer buffer [192 mM glycine, 25 mM Trizma, 10% methanol (v/v)]. Membranes were blocked in 5% non-dry milk in tris-buffered saline with Tween-20 [TBST; 150 mM NaCl, 50 mM Trizma, 5% non-fat dried milk (w/v), 0.1% Tween-20 (v/v) pH 7.4 with HCl]. Membranes with rinsed with TBST and incubated in primary antibody at 4°C overnight. Subsequently, membranes were washes three times in TBST for 5 min at room temperature and incubated in an appropriate HRP-conjugated secondary antibody for 1 h. Membranes were washes three times in TBST for 5 min at room temperature and incubated in a 1:1 mix of

ECL reagents (Amersham Biosciences). Membranes were exposed to photographic film (Roche) in the dark for 1, 5, 15 and 30 min. Antibodies used are summarised in table 2.4.

Antigen	Vendor	Buffer	Dilution
β-Actin	MERCK	TBST-5% milk	1:1000
TBP	Bio-Rad	TBST-5% milk	1:1000
VDAC	Abcam	TBST-5% BSA	1:1000
Survivin	Novus Biologicals	TBST-5% milk	1:1000
α-Tubulin	MERCK	TBST-5% milk	1:2000
XIAP	BD Biosciences	TBST-5% milk	1:4000
p53	GeneTex	TBST-5% milk	1:1000

Table 2.4 – Summary of antibodies used in immunofluorescence.

2.5.6 Protein Purification

Relevant plasmid constructs (Table 2.3) were transformed into BL21 (DE3) pLysS cells using a standard heat-shock technique. Cells were plated onto LB agar plates supplemented with ampicillin (100 mg/ml). Starter colonies were grown overnight at 37°C from which a single colony was picked and used to inoculate larger cultures at 37°C until OD_{600}=0.6. Protein expression was induced through the addition of 0.5 mM isoproprl β-d-1-thiogalactopyranoside (IPTG) and 500 μM $ZnCl_2$, and cultures were left rocking (220 rpm) overnight at 20°C. Cells were harvested at 3200 x g for 5 min and washed with TBS before resuspension in TBS supplemented with 2 mM β-mercaptoethanol, 1 μg/ml CLAP, 10 mM $MgCl_2$ and 4 units/ml DNase (Quanta Biosciences). Samples were lysed by sonication and centrifuged at 48,000 x g for 30 min. The supernatant was added to washed Glutathione Sepharose 4B beads (GE Life Sciences, 17075604) for 1 h at 4°C and collected by centrifuging at 300 x g for 5 min and eluting in elution buffer (10 mM reduced glutathione, 50 mM Tris HCl pH

8.0). Glutathione was removed through overnight incubation in wash buffer (50 mM Tris-HCl, 150 mM NaCl) in dialysis tubing.

2.5.7 GST-Pulldown

200 µl washed Glutathione Sepharose beads were bound to 1 mg purified GST-tagged protein and incubated for 1 h at 4°C before being pelleted by centrifugation at 500 x g for 15 min.

Whole cell extracts of interest were prepared using cells grown to ~80% confluency and harvested by scraping in ice cold PBS. Samples were subsequently centrifuged at 500 x g for 5 min at 4°C and resuspended in RIPA Buffer [20 mM Tris-HCl, 137 mM NaCl, 1% Nonidet P-40 (v/v), 10% Glycerol (w/v), 1% sodium deoxycholate (w/v), 0.1% SDS (w/v)] supplemented with an inhibitor cocktail [2 mM β-glycerophosphate, 1 µg/ml CLAP, 100 µm phenylmethylsulphonyl fluoride (PMSF), 20 mM Na_3VO_3, 2 mM $MgCl_2$ and 4 units/ml DNase (Quanta Biosciences)].

Pelleted beads were incubated with whole cell extracts for 2 h at 4°C. Beads were then washed in RIPA wash buffers 1 [50 mM Tris-HCl pH 8.0, 150 mM NaCl and 1% Nonidet P-40 (v/v)] and 2 [50 mM Tris-HCl pH 8.0 and 1% Nonidet P-40 (v/v)] for 15 min, then boiled at 95 °C for 10 min in 2x SDS loading dye.

2.6 Histology

2.6.1 Embedding

Decellularised lung and mammary tissue was fixed in 4% formaldehyde (Thermo Scientific) in PBS for 15 mins at room temperature. All wash step were performed at room temperature. Samples were washed twice in PBS then twice in dH_2O for 20 mins. Subsequently, samples were dehydrated by successive 20 min washes in 70%,

95% and 100% ethanol solutions before three 20 min washes in 100% xylene. Samples were then incubated in 50% paraffin in xylene (v/v) at 64°C for 20 mins before being immersed twice in 100% paraffin at 64°C and finally set in a cassette overnight at room temperature.

2.6.2 Sectioning

Paraffin embedded samples were sectioned using a Leica DSC1 microtome to form 5 µm sections. Slides were prepared by drying overnight at 42°C on a hot-plate (Thermo Scientific) and stored at room temperature.

2.6.3 Immunohistochemistry

Tissue deparaffinisation and hydration was carried out at room temperature. Tissue sections were washed twice in xylene followed by 100% ethanol, 95% ethanol, 70% and twice in dH_2O. Antigen retrieval was performed by microwaving (ProLine, 750W) section in citrate buffer [10 mM tri-sodium citrate dihydrate pH 6 with HCl] and washed three times in TBST for 5 min. Samples were blocked in blocking buffer [10% goat serum, 5% BSA in TBST] for 1 h at room temperature and washed three times in TBST before an overnight incubation with primary antibody at 4°C. Secondary only controls were instead incubated in blocking buffer overnight. Table 2.4 summarises antibody information. Tissue sections were then washed three times in TBST for 5 min before incubation with relevant fluorescent secondary antibodies (1:200 in blocking buffer) for 1 h at room temperature. Samples were counterstained in 1 µg/ml DAPI for 10 min and the then washes three times in TBST. Sections were mounted using Mowiol (Aldrich) mounting media and stored at 4°C.

Antigen	Vendor	Dilution
E-cadherin	Cell Signaling Technology	1:400
Survivin	Novus Biologicals	1:100

Table 2.4 – Summary of antibodies used for immunohistochemistry.

2.7 Microscopy

2.7.1 Live Imaging

$0.5x10^5$ cells were seeded into a well of a live imaging chamber (Ibidi) and incubated overnight under standard conditions. Before imaging, cells were treated with either 1 drop NucBlue (Life Technologies), 200 nM tetramethlrhodamine ethy ester perchlorate (TMRE, AAT Bioquest) or MitoTracker Deep Red (Thermo Fisher Scientific) diluted in complete media. Cells were incubated for 20 mins under standard conditions before replacing the media with imaging media [Pheno Red-free CO_2-independent medium (DMEM, Invitrogen) supplemented with 2 mM L-glutamine and 10% FCS]. Images were acquired on a Zeiss 200M microscope using 63x 20x (0.75 NA, air) magnification for each sample at 37°C. Excitation and emission settings are detailed in Table 2.5.

2.7.2 Fixed Sample Preparation

$1.0x10^5$ cells were seeded onto sterile Poly-L-Lysine (Merck) coated coverslips within 24-well plates (Greiner) and incubated overnight under standard conditions. Unless stated otherwise, all subsequent steps were conducted at room temperature. Samples were fixed with 4% formaldehyde for 10 mins before three 5 min washes in PBS. Samples were permeabilised in PBS containing 0.15% Triton X-100 (v/v) for 10 mins and subsequently blocked in PBA buffer [1% BSA (Merck) (w/v) and 0.1% Azide (Merck) (v/v) in PBS] for 1 hour. Coverslips were washed in PBS before incubation with primary antibody diluted in PBA buffer overnight at 4°C.

Secondary only control samples were instead incubated in PBA buffer overnight. All samples were then washed three times in PBS for 5 min before a 1 h incubation with relevant fluorescent secondary antibodies diluted in blocking buffer. Where appropriate, samples were counterstained in 1 µg/ml DAPI in PBS for 10 min. Finally, samples were washed three times in PBS for 5 min and mounted using Mowiol mounting medium (Aldrich). Images were acquired on a Zeiss 200M microscope using 63x (1.40 NA, oil-immersion) 20x (0.75 NA, air) or 10x (0.3 NA, air) magnification for each sample. Excitation and emission settings are detailed in Table 2.5.

Channel	Excitation (nm)	Emission (nm)
DAPI	390	435
GFP/FITC	475	523
TMRE/Texas Red	546	594
MitoTracker Deep Red	620	700

Table 2.5 – Summary of channel excitation and emission wavelengths.

2.7.3 Image Processing

The minimum signal threshold for channels with fluorescent secondary antibodies were determined by assessing the signal intensity of secondary only controls. Maximum values were determined by assessing images with the greater signal intensity. All images from a linked experiment were processed with the same threshold values using a macro (appendix), described in 5.2.3. Any image analysis data was collated in Microsoft Excel and transferred to GraphPad Prism software.

2.8 Statistical Analyses

All statistical analysis was performed with GraphPad Prism software. Data normality was confirmed by Shapiro-Wilks normality test and variance was assessed by *F*-test of equality of variance.

A summary of the statistical tests used based on the experimental design are given in Table 2.5. ANOVA tests were followed by *post hoc* Tukey's multiple comparisons test or Dunnett's multiple comparisons test depending on whether all samples were compared against each other or against a control sample respectively. Multiple comparisons were corrected using a false discovery rate control by a two-stage linear set-up procedure (Benjamini et al. 2006).

Sample Number	Sample Pairing	Test
2	Paired	N/A
	Unpaired	Unpaired t-test
>2	Independent	One-way ANOVA
	Repeated Measures	Two-way anova

Table 2.6 – Overview of statistical tests used by experimental design.

Chapter 3 – Survivin localisation in response to hypoxic and genotoxic stress

3.1 Overview

3.1.1 Spatial regulation of survivin during interphase

Survivin mediates a host of cellular functions and it is thought these activities are tied to its spatial localisation within the cell. During interphase, survivin resides within the cell cytoplasm and is actively excluded from the nuclear region (Fig. 3.1). This spatial confinement is enforced by CRM1-mediated nuclear export and preferential degradation within the nucleus (Connell et al. 2008). A number of export sequences have been identified within the amino acid sequence; a nonclassical export motif located between aa 119–142 was first proposed as the determinant for CRM1-mediated export (Rodríguez et al. 2002). However, later work demonstrated the ability for survivin constructs lacking this motif to exhibit nuclear export with aa 96-104 (Colnaghi et al. 2006) and the partially overlapping section aa 89-98 (Stauber et al. 2007; Knauer et al. 2006; Knauer et al. 2007) suggested as classical NES sequences. Expanding the amino acid sequence to aa 84-109 was further suggested to encompass a more complete NES, as evidenced by greater cytoplasmic localisation (Engelsma et al. 2007). This centrally located NES site notably exists within the linker region of survivin (aa 90-102), which interfaces with other survivin molecules to form homodimers (Verdecia et al. 2000). In so doing, it was demonstrated that survivin dimerization blocks interactions with CRM1 and thereby reduced nuclear export (Engelsma et al. 2007). Survivin therefore contains two identified NES sequences located in the linker region, which relies on survivin monomerization to enable CRM1 interaction, and the C-terminus.

Despite these regulatory mechanisms, survivin demonstrates nuclear accumulation during late G2 (Jeyaprakash et al. 2007) and in response to genotoxic stress

(Capalbo et al. 2010). Within malignant cells, a nuclear population has also been demonstrated with numerous studies attempting to evaluate the prognostic value of its nuclear-to-cytoplasmic ratio, albeit with inconsistent results (Stauber et al. 2007). Little is however known about the mechanisms mediating its nuclear residency, with some limited data suggesting it is actively transported (Colnaghi et al. 2006). As survivin contains no identified nuclear localisation sequence (NLS) (Villapol et al. 2008), it is possible survivin is reliant on interactions with partner proteins for its import and sustained occupancy within the nucleus. Such interactions may be mediated by post-translational modifications, which have demonstrated profound influences on the cellular activity of survivin (Nogueira-Ferreira et al. 2013; Aspe, Wall 2010). Acetylation at K129 by cAMP response element-binding protein (CBP) promotes survivin dimerization for example and leads to a nuclear accumulation as a result (Wang et al. 2010).

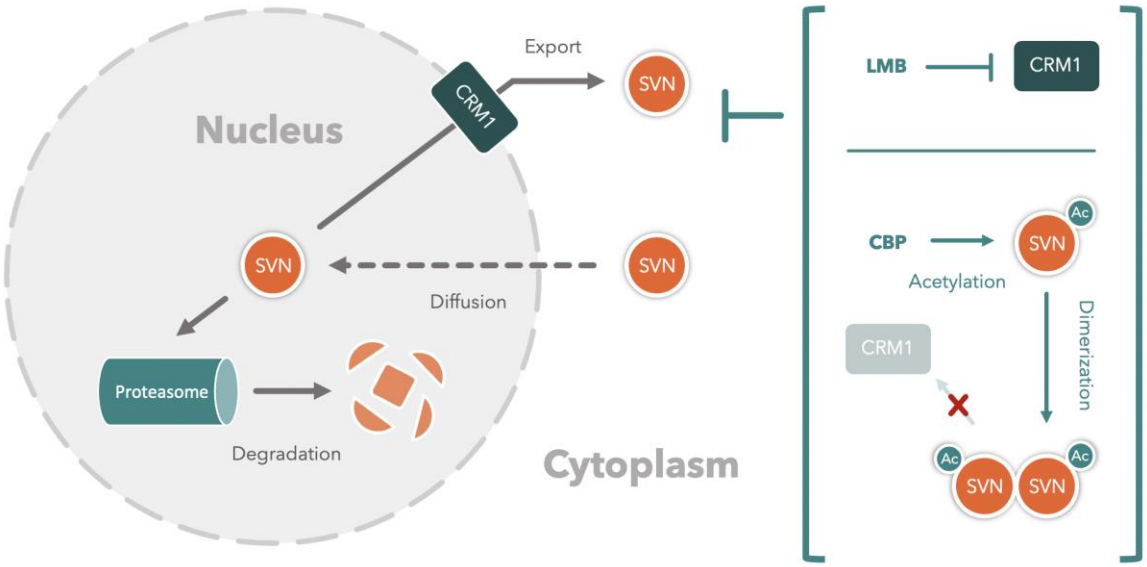


Figure 3.1 – Regulation of the cytoplasmic and nuclear positioning of survivin. Survivin is thought to passively diffusive into the nucleus where it is actively excluded, either by preferential proteasomal degradation or CRM1-mediated export. Nuclear export may

be inhibited either by chemical inhibition of CRM1 by leptomycin B (LMB) or survivin dimerization, preventing CRM1-survivin interaction. Created by author.

To date, few studies have investigated survivin localisation and activity within conditions better reflecting the tumour microenvironment, such as hypoxia, and instead opt for traditional normoxic, monolayer cultures. As a target of the hypoxic regulator, HIF1a, and its virtually universal upregulation within tumours (Velculescu et al. 1999), recapitulating conditions of the TME poses an enticing prospect to uncover further contribution of survivin to both neoplasia and normal cell activity.

3.1.2 Cell Culture Techniques

3.1.2.1 2D culture systems

Traditional cell culture techniques use a two-dimensional (2D) monolayer of cells typically grown on either glass or tissue culture polystyrene plastic to investigate cellular behaviour in vitro. It is the simplicity of this technique and its ease of implementation that has led to its near ubiquitous adoption. An estimated >80% of cancer biologists still rely on this method to obtain in vitro data (Hutmacher 2010). However, while this simplicity enables researchers to take a reductionist approach to investigate complex cellular phenomena, its reliance on culturing cells in a wholly artificial environment restricts its ability to model cellular responses in vivo. In this 2D system where cells are grown as a monolayer, they are forced to assume an apical-basal polarity; are exposed to an equal quantity of nutrients and growth factors from the surrounding medium; experience limited cell-cell and cell-ECM interaction; and are typically cultured as a single, homogeneous population of cells. This presents a striking contrast to the complex and dynamic environmental conditions of the TME. As a result, cells grown in vivo and in vitro often exhibit a large number of differences. These may include morphology, gene and protein expression, differentiation, proliferation and signal transduction (Baker, Chen 2012). This limitation is especially pertinent in the study of cancer, whose pathology

and cellular behaviour is largely influenced by the complexities eschewed in 2D culture systems.

3.1.2.2 3D culture systems

With the aim of achieving more representative cellular responses, many researchers have turned to 3D culture techniques that mimic in vivo growth conditions with greater fidelity. Indeed, transcriptome studies comparing 2D cultures and 3D spheroid cultures have revealed differential expression of multiple genes, including those involved in survival, proliferation and resistance, with 3D cultures displaying greater similarity to tumour tissue in vivo (Chang, Hughes-Fulford 2009; Cody et al. 2008; Gaedtke et al. 2007). A number of 3D culture methods have been developed of varying complexity, ranging from simplistic spheroids cultures to more intricate organ-on-a-chip technologies (Kimura et al. 2018).

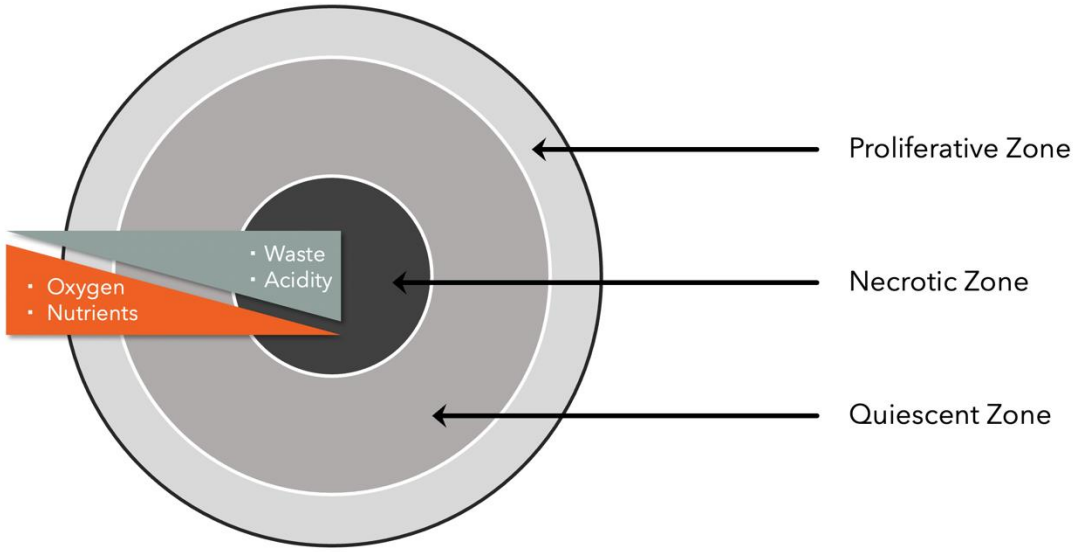


Figure 3.2 – Schematic diagram of multicellular tumour spheroids. The aggregation of cells produces distinct regions within the spheroid based on their proximity to the spheroid-media interface. Gradients are established in factors such as nutrient and oxygen

availability higher at the periphery of the spheroid while waste products and extracellular acidity accumulate at the centre. Created by author.

Multicellular tumour spheroids (MCTS) describe aggregations of tumour cells grown either in suspension or embedded in gels. Advantages of this method include its ability to grow cells within a 3D space, facilitating more natural cell-cell and cell-ECM interactions, and its capacity to establish gradients across the spheroid due the density of cells and its limitations on diffusion. This results in variable levels of oxygen, metabolites, signalling molecules, pH and waste products within the structure, giving rise to regions of cells exhibiting distinct phenotypes (Ware et al. 2016), depicted in Fig. 3.2. While hypoxia studies in 2D cultures succeed in establishing restricted oxygen availability, they fail to recreate these additional physiological perturbations naturally present in solid tumours. Factors such as acidosis have been shown to attenuate hypoxia-induced gene expression (Tang et al. 2012) and are therefore relevant in modelling in vivo responses.

Typically, cells proximal to the spheroid-media interface benefit from higher concentrations of oxygen and nutrients in the media, giving rise to a subpopulation of proliferative cells. However, as diffusion becomes increasingly restricted deeper into the spheroid, a hypoxic environment is established that is characteristically populated by quiescent cells. This simple relationship may be likened to conditions experienced by tumour cells situated at increasing distances from functional blood vessels. Larger spheroids, i.e. greater than 400 μm in diameter, have also been shown to harbour a necrotic core (Mehta et al. 2012) and may serve as a model to investigate similar regions seen in poorly vascularised tumours for example. Hence, this diversity mimics the heterogeneity seen in solid tumours. A number of different methods have been developed to generate MCTS:

Suspension cultures were first utilised in the 1970s to culture neural stem cells and have since become a popular 3D culture technique (Morrison et al. 1987). This method requires a low adhesion environment to deter monolayer formation and promote cell aggregation. Coating tissue culture plates with 1.5% agar is commonly employed to achieve this (Yuhas et al. 1977), producing spheroids of 20 μm – 1 mm in diameter (Lv et al. 2017). Additionally, serum-free may be used to enrich the population of cancer stem cells (CSCs) as highly differentiated cells die off over the course of multiple passages. This enrichment leads to increased drug and radiation resistance and therefore serves as a model to better investigate this resilient subset of tumour cells (Phi et al. 2018). The simple nature of this technique lends itself to high-throughput analysis and is compatible with many tumour cell lines. However, a lack of a defined end-point, limited success of long-term passages and variability in the size of the spheroids generated, producing aggregates with regions of differing proportions, limits the applications of this method.

Rotational bioreactors attempt to create spheroids through the continuous rotation of vessels containing cells in growth media, preventing cell adhesion to the interior and producing uniform distribution of oxygen and nutrients through constant mixing of the media (Kaur et al. 2011). These bioreactors are capable of producing many spheroids, however variability in spheroid size may still occur and potential mechanical damage can be inflicted as cells come into contact with the bioreactor wall. Nonetheless, rotational bioreactors have successfully been used to model various tumour types, including breast adenocarcinoma and hepatocellular carcinoma, and are a popular technique for generating 3D tumour cultures.

Gel embedded cultures aim to restore the cell-ECM interactions not possible with suspension cultures and arguably better recapitulate conditions experienced in vivo (Gill, West 2014). The gel substrate is a hydrophilic polymer with low stiffness, providing architectural support and signalling motifs. A range of materials are used

in gel embedding to act as ECM components including collagen, alginate and the commercially available Matrigel, which is composed of collagen IV, laminin, entactin, perlecan and a range of cytokines and growth factors (Kleinman, Martin 2005). However, the range of novel gel products is constantly expanding, such as the recently produced PathClear Grade Basement Membrane gel (AMS Biotechnology, Ltd., Abington, UK). Gel embedded cultures have demonstrated a number of differences to cells grown as a monolayer. Notably breast cancer cells form spheroids spontaneously in alginate gel and display increased resistance to chemotherapy (Zhang et al. 2008) while CSCs have been successfully enriched using alginate gel beads (Xu et al. 2014). However, gel embedded cultures fail to provide a structural support system that allows cells to grow more diffusely and similarly to cells in vivo. Additionally, more complex gels, such as Matrigel, can be costly and experience variance in their precise composition between batches (Lv et al. 2017).

Scaffold cultures attempt to reproduce the ECM by creating a framework composed of either natural or synthetic polymers to provide a physical support system that more closely resembles that of tissue in vivo. It enables cells to grow with a more faithful spatial distribution and develop appropriate cell-cell and cell-ECM interactions. Consequently, many cell lines exhibit different features when cultured in 3D scaffolds: U87 glioblastoma cells present as flat and fusiform in 2D cultures but form round cells and complex structures with cilia and microvilli in 3D scaffolds (Lv et al. 2016). Similar to other 3D culture systems, breast cancer cells grown with collagen scaffolds exhibit increased expression of CSC-associated properties and demonstrate greater tumorigenicity when transferred to an in vivo model than cells grown as a monolayer (Chen et al. 2012).

The advantages and potential limitations of scaffold systems depend on the type of polymer used. Synthetic polymers, such as polyglycolic acid, polylactic acid,

polyorthoester and their blends, offer researchers greater control over the specific scaffold properties, boasting superior versatility and consistency while typically being easier to process (Lv et al. 2017). However, these polymers offer no bioactivity. Natural polymers on the other hand, such as collagen, chitosan and glycosaminoglycans, offer decreased toxicity and greater biocompatibility. As they are derived from natural polymer materials, they are more limited in their versatility and less consistent in their composition. Moreover, the stability, porosity, tensile strength and degradability of scaffolds must be considered and controlled for, presenting an additional level of complexity.

An alternative approach to generating scaffolds is the use of decellularized tissue. This preserves the ultrastructure and ECM composition of physiological tissue whilst the process of decellularization removes native cells and cell-associated antigens (Elmashhady et al. 2017; Campbell-Ritchie et al. 2018). The resultant scaffold contains similar concentrations of growth factors, glycosaminoglycans (GAG) and basement membrane proteins to tissue in vivo. However, care must be taken during processing of the tissue to maintain its integrity. Treatment with ionic detergents and potent enzymes may breakdown GAGs and collagen and interfere with protein-protein interactions, while treatment with solvents such as ethanol can lead to crosslinking and fixation. It is therefore important to ensure the decellularization process does not alter the mechanical properties of the tissue or its bioactivity. Acquisition of viable biological material may also prove challenging. Tissue should be harvested and processed immediately post-sacrifice to limit its degradation and ensure greater consistency and reproducibility. However, acquiring ethical approval for the sacrifice of animals or use of excised tissue from patients may not be feasible for purposes of many research projects.

3.1.3 Aims

As research into the cellular activity of survivin has primarily been conducted using monolayer cell cultures under normoxic conditions, this chapter aims to assess survivin localisation when exposed to hypoxic stress and further interrogate the molecular mechanisms mediating the nuclear and cytoplasmic pools of survivin. Subsequently, it seeks to established 3D cultures that may further replicate aspects of the TME and understand their impact on survivin activity.

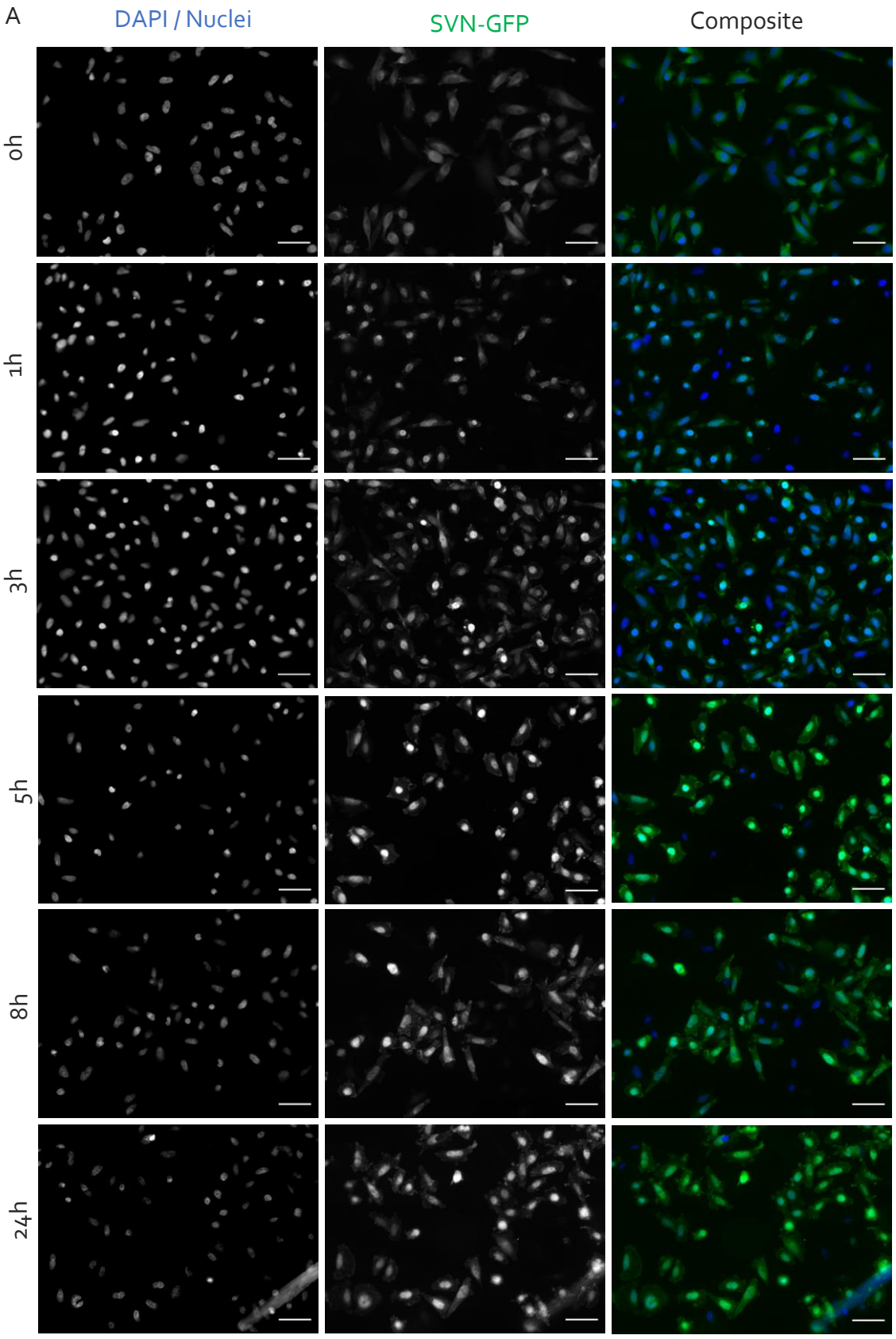
Specifically, this chapter aims to assess whether:

- exposure of cells to hypoxia (1% O_2) leads to an altered localisation and expression profile of survivin within the cell compared to normoxic conditions.
- altering the capacity of survivin constructs to bind with recognised survivin binding partners affects the subcellular localisation of survivin in response to hypoxia and agents that induce apoptosis.
- growing cells in 3D spheroid cultures leads to altered subcellular localisation of survivin compared to monolayer cultures.

3.2 Results

3.2.1 Survivin Localisation under conditions within the TME

To explore the relationship between hypoxia and survivin localisation, the cervical cancer cell line, HeLa, stably expressing a GFP tagged survivin construct (SVN-GFP), was imaged over a 24-hour period following exposure to a hypoxic 1% O_2 environment. Fig. 3.3A demonstrates the cytoplasmic localisation of survivin in interphase cells under normoxic conditions, determined by the reduced GFP signal in areas overlapping DAPI signal. Within 1-hour rapid accumulation of survivin within the nucleus is exhibited, demonstrated by increased GFP signal in the nuclear regions compared to cytoplasmic. Association of survivin with the nucleus was measured by Pearson's correlation coefficient (PCC), which was significantly increased under all hypoxic conditions compared to the normoxic control (Fig. 3.3B).


A
DAPI / Nuclei
SVN-GFP
Composite
0h
1h
3h
5h
8h
24h

B

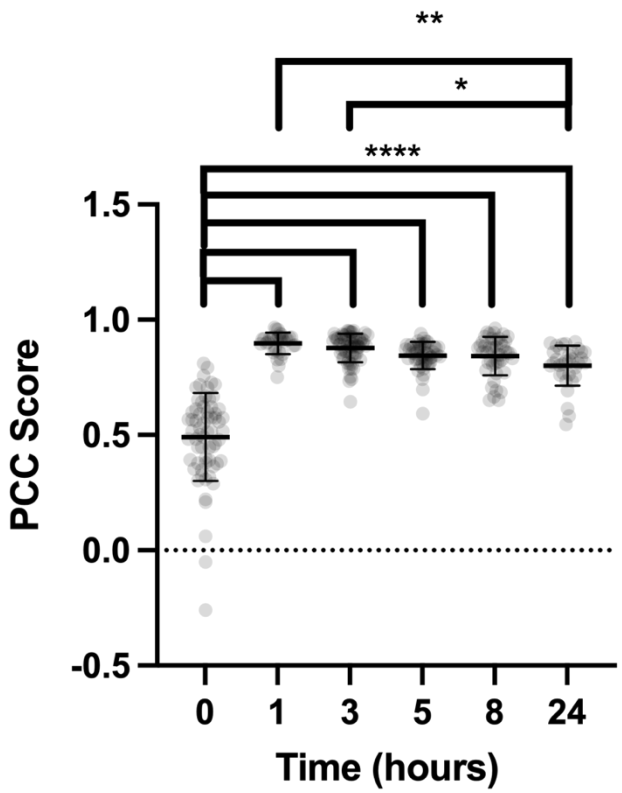


Figure 3.3 - Survivin undergoes rapid nuclear translocation in HeLa cells under hypoxic stress. (A) HeLa cells expressing a survivin-GFP construct were exposed to a hypoxic 1% oxygen environment before being fixed and imaged by fluorescent microscopy at the indicated time points. Samples were stained with DAPI to mark nuclear regions. (Scale bar = 100 μm). **(B)** Co-localisation analysis of GFP signal with DAPI demonstrated significant differences in the Pearson's Correlation Coefficient (PCC) score when exposed to hypoxia. Error bars represent SD of means from three separate experiments. (*, P<0.05; **, P<0.01; ****, P<0.0001; N=293)

A similar experiment was performed in the osteosarcoma cell lines U2OS (Fig. 3.4) and MRC5 (Fig. 3.5) cells to explore this behaviour in other cancerous and non-cancerous cell lines respectively. As with HeLa cells, SVN-GFP signal demonstrated

a cytoplasmic localisation under normoxic conditions but a distinct translocation to the nucleus 24 hours following exposure to hypoxic conditions in both cell lines.

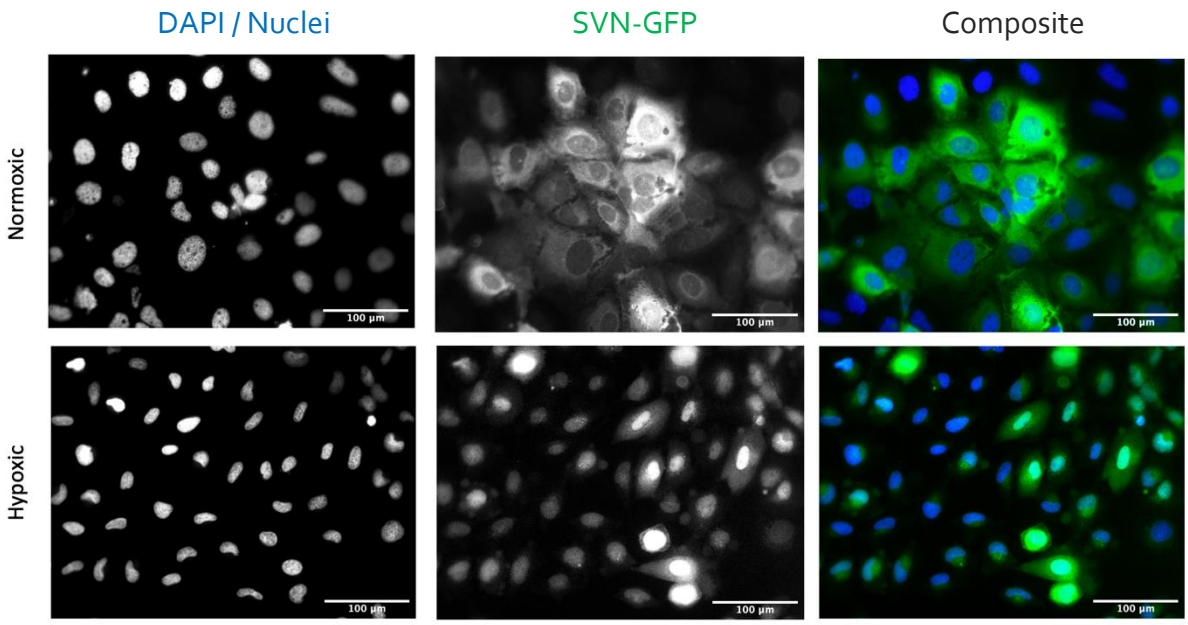


Figure 3.4 - U2OS cells exhibit nuclear localisation of survivin under hypoxia. U2OS cells expressing a survivin-GFP construct demonstrate translocation of survivin to the nucleus following 24-hour exposure to a hypoxic 1% O_2 environment. Samples were fixed, stained with DAPI to mark nuclear regions and subsequently imaged by fluorescent microscopy. Displayed is one representative out of three repeated experiments.

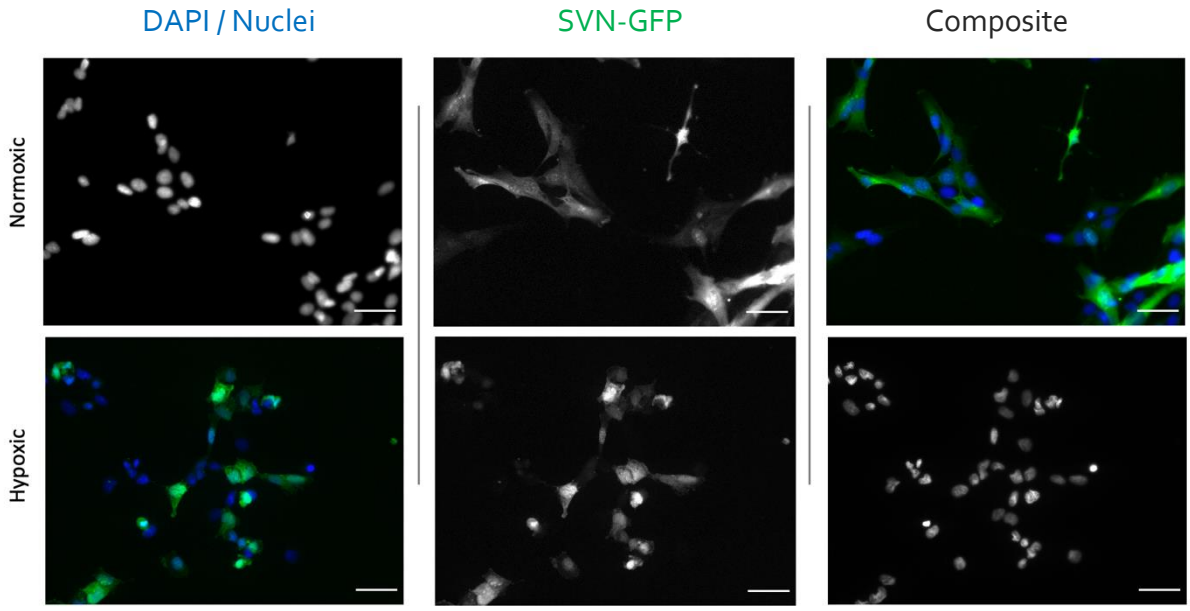


Figure 3.5 - Non-cancerous MRC5 cells demonstrate nuclear accumulation of survivin in response to hypoxic conditions. MRC5 cells expressing a survivin-GFP construct demonstrate translocation of survivin to the nucleus following 24-hour exposure to a 1% O_2 environment. Samples were fixed, stained with DAPI to mark nuclear regions and subsequently imaged by fluorescent microscopy. Displayed is one representative out of three repeated experiments. (Scale bar = 50 μm).

GFP expressing cells were immunoprobed with anti-survivin antibodies to examine the behaviour of the endogenous survivin protein (Fig. 3.6). These cells presented the same nuclear translocation as the SVN-GFP construct, indicating this was a common feature of survivin and not specific to the GFP tagged construct, evidencing SVN-GFP as a valid model of endogenous survivin activity.

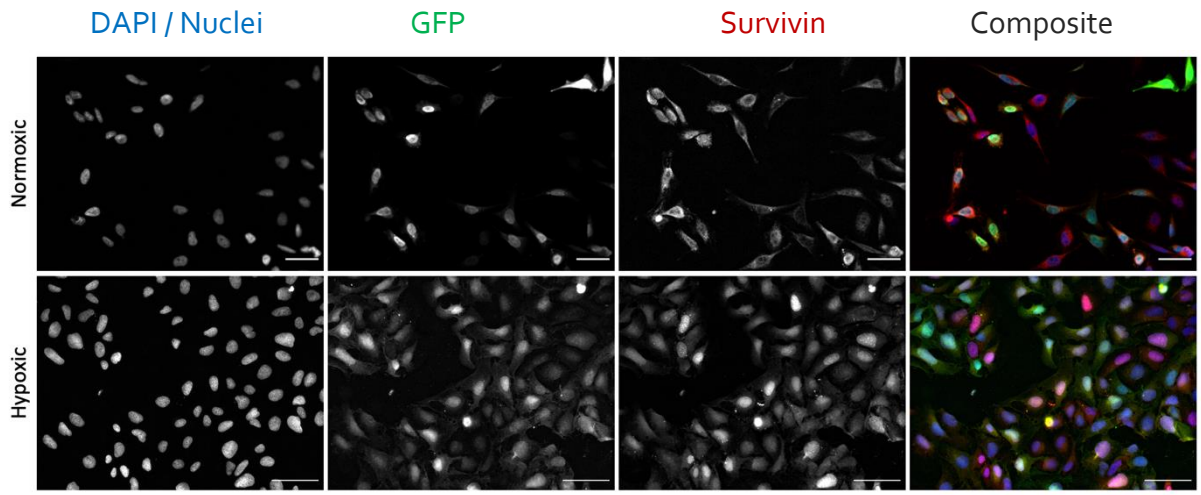


Figure 3.6 - U2OS cells exhibit nuclear localisation of endogenous survivin protein under hypoxia. Fluorescent microscopy analysis of U2OS cells expressing a GFP construct as a control were exposed to a hypoxic 1% O_2 environment for 24 hours. Samples are stained with DAPI to mark nuclear regions and immunoprobed with anti-survivin antibodies. Displayed is one representative out of three repeated experiments. (Scale bar = 50 μm).

Nuclear translocation was confirmed by performing a subcellular fractionation of cells isolated in normoxic and hypoxic conditions (Fig. 3.7A). The purity and protein concentrations of fractions were determined by blotting for specific markers of these fractions. Specifically, TATA-box binding protein (TBP) for nuclear, voltage-dependent anion channel (VDAC) for mitochondrial and α-tubulin for cytoplasmic fractions. Normoxic samples demonstrated strong signal in the whole cell extract (WCE) but only weak signal in the nuclear and mitochondrial extracts. However, the hypoxic sample demonstrated an appreciable signal increase in both extracts relative to the normoxic sample, indicating an increase in both nuclear and mitochondrial survivin. This is in agreement with the imaging experiments for nuclear accumulation. The stability was nuclear survivin was assessed through treatment with MG132 (Fig. 3.7B), an inhibitor of the 26S proteasome. Under both

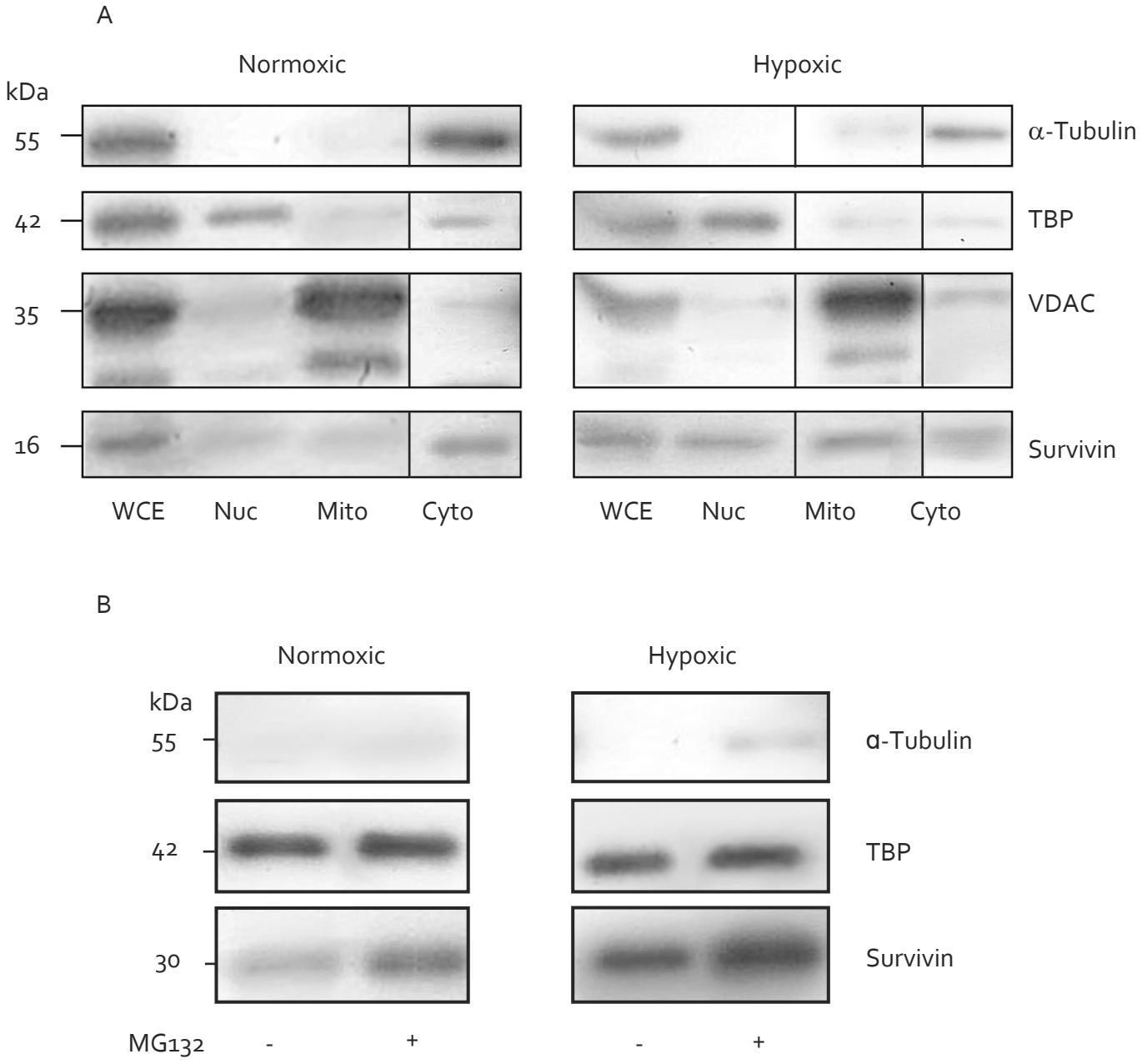


Figure 3.7 - U2OS cells demonstrate an increase in nuclear and mitochondrial survivin under hypoxia. Nuclear survivin displays similar stability under hypoxia as normoxia. **(A)** Western blot performed on subcellular fractions of control and U2OS cells exposed to hypoxia (1% O_2) for 24 hours. Samples were probed for endogenous survivin,

alpha-tubulin, TBP and VDAC. (B) Nuclear extractions of control and U2OS cells exposed to hypoxia with and without MG132 treatment to assess protein stability.

normoxic and hypoxic conditions, nuclear survivin demonstrated a similar increased with the inhibition of proteasome-mediated degradation.

3.2.2 Survivin Localisation under hypoxia

A number of SVN-GFP cells exhibited small nuclear foci under hypoxia, similar in appearance to those seen by survivin during late prophase (Uren et al. 2000). As hypoxia may induce cell cycle arrest (Ortmann et al. 2014), it was considered that nuclear survivin may be the result of cells arresting during early mitosis, where survivin normally enters the nucleus as part of the CPC. Indeed, immunoprobing for CENPA, a centromeric marker with which survivin is associated during mitosis, demonstrated significant overlap with nuclear survivin foci (Fig. 3.8A). Analysis of DNA content similarly revealed a significant increase in the G2 population of cells under hypoxia with a reduction in their S and G1 pools (Fig. 3.8B). However, this ~15% increase in G2 cells fails to account for the near universal nuclear accumulation demonstrated under hypoxia, nor cells lacking these nuclear foci.

Oxidative stress has been shown to inhibit the nuclear export machinery (Crampton et al. 2009) and is elevated during acute hypoxia (Hernansanz-Agustín et al. 2014). As survivin is actively excluded from of the nucleus to maintain its cytoplasmic localisation, the ability for nuclear export to function under hypoxic stress was assessed through the expression of a construct containing survivin's C-terminal NES sequence tagged to GFP (Fig. 3.9). Under both normoxic and hypoxic conditions, the GFP signal remaining predominantly cytoplasmic, indicating that CRM1-mediated export remained functional.

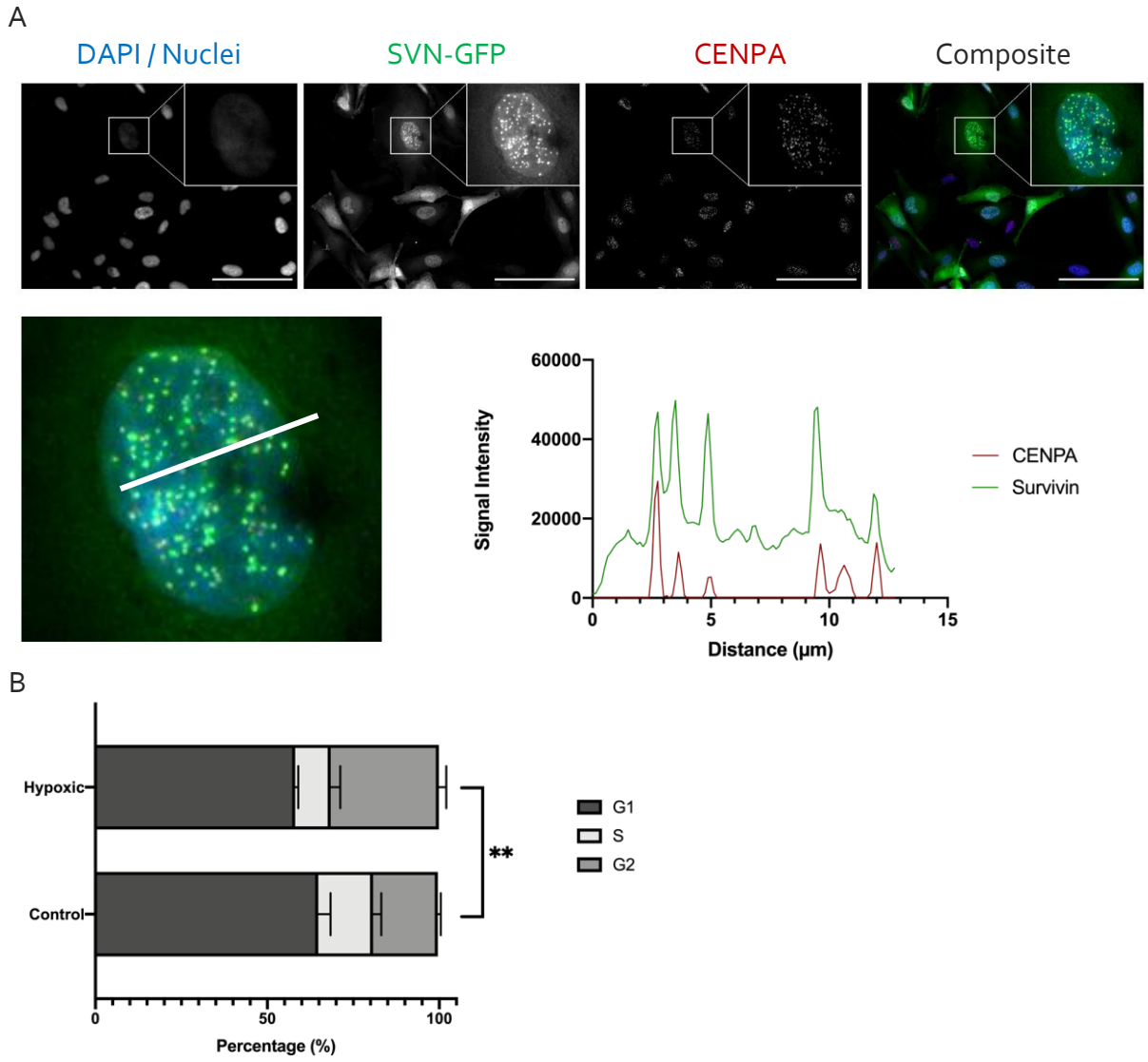


Figure 3.8 - HeLa cells undergo cell cycle arrest under hypoxia, leading to nuclear survivin foci. (A) Fluorescent microscopy analysis of HeLa cells expressing a survivin-GFP construct following 24-hour exposure to a hypoxic 1% O_2 environment. Samples were stained with DAPI to identify nuclear regions and immunoprobed with anti-CENPA antibody as a centromere marker. Displayed is one representative out of three repeated experiments. (Scale bar = 50 µm). **(B)** DNA content analysis of HeLa-SVN-GFP cells in normoxic control conditions and hypoxic 1% O_2 conditions. Error bars represents SEM of

means from three separate experiments. Asterisks indicate significant differences between the percentage of G2 cells present in each population (**, $p < 0.01$).

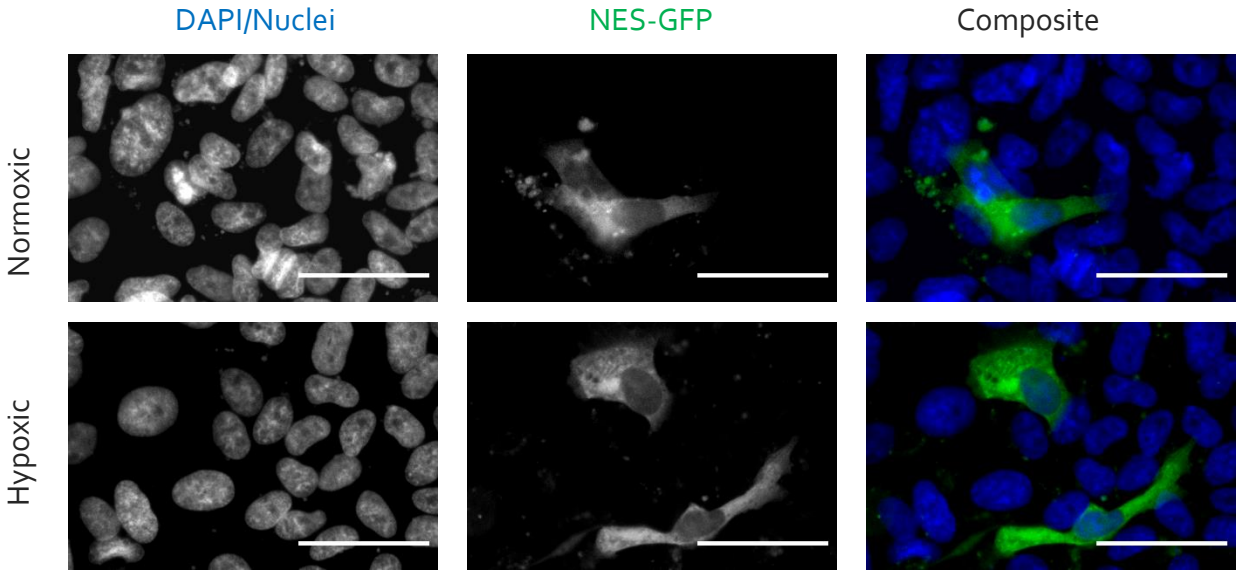


Figure 3.9 - U2OS cells demonstrate functional nuclear export under hypoxia. U2OS cells expressing NES-GFP exhibit CRM1-mediated nuclear export under both normoxic and hypoxic conditions (1% O_2). Samples were fixed, staining with DAPI to identify nuclear regions and imaged by fluorescent microscopy. (Scale bar = 50 µm).

To understand whether this nuclear translocation is reversed upon re-exposure to normoxic conditions, U2OS SVN-GFP cells were incubated in hypoxic conditions for 24 hours before being returned to normoxia and imaged after 6h (Fig. 3.10). Notably, these cells continued to exhibit a strong nuclear population of survivin. Reoxygenation presents a common event in the development of tumours (Bader et al. 2021) and is associated with reduced viability and DNA damage (Kim et al. 2007). Hypoxic stress has similarly been shown to initiate the DNA damage response (Scanlon, Glazer 2015) and therefore highlights a potential link to the nuclear translocation of survivin in response to genotoxic damage.

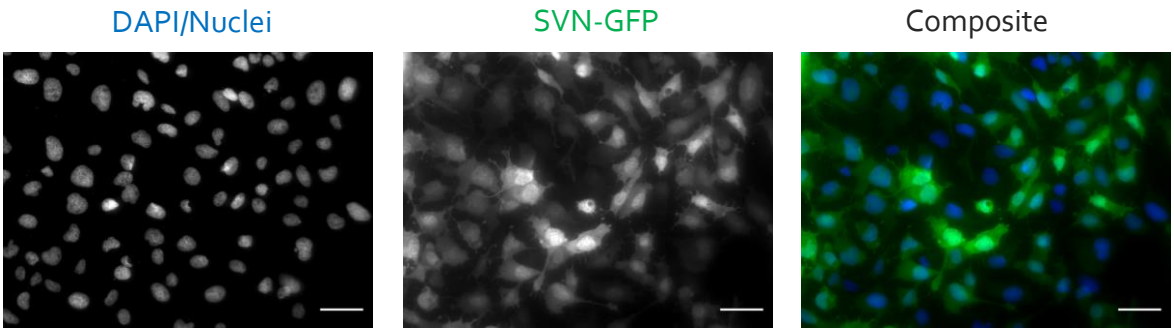


Figure 3.10 - U2OS cells maintain a nuclear survivin pool following reoxygenation. U2OS cells expressing a SVN-GFP construct were exposed to normoxic conditions for 6h following a 24h incubation in hypoxia and fixed. Samples were stained with DAPI to mark nuclear regions and subsequently imaged by fluorescent microscopy. (Scale bar = 50 μm).

Serum starvation induces cell cycle arrest and associated activation of the DNA damage response as well as reduced cell viability. U2OS SVN-GFP cells were incubated in serum free media for 24h and similarly demonstrated an elevated pool of nuclear survivin (Fig. 3.11).

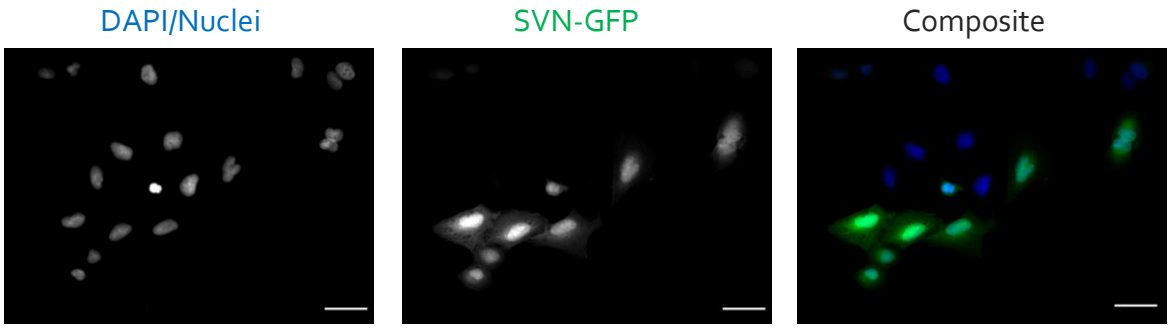


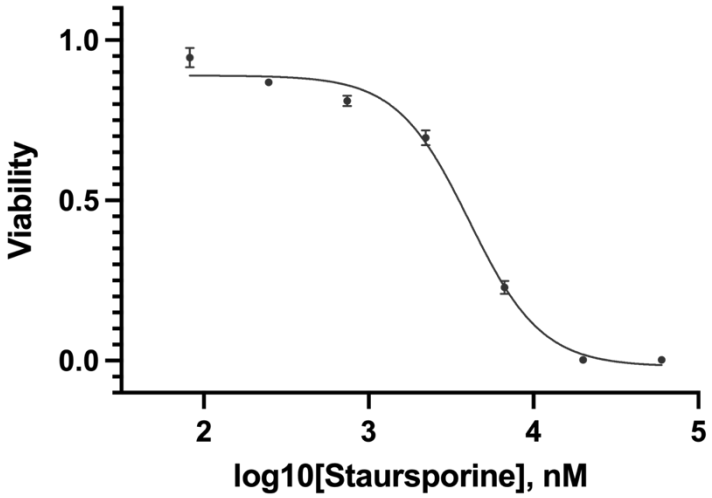
Figure 3.11 - U2OS cells demonstrate nuclear accumulation of survivin following serum starvation. U2OS cells expressing SVN-GFP were exposed to serum free culture media for 24h and fixed. Samples were stained with DAPI to mark nuclear regions and subsequently imaged by fluorescent microscopy. (Scale bar = 50 μm).

To understand whether this effect is tied to induction of apoptosis or specific to DNA damage, U2OS cells were treated with the broad acting kinase inhibitor, staurosporine, whose cytotoxicity is not reliant on DNA damage. An IC50 concentration was determined (Fig. 3.12A) and used to treat SVN-GFP expressing cells for 4 and 24 hours (Fig. 3.12B). In contrast, staurosporine failed to induce nuclear translocation of survivin, where it resided in the cell cytoplasm for all time points assessed.

3.2.3 Survivin Localisation in response to genotoxic stress

To further probe the stimuli capable of inducing nuclear translocation, U2OS cells were treated with the DNA damaging agent etoposide. An IC50 treatment concentration was determined (Fig. 3.13A) and used to treat U2OS SVN-GFP cells, inducing the nuclear localisation associated with DNA damage after 4h and this presentation persisted for the 24h time period assessed (Fig. 3.13B).

A



B

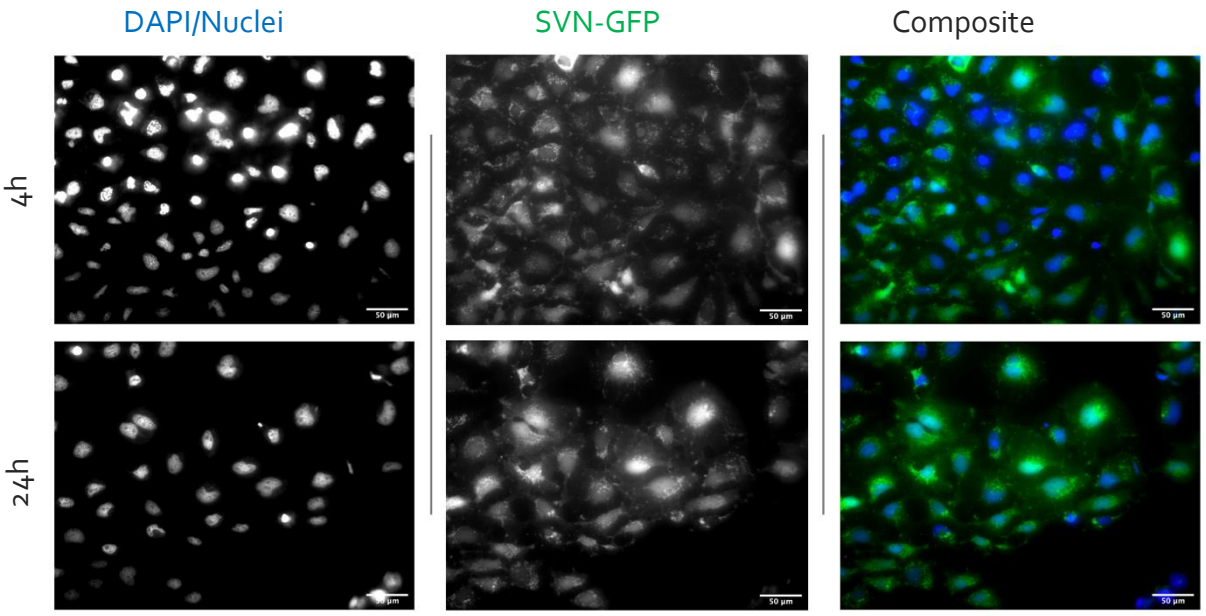
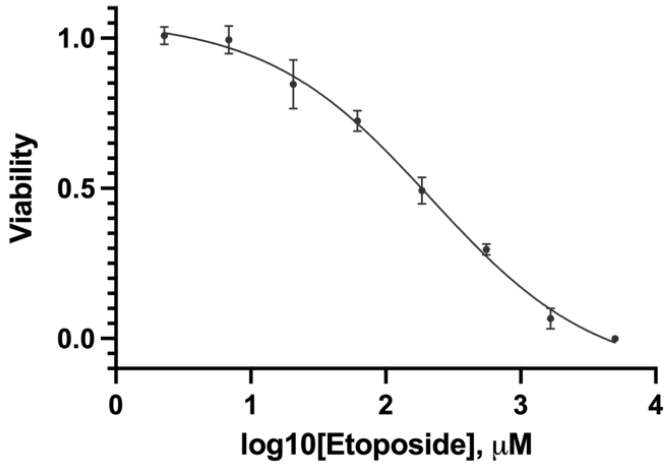


Figure 3.12 - U2OS cells exhibit cytoplasmic residency of survivin following treatment with IC50 staurosporine. (A) IC50 curve for 24h staurosporine treatment. Error bars represents SEM of means from three separate experiments. **(B)** U2OS cells expressing a survivin-GFP construct were treated with IC50 staurosporine and fixed at indicated time

points. Samples were stained with DAPI to mark nuclear regions and subsequently imaged by fluorescent microscopy. Displayed is one representative out of three repeated experiments.

A


1.0
0.5
0.0
Viability
0
1
2
3
4
log10[Etoposide], μM

B

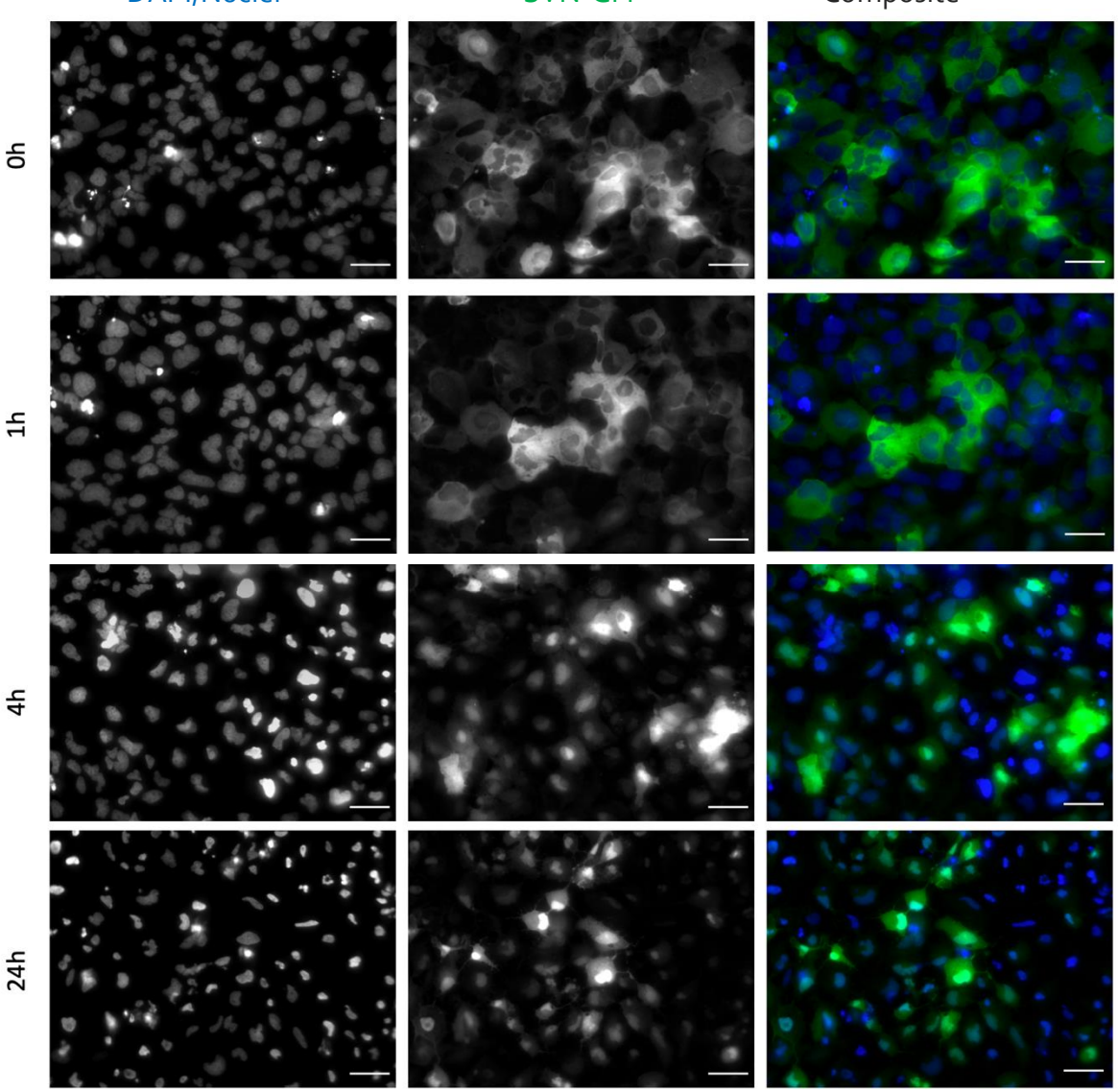
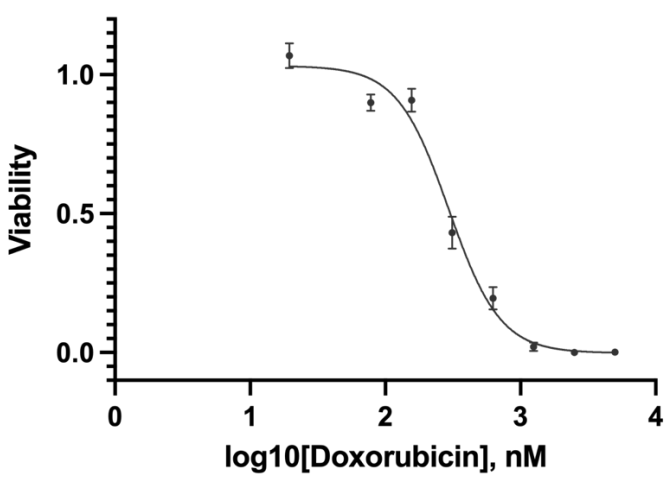

DAPI/Nuclei
SVN-GFP
Composite
0h
1h
4h
24h

Figure 3.13 - U2OS cells demonstrate a nuclear translocation of survivin following exposure to etoposide. (A) IC50 curve for 24h etoposide treatment. Error bars represents SEM of means from three separate experiments. **(B)** U2OS cells expressing a survivin-GFP construct were treated with IC50 etoposide and fixed at indicated time points. Samples were stained with DAPI to mark nuclear regions and subsequently imaged by fluorescent microscopy. Displayed is one representative out of three repeated experiments. (Scale bar = 50 μm).

Doxorubicin, like etoposide, is a TOP2 inhibitor but features attenuated DNA damage repair as a result of histone eviction. In contrast to other genotoxic stimuli tested, treatment with IC50 doxorubicin (Fig. 3.14A) failed to induce movement of survivin to the nucleus during the 24h treatment period (Fig. 3.14B), indicating nuclear transport is specifically tied to the DNA damage response and is ablated by histone eviction (Qiao et al. 2020).

A


Viability
1.0
0.5
0.0
0
1
2
3
4
log10[Doxorubicin], nM

B

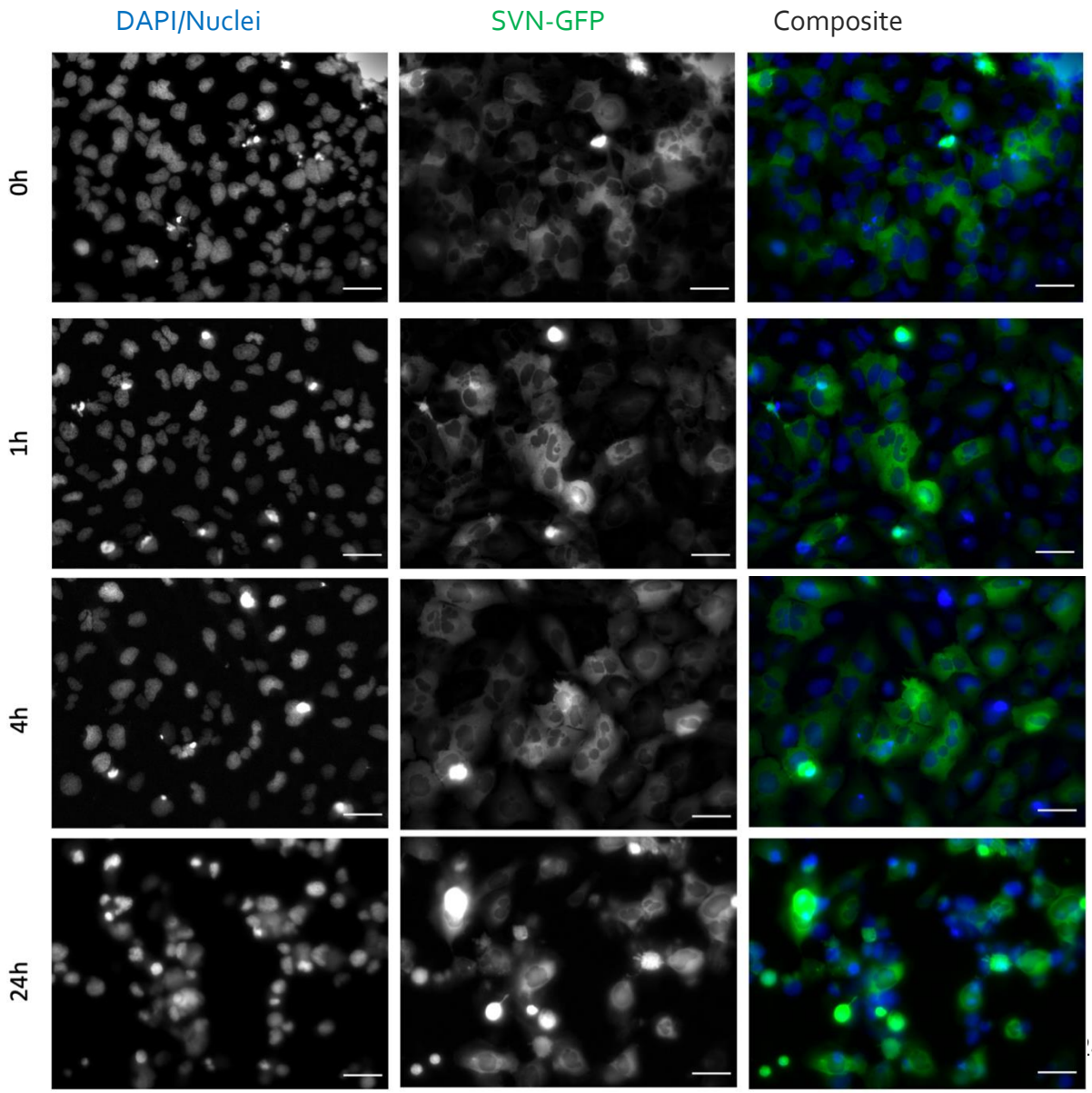
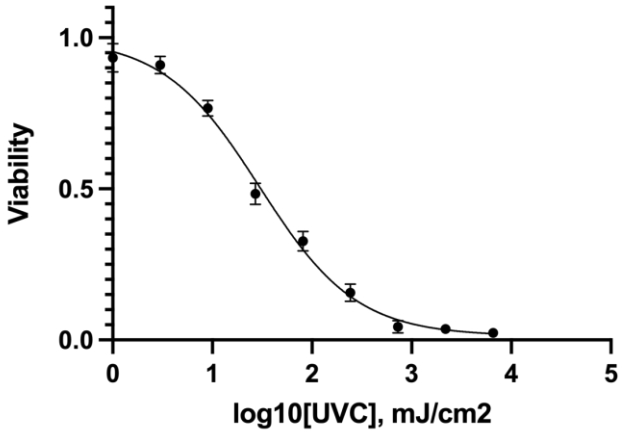

DAPI/Nuclei
SVN-GFP
Composite
0h
1h
4h
24h

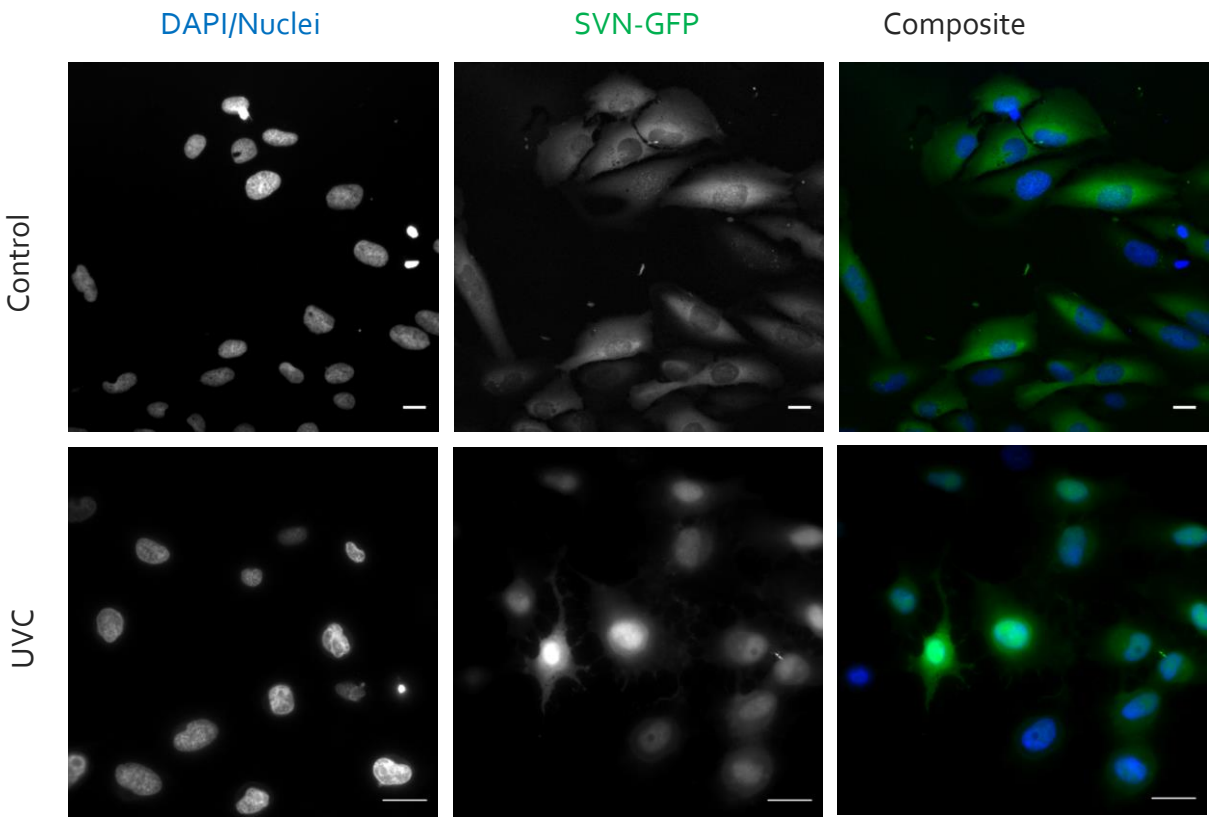
Figure 3.14 - U2OS cells maintained a predominantly cytoplasmic population of survivin upon treatment with doxorubicin. (A) IC50 curve for 24h doxorubicin treatment. Error bars represents SEM of means from three separate experiments. **(B)** U2OS cells expressing a survivin-GFP construct were treated with IC50 doxorubicin and fixed at indicated time points. Samples were stained with DAPI to mark nuclear regions and subsequently imaged by fluorescent microscopy. Displayed is one representative out of three repeated experiments. (Scale bar = 50 μm).

To further examine the potential role of the DNA repair pathway in the nuclear recruitment of survivin, U2OS cells were first treated with IC50 UVC (Fig. 3.15A) to test its ability to induce the movement of survivin to the nucleus (Fig. 3.15B). An inhibitor of DNA-PKcs and PI3K, KU-0060648, was then tested for its ability to sensitise cells to UVC by impairing the repair pathway (Fig. 3.15C). U2OS cells expressing SVN-GFP were then challenged by a combination of UVC and KU-0060648 treatment. In contrast to UVC treatment alone, inclusion of the repair inhibitor prevented survivin's nuclear recruitment (Fig. 3.15D), further evidencing survivin's nuclear localisation as a downstream product of the DNA repair pathway. As hypoxia is associated with activation of the PI3K pathway (Zhang et al. 2018) and the DNA repair response (Scanlon, Glazer 2015), it is tempting to suggest survivin's recruitment in hypoxia shares the same molecular mechanism as its translocation in response to DNA damage.

A


1.0
0.5
0.0
Viability
0
1
2
3
4
5
log10[UVC], mJ/cm2

B


DAPI/Nuclei
SVN-GFP
Composite
Control
UVC

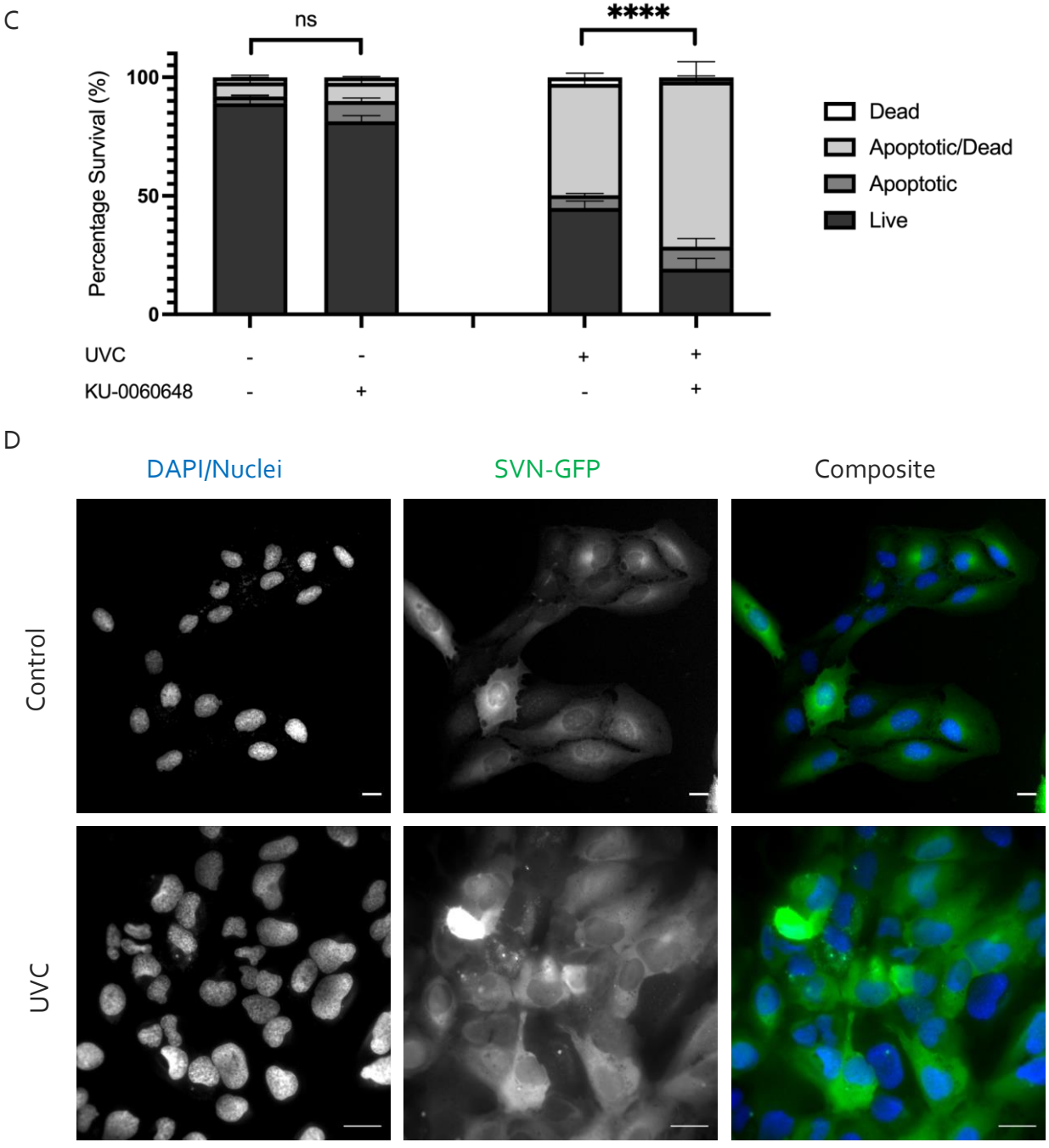


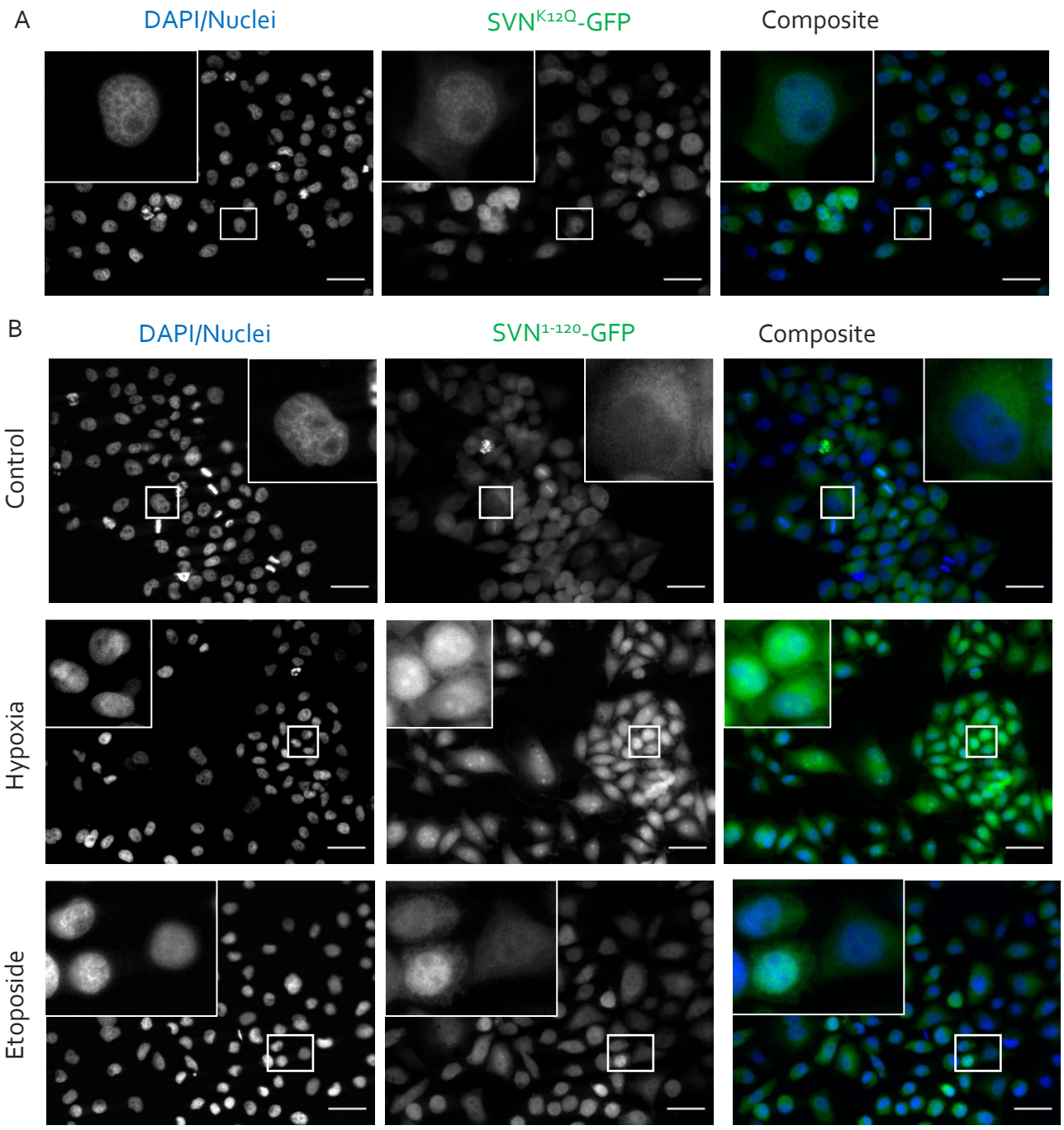
Figure 3.15 – DNA-PKcs/PI3K inhibition prevents nuclear translocation of survivin in response to UVC irradiation. (A) IC50 curve for 24h UVC treatment. Error bars represents

SEM of means from three separate experiments. **(B)** Control U2OS SVN-GFP cells or cells treated with IC50 UVC were fixed after 4h. Samples were stained with DAPI to mark nuclear regions and subsequently imaged by fluorescent microscopy. (Scale bars = 20 μm). **(C)** Flow cytometry analysis of caspase activity and membrane permeability revealed sensitisation of U2OS cells to UVC with 1uM KU-0060648 treatment. Error bars represent SEM of means from two separate experiments. (ns, not significant; ****, p <0.0001) **(D)** Control U2OS SVN-GFP cells or cells treated with IC50 UVC were both incubated with 1uM KU-0060648 and fixed after 4h. A combination of UVC and KU-0060648 treatment failed to induce nuclear accumulation of survivin. Samples were stained with DAPI to mark nuclear regions and subsequently imaged by fluorescent microscopy. (Scale bars = 20 μm).

3.2.4 Survivin localisation by post-translational modifications and protein interactions

It was considered that post-translational modifications of survivin may regulate protein interactions that lead to its nuclear accumulation. Acetylation of K129 has been shown to promote survivin dimerization and increase the nuclear pool (Wang et al. 2010). This was confirmed through the expression of a survivin K129 acetylation mimetic (K129Q) (Fig.3.16A). A truncated survivin construct (aa 1-120) tagged with GFP was expressed in U2OS cells and therefore lacked the K129 amino acid to assess its potential role in hypoxic nuclear translocation (Fig. 3.16B). Under normoxic conditions, SVN^{1-120}-GFP maintained a cytoplasmic localisation despite loss of its C-terminal NES, albeit more weakly than the wild type construct. However, under hypoxic conditions it demonstrated an increased nuclear pool. Notably this truncated form also exhibited large foci within the nuclear region. These cells were additionally exposed to etoposide to induce DNA damage and similarly demonstrated transport of survivin to the nucleus, although these cells lacked the nuclear foci seen under hypoxia. In both conditions, nuclear survivin signal appeared to be stronger than the weaker nuclear accumulation exhibited by SVN^{K129Q}-GFP. The involvement of survivin acetylation was further examined through

the use of pan-HDAC inhibitor trichostain-A (TSA). HDAC6 activity has been shown to promote survivin export via deacetylase activity (Riolo et al. 2012) and is inhibited by TSA (Hanson et al. 2018). Efficacy of the TSA treatment dosage was demonstrated by TSA-induced cell cycle arrest, as previously reported (Meng et al. 2012); TSA treatment significantly increased the G1 population with a reduction in S phase cells (Fig. 3.16C). In agreement with the SVN^{1-120}-GFP construct, preventing survivin acetylation with TSA did not affect its localisation under normoxic conditions (Fig. 3.16D).


A
DAPI/Nuclei
SVN^K12Q-GFP
Composite
B
DAPI/Nuclei
SVN^1-120-GFP
Composite
Control
Hypoxia
Etoposide

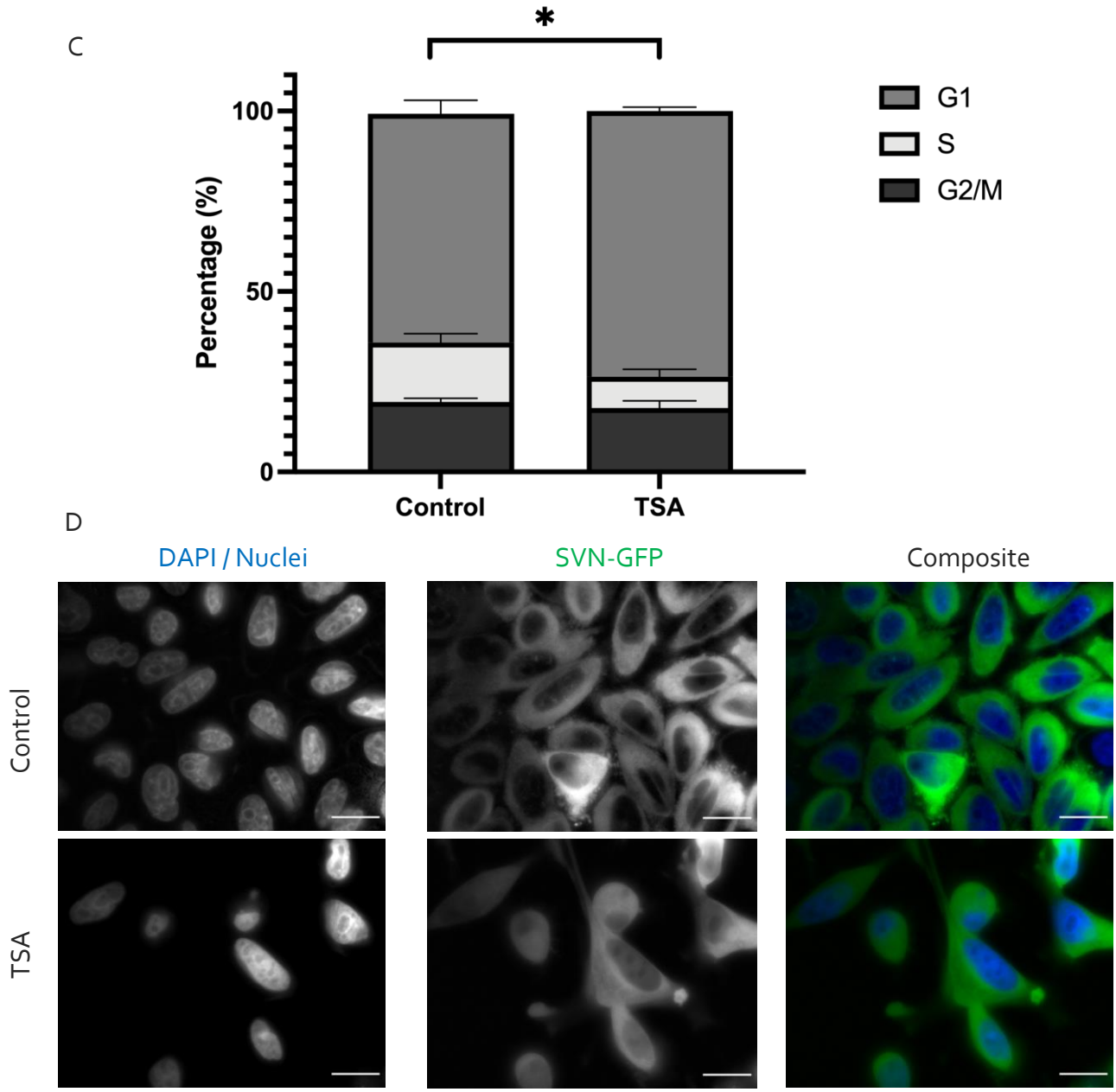


Figure 3.17 – Survivin (aa 1-120) translocates to the nucleus under hypoxia and in response to genotoxic stress. **(A)** U2OS cells expression the survivin K129 acetylation mimetic, SVN^{K12Q}-GFP, demonstrates weak nuclear accumulation under normoxic conditions. **(B)** U2OS cells expressing a $survivin^{1-120}$-GFP construct were fixed following 24h exposure to normoxia, hypoxia or etoposide-induced genotoxic stress. Samples were stained with DAPI to mark nuclear regions and subsequently imaged by fluorescent

microscopy. Displayed is one representative out of three repeated experiments. (Scale bar = 50 µm). **(C)** DNA content analysis of U2OS SVN-GFP cells treated with TSA for 48h. Error bars represent SEM of means from three separate experiments. (*, p <0.05) **(D)** U2OS cells expressing SVN-GFP construct were treated for 24h with trichostatin-A (TSA). Samples were fixed, stained with DAPI to mark nuclear regions and subsequently imaged by fluorescent microscopy. Displayed is one representative out of three repeated experiments. (Scale bar = 20 µm).

Further survivin modifications important to its protein interactions were assessed, including the phosphorylation of survivin at S20 (Fig. 3.17). Protein kinase A (PKA) phosphorylates survivin at the S20 residue and may reduce its binding affinity for XIAP with implications for apoptosis inhibition (Dohi et al. 2007). Survivin constructs containing either an S20 phosphomimetic substitution (S20D) or an S20 phosphoresistant substitution (S20A) were expressed in U2OS cells and similarly exposed to hypoxic and normoxic conditions. Both constructs continued to display the the same nuclear translocation demonstrated in wild type cells. This was further supported by treatment with forkolin, an activator of protein kinase A (PKA) (Bradbury 2000). Following 24h treatment with 10 µM forskolin, survivin's subcellular localisation remained cytoplasmic. Together suggesting that S20 phosphorylation is not necessary for survivin's import.

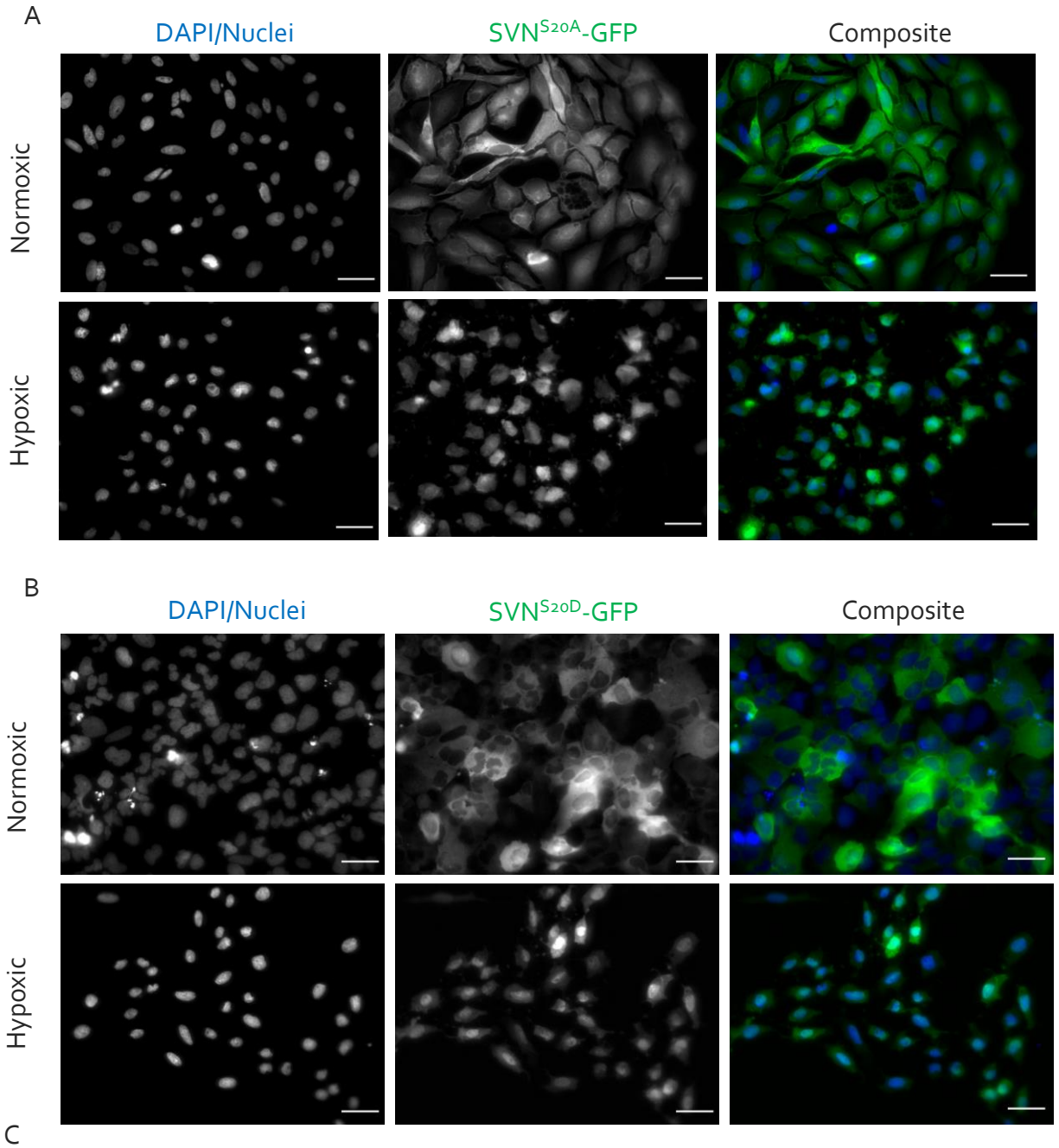

A
DAPI/Nuclei
SVN^{S20A}-GFP
Composite
Normoxic
Hypoxic
B
DAPI/Nuclei
SVN^{S20D}-GFP
Composite
Normoxic
Hypoxic
C
DAPI/Nuclei
SVN-GFP
Composite

Figure 3.17 – Survivin S20A and S20D display typical nuclear accumulation under hypoxia. U2OS cells expressing survivin-GFP constructs with either **(A)** S20A or **(B)** S20D mutations were fixed following 24h exposure to normoxic or hypoxic conditions. Samples were stained with DAPI to mark nuclear regions and subsequently imaged by fluorescent microscopy. Displayed is one representative out of three repeated experiments. (Scale bar = 50 μm). **(C)** U2OS SVN-GFP cells treated for 24h with 10 μM forskolin. Samples were stained with DAPI to mark nuclear regions and subsequently imaged by fluorescent microscopy. Displayed is one representative out of three repeated experiments. (Scale bar = 50 μm).

Survivin T34 phosphomimetic (T34E) and phosphoresistant (T34A) substitutions were also investigated (Fig. 3.18), although these similarly failed to alter the localisation profile of survivin.

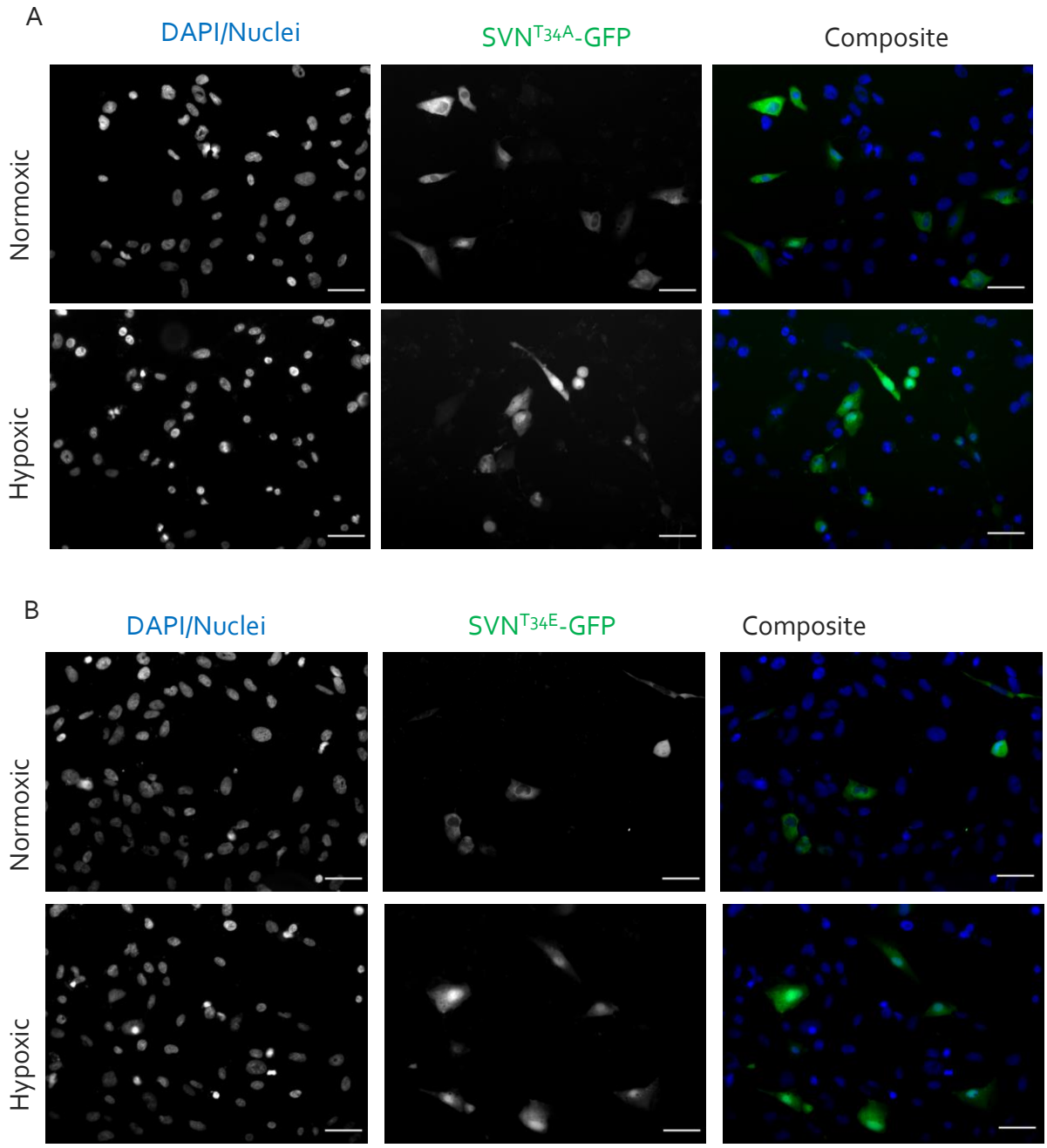


Figure 3.18 - Survivin T34A and T34E display typical nuclear accumulation under hypoxia. U2OS cells expressing survivin-GFP constructs with either T34A **(A)** or T34E **(B)** mutations were fixed following 24h exposure to normoxic or hypoxic conditions. Samples were stained with DAPI to mark nuclear regions and subsequently imaged by fluorescent

microscopy. Displayed is one representative out of three repeated experiments. (Scale bar = 50 µm).

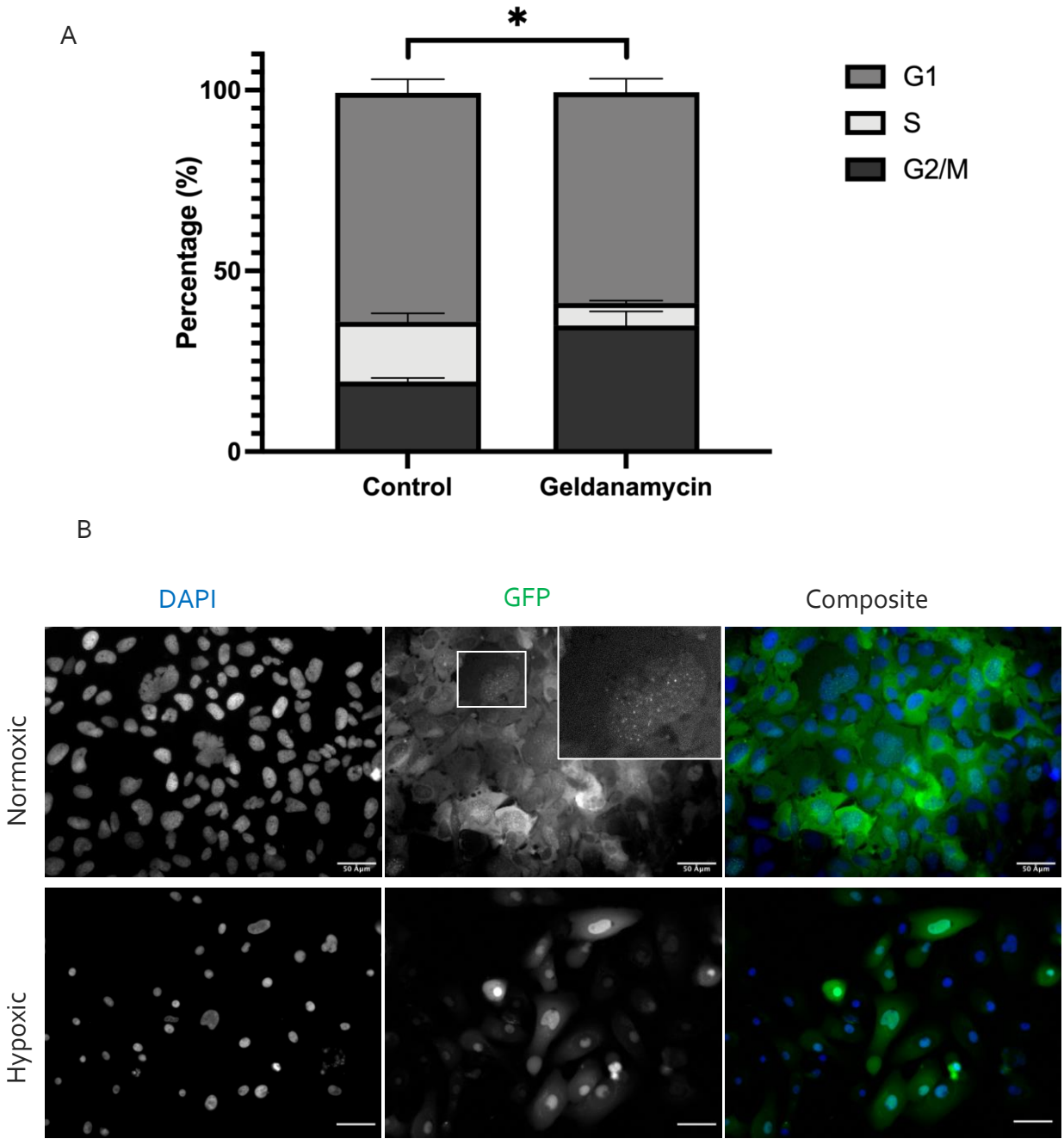


Figure 3.19 - U2OS cells exhibit cytoplasmic residency of survivin under hypoxia and nuclear survivin foci following treatment with geldanamycin. (A) DNA content analysis of U2OS SVN-GFP cells treated with geldanamycin for 24h. Error bars represents

SEM of means from three separate experiments. **(B)** U2OS cells expressing a survivin-GFP construct were treated with geldanamycin and fixed at after 24h exposure to normoxic or hypoxic conditions. Samples were stained with DAPI to mark nuclear regions and subsequently imaged by fluorescent microscopy. (Scale bar = 50 μm).

Survivin stability is facilitated by interactions with heat shock protein 90 (HSP90) (Fortugno et al. 2003). Notably, HSP90 is thought to contain a bipartite NLS sequence (Nardai et al. 1996), which may play a role in the nuclear shuttling of steroid receptors (Csermely et al. 1995). To explore a potential role for HSP90 in the nuclear shuttling of survivin within this context, the HSP90 inhibitor, geldanamycin, was used (Fig. 3.19). An effective concentration was determined by testing for geldanamycin-induced cell cycle arrest (Okamoto et al. 2008). DNA content analysis revealed a significant increase in the G2/M phase population (Fig. 3.19A) with 24h incubation with 1uM geldanamycin. However, this treatment failed to prevent hypoxia-induced nuclear transport of survivin (Fig. 3.19B).

Notably, geldanamycin treated cells under normoxia presented with nuclear survivin foci associated with late prophase cells (Uren et al. 2000). This intriguingly raised the possibility of using geldanamycin as a late prophase cell cycle inhibitor for use in cell synchronisation experiments, of which there are few available alternatives (Banfalvi 2011).

3.2.5 Geldanamycin as a cell synchronisation tool

It was first necessary to establish the ability of geldanamycin to inhibit cell growth and a suitable treatment range. The immortalised fibroblast cell line MRC-5 was treated with a broad range of geldanamycin concentrations and their growth rate over a 24-hour period was measured. Growth rate was determined by monitoring relative cell numbers through resazurin assays and compared to an untreated control to determine a relative growth rate, summarised in Fig. 3.20. A dose

dependent relationship was demonstrated and ranged from minimal inhibition of growth at low concentrations and complete arrest of cell numbers at higher concentrations. Treatment doses between 82 nM and 2.2 μM displayed significantly reduced growth rates while treatments above this range lowered cell numbers, indicating treatment toxicity at higher doses.

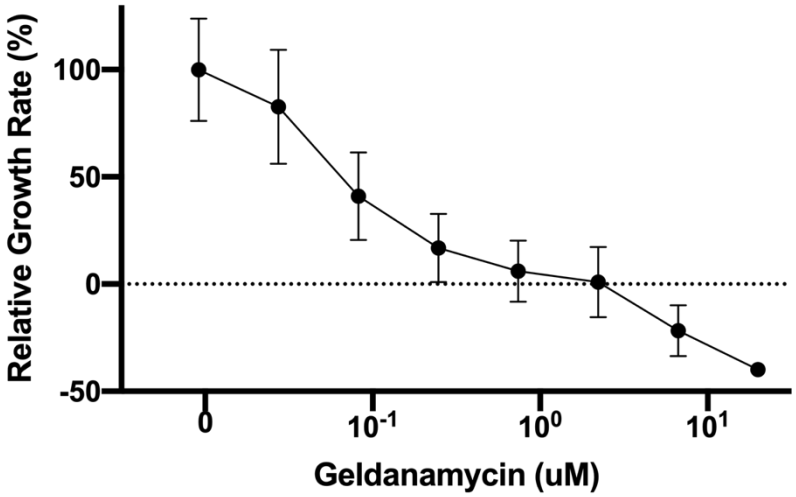
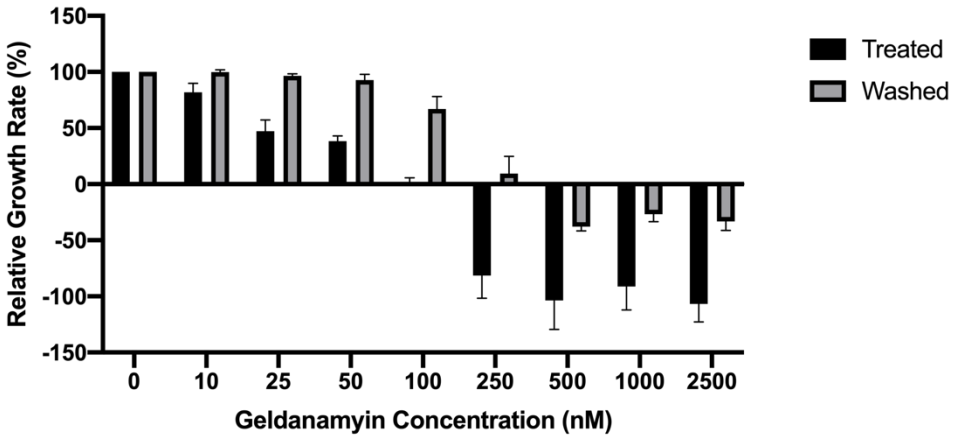


Figure 3.20 – MRC5 cells demonstrate reduced cell proliferation with geldanamycin treatment. Fibroblastic MRC5 cells were treated for 24h to a range of geldanamycin concentrations and relative growth rate to controls cells were determined by resazurin assay. Error bars represents SEM of means from three separate experiments.

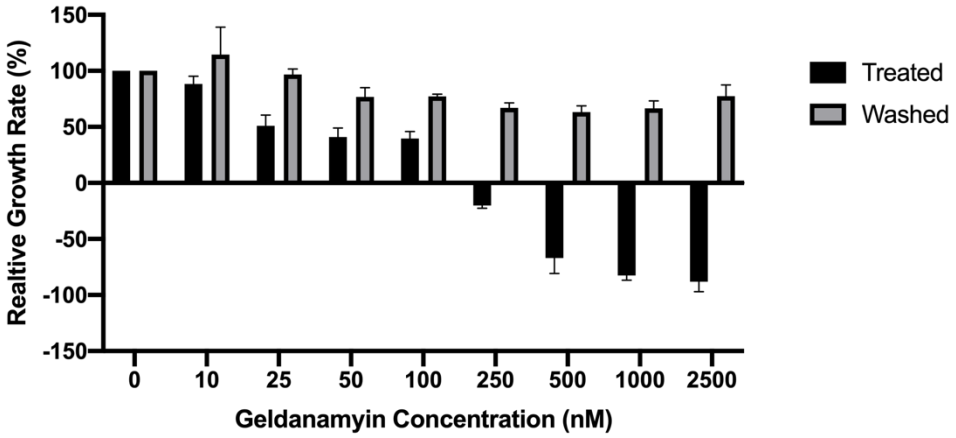
To determine whether the inhibitory effects of geldanamycin treatment could be reversed, samples were treated and then washed and incubated without geldanamycin present. Their growth rates relative to untreated controls were compared. Additionally, the range of cell lines tested was expanded to include immortalised retinal pigment epithelium (RPE) and the osteosarcoma cell line

U2OS. Treatment concentrations were assessed for their ability to induce cell cycle arrest with treatment while washed samples would return to a normal growth rate. MRC5 cells displayed a narrow treatment range fulfilling these criteria, with only the 100 nM treatment exhibiting significant recovery when cell cycle arrest was induced. Treatment concentrations exceeding 100 nM displayed a dramatic reduction in cell numbers for both washed and treated samples. U2OS demonstrated a broader range, from 250 nM to the maximum concentration tested at 2500 nM. RPE cells exhibited the greatest resistance to geldanamyin but showed significantly reduced growth at the highest concentration with complete recovery when washed. Based on these data, treatment concentrations of 100 nM for MRC5 and 2500 nM for U2OS and RPE cell lines were used moving forward.

A



B



C

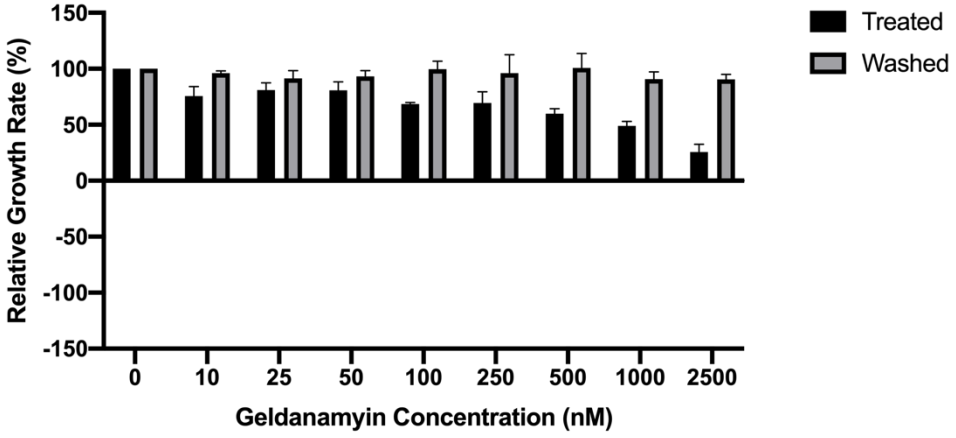


Figure 3.21 – Geldanamycin demonstrates variable cell toxicity and cell cycle arrest in human cell lines. Relative growth rate of MRC5 (A), U2OS (B) and RPE (C) cells were

determined by resazurin assay to a range of geldanamycin treatment concentrations over a 24h period.

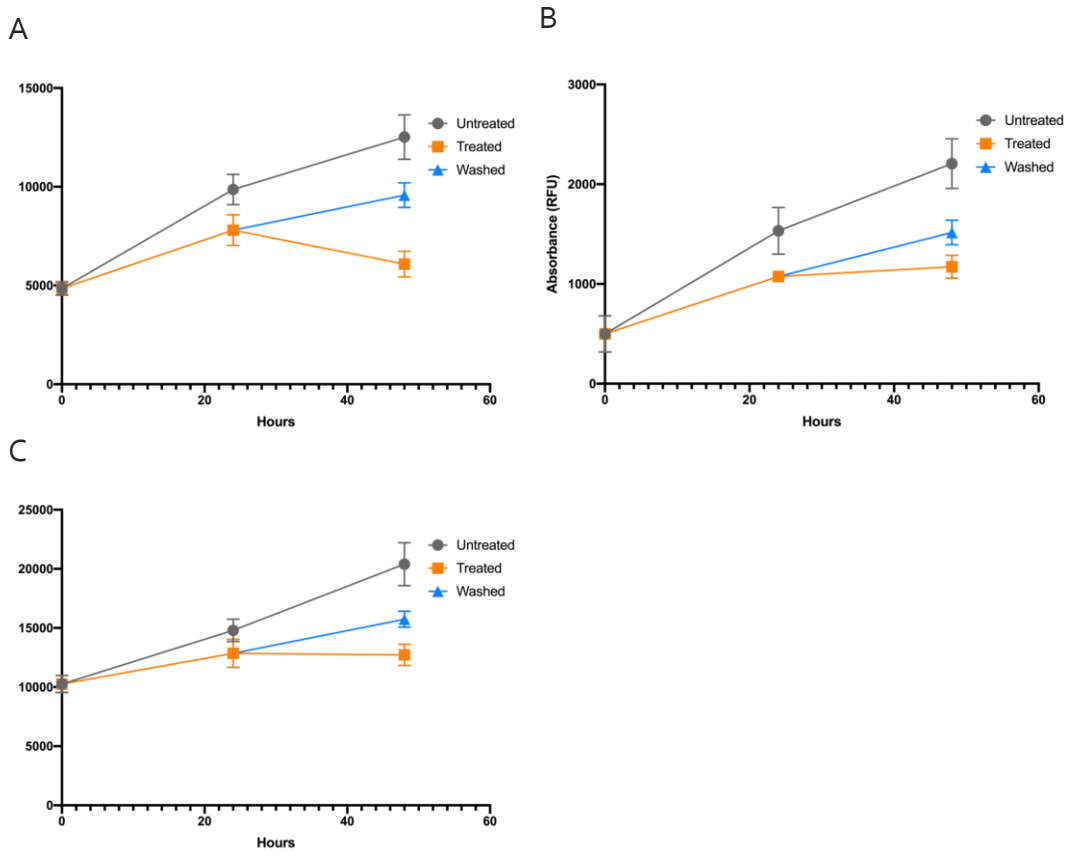


Figure 3.22 – Geldanamycin demonstrates reversible cell cycle arrest. U2OS **(A)**, RPE **(B)** and MRC5 **(C)** cells exhibit distinct growth rates depending on whether geldanamycin treatment was washed out.

To determine at which stage cell cycle arrest occurred, DNA content analysis was performed on treated samples, summarised in Fig. 3.23. MRC5 and RPE cell lines demonstrated no significant difference in the proportion of G2/M phase cells although a noticeably decrease in S phase cells was observed. Together these data might suggest geldanamycin treatment induces an arrest in both the G1 and G2/M

phases of the cell cycle. Conversely, U2OS cells demonstrated a modest but significant increase in the G2/M portion of cells, increasing from 19% to 35%

In an effort to increase a G2 arrest, cells were treated with the G1 inhibitor thymidine before being released in geldanamycin. In all cell lines, thymidine treatment successfully resulted in an increase in cells at the G1/S checkpoint. In so doing, it was hoped cells would have already progressed through the G1 phase and subsequent cell cycle arrest by geldanamycin would catch cells in the G2 phase. However, release into geldanamycin resulted in varied cell profiles. Whilst U2OS cells demonstrated the greatest G2/M increase to geldanamycin treatment alone, preceding treatment with thymidine had no significant impact of the cell cycle distribution of cells. Similarly, MRC5 cells showed little difference regardless of the treatment course employed. RPE cells however exhibited a substantial increase in the G2/M population, increasing from 17% to 52%.

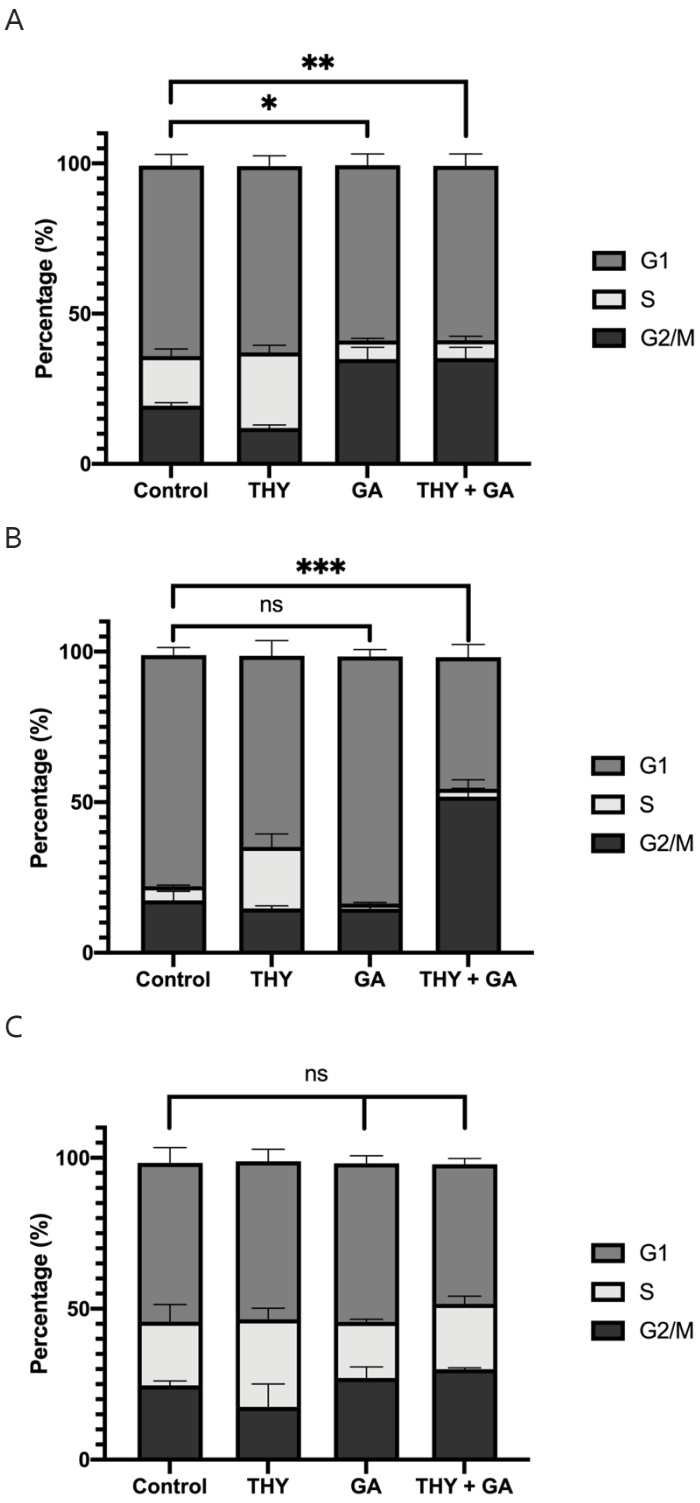
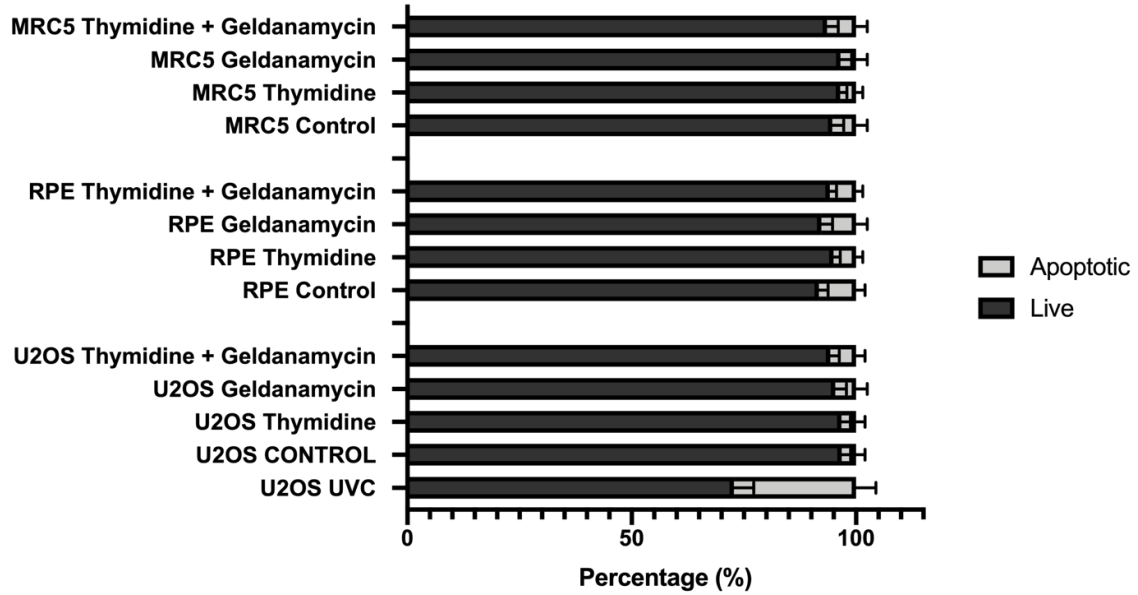


Figure 3.23 – Geldanamycin and combination treatment of thymidine and geldanamycin induce a G2/M arrest. U2OS **(A)**, RPE **(B)** and demonstrate cell cycle arrest in the G2/M phase following treatment with geldanamycin with some benefits offers by an

initial treatment with thymidine. MRC5 (C) cells display no significant difference to control cells following treatment. (ns, not significant; *, p <0.05; **, p <0.01; ***, p <0.001; n=3).

As prolonged treatment and higher treatment concentrations both demonstrated reduced cell numbers, the toxicity of these treatment concentrations was determined by a caspase 3/7 assay. Fig. 3.24. demonstrates no significant reduction in the number of live cells compared to the untreated control group in the cell synchronisation regimes tested. Similarly, no significant increase in cells with active caspase activity, indicative of apoptosis, was seen. U2OS cells treated with UVC radiation to induce apoptosis was used as a positive control.

A



B

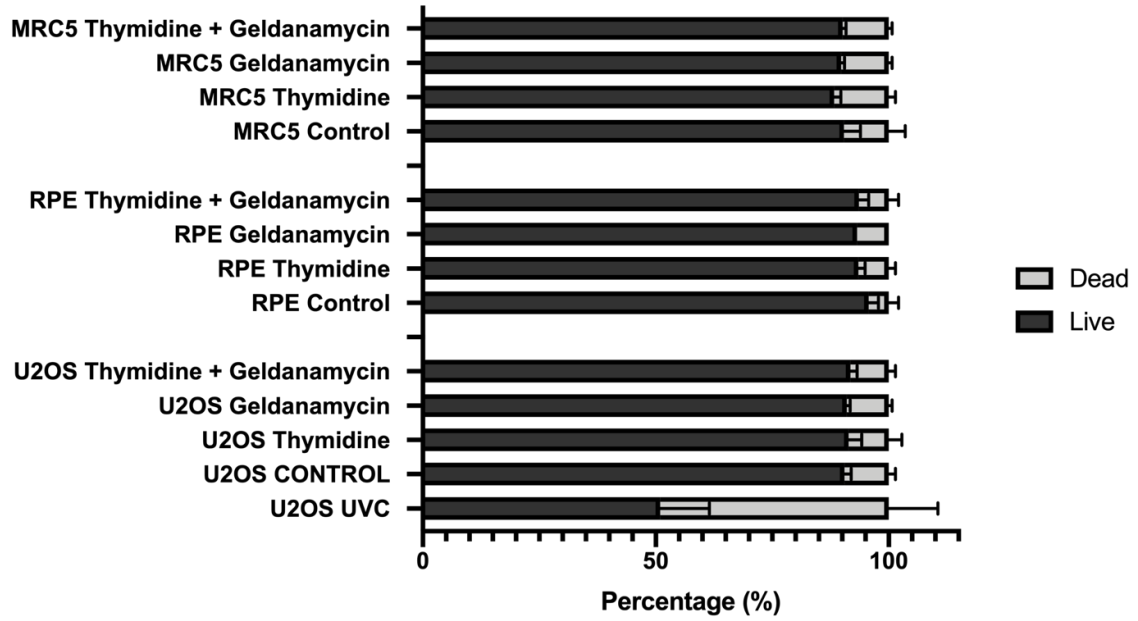


Figure 3.24 – Geldanamycin treatment display no significant toxicity at the treatment concentrations determined. MRC5, RPE and U2OS cells were treated with either

thymidine, geldanamycin or a combination treatment for 24h **(A)** or 48h **(B)** to determine treatment toxicity.

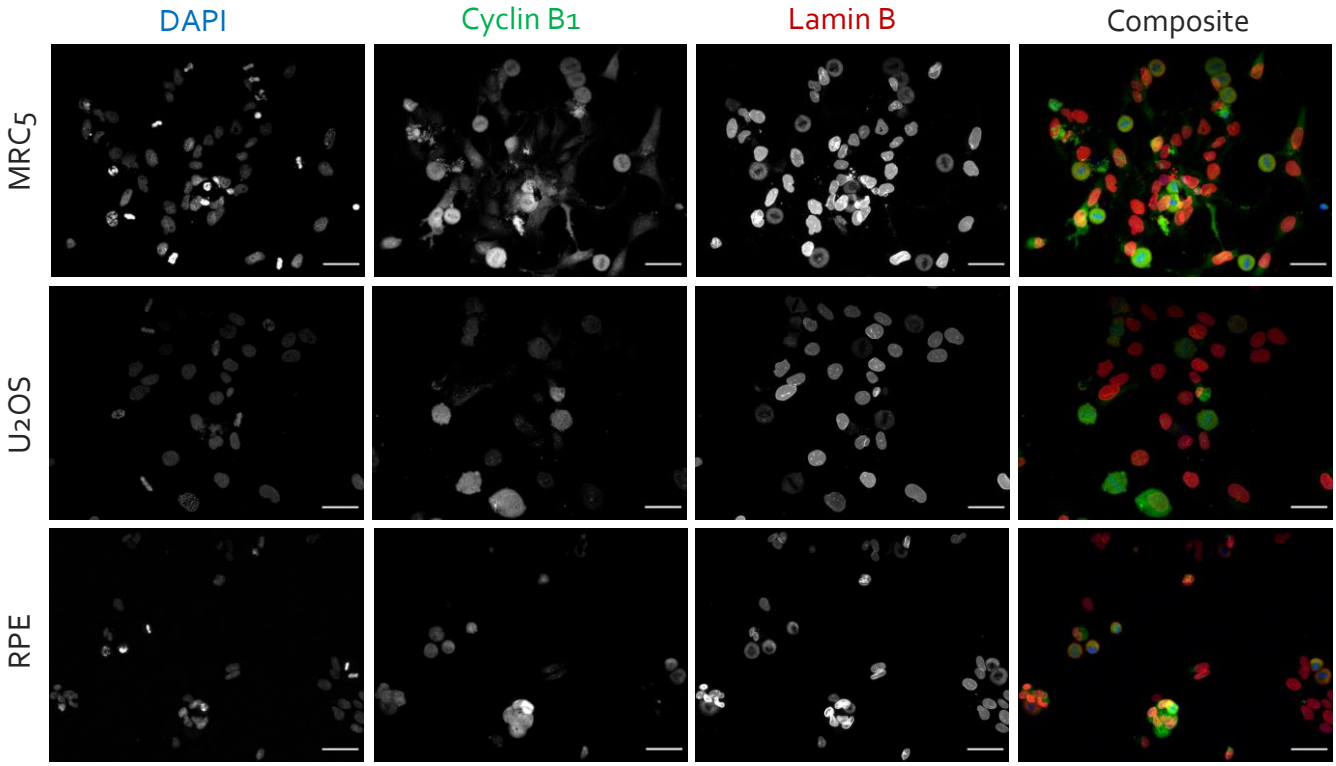


Figure 3.25 – Combined Thymidine and Geldanamycin treatment induces cell cycle arrest in metaphase. MRC5, U2OS and RPE cells were treated with thymidine and geldanamycin before fixing. Samples were stained with DAPI and immunoprobed for cyclin B1 and lamin B to assess cell cycle stage. (Scale bar = 50 μm).

To specially determine the cell cycle stage at which were arrested with a combined treatment regime, cells were fixed and immunoprobed with cyclin B1 and lamin B (Fig. 3.25). Nuclear cyclin B1 expression occurs during prophase-metaphase whilst lamin B (Toyoshima et al. 1998), as a constituent of the nuclear lamina, is associated with the nucleus until its dissolution during prometaphase. In contrast to prophase

arrest suggested by geldanamycin treatment alone, imaging treatments of thymidine and geldanamycin revealed an increase in the metaphase population of cells, as determined by breakdown of the nuclear envelope and DNA condensation.

3.2.6 Development of 3D culture techniques

To further replicate the TME, preliminary work was carried out to generate 3D cultures that might better recapitulate conditions of tumour cells, namely spheroids and decellularized matrices.

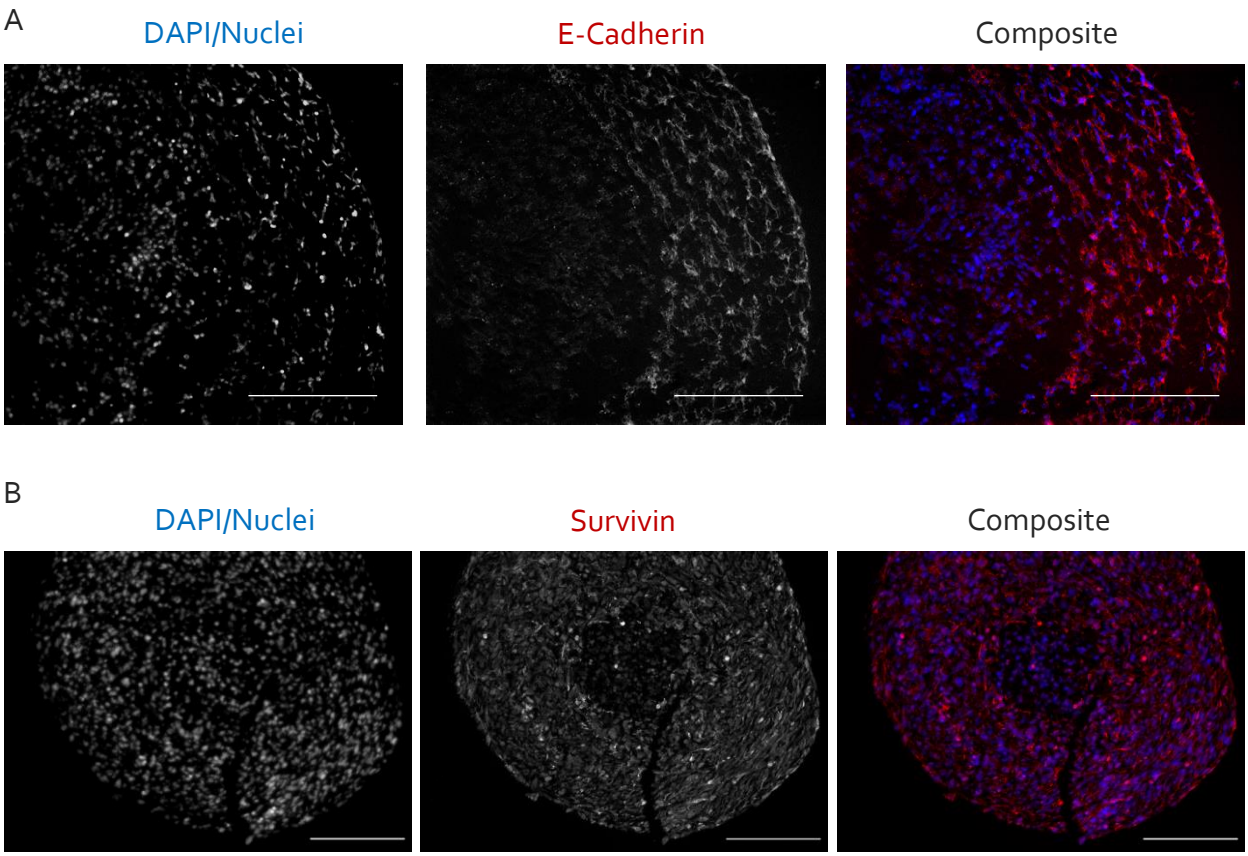


Figure 3.26 – MRC5 spheroid demonstrate generate distinct cell populations with different expression profiles. MRC5 SVN-GFP cells cultured in a rotational bioreactor generated spheroid cultures. Immunoprobing of fixed cells with E-cadherin **(A)** and survivin

(B) revealed distinctive expression phenotypes depending on the position within the spheroid. (Arrows indicate the spheroid-media interface; Scale bar = 200 μm).

Use of a rotational bioreactor successfully generated spheroid cultures of MRC5 SVN-GFP over 600 μm in diameter (Fig. 3.26). However, imaging of GFP signal demonstrated significant quenching (data not shown), likely as a result of the fixation and paraffinization process. Survivin signal was recovered by performing antigen retrieval and immunoprobing with survivin antibodies. Immunoprobing of spheroid sections for E-cadherin (Fig. 3.26A) and survivin (Fig. 3.26B) revealed distinct expression phenotypes based on their proximity to the media interface. E-cadherin signal was significantly reduced at a distance of approx. 200 μm from the spheroid edge. Cell density additionally appeared more variable near the centre of the spheroid mass with a less structured organisation. Similarly, survivin signal was reduced at the spheroid centre and colocalised more strongly with DAPI. However, a distinctly cytoplasmic localisation was not clear from cells at the spheroid edge either. Together these data suggest the spheroid culture was successful in generating different microenvironmental conditions and gave rise to cellular populations with distinct expression profiles.

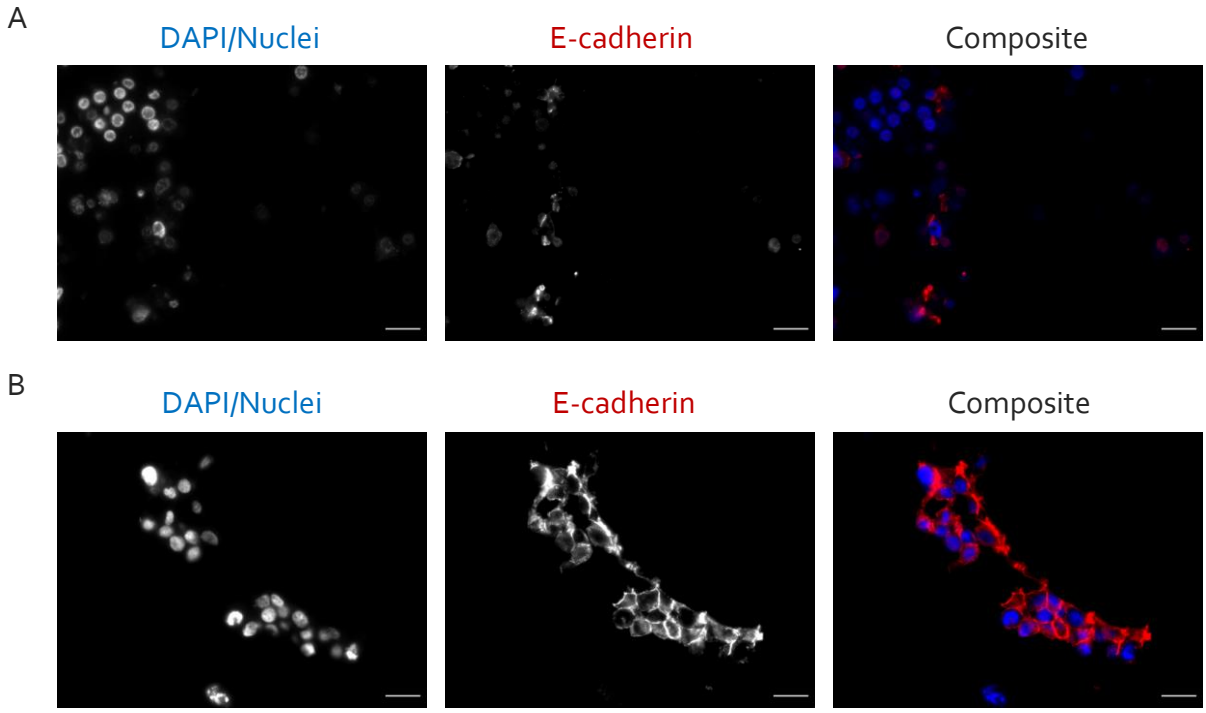


Figure 3.27 – MCF7 cells demonstrate reduced E-cadherin expression within the inner regions of spheroids. **(A)** MCF7 cells within the inner regions of spheroids exhibit reduced E-cadherin expression with some nuclear localisation. **(B)** Cells positioned on the edge of the spheroid demonstrated greater E-cadherin levels with typically expression at the outer membrane. (Scale bars = 50 μm).

Spheroids were also generated using the breast cancer cell line, MFC7 (Fig. 3.27) Similarly this cell line developed subpopulations of cells with distinctive phenotypes based on their distance to the spheroid-media interface. Cells positioned at the edge of the spheroid maintained a more structured organisation with greater cell adhesion whilst those within the inner regions exhibited an almost total loss of cell structure. Immunoprobing for E-cadherin highlighted increased expression within the outer regions (Fig. 3.27B) and a characteristic localisation to the outer membrane and cell junctions. In contrast, inner regions exhibited significantly reduced expression and staining that colocalised with DAPI signal (Fig. 3.27B).

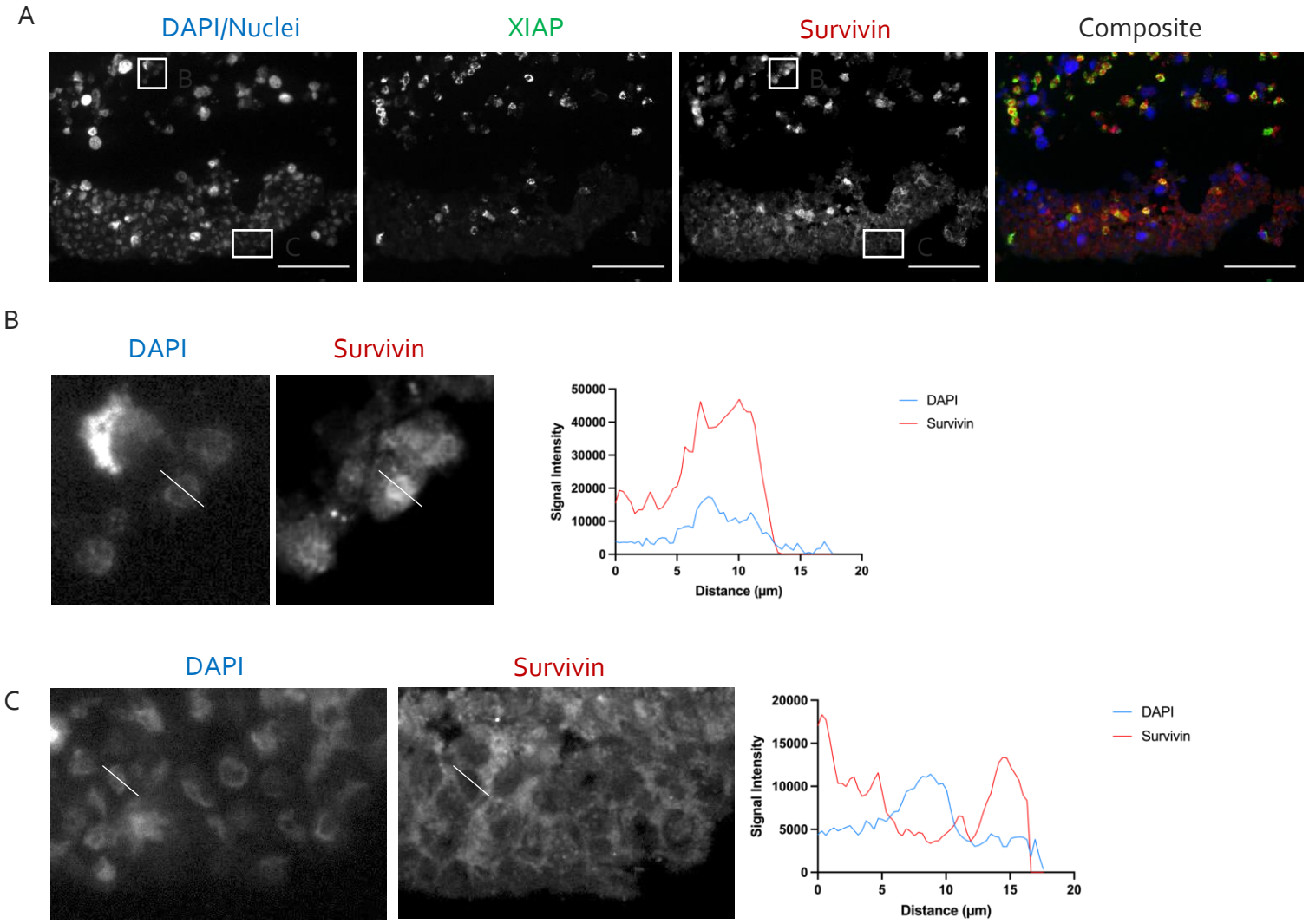


Figure 3.28 – MCF7 cells exhibit increased XIAP expression and a nuclear translocation of survivin within the inner regions of spheroids. (A) MCF7 cells demonstrate distinct morphological and expression phenotypes between cells situated near the media interface (indicated by arrows) and the inner regions of the spheroids. (Scale bar = 200 μm). Immunoprobing for XIAP and survivin revealed increased XIAP expression within the inner sections while survivin exhibited nuclear accumulation in the inner regions (B) compared to the edge of the spheroid (C).

Immunoprobing of MCF7 spheroids for XIAP and survivin also revealed increased expression within the inner regions. Survivin notably demonstrated a more nuclear localisation in the inner regions (Fig. 3.28B) compared to a predominantly cytoplasmic appearance at the spheroid periphery (Fig. 3.28C), indicative of a hypoxic environment.

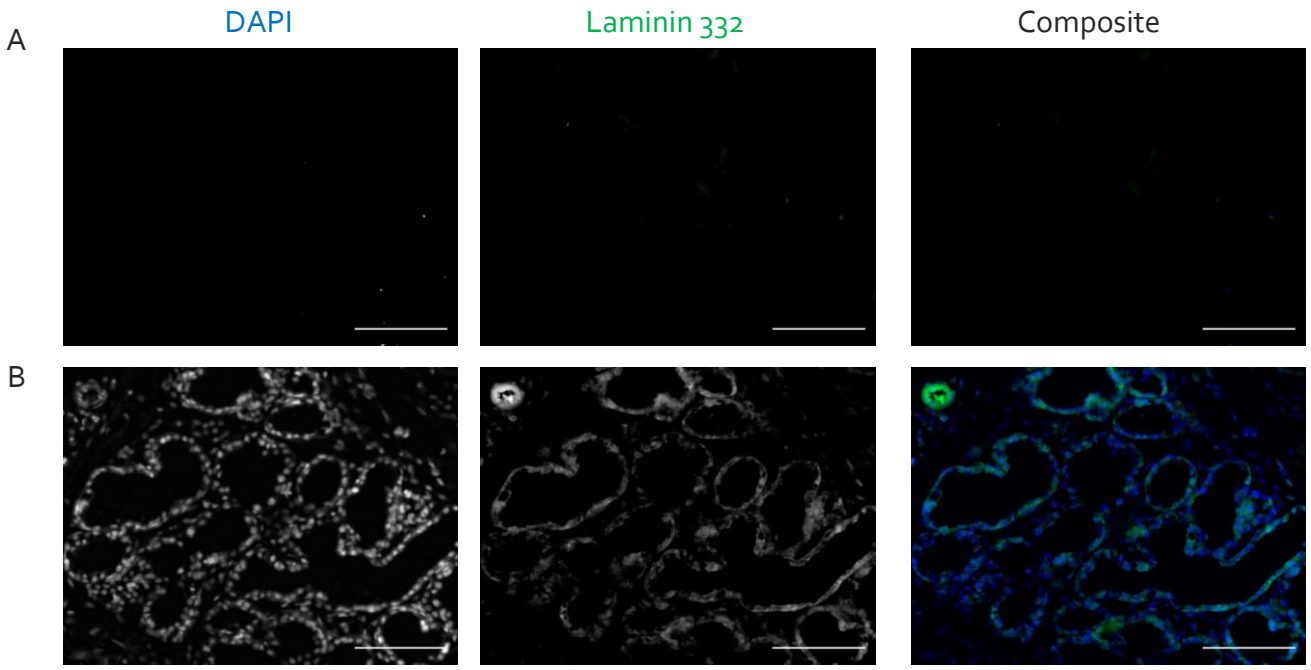


Figure 3.29 – Decellularized rat mammary tissue supports the colonisation of MCF7 cells and expression of laminin 332. Decellularization of mammary tissue harvested from sacrificed rats successfully removed the native cell population **(A)** and supported the colonisation of the tissue matrix by MCF7 cells following a 7-day incubation period **(B)**. Tissues were fixed, stained with DAPI and immunoprobed for laminin 332. (Scale bar = 200 µm).

The use of decellularized tissue matrices was also investigated as a scaffold for tumour cell colonisation. Tissue was excised from mammary glands of rats immediately post-sacrifice. The successful removal of native cells during the decellularization process was assessed by DAPI staining (Fig. 3.29A); the resultant

tissue contained no significant cellular population. However, incubation of the tissue with MCF7 cells revealed it had been successfully colonised (Fig. 3.29B). The tissue was also immunoprobed for laminin 332, a cell adhesion molecule deposited by MC7 cells in monolayer cultures and may promote cell migration (Carpenter et al. 2009). Similarly, the decellularized tissue did not stain positively for laminin 332 whereas colonised tissue did, suggesting *de novo* synthesis.

The spheroid cultures and decellularized matrices produced therefore serve as functional models to further investigate tumour cell behaviour within a context more reflective of the TME. Spheroid cultures successfully demonstrated distinct cell subpopulations indicative of altered environmental conditions and supported the nuclear localisation of survivin presented within hypoxic monolayer cultures.

3.3 Discussion

As a downstream target of the HIF1a transcription factor, survivin upregulation occurs in response to hypoxic conditions. Despite the similarities between the cellular adaptations demonstrated in hypoxia and the associated effects of survivin expression, such as altered cell metabolism and therapeutic resistance, few studies have investigated the role survivin may play in realising these adaptations. Given the link between survivin's subcellular localisation and its functional activity, an understanding of its expression profile in this context might be informative to its contribution to cellular adaptations.

3.3.1 Hypoxia induces translocation of survivin to the cell nucleus and mitochondria.

Rapid accumulation of survivin within the nucleus of HeLa cell was demonstrated upon exposure to a hypoxic 1% oxygen environment that is characteristic of cervical tumours (Vaupel et al. 2007c) and was maintained for the duration of the 24h time period tested. A small but gradual decline in DAPI colocalization suggests this translocation may be a transient and further decline over time, although reversal to a predominantly cytoplasmic population was not observed in the time frame tested. Similar results were also obtained using the cancerous U2OS cell line and non-cancerous MRC5 cell line, suggesting this may be a universal cell response and not specific to cancerous cells.

The rapid nuclear translocation demonstrated is suggestive of post-translational modifications or protein interactions rather than de novo protein expression. Notably these results were obtained using a survivin-GFP construct with a molecular weight of approx. 45 kDa, which may be to be inhibitory to passive nuclear diffusion (Connell et al. 2008) and indicative of an active transport mechanism. However,

more recent research has suggested the upper limits for passive diffusion are considerably larger than once thought (Wang, Brattain 2007) or have disputed the notion of a hard limit (Timney et al. 2016). The ability of SVN-GFP to model behaviour of endogenous survivin protein was determined both through immunofluorescent imaging and immunoblotting of subcellular fractions. Both confirmed a nuclear translocation of survivin while immunoblotting additionally revealed an increased mitochondrial pool. Determination of mitochondrial survivin through imaging is often difficult due to obfuscation by the cytoplasmic population (Beghein et al. 2016). This is consistent with the Dohi et al. study investigating the subcellular localisation of survivin under hypoxic conditions, in which they similarly found an increased mitochondrial population but failed to investigate any alterations in the nuclear population (2004). This novel finding poses interesting questions for nuclear survivin's functional role under these environmental conditions. Nuclear translocation of survivin is largely associated with its role in mitosis during its entry in late G2, yet hypoxia is associated with decreased cell proliferation rates (Hubbi, Semenza 2015). Furthermore, nuclear survivin is regarded as lacking cytoprotective qualities (Connell et al. 2008), however cells under hypoxic conditions typically demonstrate increased apoptosis resistance (Harris 2002). It appears counterintuitive cells would invest in survivin upregulation under adverse environmental conditions only to relegate the protein to a subcellular location in which it has no clear functional role. Whilst a direct link between nuclear survivin and hypoxia has not been observed before, numerous studies have observed altered nuclear-to-cytoplasmic ratios with the aim of assessing its prognostic value, although with inconsistent findings (Rexhepaj et al. 2010; Brennan et al. 2008; Vischioni et al. 2004; Kim, McNiff 2008).

Under hypoxic conditions, all three cell lines tested demonstrated nuclear survivin foci in a subset of cells. DNA content analysis revealed hypoxia-mediate cell cycle arrest, consistent with previous research (Hubbi, Semenza 2015), with an

accumulation of late S/G2 phase cells. These foci additionally colocalised with CENPA, which is typically associated with centromeres, and is consistent with survivin's expression pattern during the G2/M transition (Beardmore et al. 2004). Whilst this may clarify the foci developed in a minority of cells, it fails to explain the near ubiquitous nuclear translocation observed nor its short time frame given the 30-hour doubling time of U2OS cells (Musa et al. 2013).

Transport of survivin to the cell nucleus is also documented in response to genotoxic stress (Capalbo et al. 2010) with a link to hypoxia through activation of the DNA repair pathway in response to low oxygen levels (Scanlon, Glazer 2015). This effect was shown to be specific to genotoxic stress rather than all apoptosis-inducing agents, such as the broad acting ATP-kinase inhibitor staurosporine (Belmokhtar et al. 2001). Indeed, treatment with DNA damaging agents, UVC and etoposide, induced rapid nuclear accumulation of survivin. However, treatment with doxorubicin failed to replicate this response. Like etoposide, doxorubicin also functions as a topoisomerase II inhibitor capable of inducing DSBs but exhibits the additional ability to induce histone damage and eviction (Qiao et al. 2020). As H2AX histone phosphorylation is an important step in the recruitment of DNA repair machinery and its consequent repair, doxorubicin is thought to attenuate the DNA damage response (Pang, Qiao, Janssen, Velds, Groothuis, Kerkhoven, Nieuwland, Ovaa, Rottenberg, Van Tellingen, et al. 2013). Similarly, addition of the DNA-PKcs/PI3K inhibitor, KU-0060648, ablated nuclear transport when combined with UVC irradiation. This would further suggest nuclear translocation occurs as a downstream product of the DNA repair pathway and is contingent on DNA-PKcs and/or PI3K activity in this context. As recent research as linked survivin with DNA repair and possibly direct interaction with NHEJ machinery (Cheng et al. 2021b; Capalbo et al. 2010), these findings are consistent with an implicated role for survivin in the DNA damage response. Further links to the TME were also demonstrated with sustained nuclear survivin in response to reoxygenation and

serum starvation, with cyclical hypoxia (Kim et al. 2007) and nutrient deprivation (White et al. 2020) constituting key characteristics of tumour development and are associated with activation of the DNA repair pathway. However, it remains to be determined whether nuclear accumulation under hypoxia operates with the same molecular mechanism.

A clearer role for the elevated mitochondrial pool may be suggested, with previous research demonstrating increased apoptosis resistance (Dohi, Beltrami, et al. 2004) and reduced oxidative phosphorylation (Townley, Wheatley 2020). These downstream effects are consistent with the adaptations noted in hypoxic cells, in which therapeutic resistance (Cuvillier et al. 2013) and an increased reliance on glycolysis for energy production are key characteristics (Robey et al. 2005).

Overall, these data demonstrate clear nuclear and mitochondrial localisation of survivin in response to hypoxia, whose downstream impacts remain to be fully explored.

3.3.2 Nuclear translocation is not reliant on K129, S20 or T34 modifications.

Numerous post-translational modifications are associated with alterations to survivin's function and localisation within the cell. Acetylation of K129 is thought to promote surivivin dimerization and concomitant obstruction of its central NES sequence, diminishing nuclear export. K129 acetylation is associated with increased STAT3 repression (Wang et al. 2010) and its dysregulation may lead to mitotic defects (Aljaberi et al. 2015). Despite a clear link to nuclear localisation, expression of a construct lacking the K129 amino acid failed to prevent this phenotype.

Phosphorylation of survivin at S20 is mediated by PKA and is associated with altered XIAP binding capacity with downstream implications for its cytoprotective role

within the cell (Dohi et al. 2007). XIAP has similarly demonstrated a nuclear translocation to the cell nucleus following hypoxia-ischemia (Russell et al. 2008). It was therefore considered that survivin may also be transported with XIAP. However, inhibiting this binding interaction through an S20 phosphomimetic similarly failed to the retain survivin within the cytoplasm. One caveat is, whilst S20 phosphorylation have previously been shown to determine the ability of survivin to bind to XIAP (Dohi et al. 2007), this study did not confirm XIAP binding in these S20 constructs.

Similarly, T34 plays dual role depending on its phosphorylation status (Barrett et al. 2009). In its unphosphorylated form, survivin promotes proliferation at the expense of its cytoprotective effects. Conversely, cdk1 mediated phosphorylation retards cell proliferation but confers greater resistance to TRAIL and X-irradiation, promoting cell survival (Barrett et al. 2009). This phenotype presents clear similarities to the reduced cell growth and increase therapeutic resistance of tumour cells in hypoxia. However, neither phosphomimetic nor phosphoresistant T34 substitutions impacted survivin localisation. It should be noted that while these modifications did not alter localisation, these finding do not preclude their potential role in hypoxia.

Assessment of HSP90, a survivin binding partner with implicated roles in the nuclear transport of other proteins (Csermely et al. 1995), also failed to alter nuclear accumulation. However, treatment with its inhibitor, geldanamycin, notably induced cell cycle arrest with evidence this occurred during the late G2 phase. This raised the intriguing possibility of repurposing geldanamycin as tool for cell synchronisation.

3.3.3 Geldanamycin as a tool for cell synchronisation

3.3.3.1 - Cell Synchronisation

The tightly orchestrated and complex process of cell division has garnered widespread interest amongst researchers for its fundamental role in biological and pathological development. Experimental procedures isolating mitotic cells have been a mainstay of cell cycle research and range from physical fractionation to chemical blockades (Banfalvi 2011), with the aim of enriching distinct subpopulations of cells at various stages of the cell cycle.

Whilst the isolation of these subpopulations is a fundamental prerequisite of cell synchronisation techniques, biological research often requires multiple additional criteria to be met. These may include non-toxicity, reversibility and otherwise limited alteration of cellular pathways. Despite the array of techniques available, none perfectly satisfy all conditions. For example, chemical techniques reliant on the inhibition of DNA synthesis (e.g., thymidine and hydroxyurea treatments) or mitotic spindle formation (e.g., nocodazole treatment) exhibit toxicity and growth imbalance (Banfalvi 2011).

Here we explored the potential role of geldanamycin as a cell synchronisation agent. Whilst discovery of HSP90 is owed to its elevated expression during the heat shock response, HSP90 plays essentials roles in multiple pathways under physiological conditions. Functioning as a molecular chaperone, HSP90 aids the folding, assembly, maturation and stabilisation of numerous client proteins (Zhang, Burrows 2004).

Of particular note is the serine/threonine protein specific kinase Akt, which is reliant on HSP90 to maintain its activity by preventing protein phosphatase 2A (PP2A)-mediated dephosphorylation and consequent inhibition (Sato et al. 2000). As part

of the phosphatidylinositol 3'-kiniase (PI3K)-Akt signalling pathway, Akt is responsible for a variety of cellular processes including the cell cycle, growth and cell survival (Madhunapantula et al. 2011). Following PI3K activation, Akt is recruited to the membrane and fully activated by phosphoinositide-dependent kinases PDK1 and PDK2 (Cantley 2002; Partovian, Simons 2004). Additionally, HSP90 has been shown to maintain the stability and activity of PDK1 (Fujita et al. 2002). Downstream targets of this pathway include cyclin D through the inactivation of the cell-cycle-dependent kinase (CDK) inhibitors $p27^{KIP}$ and $p21^{WAF}$. Cyclin D in turn promotes the G_1/S transition by inhibiting retinoblastoma protein (Rb) (Musgrove et al. 2011). Furthermore, Akt activity is thought to promote G_2/M transition. Whilst the precise mechanism of Akt-mediated regulation at this point is not well characterised, it has been suggested Akt mediates $p21^{WAF}$ localisation and subsequent phosphorylation (Wu et al. 2011).

3.3.3.2 - Geldanamycin

Geldanamycin is thought to bind to the amino acid terminus of HSP90, a region responsible for adenosine triphosphatase activity. Competitive binding with this region inhibits HSP90's ability to function as a chaperone and consequently destabilises its downstream targets.

Whilst the inhibitory effects of geldanamycin and its derivatives on cell growth have been reported in numerous previous studies (Kim et al. 1999; McIlwrath et al. 1996; Karkoulis et al. 2013), these aim to explore geldanamycin treatment as a potential anti-cancer strategy. As such, aspects of drug treatment such as reversibility and subsequent cell tolerance were not explored. Measurements of relative growth rates compared to control cells in U2OS, MRC5 and RPE cell lines demonstrated reversible cell cycle arrest, although a narrow treatment range that supported recovery from HSP90 inhibition was observed in MRC5 cells. Moreover, the treatment concentration could vary significantly between cell lines; RPE and U2OS

were tolerant of concentration up to 2.5 μM while 500 nM treatment of MRC5 cells exhibited significant toxicity. Appropriate treatment concentrations that supported reversible cell cycle arrest with minimal cell toxicity were however demonstrated.

Despite lowered proliferation rates, DNA content analysis revealed that changes to the distribution of cell cycle phases varied between cell lines. This may be due to dual action of geldanamycin in inducing cell cycle arrest, with reports of both G1 (Karkoulis et al. 2013) and G2 (Lee 2018) arrest. Pre-treatment and release of cells from thymidine treatment was employed in an effort to arrest cells as they progressed through G2, enriching the G2/M specific population. Results were similarly varied however. Whilst RPE cells responded effectively to this regime, U2OS cells, which demonstrated significant G2/M enrichment already, and MRC5 cells saw little to no increase. Moreover, image analysis of cell lines following combination treatment revealed an increase in their metaphase populations rather than late G2 phase cells, as suggested by geldanamycin treatment alone.

Together these data suggest geldanamycin may function as a cell synchronisation agent, with reversible cell cycle arrest and minimal toxicity. However, treatment concentrations and its specific enrichment of cell cycle populations appear to be dependent on the cell line used. Its utilisation would therefore require further testing to determine specific effects and parameters for different cell lines.

3.3.4 Spheroid cultures and decellularized matrices reveal unique cell phenotypes

The generation of viable tissue matrices requires the removal of the native cell population and preservation of the matrix ultrastructure to support the establishment of cell colonies subsequently introduced. The excision of rat mammary tissue and its subsequent decellularization appeared to successfully generate a sterile tissue scaffold that supported colonisation by the MCF7 cell line.

The capability of the matrix to function as a biomimetic scaffold additionally requires the conservation of tissue bioactivity, however. Whilst the removal of the native cell population was evidenced by the lack of DNA staining, the preservation of native ligands during the decellularization process remains to be established. These key protein constituents may regulate a wide range of cell responses, including cell adhesion, migration and differentiation (Kim et al. 2011). Mammary tissue specifically has been shown to contain a range of protein elements within its ECM, including collagens I-VI, fibronectin and periostin, and are together associated with modulating tumour progression, proliferation and metastasis (Zhu et al. 2014; Rijal, Li 2017). Proteomic analysis of the tissue matrix by mass spectrometry would enable the systematic identification of the protein constituents (Rijal, Li 2017), which may be further verified by immunoblotting of tissue extracts.

The preliminary work on 3D spheroid cultures aimed first to assess their ability to recapitulate the varied environmental conditions of the TME. Both the MRC5 and MCF7 spheroids generated exhibited distinct expression phenotypes within different regions depending on their relative distance to the spheroid-media interface. As media must diffuse through the spheroid, nutrient and oxygen availability transitions from regions that support proliferation to hypoxic regions limited in nutrient availability. Similarly, cells near the centre are subject to waste build up and changes in extracellular acidity. Necrotic regions may also lead to cell death and release of signalling molecules, such as damage associated molecular patterns (DAMPs), that may initiate a range of cell pathways (Geck et al. 2018). The generation of different phenotypic subpopulations therefore suggested that the spheroids successfully established varied microenvironments that may be used to examine cell behaviour within the context of the heterogenous TME.

Both MRC5 and MCF7 cells exhibited reduced E-cadherin expression. As a key component of the adherens junctions, E-cadherin plays a core role in the

maintenance of cell adhesion and cell junction formation with a cytoplasmic tail that initiates intracellular signalling, including the Wnt, TGFβ and Hippo growth factor pathways (Mendonsa et al. 2018). Loss of E-cadherin is associated with the epithelial-mesenchymal transition (EMT), a process in which cells undergo biochemical changes that result in characteristics of mesenchymal cells, such as increased migratory capacity and production of EMC components (Kalluri, Weinberg 2009). Hypoxia-induced EMT constitutes a key event in the development of aggressive, metastatic tumours (Tam et al. 2020). MCF7 cells additionally exhibited nuclear localisation of E-cadherin. Whilst typically localised at the cell membrane, nuclear E-cadherin has also been observed in tumour tissues and is associated with tumorigenesis via enhanced β-catenin activity (Y. Zhao et al. 2019). Survivin localisation was also shown to differ between the outer spheroid regions, which experience higher oxygen and nutrient availability, and the hypoxic inner regions. Together these data support the findings of hypoxic monolayer cultures seen previously. Spheroid cultures therefore demonstrate the unique benefits of 3D culture models by reflecting the heterogeneity of tumour cell populations to unveil cell behaviours that may not be replicated by traditionally normoxic monolayer cultures.

3.3.5 Summary

These data reveal a unique nuclear and mitochondrial localisation of survivin in response to hypoxic conditions, although the molecular mechanisms underpinning this process remain to be elucidated. Nuclear translocation may possibly be linked to its accumulation within the nucleus seen in response to genotoxic stress, which appears to be contingent on the PI3K pathway. Initial work generating 3D cultures to further probe cancer cell activity successfully replicated these observations within the hypoxic spheroid regions. However, the downstream consequence of these subcellar pools requires further investigation.

Chapter 4 – Nuclear survivin is cytoprotective

4.1 Overview

4.1.1 Survivin inhibits apoptosis within the cytoplasm

The role of survivin in enhancing cancer cell survival and therapeutic resistance is well established and has been attributed to a number of proposed mechanisms, summarised in Fig. 4.1. It was speculated survivin may directly inhibit caspase enzymes (Tamm I et al. 1998). However, structural analysis suggests survivin lacks the moiety responsible for caspase-3 docking to the BIR domain (Eckelman et al. 2006). In contrast, XIAP utilises a two-site binding mechanism with caspase molecules to directly inhibit their activity in a manner unique to IAP members (Eckelman et al. 2006). Survivin may form a complex with XIAP to protein stabilisation and thereby facilitate caspase inhibition indirectly (Altieri 2010; Dohi, Okada, et al. 2004), although this mechanism has been challenged (Zumbrägel et al. 2017). Alternatively, survivin may cooperate with Hepatitis B X-interacting protein (HBXIP) to inhibit APAF1 recruitment and the resulting formation of the apoptosome, preventing caspase-9 activation (Marusawa et al. 2003).

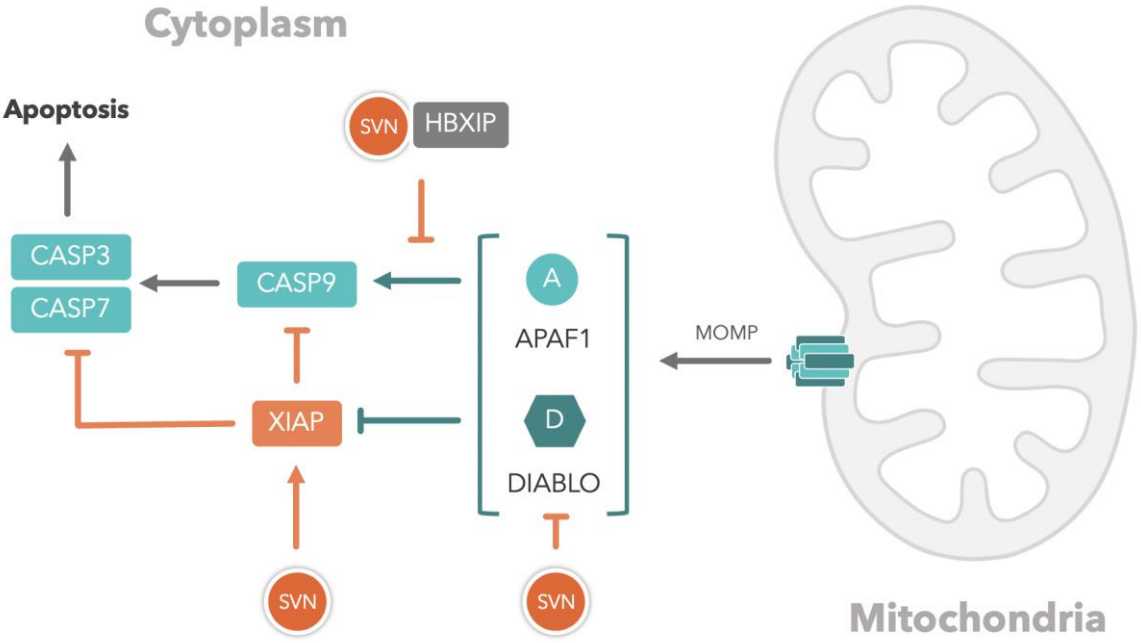


Figure 4.1 – Inhibition of the intrinsic apoptotic pathway by survivin. Following the release of pro-apoptotic factors form the mitochondria, survivin can bind to DIABLO and prevent its inhibition of the anti-apoptotic protein XIAP. Further, survivin may coordinate with HBXIP to prevent APAF1 recruitment and subsequent activation of caspase 9 as well as XIAP to facilitate inhibition of caspase proteins directly. Created by author.

The mitochondrial pool of survivin, identified exclusively within cancerous cell lines, is also thought to promote cell survival. Induction of apoptosis rapidly discharged more than 70% of mitochondrial survivin into the cytosol within 4 hours and exhibited enhanced anti-apoptotic activity (Dohi, Beltrami, et al. 2004). The underlying mechanism mediating this augmented cytoprotection remains to be characterised.

Notably, these anti-apoptotic pathways are reliant on interactions within the cell cytoplasm and forced localisation of survivin to the nucleus has been associated with a loss of cytoprotective capabilities (Connell et al. 2008) (Knauer et al. 2007).

These studies would therefore suggest the anti-apoptotic capabilities of survivin are tied to its cytoplasmic residency.

4.1.2 Survivin influences DNA repair and genotoxic resistance.

A number of reports have implicated a role for survivin in mediating the cell response to DNA damage. The precise mechanism and downstream consequences of survivin expression within this context remain unclear, however. Whilst survivin expression may potentiate genomic instability within cancer cells (Conde et al. 2017b), numerous studies have suggested survivin may protect against genotoxic stress, facilitate DNA repair and ultimately promote cell survival (Reichert et al. 2011; Güllülü et al. 2021; Véquaud et al. 2016; Hu et al. 2015). A number of potential mechanisms have been proposed (summarised in Fig. 4.2), including upregulation of HR genes to promote DNA repair and mitigation of excessive autophagy to reduce ROS-mediated DNA damage (Cheng et al. 2021). A direct interaction with DNA repair proteins has also been demonstrated where DNA damage was shown to induce nuclear accumulation of survivin and colocalisation with DNA repair proteins (Capalbo et al. 2010). Later work demonstrated binding of survivin to DNA-PKcs, which may alter substrate specificity and aid DNA repair (Güllülü et al. 2021). Survivin was shown to switch DNA-PKcs activity towards substrates with a S/T-P motif and away from those containing S/T-Q motifs, which paradoxically includes a number of NHEJ factors (e.g., Artemis, Ligase IV and XRCC4). Instead, it was proposed survivin may lead to DNA-PKcs-mediated phosphorylation of proteins such as Foxo3, high-mobility group AT-hook 2 (HMGA2) and filamin-A, leading to downregulation of pro-apoptotic factors and increased DNA-PKcs complex activity and stabilisation respectively (Güllülü et al. 2021). Again, the precise role survivin may play in mitigating genotoxic stress and its mechanism are not well characterised.

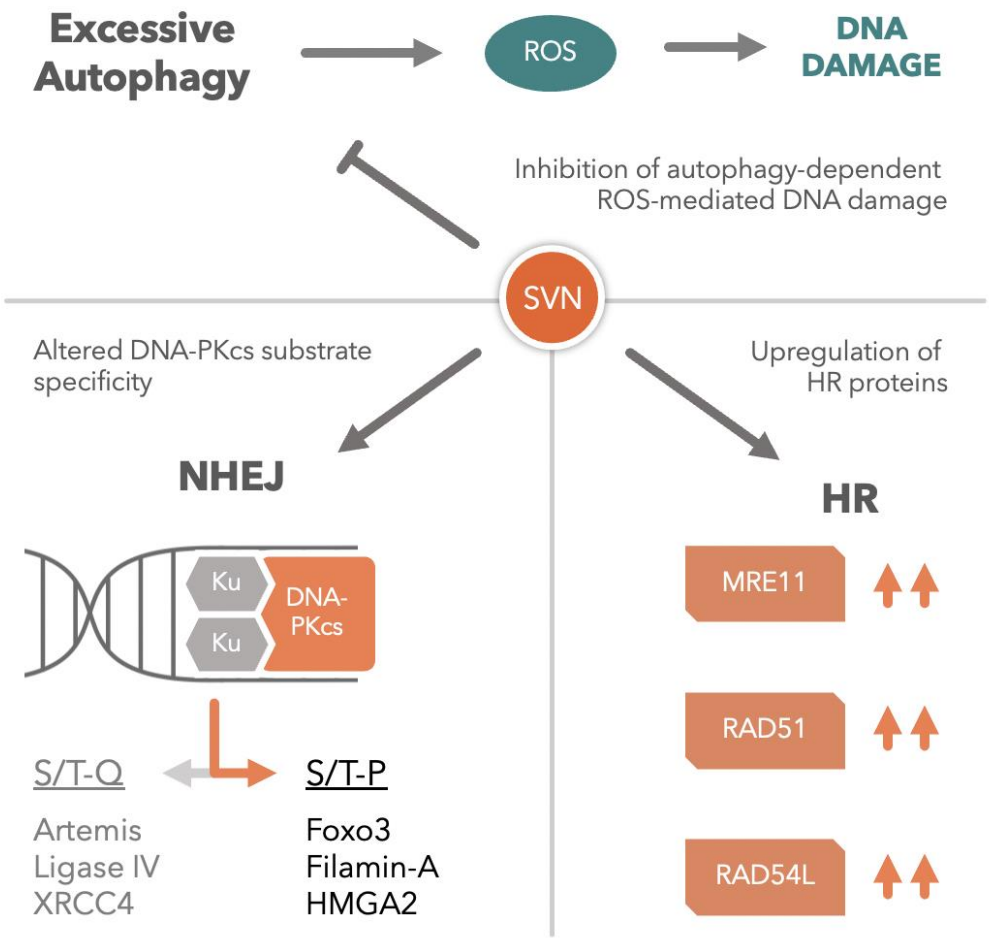


Figure 4.2 – Implicated roles for survivin in mitigating DNA damage. Recent studies have implicated a number of roles for survivin in the management of DNA damage and induction of cell death pathways. Survivin may inhibit excessive autophagy to limit ROS production and thereby reduce ROS-mediated DNA damage (Cheng et al. 2021). The binding of survivin to DNA-PKcs may alter its substrate specificity and redirect activity to targets involved in the expression of pro-survival genes and DNA-PKcs stability (Güllülü et al. 2021). Finally, survivin may facilitate DNA repair indirectly via upregulating proteins involved in HR (Cheng et al. 2021). Created by author.

4.1.3 Aims

With the impact of nuclear and mitochondrial survivin localisation on cytoprotection being unknown, this chapter aims to investigate whether survivin is able to facilitate apoptosis resistance under hypoxia and the role of these subcellular pools in mediating this response. It further aims to assess the potential contribution of DNA repair pathways in survivin-mediated cell survival.

Specifically, this chapter aims to assess whether:

- over-expression or siRNA-mediated inhibition of survivin correlates with cell viability following treatment with cytotoxic agents.
- this potential correlation is maintained under hypoxic conditions compared to normoxic cells.
- survivin expression levels correlate with cell survival following treatment with genotoxic agents when DNA repair pathways have been inhibited.

4.2 Results

4.2.1 Survivin is cytoprotective under normoxic and hypoxic conditions

To understand the downstream implications of survivin repositioning under hypoxia, U2OS cells were challenged with the apoptosis inducing agent zeocin to assess survivin-mediated cytoprotection. As a radiomimetic, zeocin induces DSBs in the DNA and initiates the intrinsic apoptotic pathway as a consequence (Petering et al. 1990). Cells were treated with zeocin for 4h followed by a 20h recovery period to imitate the initial burst of DNA damage produced by X-radiation used in therapy and assess the influence of subsequent DNA repair on cell survival. An IC50 concentration for this treatment was first determined (Fig. 4.3A). U2OS cell lines were pre-treated with siRNA to establish a range of intracellular survivin levels (Fig. 4.3B): U2OS GFP cells treated with survivin siRNA (low survivin levels), U2OS GFP cells treated with control siRNA (normal survivin levels) and U2OS SVN-GFP cells treated with control siRNA (high survivin levels). SVN-GFP constructs notably included a silent C56G mutation, conferring exogenous survivin a resistance to siRNA knockdown. An effective knockdown of endogenous survivin (~80%) was verified by western blot analysis of treated samples (Fig. 4.3D). Additionally, cells were placed in either normoxic or hypoxic conditions and then the impact of zeocin treatment on apoptotic response was determined by caspase assay.

A clear relationship between zeocin resistance and survivin expression was established in normoxic conditions, with cell survival significantly increasing with survivin levels (Fig. 4.3B). Although a similar trend was observed under hypoxia, all groups exhibited reduced sensitivity and limited cell death within this context. Differences between hypoxic groups were therefore less clear, albeit a significant increase in survival was seen between survivin siRNA and control siRNA treated GFP cells and is supported by similar results in Fig. 4.7B.

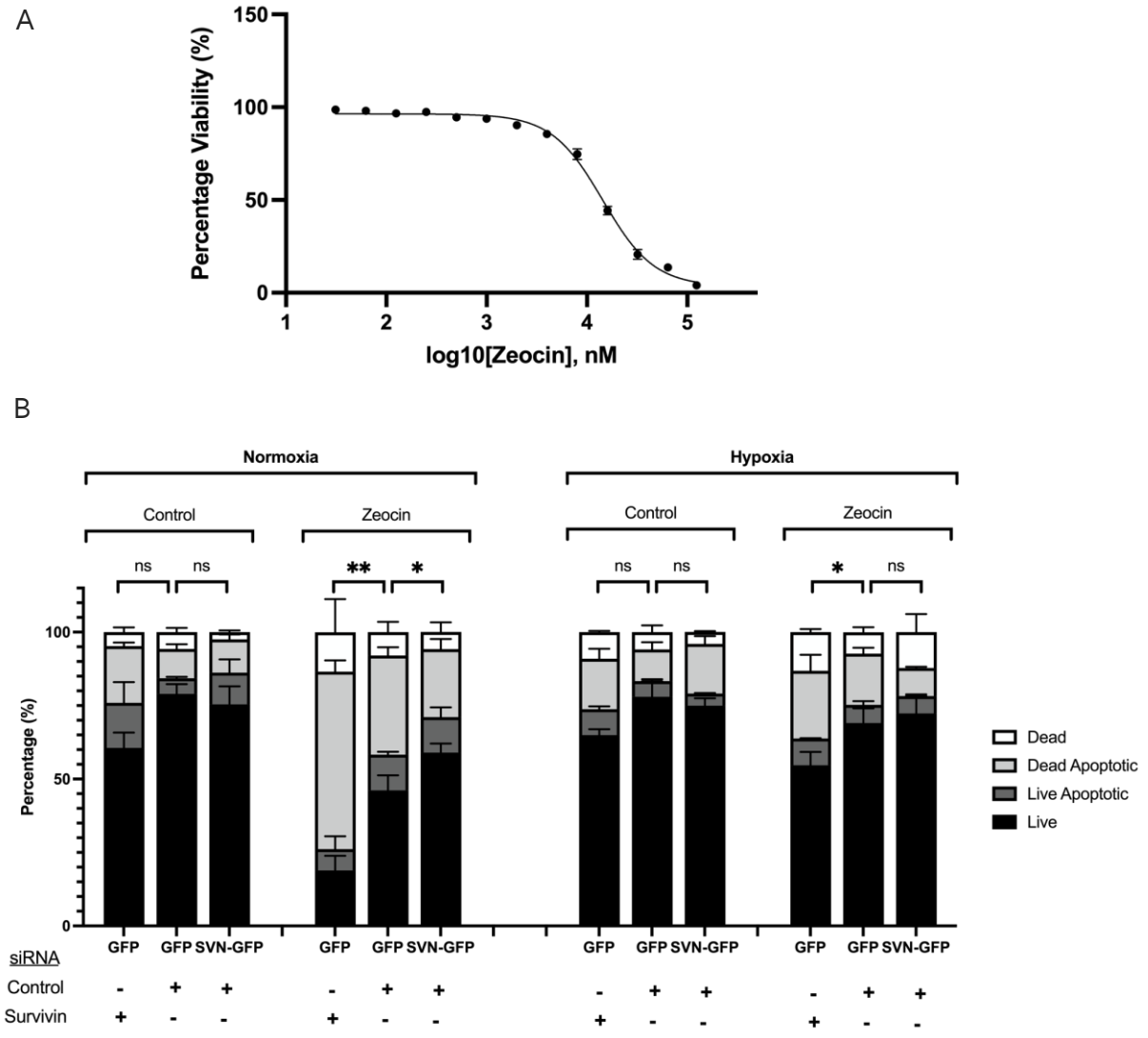


Figure 4.3 – Survivin protects against genotoxic damage in both normoxia and hypoxia. (A) IC50 curve for 4h zeocin treatment followed by a 20h recovery period. Error bars represents SEM of means from three separate experiments. **(B)** Comparison of apoptosis between normoxic and hypoxic samples and its relationship with survivin expression. Error bars represent SEM of means from two separate experiments. (ns, not significant; **, p <0.01; *, p <0.05)

4.2.2 Survivin regulates expression of cell survival proteins

As the cytoplasmic residency of survivin is thought to be necessary for its cytoprotective protein interactions, yet survivin appears to be nuclear under hypoxia (Chapter 3.2.1), the mechanism through which survivin promotes treatment resistance are unclear. The expression of survivin and other factors involved in regulating apoptosis, namely XIAP and p53, were subsequently assessed in response to siRNA treatments under these conditions (Fig. 4.4A). No significant differences were observed in the protein levels of XIAP under normoxia (Fig 4.4B). However, a significant increase was seen with survivin overexpression under hypoxia, suggesting XIAP may be stabilised as a consequence of survivin expression and may facilitate therapeutic resistance in this context. The apoptosis inducing protein, p53, exhibited a negative correlation with survivin expression under normoxia (Fig. 4.4C), as previously reported (Wang et al. 2004). In contrast, p53 was downregulated under all conditions under hypoxia, with no clear relationship to survivin levels. While this expression profile may support hypoxia-mediated resistance, it fails to explain the cytoprotection conferred by survivin within this setting. Finally, levels of the endogenous survivin protein were also assessed (Fig. 4.4D). As previously commented, siRNA treatments induced significant knockdown of survivin under both normoxic and hypoxic conditions. Moreover, hypoxia led to a significant increase in survivin levels, further supporting a role for hypoxia induced resistance through altered expression of apoptotic factors.

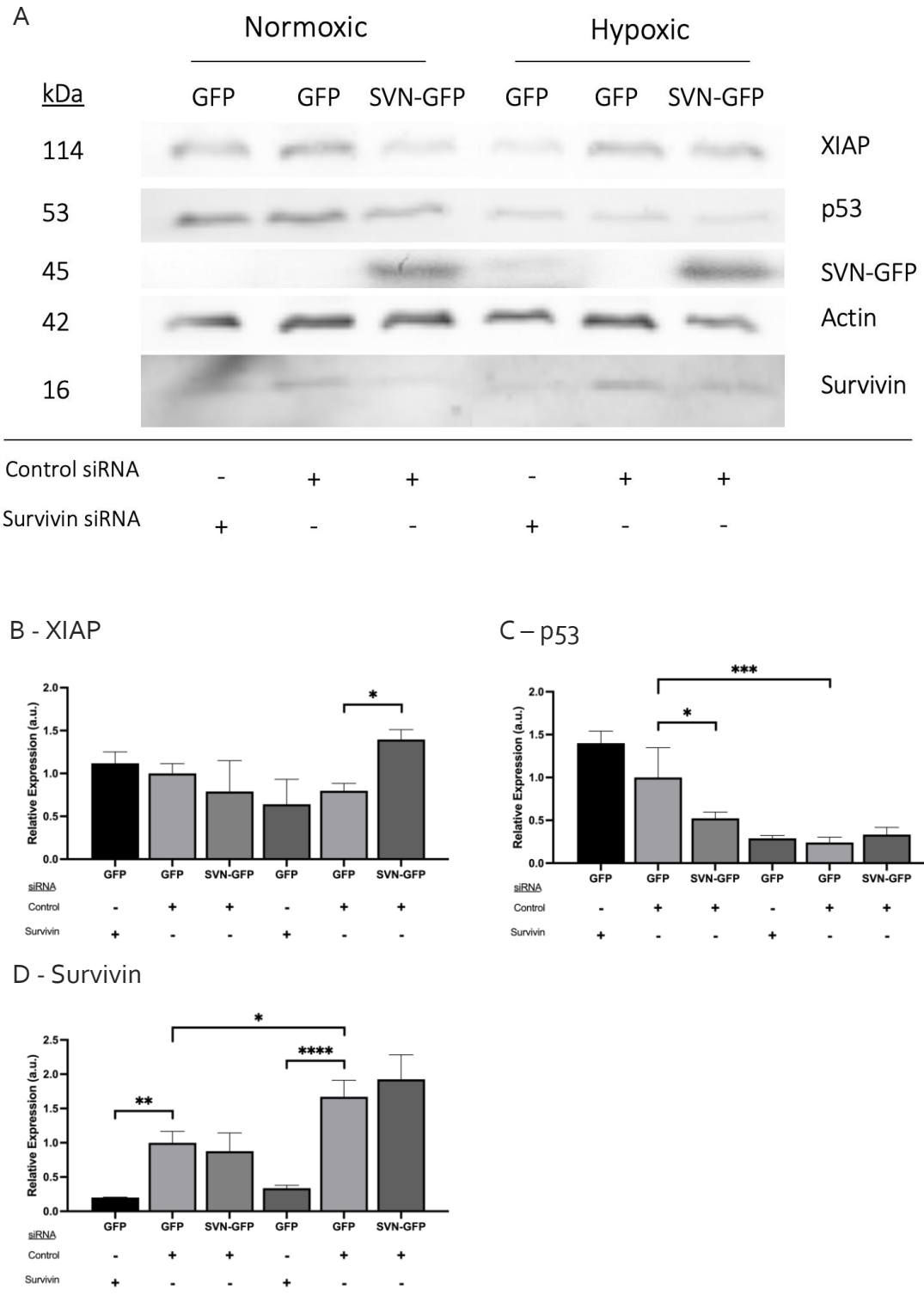


Figure 4.4 – Expression of apoptotic regulators by hypoxia and survivin. (A) Immunoblot of U2OS GFP and SVN-GFP cells treated with control or survivin siRNA followed by 24h

incubation under normoxic or hypoxic conditions. Semi-quantitation of immunoblots probed for XIAP **(B)**, p53 **(C)** and survivin **(D)**. Values are normalised to actin and expressed as relative expression to normoxic GFP samples treated with control siRNA. Error bars represent SD of means. (****, p <0.0001; ***, p <0.001; **, p <0.01; *, p <0.05; n=3)

Next, transcriptional regulation of genes mediating cell survival was assessed by RT-PCR of mRNA extracts from U2OS GFP and SVN-GFP cells incubated under normoxic or hypoxic conditions for 24h (Fig. 4.5). Identification of suitable reference genes was determined by comparing the relative threshold breaking cycle (C_T) values of TBP, actin and tubulin transcripts between samples conditions (Fig. 4.5A). TBP and actin were shown to be expressed most uniformly between conditions and were subsequently used for normalisation.

Due to the additionally expression of the ectopic survivin constructs, SVN-GFP cells demonstrated significantly increased survivin mRNA levels under normoxic and hypoxic conditions (Fig. 4.5B). However, transcription of survivin within GFP cells was not shown to increase under hypoxia, contrasting with the elevated protein levels previously observed, together suggesting survivin may be stabilised under these conditions.

HIF1a mRNA levels were also shown to remain stable in both conditions. Whilst elevated HIF1a protein is associated with hypoxia, expression levels are variable and largely determined by the timeframe investigated, demonstrating a rapid increase upon initial exposure and declining over time (Ravenna et al. 2014; Lee et al. 2019). Its stable expression at 24h in hypoxia mirrors the expression pattern of survivin, in line with its role a transcriptional regulator of BIRC5.

VEGF expression demonstrates upregulation under hypoxia compared to normoxic conditions for both GFP and SVN-GFP cells (Fig. 4.5B) and is consistent with other

HRE genes, such as GLUT1 and CA-IX (Lin et al. 2011) explored in 5.2.1. Unexpectedly however, expression within SVN-GFP cells was downregulated relative to GFP cells under both conditions. As an angiogenic factor (Li et al. 2018), this may suggest survivin impairs the induction of new blood vessel formation and promotes tumour hypoxia as a result.

Anti- and pro-apoptotic factors, XIAP and p52 respectively, also demonstrated unchanged mRNA expression under hypoxia (Fig. 4.5B), suggesting their altered protein levels are governed by post-transcriptional processes.

Apoptosis inducing factor mitochondria associated 1 (AIFM1) demonstrated downregulation under hypoxia specifically in SVN-GFP cells (Fig. 4.5B). As a factor involved in mediating oxidative phosphorylation and apoptosis, its downregulation is associated with reduced OXPHOS and increased apoptotic resistance (Xiong et al. 2016; Zhang et al. 2019).

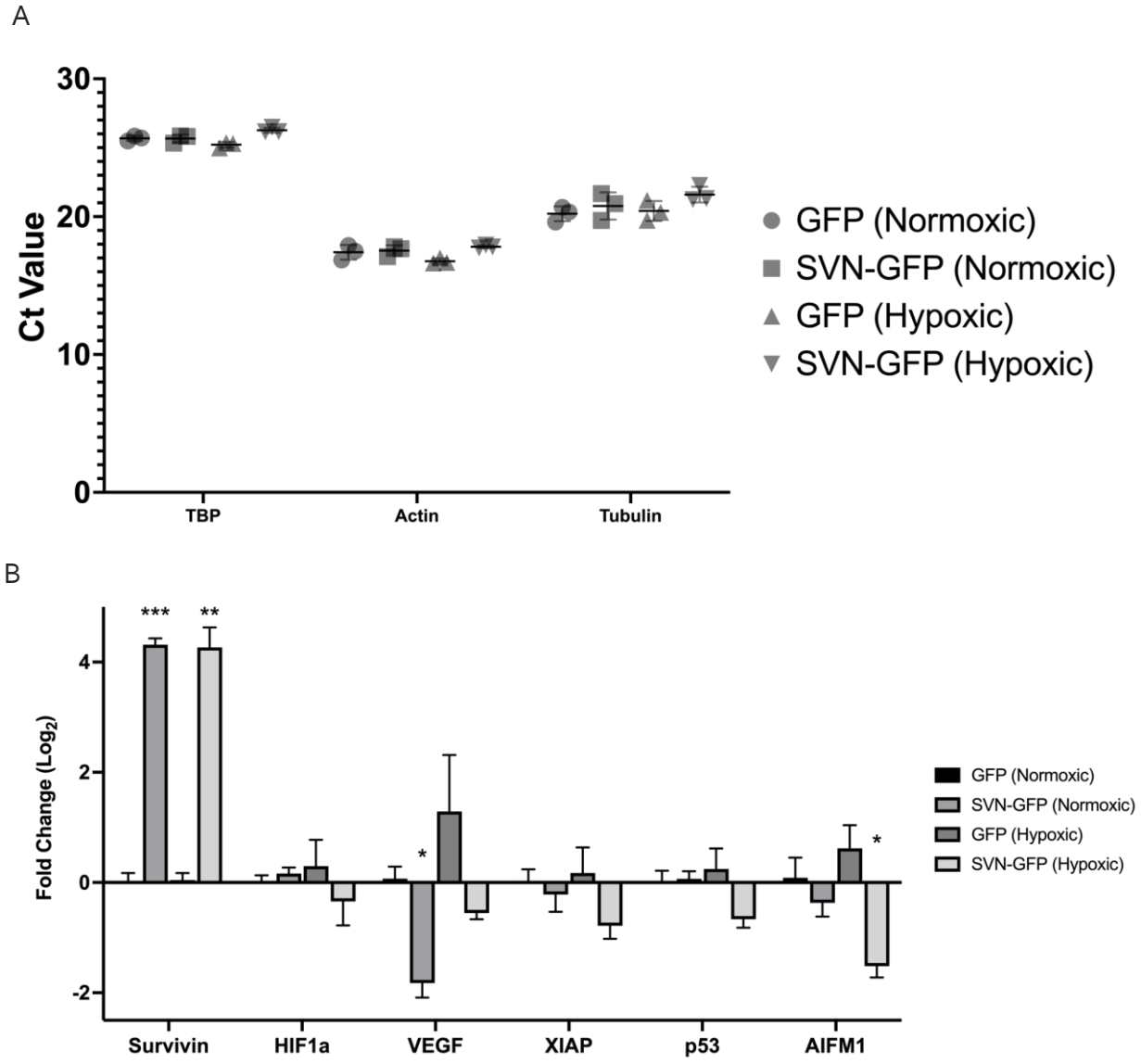


Figure 4.5 – Differential expression of cell survival genes by survivin. **(A)** Comparison of candidate reference genes, TATA-Box Binding Protein (TBP), actin and tubulin in treatment conditions. **(B)** Expression of genes involved in hypoxia and cell survival. Error bars represent SD of means (***, p <0.001; **, p <0.01; *, p <0.05; n=3).

4.2.3 Nuclear and mitochondrial targeted survivin is cytoprotective

To further examine the potential cytoprotective capabilities of mitochondrial and nuclear pools of survivin, SVN-GFP constructs containing either an NLS (SVN-NLS-GFP) or MTS sequence (MTS-SVN-GFP) were stably expressed in U2OS cells. Correct localisation of these constructs was determined by imaging fixed samples with nuclear and mitochondrial markers. Specifically, GFP signal overlap with DAPI staining was used as a measure of nuclear localisation whilst signal overlap with MitoTracker was used as a measure of mitochondrial localisation (Fig. 4.6). Results were quantified by comparing mean GFP signal intensity in the region of interest to the cytoplasmic signal intensity. These ratios were compared to control cells expressing a survivin-GFP construct. While MTS-SVN-GFP was expressed exclusively within the mitochondria, SVN-NLS-GFP retained some cytoplasmic signal, although the average signal intensity was significantly higher in the nucleus.

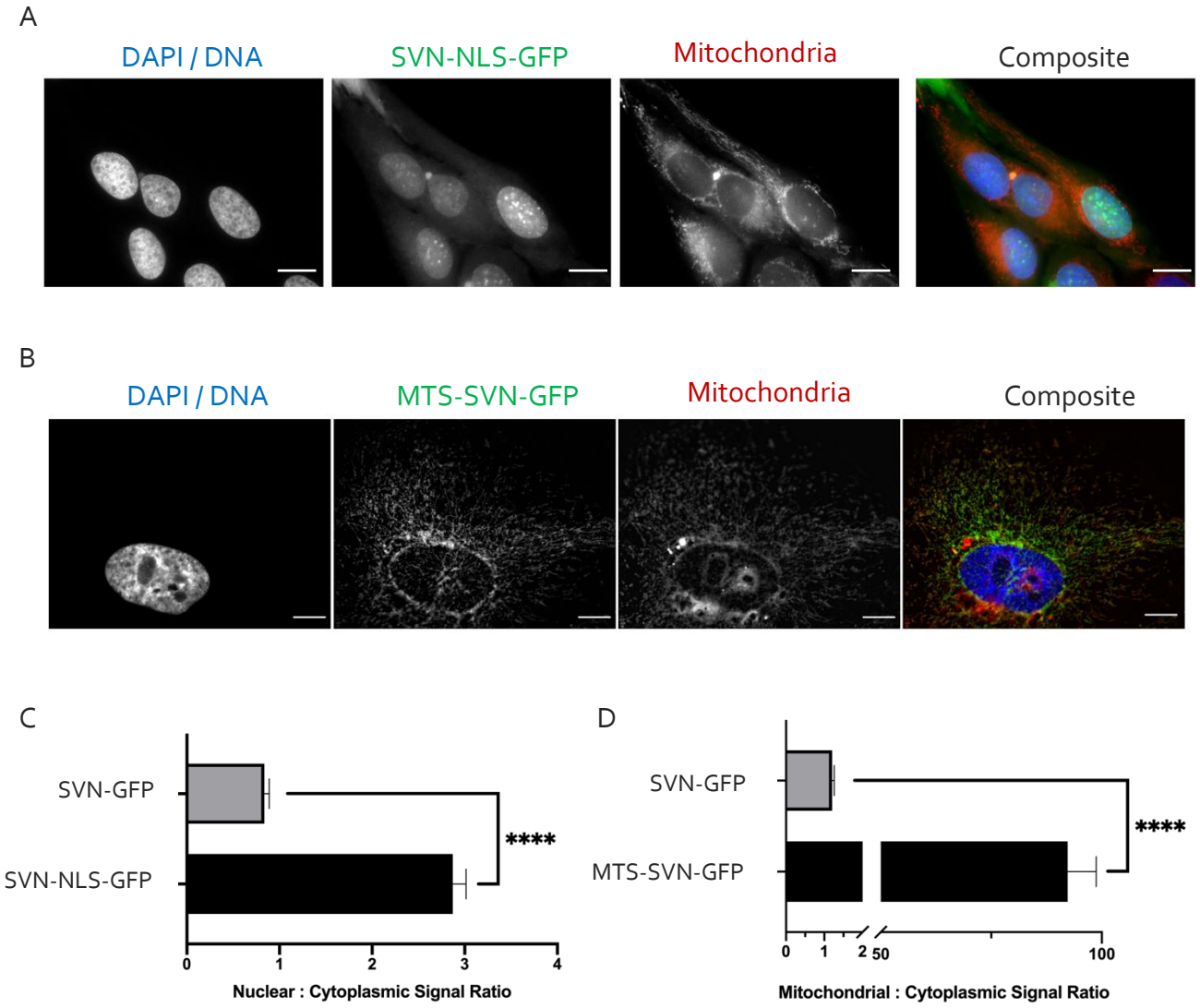


Figure 4.6 - Analysis of subcellular localisation of MTS-SVN-GFP and NLS-SVN-GFP constructs stably expressed in U2OS cells. **(A)** Immuno-fluorescent microscopy analysis of U2OS cells stably expressing NLS-SVN-GFP. **(B)** Immuno-fluorescent microscopy analysis of U2OS cells stably expressing MTS-SVN-GFP. Cells were stained with DAPI and MitoTracker to mark nuclear and mitochondrial regions respectively. Displayed is one representative out of three repeated experiments. (Scale bar = 50 μm). **(C)** Analysis of the ratio of mean fluorescent GFP signal intensity in the nucleus compared to signal within the cytoplasm of control SVN-GFP and NLS-SVN-GFP expressing cells. **(D)** Analysis of the ratio

of mean fluorescent GFP signal intensity in the mitochondria compared to signal within the cytoplasm of control SVN-GFP and MTS-SVN-GFP expressing cells. Error bars represents SEM of means from three separate experiments (**** $p < 0.0001$; N=60).

The cytoprotective properties of these relocated versions of survivin was assessed by caspase assays (Fig. 4.7). To induce apoptosis independent of DNA damage, cells were exposed to the broad acting kinase inhibitor, staurosporine. As shown In Figure 4.7B, all survivin expressing cell lines tested conferred increased cell survival relative to cells expressing GFP alone, but this was lowest for SVN-NLS-GFP. The role nuclear survivin may play in protecting cells from staurosporine mediated apoptosis is unclear. It is possible the small pool of cytoplasmic SVN-NLS-GFP identified may be responsible for this effect rather than a direct consequence of nuclear survivin.

In contrast, when treated with the DNA damaging agents UVC and etoposide (Fig. 4.7C-D), greater survival was observed for nuclear targeted survivin compared to mitochondrial survivin, although all cell lines saw increased resistance. This may support the role of survivin in promoting DNA repair, as previously suggested (Capalbo et al. 2010; Véquaud et al. 2016; Hu et al. 2015; Güllülü et al. 2021). However, SVN-NLS-GFP expressing also demonstrated increased resistance to doxorubicin, which attenuates DNA repair via histone eviction. While direct targeting of survivin to the nucleus may facilitate interactions with DNA repair proteins, this finding raises the possibility of an alternate pathway in which survivin may confer therapeutic resistance when it is present in the nucleus.

Finally, to assess the impact of survivin expression on cell viability when challenged with nutrient deprivation (another characteristic of the TME), cells were starved of serum for 48h. However, no significant differences were observed between the different lines (Figure 4.7F).

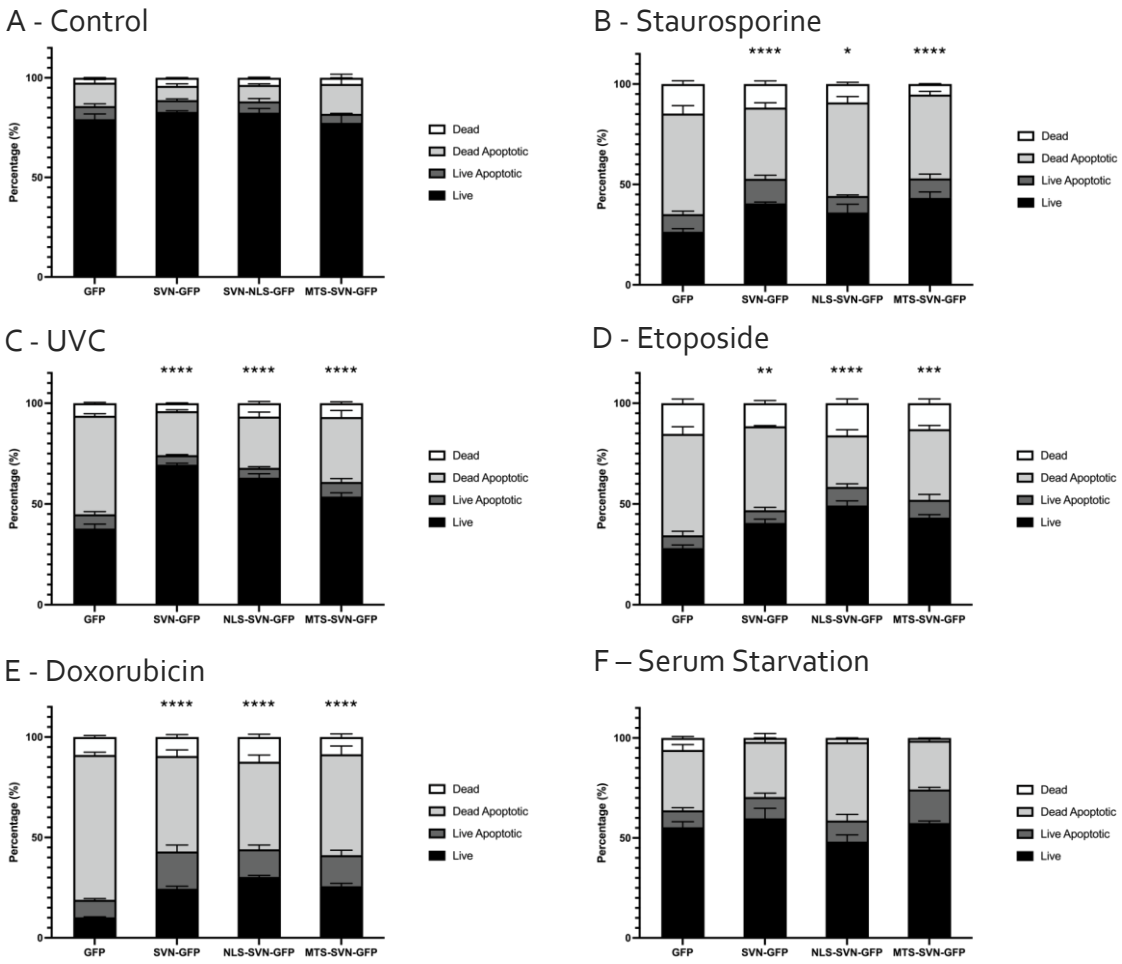


Figure 4.7 – Survivin directed to both the nucleus and mitochondria maintains anti-apoptotic activity. A caspase 3/7 flow cytometry assay was performed on U2OS cells stably expressing GFP, SVN-GFP, SVN-NLS-GFP and MTS-SVN-GFP constructs. **(A)** Control demonstrated no differences in viability between the cell lines. Cells were challenged with 24h treatments of **(B)** staurosporine **(C)** UVC **(D)** etoposide and **(E)** doxorubicin or **(F)** 48h serum starvation. Cells are defined as either alive with no caspase activity ('Live'), alive but with caspase activity ('Apoptotic'), dead with caspase activity ('Apoptotic/Dead') or dead with no detectable caspase activity ('Dead'). Cell survival for each cell lines was compared

to GFP control cells. Error bars represent SEM of means. (****, p <0.00001; ***, p <0.0001; ***, p <0.001; **, p <0.01; *, p <0.05; n=3).

Mitochondrial survivin has previous been shown to exit the mitochondria in response to apoptotic stress and to have enhanced cytoprotective capabilities (Dohi, Beltrami, et al. 2004). In an attempt to verify this, MTS-SVN-GFP cells were treated with IC50 UVC and imaged at 4h However, as shown in Figure 4.8, MTS-SVN-GFP signal persisted to colocalise with mitotracker under these conditions, suggesting it was still retained by the mitochondria both at 1h and 24h time points (data not shown). It should be noted that the MTS sequence utilised is derived from cytochrome c transcripts, which resides within the intermembrane space rather than the mitochondrial matrix to which survivin is thought to localise.

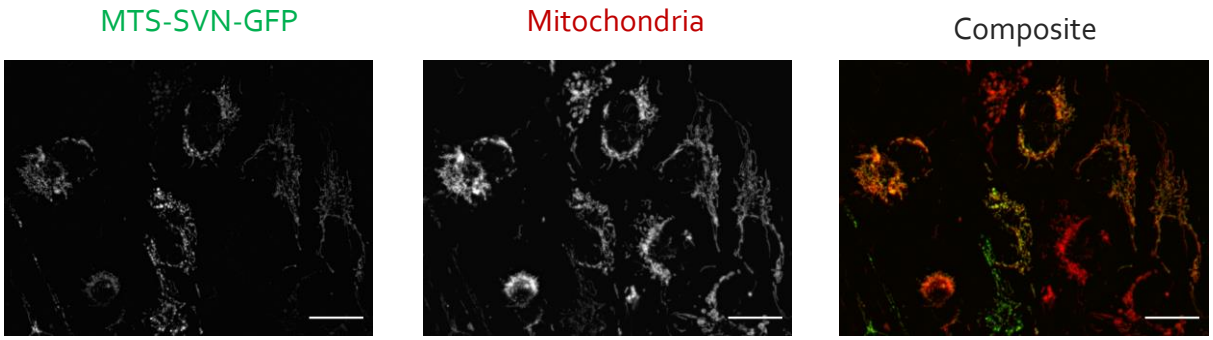


Figure 4.8 – MTS-SVN-GFP is retained within the mitochondria of UVC irradiated cells U2OS MTS-SVN-GFP cells, treated with IC50 UVC for 4h, were staining with MitoTracker and fixed before being imaged by fluorescent microscopy. (Scale bars = 20 μm).

4.2.4 Identification of putative binding partners involved in DNA repair and apoptosis

Mass spectrometry analysis of GST-pulldown samples (performed by Hana Abdelkabir), identified numerous protein interactors associated with the DNA damage response. These included DNA-PKcs (PRKDC), Ku80 (XRCC5), CDKN2A interacting protein (CDKN2AIP), Y-box binding protein 1 (YBX1) and Flap structure-specific endonuclease 1 (FEN1). DNA-PKcs and Ku80 have previously been described as survivin binding partners (Güllülü et al. 2021). Additionally, voltage dependent anion-selection channel protein 2 (VDAC2) and DnaJ homolog subfamily A member 1 (DNAJA1) were also identified. These proteins have been associated with apoptosis through regulation of BAX/BAK activity (Chin et al. 2018; Gotoh et al. 2004) and are an interesting prospective pathway for future research to investigate the anti-apoptotic mechanisms of survivin.

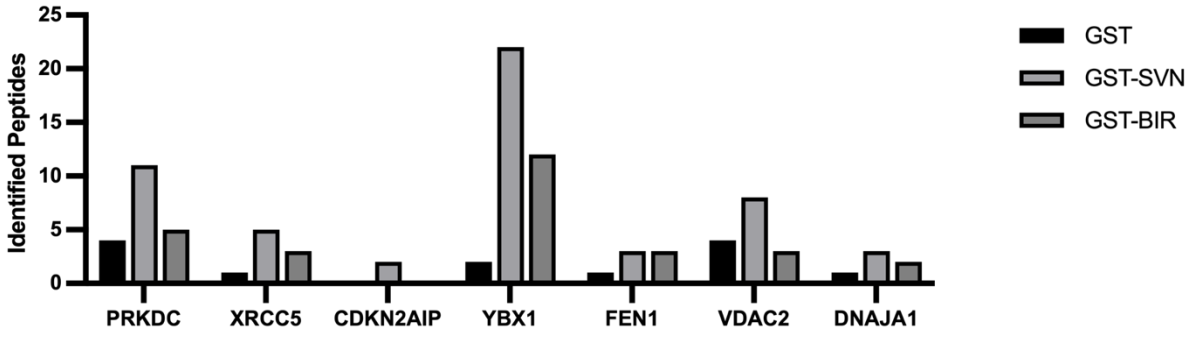


Figure 4.9 – Survivin pulls down numerous proteins associated with DNA repair and apoptosis. Mass spectrometry analysis of GST pulldown assays comparing control GST samples to survivin and survivin BIR domain constructs.

4.2.5 Cytoprotection by nuclear survivin is not conferred through DNA repair.

Doxorubicin, which induces apoptosis via DNA damage and attenuates DNA repair, failed the elicit nuclear localisation of survivin. To assess whether nuclear survivin still promotes cell survival, even when DNA repair has been inhibited, cells were treated with doxorubicin alone and in combination with leptomycin B (LMB) under normoxic and hypoxic conditions. LMB is a CRM1 inhibitor, abrogating nuclear export and thus promoting nuclear accumulation of survivin as a result. This was verified through imaging of U2OS cells treated with a combination of doxorubicin and LMB (Fig. 4.10A). Notably, U2OS SVN-GFP cells were observed to be more resistant to doxorubicin-mediated apoptosis under all conditions than cells expressing GFP alone (Fig. 4.10B). While the cytoplasmic pool, present when treated with doxorubicin alone, may inhibit apoptosis through interactions with pro-apoptotic proteins, the role of survivin within the nucleus is unclear.

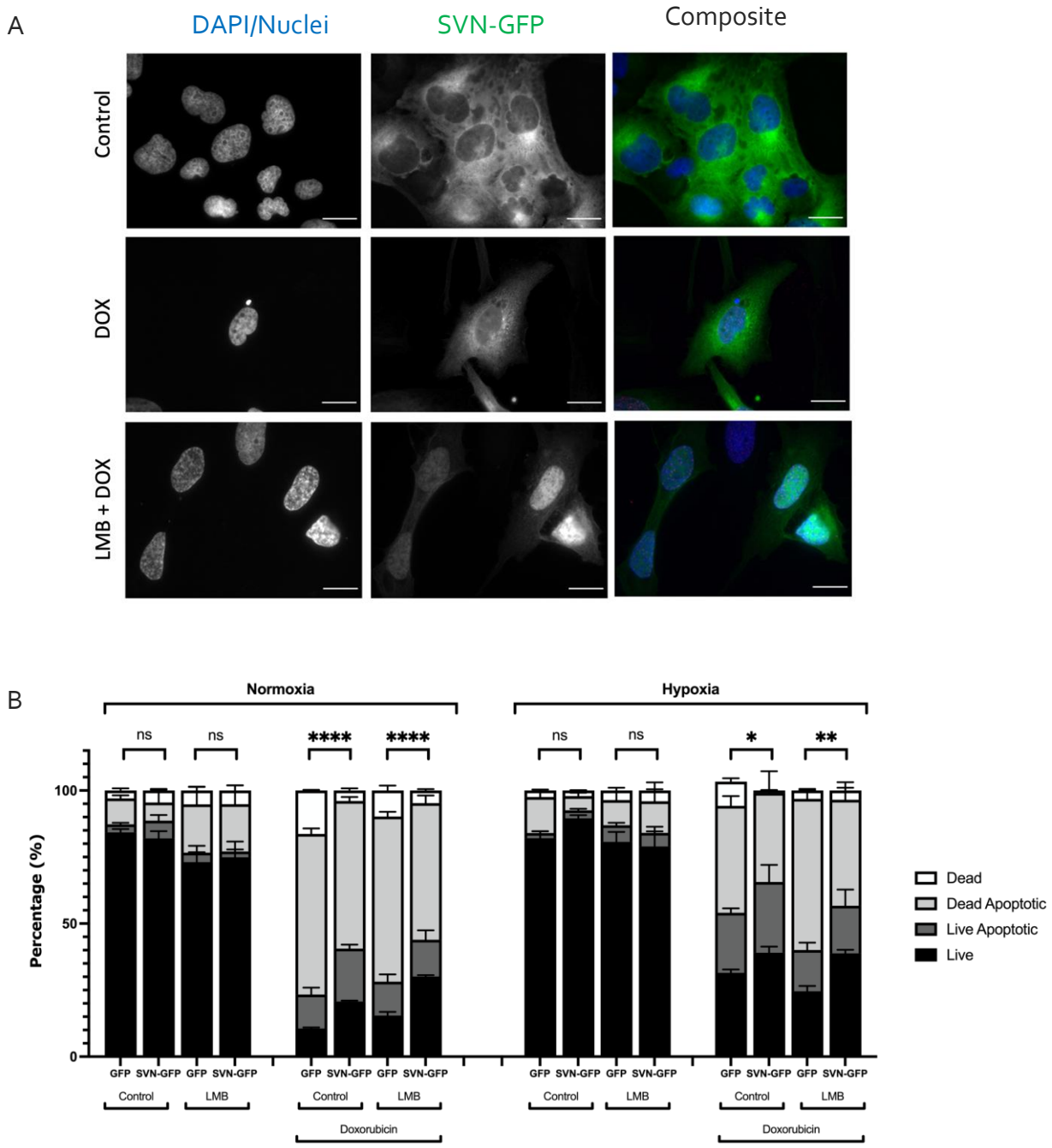


Figure 4.10 – Survivin confers doxorubicin resistance in the nucleus of normoxic and hypoxic cells. **(A)** Combined treatment of U2OS cells with doxorubicin and LMB induces localisation of survivin within the nucleus (Scale bar = 20 μm) **(B)** Comparison of doxorubicin

induced apoptosis in normoxic and hypoxic cells treated with LMB. Error bars represent SD of means. (****, p <0.00001; ***, p <0.0001; ***, p <0.001; **, p <0.01; *, p <0.05; n=2)

In support of a role for survivin in DNA repair, colocalization of survivin with sites of DNA damage has previously been reported (Capalbo et al. 2010). However, while 4h UVC treatment successfully generated g-H2AX foci and induced nuclear localisation of survivin (Fig. 4.11A), the SVN-GFP foci formed did not colocalise with the g-H2AX signal (Fig. 4.11B) either at 1h (Figure 4.11C) or 24h (data not shown). Therefore, an interaction between survivin and DNA repair machinery could not be established within this context and may be suggestive of alternative pathways utilised by survivin in support of cell survival.

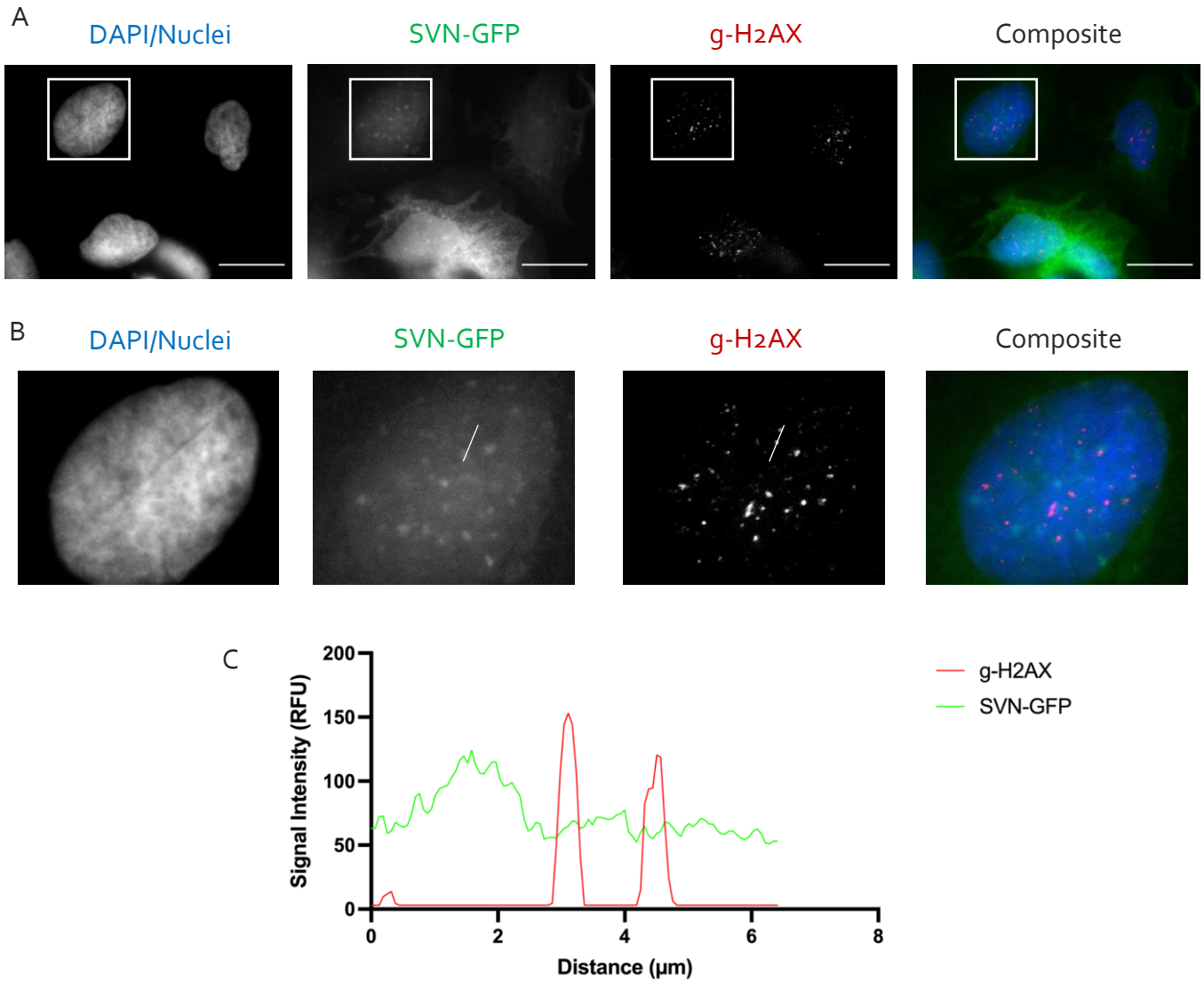


Figure 4.11 – Survivin foci do not colocalise with sites of UVC-mediated DNA damage. **(A)** U2OS SVN-GFP cells treated with IC50 UVC irradiation induced nuclear survivin localisation and g-H2AX foci. (Scale bar = 20 µm) **(B)** Enlarged images of the region outlined in A. **(C)** Multiplot line analysis of g-H2AX and SVN-GFP signal across the white line shown in B.

To further investigate the role of nuclear survivin, U2OS GFP and SVN-GFP cells were treated with the DNA-PK/PI3K inhibitor, KU-0060648, and LMB to accumulate

survivin within the nucleus. Cells were subsequently challenged with etoposide and UVC damage (Fig. 4.12A-B). Notably, survivin overexpression correlated with increased survival under all conditions. These results were similarly extended to the non-cancerous MRC5 cell line (Fig. 4.13). Together these data implicate a role for nuclear survivin in apoptosis resistance that functions independently of DNA repair.

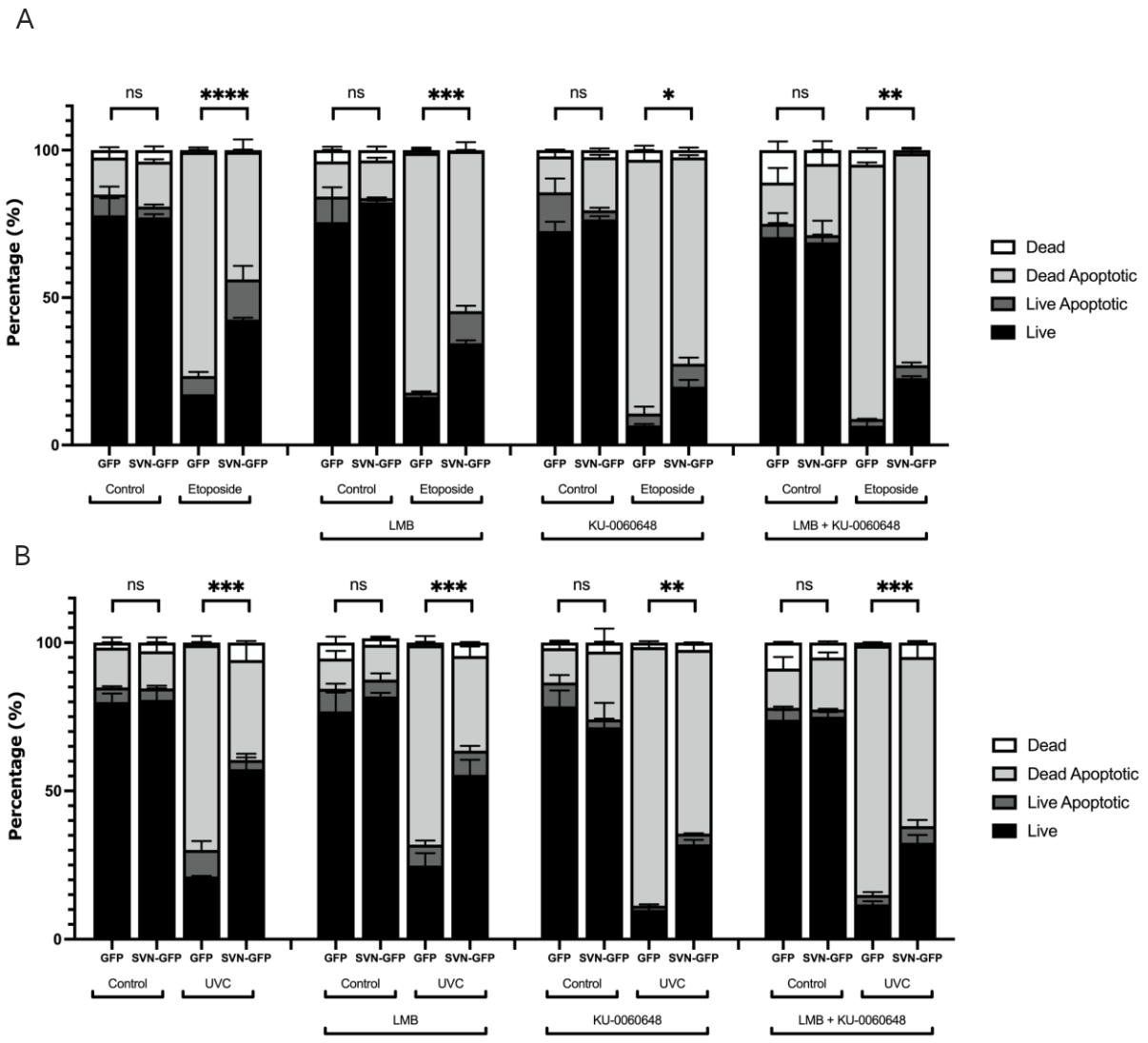


Figure 4.11 – Survivin retains cytoprotective qualities within the nucleus of cancerous cells with attenuated DNA repair. Survivin promotes the survival of U2OS cells from etoposide treatment **(A)** and UVC irradiation **(B)**, both with and without inhibited nuclear export and DNA repair. Error bars represent SD of means. (****, p <0.00001; ***, p <0.0001; ***, p <0.001; **, p <0.01; *, p <0.05; n=2).

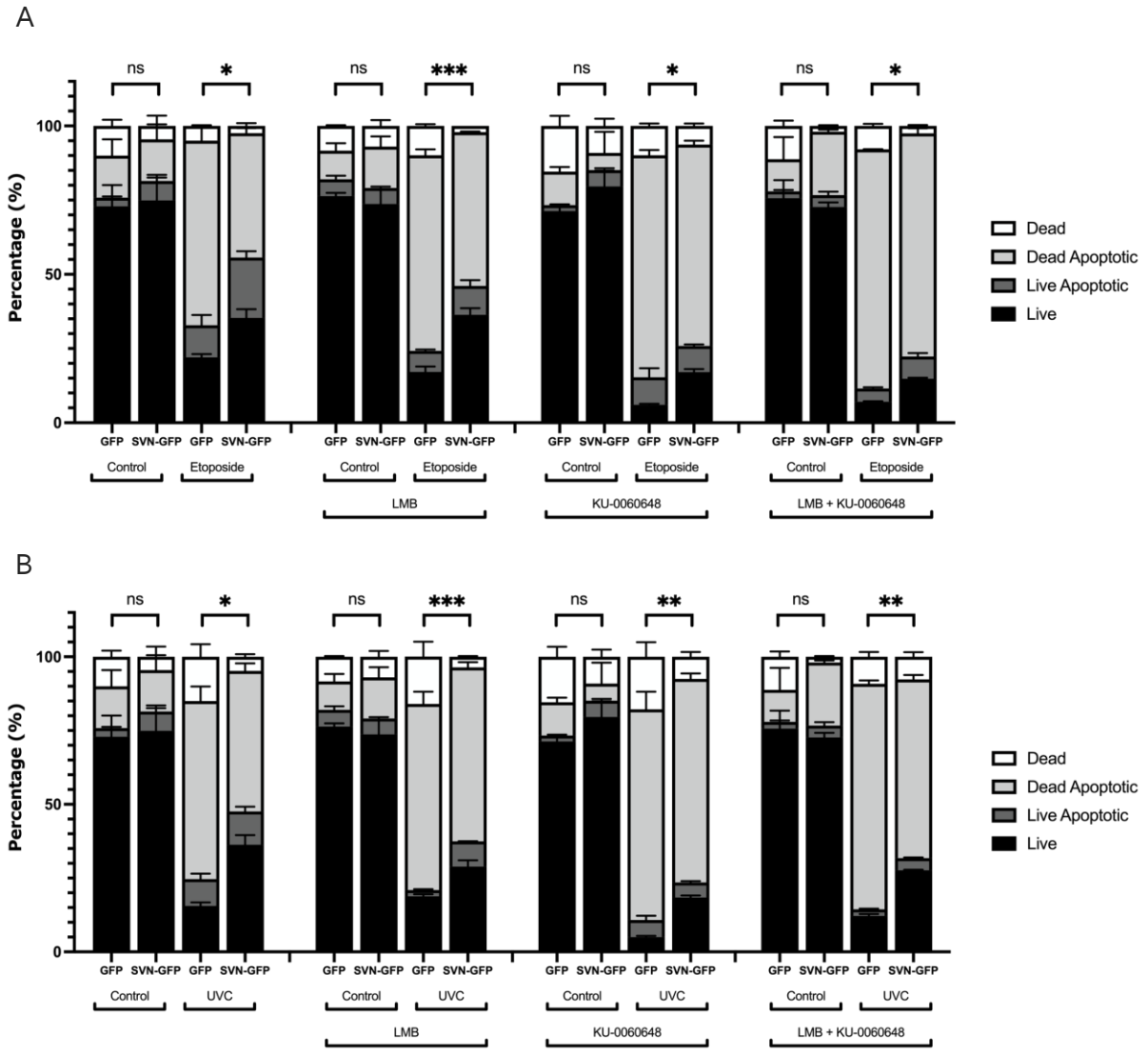


Figure 4.12 – Survivin retains cytoprotective qualities within the nucleus of non-cancerous cells with attenuated DNA repair. Survivin promotes the survival of MRC5 cells from etoposide treatment **(A)** and UVC irradiation **(B)**, both with and without inhibited nuclear export and DNA repair. Error bars represent SD of means. (***, p <0.0001; ***, p <0.001; **, p <0.01; *, p <0.05; n=2)

4.3 Discussion

The role of survivin as an apoptotic inhibitor has been well established, however the mechanisms by which this is achieved remain unclear. A diverse range of interactions have been proposed, including inhibition of caspase enzymes (Tamm I et al. 1998), stabilisation of XIAP (Altieri 2010; Dohi, Okada, et al. 2004), inhibition of Smac (Sun et al. 2005) and facilitation of DNA repair (Güllülü et al. 2021). Indeed, survivin-mediated inhibition of apoptosis and its promotion of cell survival may be multifaceted. Furthermore, survivin may localise to distinct subcellular compartments during interphase to achieve these activities. Given the nuclear and mitochondrial localisation demonstrated in 3.2.1, an understanding of their potential impact on cytoprotection was sought.

4.3.1 Nuclear and mitochondrial survivin promote cell survival under hypoxia

A clear correlation was established between intracellular levels of survivin and resistance to zeocin and doxorubicin under normoxic conditions, with a similar trend demonstrated under hypoxia. Collectively, these data confirm that survivin can be cytoprotective in both conditions. Intriguingly, this raises questions as to its functions within these locations.

The ability of survivin to inhibit apoptosis has traditionally been associated with its residency in the cytoplasm (Connell et al. 2008) (Knauer et al. 2007). Indeed, these studies showed forced nuclear localisation of survivin increased sensitivity to DNA damaging agents, such as X-irradiation and cisplatin. However, nuclear localisation of survivin in response to DNA damage has also been established (Capalbo et al. 2010; Hu et al. 2015; Güllülü et al. 2021) and has its protective role to genotoxic stress (Rödel et al. 2005; Obexer et al. 2009; Al-Khalaf, Aboussekhra 2013). Here, using hypoxic and LMB treatments as well as an SVN-NLS-GFP construct to regulate

its localisation, it was established that nuclear survivin can support cell survival under all conditions tested.

An increase in the mitochondrial pool was also demonstrated. It has previously been suggested this population of survivin molecules is discharged when challenged with apoptotic inducing agents with elevated anti-apoptotic activity (Dohi, Beltrami, et al. 2004). However, UVC treatment failed to elicit the same response here. Nonetheless, MTS-SVN-GFP expressing cells exhibited increased treatment resistance, even when survivin failed to be discharged. Previously suggested mechanisms governing inhibition of the intrinsic pathway by survivin have pointed to interactions downstream of MOMP. However, VDAC2 and DNAJA1 were identified has putative survivin binding partners. VDAC2 interfaces with Bak and inhibits oligomerisation, impeding formation of a lipid pore that facilitates MOMP (Cheng et al. 2003). Whether survivin binds directly remains unclear, although VDAC2 regulation by receptor of activated protein kinase C 1 (RACK1) as a substrate of the Src-survivin complex is a possible pathway (Chang et al. 2002; Lin et al. 2015; Dunajová et al. 2016). Likewise, DNAJA1 functions as a co-chaperone of heat shock protein 70 (HSP70) and negatively regulates the translocation of Bax to the mitochondria to inhibit MOMP (Gotoh et al. 2004). These offer alternative avenues through which survivin may influence apoptotic events within the mitochondria of cancerous cells.

4.3.2 Cytoprotection by nuclear survivin is not contingent on DNA repair

Given the proposed role of survivin in DNA repair (Hu et al. 2015; Capalbo et al. 2010; Véquaud et al. 2016; Güllülü et al. 2021), the impact of attenuating this pathway on genotoxic resistance were assessed. Both treatment with doxorubicin, which inhibits the DNA repair response, and combined treatments with genotoxic agents and a DNA-PKcs/PI3K inhibitor failed to abrogate survivin-mediated

resistance. While mass spectrometry analysis of survivin pulldown assays revealed a number of potential binding partners associated with DNA repair, the functional relevance of these interactions remains unclear. Moreover, SVN-GFP foci failed to colocalise with g-H2AX in response to DNA damage, as previously observed (Capalbo et al. 2010). These results may therefore suggest an alternative mechanism mediating the cytoprotective role of survivin within the nucleus.

4.3.3 Survivin differentially regulates the expression of cell survival proteins under hypoxia

Despite the identification of BIRC5 as a HIF gene target (Bai et al. 2013), transcription of survivin remained stable at the 24h timepoint tested. This is possibly due to the variable or transient nature of HIF1a upregulation in response to hypoxia, which experiences a rapid initial increase in activity and subsequently subsides to normal or reduced levels at 24h and above (Ravenna et al. 2014; Lee et al. 2019). Analysis of both protein and mRNA levels in response to survivin expression revealed altered regulation of apoptosis-associated genes under normoxic and hypoxic conditions. Survivin has been shown to promote XIAP stabilisation (Dohi, Okada, et al. 2004) while XIAP has also been shown to localise to the nucleus under hypoxic conditions (Russell et al. 2008). Here, a role in the stabilisation of XIAP under hypoxia was also supported, in which XIAP mRNA levels were unaffected by survivin expression under hypoxia, but protein levels were increased. While a previous survivin mutant (survivin^{S20D}) thought to prevent this interaction (Fig. 3.17) failed to alter survivin localisation, survivin may still aid its stabilisation within this compartment. Moreover, nuclear XIAP is thought to enhance the expression of HRE genes by mediating HIF1a polyubiquitination via interactions with the E2 ubiquitin conjugating enzyme, UBC13 (Park et al. 2017). Rather than altering the stability of HIF1a, Lys63-linked polyubiquitination promoted the nuclear retention of HIF1a to

facilitate HRE transcription, together outlining a pathway in which survivin may indirectly regulate expression of HIF1a target genes (outlined in Fig. 4.13).

The binding of survivin to DNA-PKcs, demonstrated here and in previous research (Güllülü et al. 2021), may also be associated with the regulation of gene transcription. While the role of DNA-PKcs in DNA repair is well characterised, this multifunctional enzyme is also associated with regulating gene transcription, cell cycle progression and telomere maintenance (Mohiuddin, Kang 2019). Indeed, DNA-PKcs has been shown to activate in response to mild hypoxia (Bouquet et al. 2011) and recently support HIF1a-medaited gene transcription in hypoxia (Yang et al. 2022). Proteomic and phosphoproteomic analysis by Güllülü et al. demonstrated a shift in DNA-PKcs substrate specificity upon survivin binding, reducing the phosphorylation of NHEJ partners and increased phosphorylation of factors such as Foxo3, associated with decreased expression of pro-apoptotic proteins (2021). DNA-PKcs may therefore represent another mechanism by which survivin may regulate gene transcription to facilitate cell survival and the adaptation of cells to hypoxia.

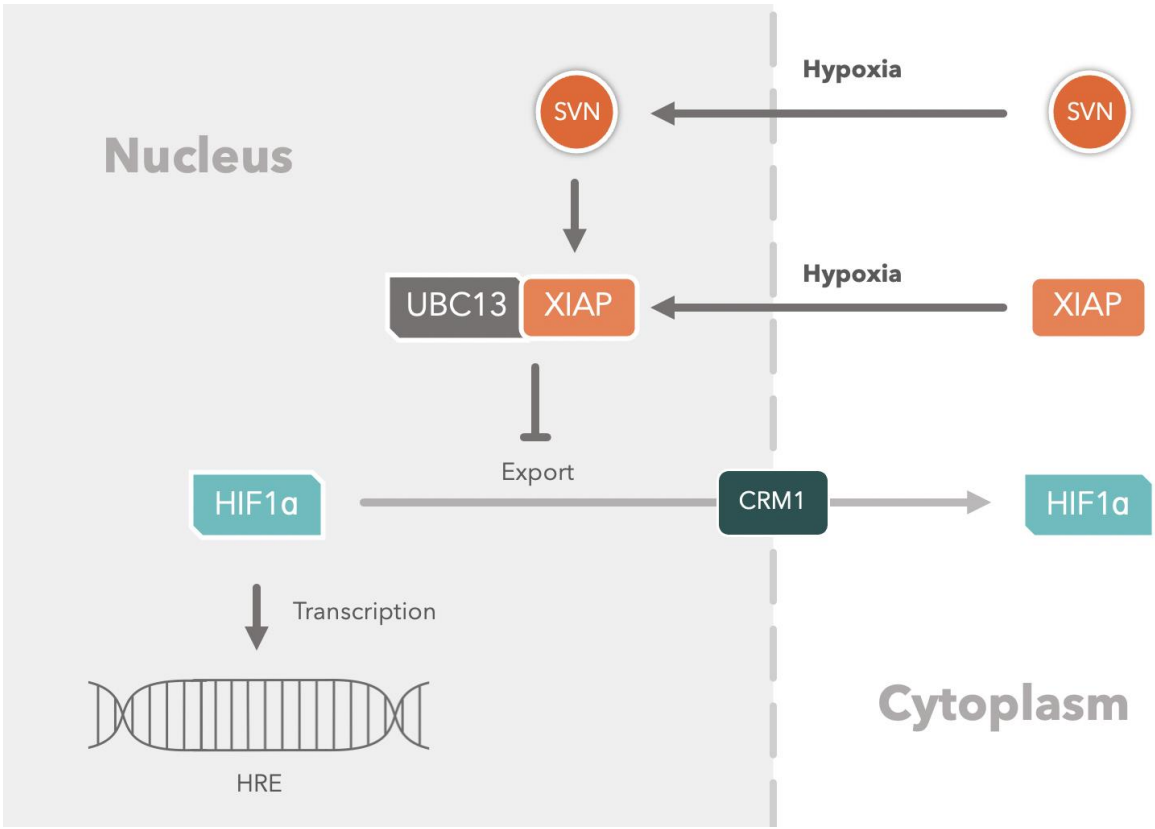


Figure 4.13 – Model of HIF1a regulation by survivin through interactions with the XIAP-UBC13 complex. Created by author.

As previously observed, p53 demonstrated stable transcription but altered protein levels in response to survivin under normoxia (Wang et al. 2004). This is thought to be achieved indirectly, with survivin regulating MDM2 levels post-translationally via inhibition of caspase-mediated cleavage, resulting in increased p53 degradation. Under hypoxia, survivin did not correlate with p53 levels, possibly as a result of its altered localisation. While hypoxia has traditionally been associated with increased p53 expression, recent research has suggested this relationship is far more variable and cell line dependent (Sermeus, Michiels 2011). Downregulation of p53 under hypoxic conditions may therefore promote treatment resistance, as demonstrated in response to the apoptotic agents tested here.

4.3.4 Summary

Survivin appears to retain its cytoprotective role, both in hypoxic conditions and when forcibly expressed within the nucleus. However, the mechanism by which this is achieved remains unclear. Despite potential interactions with DNA-PK and associated repair proteins, its ability to promote cell survival does not appear to be contingent on this pathway. Alternatively, survivin may regulate the stability of other cell survival proteins with a potential pathway to influence gene transcription, portentially via HIF1a and/or DNA-PKcs.

Chapter 5 – Survivin Mediates Cell Metabolism

5.1 Overview

5.1.1 Proposed roles for survivin in cellular metabolism

Numerous studies have implicated survivin in cellular metabolism, with a distinct focus on its mitochondrial pool and associated impact on mitochondrial activity. Notably, the mitochondria have been shown to harbour survivin exclusively within cancerous cells and are yet to be identified within non-cancerous cell lines (Dohi, Beltrami, et al. 2004). These organelles play a key role in the cellular adaptations necessary to support tumour survival within the adverse conditions of the TME. Mitochondria host the enzyme complexes that mediate OXPHOS and associated oxygen consumption and ROS production. The decreased oxygen levels experienced by many tumours require compensatory changes to the mitochondria in response. Hypoxia is therefore linked with decreased OXPHOS and a shift in cellular metabolism to glycolysis as the primary ATP production pathway (al Tameemi et al. 2019).

However, studies investigating a potential relationship with survivin have attributed it contradictory roles with inconsistent experimental results. Early work correlated survivin expression with mitochondrial fragmentation and a consequent reduction in aerobic glycolysis (Hagenbuchner et al. 2013), summarised in Fig. 5.1. This was later disputed, with survivin instead shown to promote oxidative phosphorylation through complex II stabilisation and a role in cell migration via trafficking of the mitochondria to the cortical cytoskeleton (Rivadeneira et al. 2015). Most recently, evidence supporting increased glycolysis has been published, albeit in the absence of mitochondrial fission and instead a proposed role for mitophagy that ultimately impacts cellular respiration (Townley, Wheatley 2020). This study demonstrated

reduced mitochondrial turnover as a consequence of failed Parkin localisation to the OMM, resulting in greater mitochondrial mass and decreased quality of mtDNA. Mitochondria are complex and highly dynamic organelles, which employ multiple regulatory systems to respond to both intra- and extra-cellular signals. The role for survivin in their activity may therefore be multifaceted and give rise to multiple phenotypes that may differ between cell and cancer types.

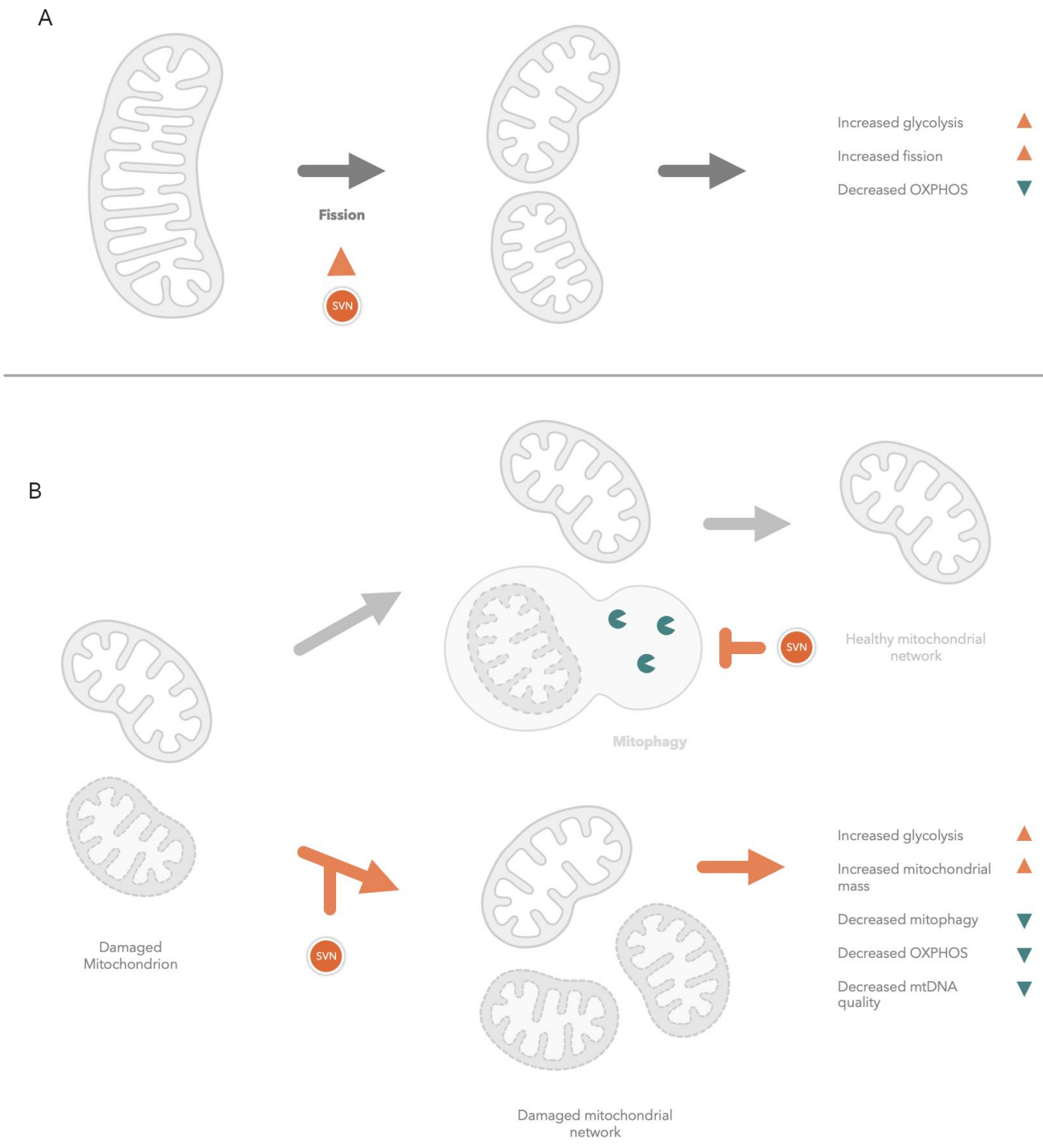


Figure 5.1 – Proposed roles of survivin in mediating mitochondrial activity. (A) Survivin promotes mitochondrial fission, reducing the capacity of mitochondria to perform OXPHOS and facilitates glycolysis (Hagenbuchner et al. 2013). (B). Survivin inhibits

mitophagy, preventing the degradation of dysfunctional mitochondria with diminished OXPHOS capacity (Townley, Wheatley 2020). Created by author.

5.1.2 Regulation of mitochondrial respiration

OXPHOS activity is regulated by numerous cellular elements. The respiratory capacity of the mitochondria is thought to be linked to the interconnectivity of its network (Silva Ramos et al. 2016). Fusion promotes mitochondrial health, particularly in regulating mtDNA levels, and increases their efficiency in energy generation (Mishra, Chan 2016). The union of healthy mitochondria with damaged ones may aid in the maintenance of mitochondrial respiration by sharing gene products and metabolites, increasing the respiratory capacity of the network as a whole (Westermann 2012). In contrast, mitochondrial fission diminishes OXPHOS activity and is linked with the release of apoptotic factors during the intrinsic apoptosis pathway (Suen et al. 2008). Mitochondria fission is thought to precede mitophagy, functioning as a necessary process to separate healthy from damaged mitochondria (Twig et al. 2008). However recent work has challenged this proposition and their relationship may be more complex, with FIS1-mediated fission demonstrating a dispensable role in mitochondrial turnover (K. Ma et al. 2020). Indeed, increased mitochondrial fusion, driven by either DRP1 suppression or MFN2 overexpression, was shown to increase mitophagy and result in lowered mitochondrial mass and OXPHOS activity (M. Yu et al. 2019). The downstream impacts on mitophagy may therefore be context dependent with greater interplay between regulatory elements than originally thought.

The generation of ATP via respiration is reliant on the development of a proton gradient between the intermembrane space and mitochondrial matrix. This is established through the activity of ETC complexes and subsequently harnessed by ATP synthase to phosphorylate ADP molecules in the generation of ATP (R. Z. Zhao

et al. 2019). Cristae are a key feature of the IMM and serve as an important evolutionary adaptation, substantially increasing the available surface area within the mitochondria to accommodate a greater number ETC complexes. Cristae biogenesis and curvature is regulated by the MICOS protein complex whilst maintenance of cristae junctions is overseen by OPA1 activity (Giacomello et al. 2020). Together these elements may regulate both the structure and functional capacity of the mitochondria (Li et al. 2015).

Maintenance of this established proton gradient relies on the sequestration of protons to specific mitochondrial regions with controlled proton reflux. Whilst a basal level of proton leakage naturally occurs, this process may be facilitated by the expression uncoupling proteins (UCPs). These transmembrane proteins undermine the proton gradient to reduce OXPHOS activity and associated ROS production. Their expression is linked with increased glycolysis and may support the Warburg Effect (Samudio et al. 2009). Moreover, UCP activity may facilitate the initiation, development and chemoresistance of tumours (Valle et al. 2010).

5.1.3 Cell Metabolism

Reduced OXPHOS activity requires metabolic adaptations to meet cellular energy demands. The Warburg Effect and hypoxia both mediate an increase in glycolysis, generating ATP in an oxygen-independent manner. However, the inefficiency of this process greatly increases glucose consumption and necessitates greater glucose import to maintain ATP production. Simultaneously, cells must also mediate the export of lactate, an acidic waste product, produced as a result of glycolysis.
Numerous enzymes facilitate this process and their expression is associated with tumour development and aggression (Sinkala et al. 2019) as well as adaptations to hypoxia (al Tameemi et al. 2019). These include factors such as Glut1, a glucose

transporter; LDHA, which preferentially binds to pyruvate and converts it to lactate; and CA-IX, a lactate transporter associated with extracellular acidification.

5.1.4 Aims

This chapters aims to evaluate the role of survivin in cell metabolism in light of previously inconsistent experimental findings and its potential role in mediating metabolic and mitochondrial adaptations to hypoxia, necessary for cancer cell survival and proliferation within tumours. Specifically, it aims to identify broad metabolic changes and probe the molecular interactions underpinning them.

Specifically, this chapter aims to assess whether:

- survivin over-expression correlates with an elevation in cellular OXPHOS and/or glycolysis under both normoxic and hypoxic conditions.
- survivin over-expression correlates with the expression of proteins involved in glycolysis.
- over-expression of survivin and survivin constructs targeted to the nucleus and mitochondria alter the morphology of the mitochondrial network with either greater interconnectivity or fragmentation. Moreover, does survivin expression correlate with an altered expression of mitochondrial fusion and fission factors.

5.2 Results

5.2.1 Survivin promotes aerobic glycolysis

With contradictory reports of survivin supporting both glycolysis and OXPHOS, its role in normoxic and hypoxic conditions was investigated by assessing glucose consumption rates (Fig. 5.2A). This was determined by measuring levels of glucose within the cell growth media. As cells consumed glucose, levels would decrease and therefore a greater reduction in glucose would indicate an increased rate of glycolysis. U2OS cells overexpressing SVN-GFP demonstrated significantly decreased glucose levels after 24h and 48h in normoxic conditions compared to control cells expressing a GFP construct, with a non-significant reduction at all time points. Under hypoxic conditions, both cell lines demonstrated increased consumption of glucose relative to normoxia, however differences between the cell lines were less apparent (Fig. 5.2B). A similar trend was seen in lactate generation, produced as a waste product of glycolysis. SVN-GFP expressing cells produced significantly increased lactate at 24h and 48h with a non-significant increase seen at all time points under normoxia (Fig. 5.2C). This trend was shared under hypoxic conditions, although differences between the two cell lines were reduced and not statistically significant (Fig. 5.2D).

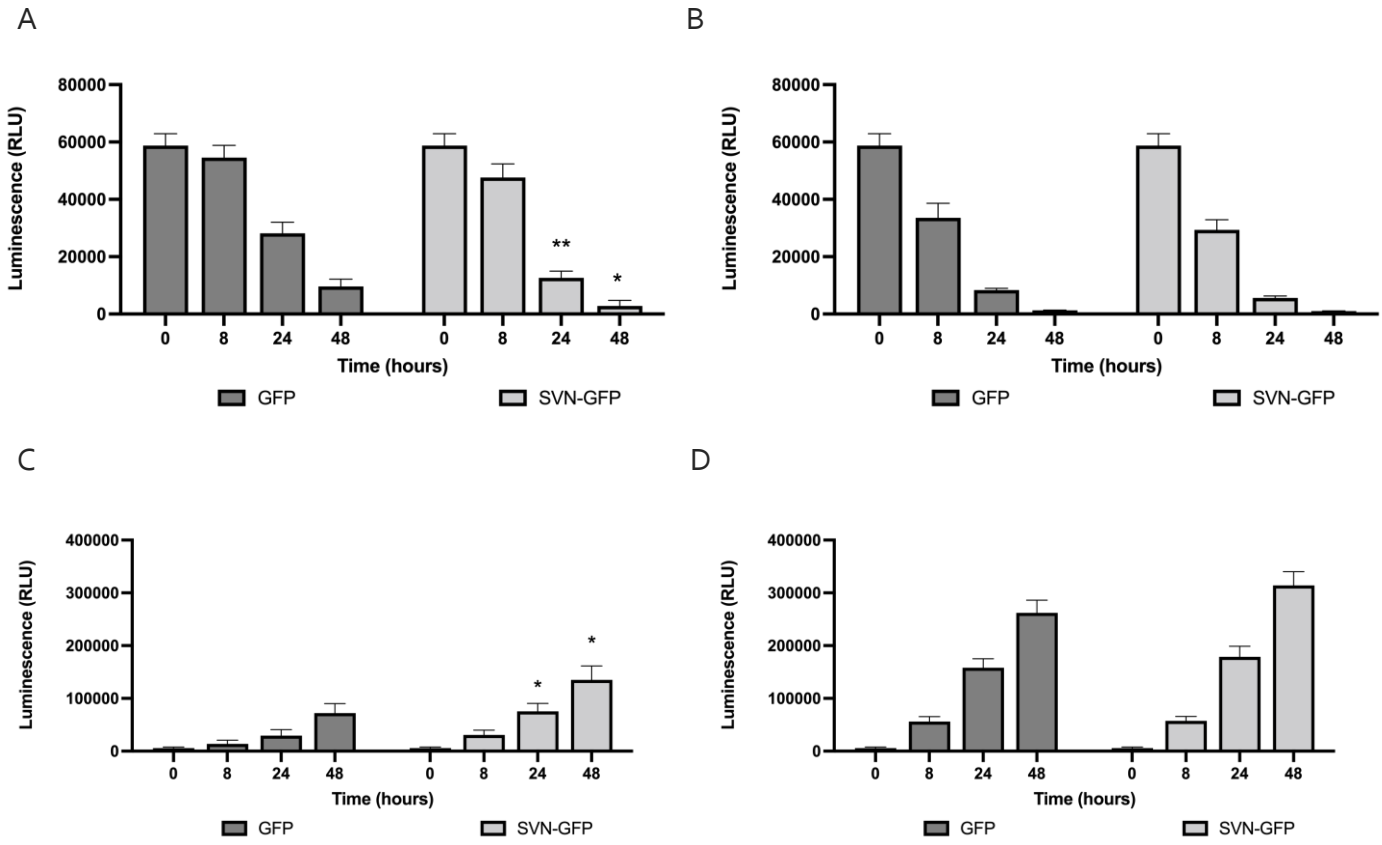


Figure 5.2 – Survivin expression correlates with increased glycolysis Glucose consumption of U2OS cells under normoxic **(A)** and hypoxic conditions **(B)**. Lactate production in normoxia **(C)** and hypoxia **(D)**. Error bars represent SD of means (*, P<0.05; **, P<0.01; N=2).

To probe the underlying mechanisms governing these metabolic differences under normoxic conditions, transcriptional expression of GLUT1 and CA-IX were determined (Fig. 5.3). SVN-GFP cells demonstrated significantly elevated expression of the glucose transporter GLUT1 mRNA, supporting a role for survivin in the transcriptional activation of glycolytic proteins. In a similar fashion to glucose consumption, hypoxia diminished cell line differences with similar expression levels exhibited for both GFP and SVN-GFP expressing cells. CA-IX, a transmembrane

protein involved in the export of intracellular lactate, was paradoxically downregulated by survivin under both normoxic and hypoxic conditions compared to the GFP control cell line and contrasts with the lactate assay results. Whilst CA-IX is not directly involved in the glycolytic process, its expression is commonly associated with increased glycolysis and mediates acidification of the extracellular environment.

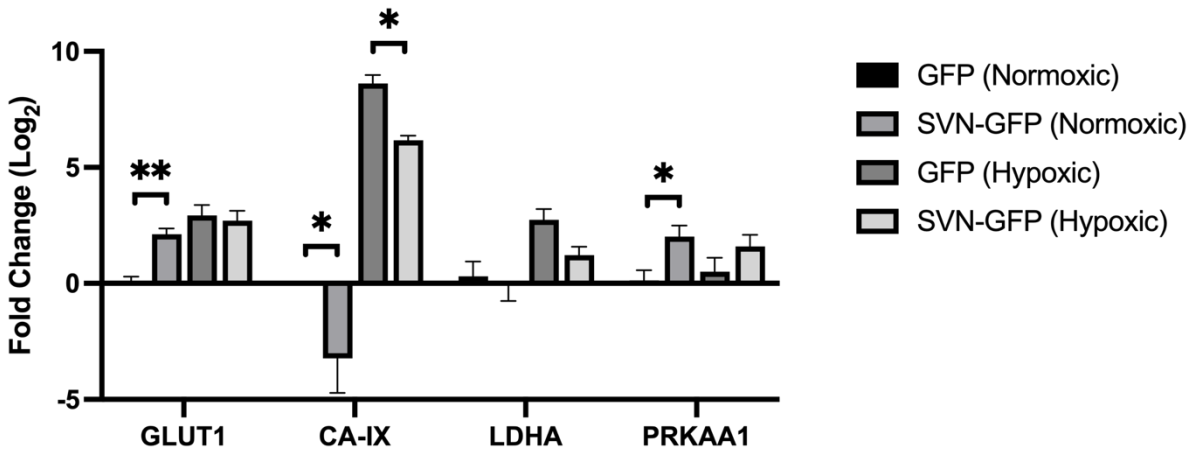


Figure 5.3 – Differential expression of glycolysis associated genes (*, P<0.05; **, P<0.01; n=3).

Expression of LDHA, an enzyme which facilitates the conversion of pyruvate to lactate, was investigated to examine proteins directly involved in lactate metabolism. Under normoxic and hypoxic conditions, both cell lines demonstrated similar mRNA levels with no significant differences, suggesting expression of lactate transporters but not enzymes involved in production were downregulated by survivin. AMPK expression, determined by mRNA levels of its catalytic subunit, protein kinase AMP-activated catalytic subunit alpha 1 (PRKAA1), was also upregulated with survivin overexpression. As a key and broad acting regulator of metabolic and mitochondrial homeostasis, AMPK promotes catabolic processes, including glucose metabolism (Herzig, Shaw 2018). AMPK activity is sensitive to

energy stress and it is not clear whether its expression drives or responds to these metabolic changes.

5.2.2 Survivin inhibits OXPHOS

As a switch to glycolysis is typically associated with a reduction of OXPHOS, mitochondrial respiration was assessed by resazurin assays in cell lines expressing different survivin constructs, detailed in 4.2.3 (Fig. 5.4). Reduction of resazurin to fluorescent resorufin is mediated by cellular NADH, primarily produced through OXPHOS. However, NADH may also be produced as part of the TCA cycle. The contribution of this pathway was assessed by oligomycin treatment, an ATP synthase inhibitor. Control GFP cells exhibited elevated resorufin production with dramatic reduction in cells expressing survivin constructs.

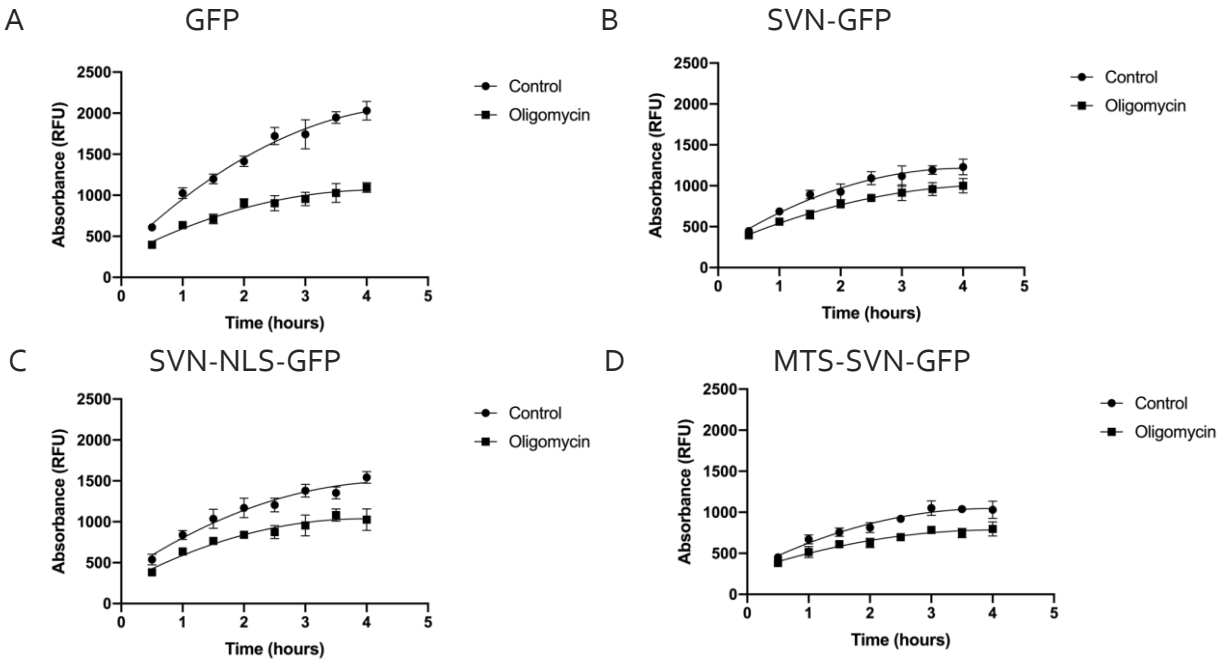


Figure 5.4 – Comparison of OXPHOS activity between survivin constructs. Resazurin assay of U2OS cells, either control or oligomycin treated, expressing either GFP **(A)**, SVN-GFP **(B)**, SVN-NLS-GFP **(C)** or MTS-SVN-GFP **(D)**.

5.2.3 Development of a mitochondrial analysis workflow and software

To determine the morphological features and interconnectivity of mitochondria, which are frequently used measures of mitochondrial dynamics, an image analysis workflow was developed within the FIJI software (Schindelin et al. 2012). A maximum-intensity projection of Z-stack images of U2OS cells stained with MitoTracker enabled all mitochondria to be captured and was used to generate initial images (Fig. 5.5A). These were subsequently processed by rolling ball background subtraction, which removed non-specific staining; application of a unsharp mask filter, which increases image sharpness to aid in differentiation of individual mitochondria as well as enhancement of local contrast to amplify the signal of weakly stained mitochondria; and finally limited adaptive histogram equalization to further enhance local contrast with limited noise. This produced high contrast images with well-defined mitochondria and limited background noise.

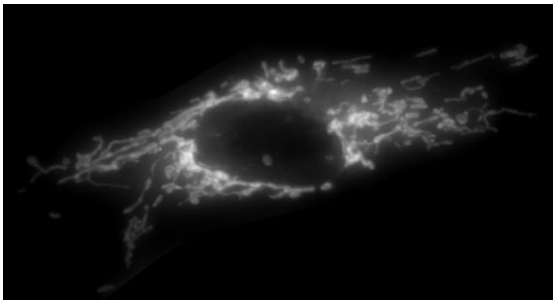
To assess mitochondrial features such as area and mitochondrial circularity, images were binarized. This process aims to designate each pixel as belonging either to background or to a mitochondrion. A selection of common binarization techniques were compared (Fig. 5.5B). Signal thresholding simply binarizes pixels based on their relative intensity to a set value. Whilst this approach successfully identified all mitochondria within the image when using a lower threshold, diffusive non-specific staining was commonly identified leading to the merging of individual mitochondria and consequent overestimation of mitochondrial area and connectivity. Alternatively, the ridge detection plugin utilises a line detection algorithm (Steger 1998) to identify curvilinear structures within an image. In contrast to signal thresholding, ridge detection was able to separate individual mitochondria and was less affected by non-specific staining. However, this approach often failed to identify highly circular mitochondria and underestimated mitochondrial area. Trainable

Weka Segmentation (Arganda-Carreras et al. 2017) utilises machine learning algorithms to automate image segmentation. Manually annotated images of mitochondria were used to train the plugin and generate a classifier (appendix) through a random forest classification algorithm (Breiman 2001). This system identified all mitochondria within the image, demonstrated greater separation of mitochondria than signal thresholding and most accurately determined mitochondrial regions. On this basis, the Weka segmentation approach was used moving forward.

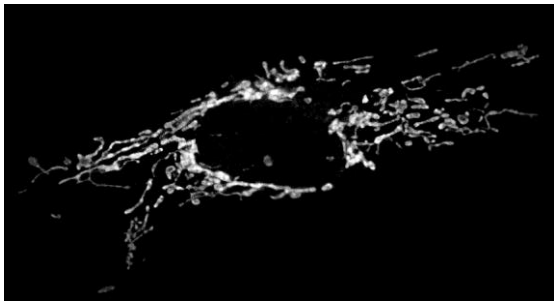
Distinct regions within these binary images were then analysed using the 'analyse particles' function, giving individual measurements of area, circularity and roundness. A statistic for weighted circularity was also calculated: this took the circularity score for each mitochondrion identified and weighted it based on its relative area to the total network within a cell. Additionally, these binary images were skeletonised (Arganda-Carreras et al. 2010) to generate line structures to determine the number of linked branches and their length.

To validate the ability of this workflow to quantify features of the mitochondrial network and differentiate fused mitochondria from fragmented ones, images of either control mitochondria or fragmented mitochondria following UVC treatment were assessed (Fig. 5.5C). Measurements of the average number of branches, average branch length and average weighted circularity clearly indicated control cells harboured a more interconnected mitochondrial network than UVC treated cells, which exhibited far fewer and shorter branches with a more circular morphology (Fig. 5.5D). Together these data verified the ability of the workflow to assess differences in mitochondrial networks.

A

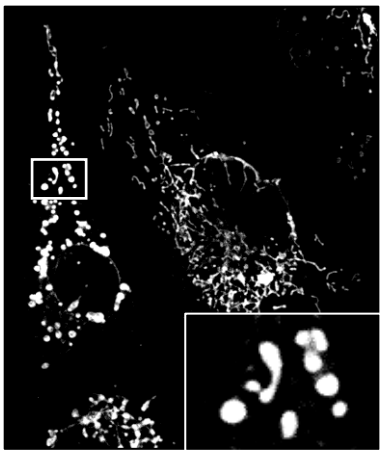


Original

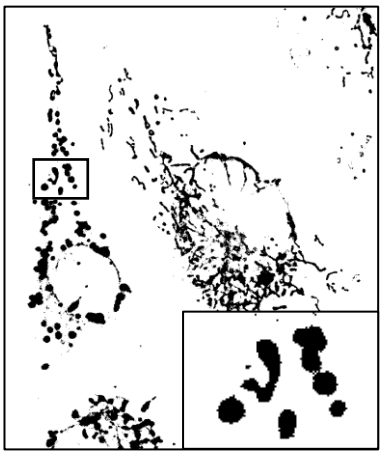


Processed

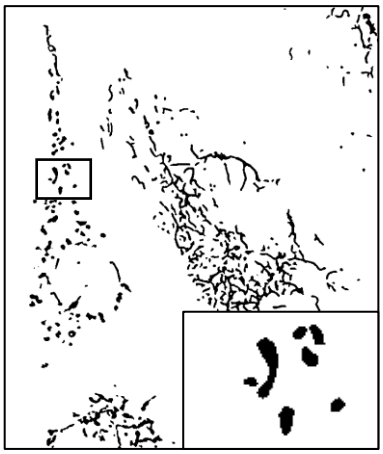
B



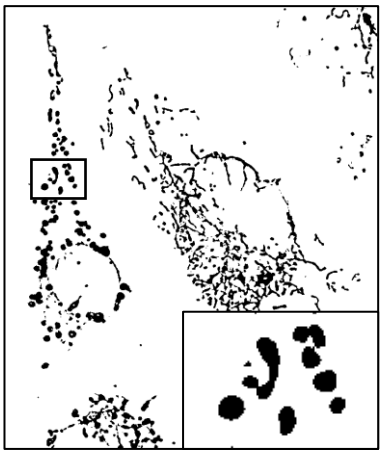
Input



Thresholding



Ridge Detection



WEKA Segmentation

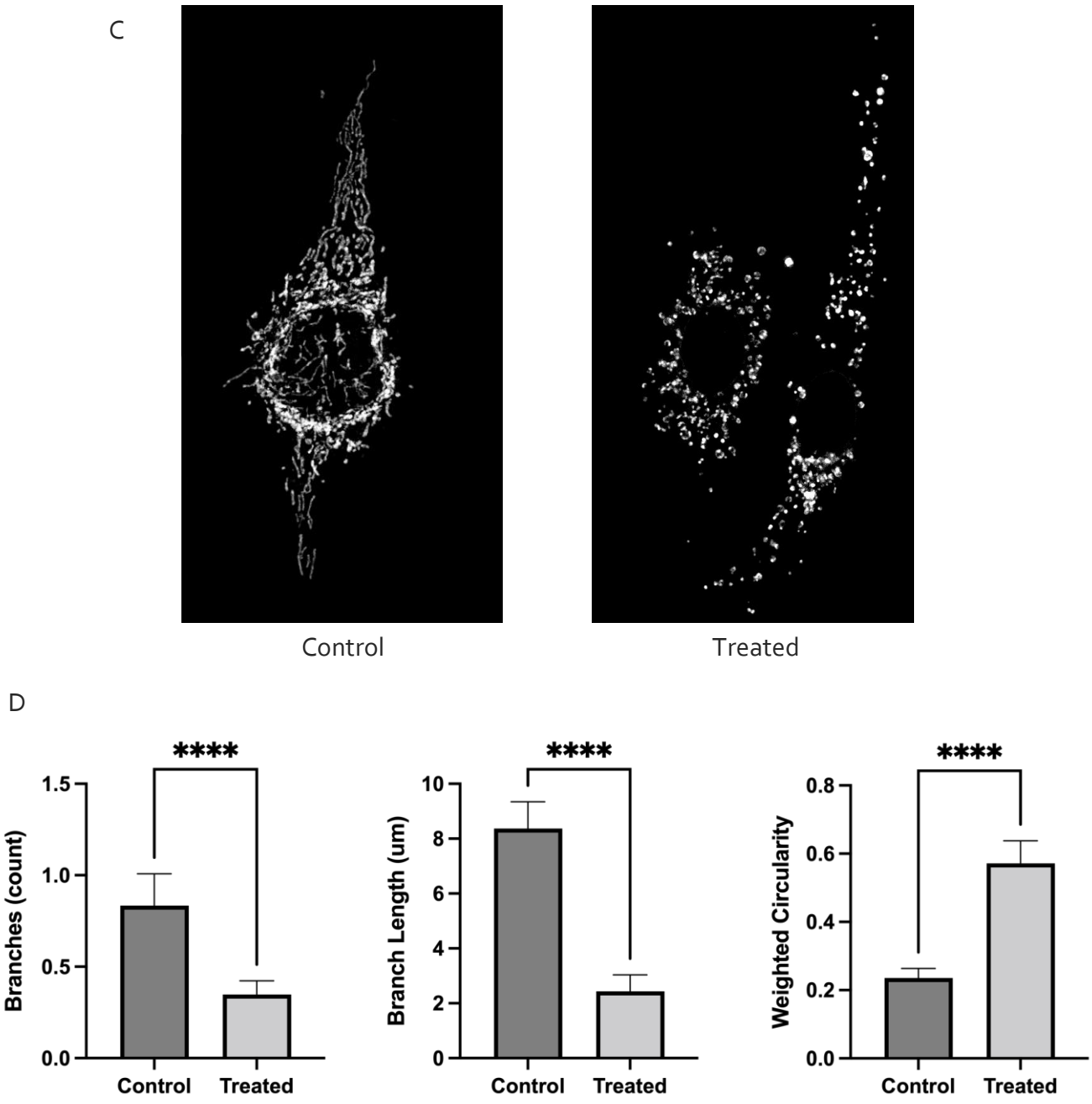


Figure 5.5 – Development and validation of a mitochondrial analysis workflow. (A) Pre-processing of widefield images to generate high contrast images of mitochondria. **(B)** Comparison of image binarization techniques. **(C)** Processed images of mitochondria generated from either control or UVC treated cells to induce fragmentation. **(D)** Analysis of control and UVC treated mitochondria finds significant differences in measurements of

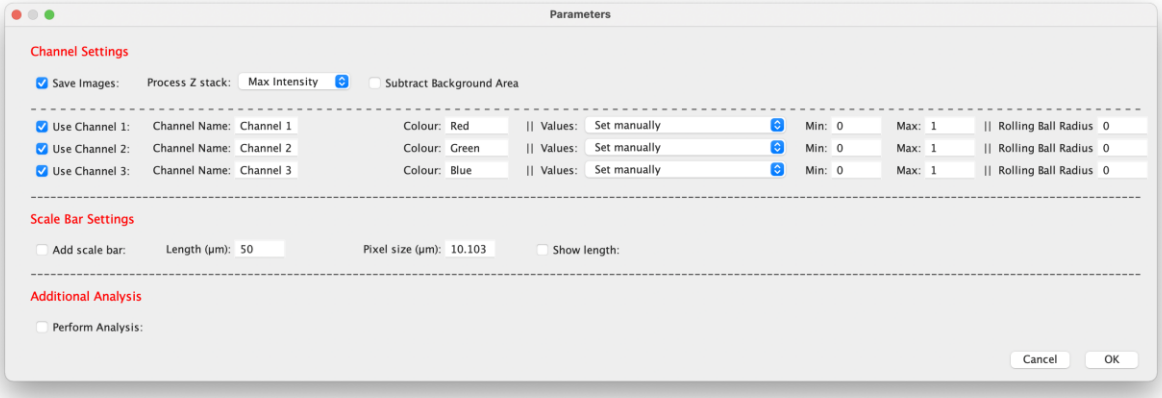
mitochondrial connectivity and morphology. Error bars represent SD of means (****, P<0.0001; n=2; N=75)

This workflow was incorporated into a larger macro (appendix) that runs within the FIJI software. This macro aims to facilitate high throughput image processing and analysis in an automated or semi-automated fashion with no requirements by the user to understand or write software code. The macro instead generates a user interface (UI) when run to handle user inputs and establish parameters for subsequent processing and analysis of images (Fig. 5.6A). Elements of the UI are generated dynamically based on the properties of the input image, such as fields for Z-stack processing if the image contains multiple image slices and parameters for each channel contained in the file. This first window allows the user to set parameters for the production of individual PNG image files, such as producing a maximum-intensity Z projection, which channels are used to produce images, the minimum and maximum signal intensities for each channel and the addition of a scale bar. This will subsequently produce an individual grey-scale PNG file for each channel as well as a coloured composite image based on the user's input. A processed version of the image file will also be generated in TIF format, retaining the image meta-data, that can be altered or analysed without requiring the user to repeat these initial steps.

A second window may also appear for image analysis (Fig. 5.6B). This further allows users to designate specific regions within a single image to be analysed separately, such as highlighting individual cells within a field displaying the desired phenotype or limiting analysis to particular subcellular locations. Types of analysis include analysis of mitochondrial features, described above, and measurements of signal intensities between channels. Signal analysis may be further gated by thresholding specific channels, such as a DAPI stained image to limit analysis to nuclear regions. Conversely, regions may also be excluded from analysis via the same process, such using the DAPI channel to enable analysis of cytoplasmic regions specifically.

Measurements may then be taken within the region to determine features such as average signal intensity for each channel. Colocalization analysis may also be conducted, evaluating the intensity of a pixel in one channel specified by the user and comparing it against values in a second channel. This generates measurements such as the Pearson's correlation coefficient (Karl Pearson 1896), Manders overlap coefficient and the Manders colocalization coefficients, M1 and M2 (Manders et al. 1993). All statistics produced are saved as csv files alongside the image file in a tabular format. This provides a powerful feature set than can be applied to either a single image or a folder of like images to quickly process large volumes of imaging data with an emphasis on accessibility and user control.

A



B

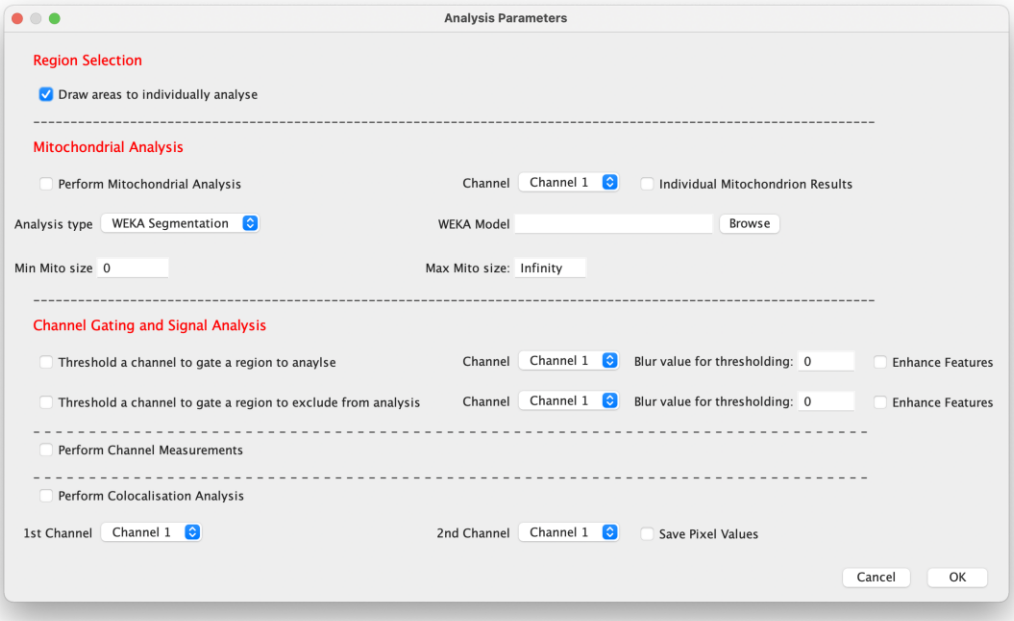


Figure 5.6 – Macro user interface allows users to more easily set **(A)** parameters for processing multi-dimensional images before export in batch mode and **(B)** carry out image analysis.

5.2.4 Survivin influences mitochondrial mass but not fission/fusion

The expression of genes involved in regulating mitochondrial dynamics were assessed by RT-PCR (Fig. 5.7). Analysis of mRNA extracts revealed no significant differences between cell lines.

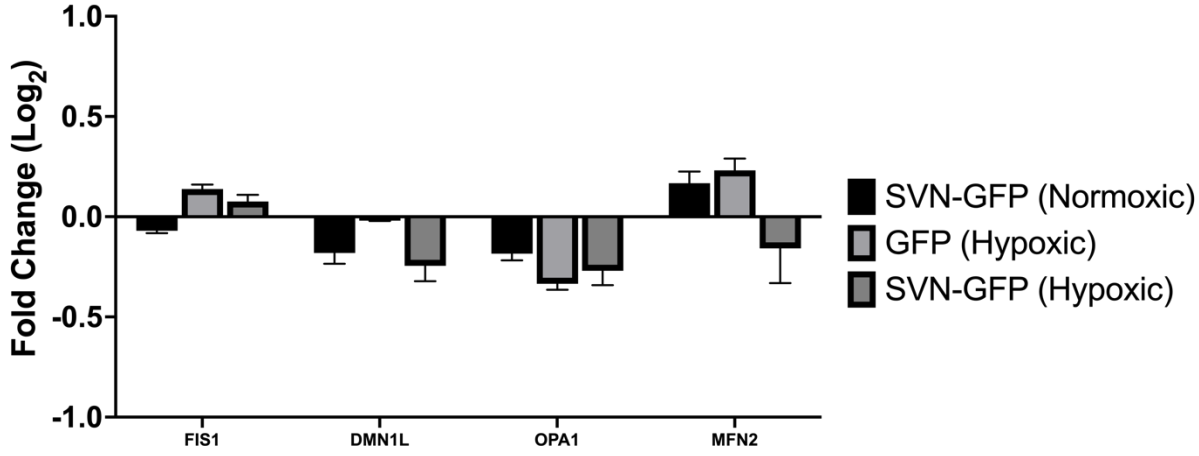
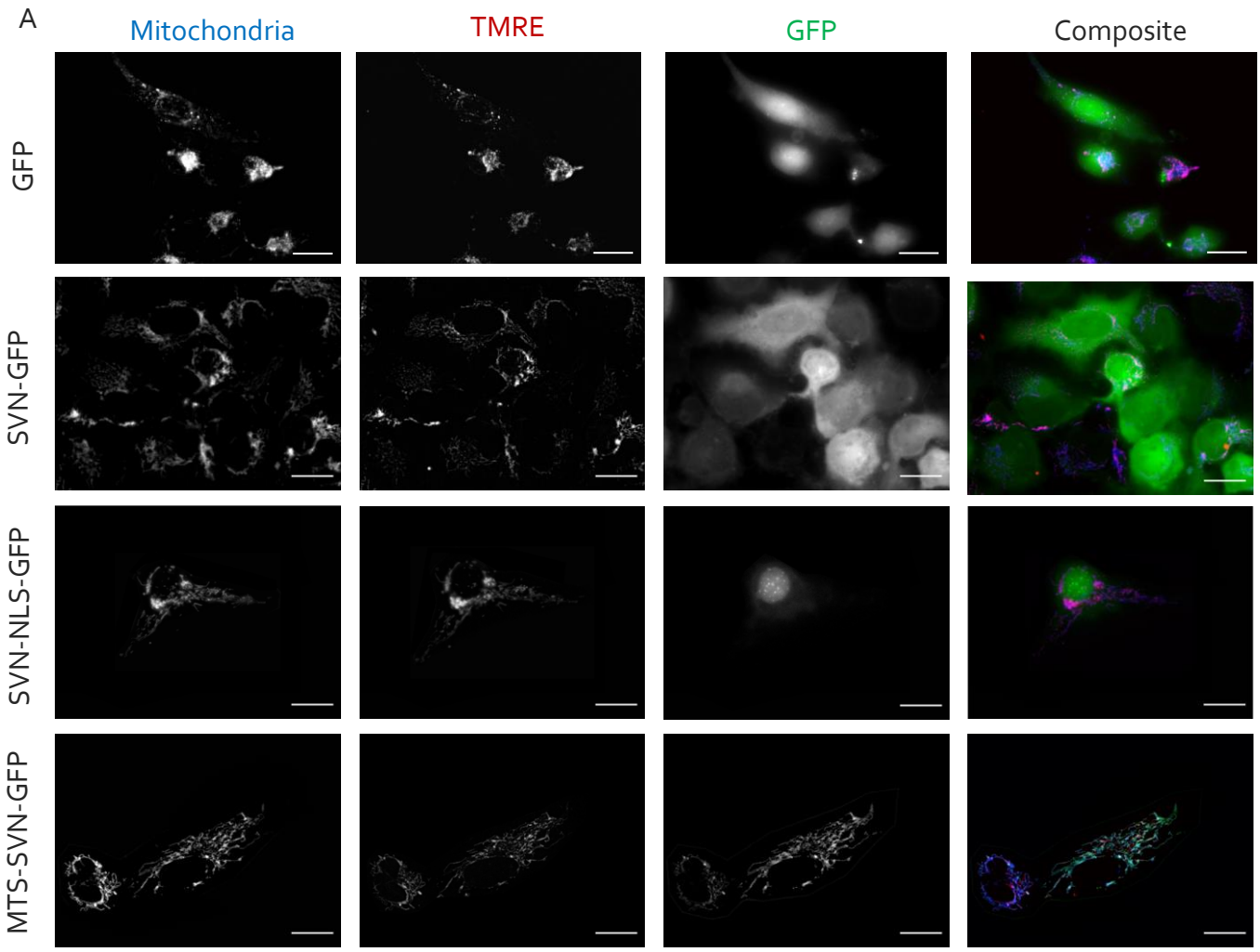
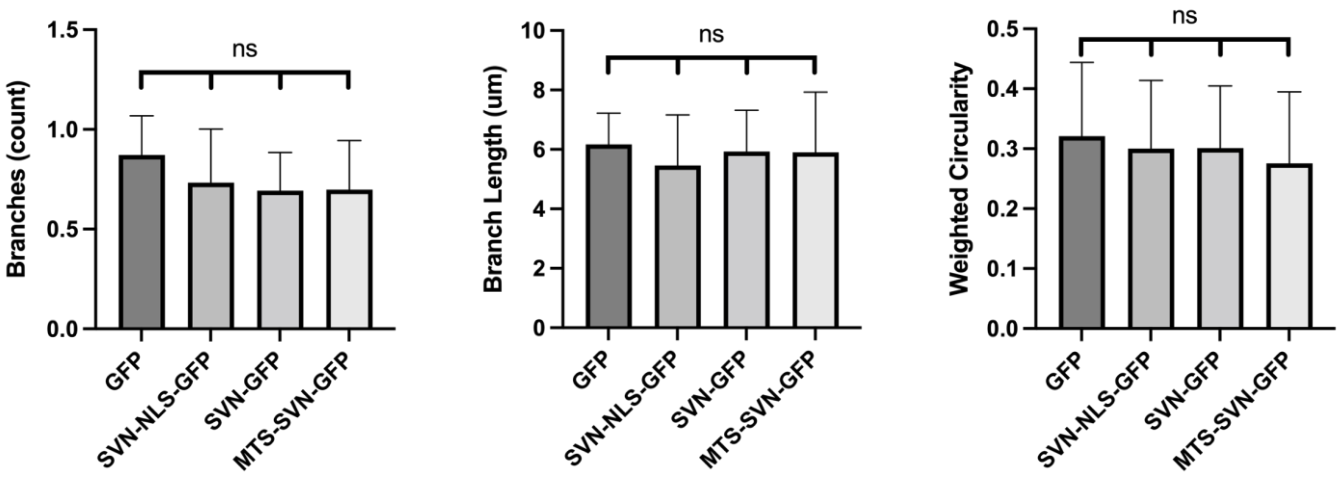


Figure 5.7 – Survivin expression had no significant impact on the expression of mitochondrial fission and fusion genes.

This was followed by analysis of the mitochondrial networks under normoxic conditions within U2OS cells expressing survivin constructs (Fig. 5.8). Measurements of mitochondrial branches and mitochondrion circularity revealed no significant differences, suggesting fusion and fission of mitochondrial were not influenced by survivin expression, which concurs with the gene expression data (Fig 5.7). However, in cells expression SVN-GFP and MTS-SVN-GFP a significant increase in the total area of the cellular mitochondrial network was observed (Fig. 5.8C), indicative of decreased mitochondrial degradation and/or increase in mitochondrial biogenesis. A smaller but non-significant increase was also demonstrated in SVN-NLS-GFP cells.


A
Mitochondria
TMRE
GFP
Composite
GFP
SVN-GFP
SVN-NLS-GFP
MTS-SVN-GFP

B



C

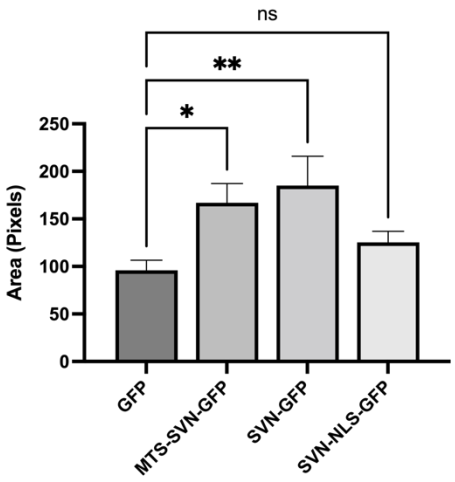


Figure 5.8 – Analysis of mitochondrial dynamics. (A) U2OS cell lines expressing control or survivin constructs. Cells were stained with MitoTracker and TMRE and imaged by fluorescent microscopy. Displayed is one representative of three repeated experiments. (Scale bar = 20 μm). **(B)** Comparison of average mitochondria branches, branch length and weighted mitochondrion circularity. **(C)** Comparison of mitochondrial area (*, $P<0.05$; **, $P<0.01$; n=3).

5.2.5 Survivin reduces mitochondrial membrane potential in cancer cells

Next, mitochondrial membrane potential was assessed through TMRE staining (Fig. 5.9A), which accumulates preferentially in polarised mitochondria (Perry et al. 2011). In line with measurements of OXPHOS activity, a significant reduction was demonstrated in SVN-GFP and MTS-SVN-GFP expressing cells with a non-significant reduction in SVN-NLS-GFP cells. To further probe the correlation of survivin with membrane potential, cells were treated with control siRNA or survivin siRNA, creating three conditions with increasing expression of survivin protein (Fig. 5.9B). Cells generated the highest average TMRE signal with survivin knockdown and lowest with its overexpression, establishing a clear relationship between the two. As mitochondrial fission was not previous exhibited, other factors influencing polarisation were examined. Transcriptional expression of the membrane uncoupling proteins, UCP2 and UCP3, were shown to correlate with survivin overexpression, both under normoxic and hypoxic conditions (Fig. 5.9C). An increase for UCP2 also seen in GFP cells under hypoxia.

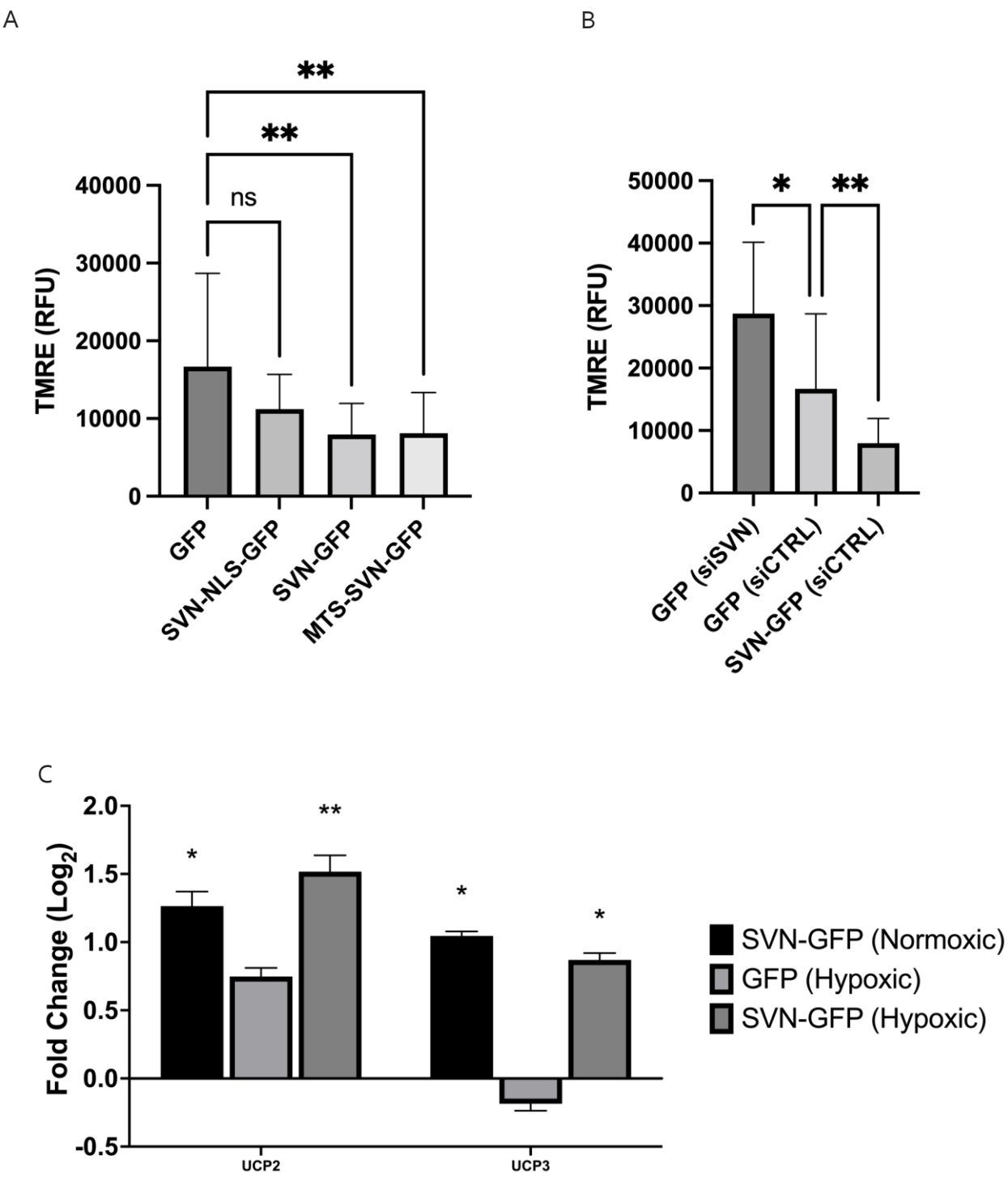


Figure 5.9 – Survivin reduced mitochondrial membrane potential (A) Average TMRE signal of U2OS cell lines expression control survivin constructs. (B) Average TMRE signal of

control or SVN-GFP cells treated with control or survivin siRNA. (C) Expression of UCP mRNA by control or SVN-GFP expressing cells in normoxic or hypoxic conditions compared to normoxic GFP expressing cells. (*, P<0.05; **, P<0.01; n=3).

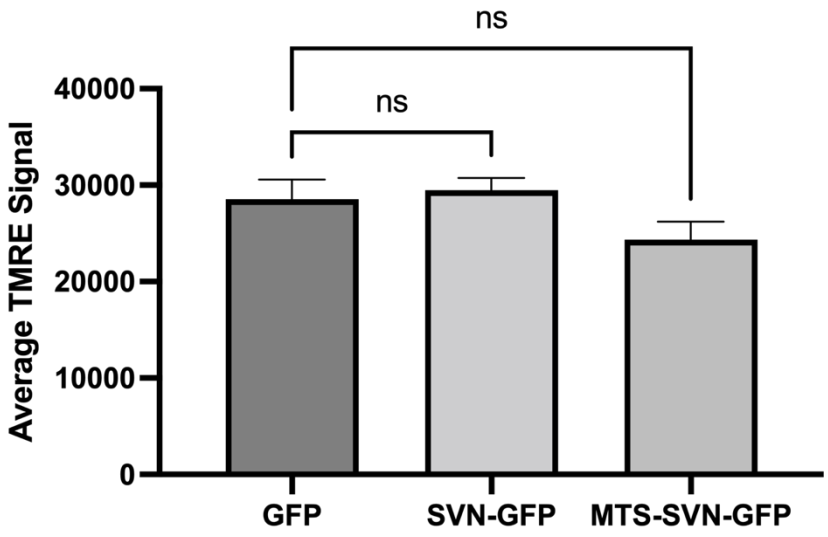


Figure 5.10 – Survivin expression does not induce significant mitochondrial depolarisation in MRC5 cells. Average TMRE signal of MRC5 cells expression control or survivin constructs.

The influence of survivin on non-cancerous MRC5 cells was also investigated (Fig. 5.10). Whilst SVN-GFP had shown significant decreases in U2OS cells, no demonstrable decrease was exhibited in MRC5 cells. MTS-SVN-GFP additionally demonstrated a non-significant reduction in TMRE staining in these untransformed fibroblasts.

5.2.6 Survivin may interact with numerous metabolic proteins

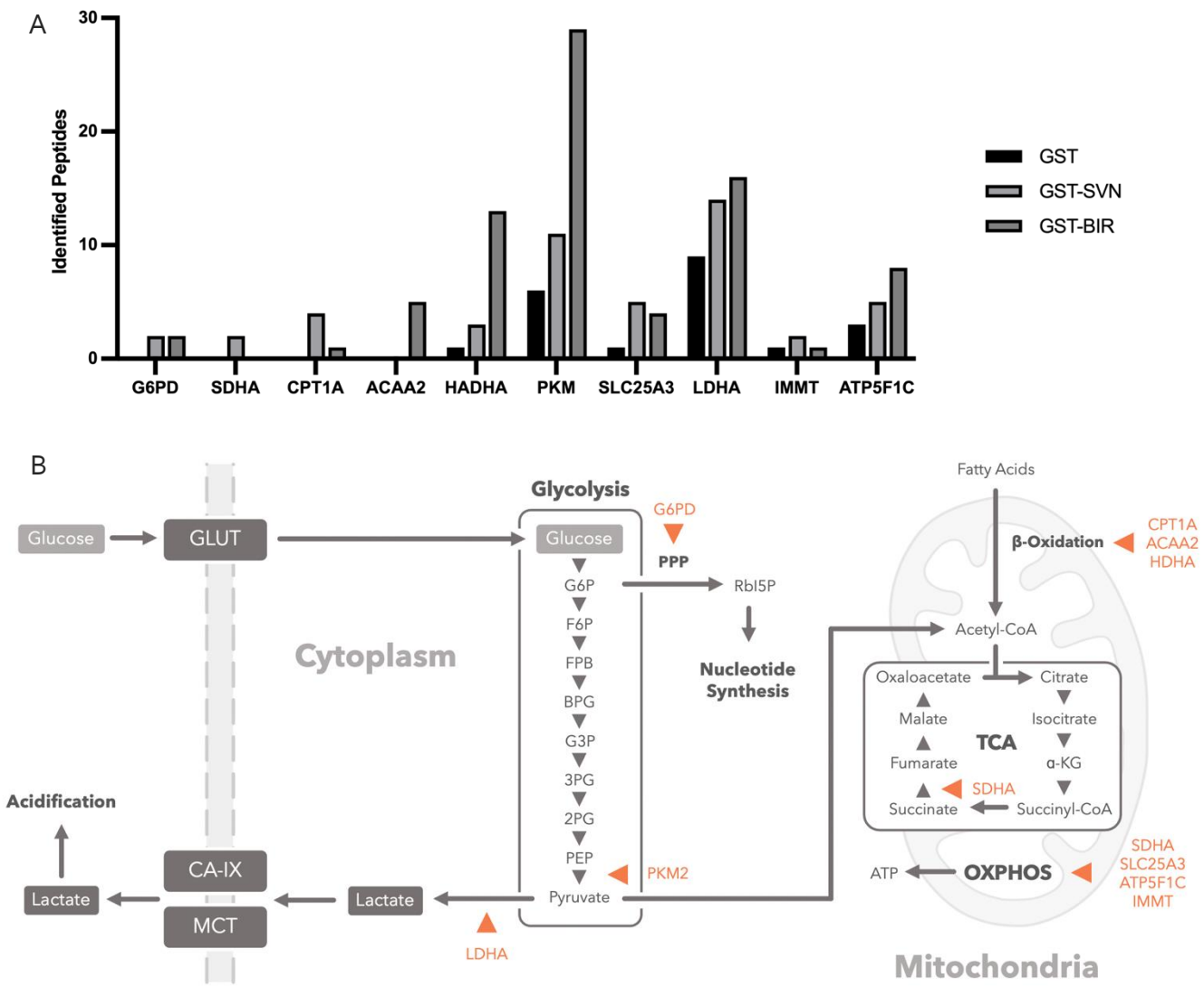


Figure 5.11 – Survivin pulls down numerous metabolic proteins. **(A)** Mass spectrometry analysis of GST pulldown assays comparing control GST samples to survivin (GST-SVN) and survivin BIR domain (GST-BIR) constructs. **(B)** Overview of putative binding partners and their role in cell metabolism. Created by author.

To assess other protein interactors that work together with survivin to influence metabolism, mass spectrometry analysis of a GST pull-down assay (performed by Hana Abdelkabir) was performed using HeLa cells expressing either a GST control, GST-tagged full length survivin (GST-SVN) or GST-tagged survivin BIR domain (GST-BIR) (Fig. 5.11A). This revealed a number of potential binding partners associated with cell metabolism, including succinate dehydrogenase (SDHA), lactate dehydrogenase A (LDHA) and pyruvate kinase (PKM). Proteins associated with other mitochondrial functions were also identified, including MICOS complex subunit MIC60 (IMMT), ATP synthase subunit gamma (ATP5F1C). Together these raise the possibility of multiple points (summarised in Fig. 5.11B) at which survivin may influence, or be influenced by, cellular metabolic pathways.

5.3 Discussion

Numerous studies have demonstrated links between survivin expression and metabolic alterations. However, no consensus on its mechanism nor metabolic impact prevails, and these studies have been focused on its role under normoxia, limiting their generalisation to in vivo conditions. As survivin localises to both the nuclear and mitochondrial compartments under hypoxia in cancer cells, an understanding of its impact within these regions may further inform its mechanistic role within the context of metabolic and mitochondrial pathways.

5.3.1 Survivin promotes glycolysis in cancer cell lines

The Warburg effect describes the propensity for cancer cells to perform glycolysis to meet their energy demands, even in conditions supportive of OXPHOS (Liberti, Locasale 2016). Survivin expression has been shown to both support (Hagenbuchner et al. 2013; Townley, Wheatley 2020) and inhibit (Rivadeneira et al. 2015) this metabolic rewiring, with different proposed mechanisms. In this study, glucose and lactate assays performed on U2OS cells correlated survivin expression with both elevated glucose consumption and lactate production under normoxia, supporting a role for survivin in the promotion of aerobic glycolysis. However, under hypoxic conditions, the influence of survivin was abolished. Both cell lines experienced increased glucose consumption and lactate production, although less dramatically in survivin overexpressing cells. Together these data may indicate a commonality in the underlying mechanisms by which survivin and hypoxia promote glycolysis, resulting in a diminished combined effect as similar pathways are utilised. This is demonstrated in the transcriptional expression of GLUT1, in which both survivin and hypoxia correlate with its upregulation. Alternatively, it may be suggested survivin adopts new roles under hypoxia in line with redistribution within the cell. Its mediation of metabolic processes under normoxia may therefore be

altered as survivin accumulates within the mitochondrial and nuclear compartments.

Despite increased lactate production and normal expression of LDHA, which mediates the conversion of pyruvate to lactate, lactate transporter CA-IX demonstrated significant downregulation with survivin expression. Whether this resulted in decreased lactate export and concomitant cytoplasmic acidification remains unclear; numerous transport proteins mediate this process, including the monocarboxylate transporters commonly upregulated in cancer (Sun et al. 2020).

Survivin was also shown to mediate p53 expression (Fig. 4.4). Whilst typically associated with regulating cell death, p53 activity is also linked with inhibition of glycolysis via the regulation of glycolytic proteins (Zhang et al. 2010). These include upregulation of TP53-induced glycolysis regulator (TIGAR), which degrades fructose-2,6-biphosphate (Bensaad et al. 2006), and downregulation of fructose-2,6-biphosphatase (Zhang et al. 2010) and the glucose transporter proteins, Glut1 and Glut4 (Schwartzenberg-Bar-Yoseph et al. 2004). P53 downregulation by survivin (Fig. 4.4) may therefore relinquish its inhibitory effects on cellular glycolysis and promote the Warburg effect.

Identification of PKM, which facilitates the generation of pyruvate from phosphoenolpyruvate and transcription of glycolytic enzymes (Yang et al. 2012), and LDHA as potential protein interactors may further implicate survivin as a complex regulator of cellular metabolism. Of note, LDHA (Jin et al. 2017) and SDHA (Ogura et al. 2012) are regulated by the tyrosine-protein kinase Src, a known binding partner of survivin (Dunajová et al. 2016). Src activity has been linked with a similar metabolic phenotype with increased glycolysis and supressed OXPHOS activity (Djeungoue-Petga et al. 2019; H. Ma et al. 2020; Ogura et al. 2012). Src activity has also been shown to inhibit mtDNA replication and result in decreased

mtDNA levels (Djeungoue-Petga et al. 2019), mirroring results demonstrated with survivin overexpression (Townley, Wheatley 2020). While survivin has been shown to activate Src and mediate cell-adhesion (Capra, Eskelinen 2017; Dunajová et al. 2016), the potential role of this pathway in cell metabolism and mitochondrial activity remains unexplored. These putative interactions may therefore be mediated by the survivin-Src complex.

5.3.2 Survivin inhibits OXPHOS and mitochondrial membrane polarisation.

In line with increased glycolysis, survivin expression correlated with reduced OXPHOS. This mechanism by which this is mediated remains unclear however. Mitochondrial dynamics demonstrated no measurable alterations with survivin expression, disputing the increased fission observed by Hagenbuchner et al. (2013) and supporting the findings of our lab (Townley, Wheatley 2020). Discrepancies may be attributed to different cancer types investigated between studies, with Hagenbuchner using neuroblastoma cells while Townley and Wheatley examined mitochondrial dynamics in cervical cancer (HeLa) cells and osteosarcoma cells (U2OS) were used here. In agreement with this study, a significant increase in the mitochondrial area of survivin overexpressing cells was also demonstrated, supporting altered mitochondrial turnover. Whereas Townley and Wheatley (2020) observed no significant decrease in membrane potential, a significant difference was demonstrated in U2OS cells here. This too may be attributed to reduced mitophagy and a consequent failure to clear dysfunctional and depolarised mitochondria (Twig, Shirihai 2011).

Interestingly, UCP2 and 3 were additionally found to be upregulated by survivin and may mediate membrane uncoupling, reducing the respiratory capacity of affected mitochondria. Notably, differences in membrane potential were not demonstrated in MRC5 cells however. This may be attributed to the lack of a mitochondrial pool

of survivin in non-transformed cells (Dohi, Beltrami, et al. 2004). However, ectopic expression of MTS-SVN-GFP in MRC5 cells, which presents a clear mitochondrial population, did result in a greater, but not significant, reduction of membrane potential in these cells.

In line with its inhibition of glycolysis, p53 has been linked with increased OXPHOS activity. P53 directly regulates synthesis of cytochrome *c* oxidase (SCO2), which mediates the assembly of the cytochrome *c* oxidase complex (complex IV) and supports the ETC (Matoba et al. 2006). Additionally, glutaminase 2 (GLS2) has been identified as a p53-regulated protein and increases the production of glutamate and α-ketoglutarate to support mitochondrial respiration (Hu et al. 2010). Survivin-mediated suppression of p53 may consequently inhibit OXPHOS and mitochondrial function.

5.3.2 Identification of putative mitochondrial partners of survivin in cancer cells.

Mass spectrometry data additionally revealed a number of potential binding partners. Although their interactions remain to be confirmed, these candidates highlight prospective pathways by which survivin may further influence cell metabolism through inhibition or stabilisation. A number of proteins thought to support the ETC were identified: IMMT constitutes a critical component of the MICOS complex, involved in the generation of mitochondrial cristae; SDHA, a member of the ETC, and ATP synthase were also highlighted and a potential interaction with survivin has previously been observed (Rivadeneira et al. 2015); the phosphate carrier and copper transport protein SLC25A3 facilitates the ETC through the import of phosphate ions and copper molecules, involved in the activity of complex IV (Boulet et al. 2018). Together these proteins may further regulate mitochondrial membrane potential and consequently alter the respiratory capacity of the mitochondria. A series of proteins involved in beta-oxidation were also

identified, including CPT1A, ACAA2 and HADHA. Oxidation of fatty acids functions as an alternative pathway for the generation of acetyl-CoA to support the TCA cycle and downstream OXPHOS activity (Vishwanath 2016).

Mitochondria are sensitive to the metabolic state of the cell and adapt accordingly. These alterations may therefore reflect the response of a metabolism shifted towards glycolysis and thus deficient in metabolites such as acetyl-CoA, inducing mitochondrial adaptations as result (Ježek, Plecitá-Hlavatá 2009). Vice versa, reduced OXPHOS activity may similarly promote the expression of glycolytic enzymes to meet the shortfall in ATP production.

A further putative interactor identified by mass spectrometry analysis was G6PD, which normally facilitates the entry of glucose-6-phosphate into the pentose phosphate pathway (PPP) and acts as the rate-limiting step. PPP generates ribose 5-phosphoate, assisting cell proliferation through nucleotide synthesis, in addition to NADPH, which maintains reduced glutathione levels within the cell (Williams, Ford 2004). Glutathione in turn protects the cell from oxidative stress and mitigates ROS-mediated damage. G6PD activity is critical to the viability of red blood cells, where high polyunsaturated fatty acid content within the membrane and haemoglobin auto-oxidation within the cell renders them susceptible to oxidative stress (Jewell et al. 2013). A deficiency of G6PD is thus associated with haemolytic anaemia (Richardson, O'Malley 2021). Notably, survivin is unusually expressed throughout the maturation of erythroid cells (Gurbuxani et al. 2005) and may facilitate cell survival through G6PD stabilisation.

5.3.3 Development of mitochondrial and image analysis software

A robust macro, running within the free FIJI software, presents a useful and accessible tool for researchers to quickly process and analyse large volumes of microscopy images without requiring custom code written to handle their data set. As part of this software, a workflow for mitochondrial image analysis was also developed. Utilising a combination of pre-processing techniques and a segmentation process developed through machine learning algorithms, an accurate and precise system for analysing mitochondrial dynamics from low contrast widefield images was produced.

5.3.4 Summary

These findings support a role for survivin in causing the metabolic shift towards glycolysis and a reduced reliance on OXPHOS activity. How this is achieved appears to be highly complex and may be accomplished via multiple means, e.g. reduction of mitochondrial membrane potential, regulation of OXPHOS and glycolysis proteins as well interactions with linked metabolic pathways, such as fatty acid synthesis. Further still, survivin may modulate broad acting gene regulators, including AMPK, p53 and potentially HIF1a (discussed in 4.3.2). Survivin may therefore function as a multifaceted regulator of metabolism, intersecting with multiple cellar pathways.

Chapter 6 – General Discussion

6.1 Overview

As a member of the IAP family and constituent of the CPC complex (Li et al. 1999), survivin has largely been associated with its roles in apoptosis inhibition and mitosis respectively. However, whilst survivin contains no intrinsic enzymatic activity, research has revealed an extensive functional repertoire, attributed to the numerous interactions it maintains with intracellular proteins. These functions extend to autophagy, metabolism, mitochondrial dynamics and DNA repair (Wheatley, Altieri 2019; Garg et al. 2016). Together with its differential expression within cancers (Velculescu et al. 1999), survivin has been highlighted as an appealing target for the development of cancer therapeutics. Mediation of its intracellular interactions and concomitant functions are thought to be governed by its temporal expression, spatial positioning and post translational modifications, establishing complex regulatory systems with potential crosstalk between cell pathways (Wheatley, Altieri 2019; Garg et al. 2016). Despite its discovery over two decades ago (Ambrosini et al. 1997), the precise mechanisms through which survivin realises its metabolic and anti-apoptotic effects as well as its subcellular localisation remain poorly characterised. Elucidation of these key aspects are vital to development of potential anti-cancer strategies as well as our understanding of cellular homeostasis.

The development of solid tumours during the progression of cancer establishes a spectrum of microenvironmental conditions with differing concentrations of factors such as oxygen, nutrients, signalling molecules and waste products (Yuan et al. 2016). These in turn initiate a cascade of intracellular signalling pathways and adaptations, influencing a broad range of cancer cell behaviours with significant consequences for patient outcome. With many tumours generating diminished

oxygen availability, hypoxia is a key mediator of cancer development with implications for tumour aggression, treatment resistance and patient relapse (Muz, de la Puente, Azab, Azab 2015; Wilson, Hay 2011). Adaptations to this milieu are primarily orchestrated of the HIF transcription factors, regulating the expression of an extensive range of genes involved in various cell processes, including cell metabolism, apoptosis resistance, motility and proliferation (Muz, de la Puente, Azab, Azab 2015).

Survivin constitutes a HIF gene target and is linked with a number of associated pathways, such as treatment resistance and mitochondrial and metabolic regulation (Wheatley, Altieri 2019; Garg et al. 2016). Its potential role in mediating the adaptation and consequent development of cancers to TME is of great interest. This thesis therefore set out to explore the spatial regulation of survivin within the context of hypoxia; the mechanisms governing its localisation, including nuclear accumulation observed in response to genotoxic stress; the cytoprotective capabilities of survivin within hypoxia and the potential involvement of DNA repair pathways; and the influence of survivin on cell metabolism and mitochondrial function.

6.2 Survivin localisation within the TME

With an understanding of the disparity between traditional normoxic culture techniques and the TME, this thesis aimed to investigate survivin behaviours within a context that better replicated normal tumour conditions. In testing the influence of hypoxia, survivin exhibited altered subcellular positioning, with greater concentrations of its nuclear and mitochondrial pools. This was further supported by 3D spheroid cultures, demonstrating altered survivin locals within different domains of the tumour. While the presence of nuclear survivin has been observed within patient tumour tissue for some time, with numerous reports attempting to

evaluate its prognostic value (Rexhepaj et al. 2010; Brennan et al. 2008; Vischioni et al. 2004; Kim, McNiff 2008), little is known regarding the molecular mechanisms regulating its cytoplasmic/nuclear residency nor its functional implications. Indeed, under standard laboratory growth conditions (i.e., monolayer cultures under normoxic conditions with optimised growth media), if expressed in interphase, survivin appears exclusively within the cytoplasm (Stauber et al. 2007). These findings would suggest survivin activity is therefore strongly linked to the environmental circumstances in which cell are cultured and that traditional laboratory conditions may misrepresent or limit the full diversity of its roles.

6.3 Nuclear survivin and links to the DNA damage response

The TME is characterised by a reduction to both oxygen and nutrient availability. Interestingly, both of these environmental deficiencies have been shown to initiate the DNA damage response within cells (White et al. 2020), even in the absence of detectable DNA damage (Hammond et al. 2002). Exposure to such challenges here was shown to induce the nuclear accumulation of survivin in a similar manner to exposure to genotoxic stress. As further examination of nuclear survivin demonstrated a reliance on the DNA damage response pathway to initiate its accumulation when challenged with DNA damaging agents, it is possible these responses may share a linked mechanism to regulate the spatial distribution of survivin. Further interrogation of these pathways is required to characterise the molecular mechanisms governing their activity. Inhibition of early DNA damage response steps would therefore be expected to prevent downstream events, such as survivin relocalisation, from occurring when exposed to the same environmental stresses. This may be tested through the use of chemical inhibitors, as used in this study, or CRISPR-mediated knockout / siRNA-mediated knockdown of relevant genes before observing surviving localisation through imaging or western blots of

subcellular fractions to determine its distribution through the cell following treatment.

6.4 Nuclear and mitochondrial-localised survivin is cytoprotective

Unexpectedly, survivin under hypoxia facilitated cell survival despite altered subcellular distribution. The anti-apoptotic activity of survivin has been attributed to a number of pathways occurring within the cytoplasm following MOMP and nuclear occupation is thought to abrogate its pro-survival functions (Connell et al. 2008). However, survivin expression, both knockdown and overexpression, correlated with cell survival in response to a number of apoptotic agents under hypoxia, where it resides within the nucleus. This was further supported by survivin constructs targeted to the nucleus via an NLS sequence and when forced into the nucleus by inhibiting nuclear export. Whilst this initially appears inconsistent with previous research, a number of studies have also shown survivin to both accumulate within the nucleus in response to DNA damage and promote genotoxic resistance (Rödel et al. 2005; Obexer et al. 2009; Al-Khalaf, Aboussekhra 2013). Yet, this clear contradiction does not seem to be widely acknowledged. As the underlying mechanisms mediating cell resistance remains to be clarified within this context, it is unclear whether cell type, treatment duration or the apoptotic agent used may affect survivin-mediated protection and thus result in differing experimental conclusions.

One possible mechanism is the proposed link between survivin and DNA repair, in which a number of reports have correlated survivin expression with increased repair of DNA damage. While several prospective mechanisms have been offered, the interaction of survivin with NHEJ machinery, specifically DNA-PKcs, represents the most well characterised pro-survival role for survivin within the nucleus (Güllülü et

al. 2021). However, the present study failed to replicate these findings, although a pulldown assay identified DNA-PKcs as a putative binding partner, alongside a number of other DNA repair proteins. Moreover, survivin failed to colocalise with g-H2AX foci in response to DNA damage and inhibition of NHEJ failed to abolish cytoprotection. Indeed, the altered substrate specificity previously reported (Güllülü et al. 2021), which suggested survivin interaction with DNA-PKcs reduced phosphorylation of many NHEJ substrates, may suggest survivin does not directly facilitate NHEJ but instead may promote alternative pro-survival mechanisms, including inactivation of the pro-apoptotic transcription factor, FOXO3. The rate of DNA repair, phosphorylation of FOXO3 and expression of FOXO3-target genes are therefore expected to correlate with survivin levels within the cell. Survivin expression levels may be modulated through the over-expression of an exogenous survivin construct or knocked down with siRNA as used in this study. DNA repair may be monitored directly via a time course of comet assays to measure DNA damage following treatment with a genotoxic agent. Antibodies against FOXO3 and phosphorylated FOXO3 may be used in western blots to determine the level of phosphorylation that has occurred as well as protein stability while qPCR analysis of target genes could be used to measure its transcriptional activity.

In line with this mechanism, survivin expression correlated with altered expression of numerous proteins implicated in cell survival, including downregulation of the pro-apoptotic proteins p53 and AIFM1. Under hypoxia, survivin notably increased XIAP stabilisation. While this interaction has been demonstrated before under normoxic conditions and was found to promote XIAP-mediated suppression of caspase activity, under hypoxia XIAP accumulates in the nucleus (Russell et al. 2008; Park et al. 2017), which may spatially separate it from cytoplasmic caspase enzymes during early apoptosis. However, both initiator and executioner caspase enzymes have been observed within the nucleus and facilitate the proteolytic cleavage of nuclear substrates during the later stages of apoptosis (Prokhorova et al. 2018).

Nuclear XIAP stabilisation may therefore facilitate caspase inhibition in the later stages of apoptosis within this compartment to promote cell survival. Survivin levels would therefore correlate with complexation of XIAP and caspase enzymes within the nucleus of cells exposed to hypoxic conditions and treated with apoptotic stimuli. This may be assessed by immunoprecipitation assays of nuclear extracts using a cleaved caspase-7 antibody and observing XIAP levels after modulating survivin expression levels, as outlined previously. Furthermore, XIAP regulates the nuclear localisation of HIF1a, facilitating transcriptional expression of HIF target genes (Park et al. 2017). Downstream HIF targets include a large of number of genes involved in multiple pathways (Yu et al. 2017; Karakashev, Reginato 2015), summarised in table 1.1, and facilitate treatment resistance and promote glycolysis, concordant with the phenotype exhibited by survivin expression. Modulation of survivin levels would therefore correlate with the levels of HIF1a within the nucleus and concomitant expression of HIF1 target genes. Knockdown and overexpression of survivin may be paired with western blots of nuclear fractions and fluorescent microscopy to examine this potential relationship alongside qPCR analysis of HIF1 gene targets.

Survivin targeted to the mitochondria was found to promote cell survival. Whilst apoptotic resistance has previously been attributed to the release of mitochondrial survivin into the cytosol (Dohi, Beltrami, et al. 2004), MTS-SVN-GFP was retained within the mitochondria following exposure to genotoxic stress. This cell survival function may be mediated by a putative interaction with transmembrane protein, VDAC2 (summarised in Fig. 6.1), which is responsible for mediating BAK activity and downstream MOMP (Cheng et al. 2003). Inhibition of BAK-BAX oligomerisation would prevent the release of pro-apoptotic factors and initiation of the intrinsic pathway. Complexation of survivin and VDAC2 would there be expected to occur in response to the induction of apoptosis. Immunoprecipitation or FRET based approaches may be used to determine protein complexation. The functional

implications of this potential interactions may be determined by monitoring the release of mitochondrial pro-apoptotic proteins, such as cytochrome c, in response to apoptotic stimuli. This may be monitored through western blots of cytoplasmic and mitochondrial extracts and the immunoprobing and imaging of fixed samples by fluorescent microscopy. Should survivin facilitate cell survival via this mechanism, greater retention of cytochrome c would be expected compared to cells with a knockdown of survivin.

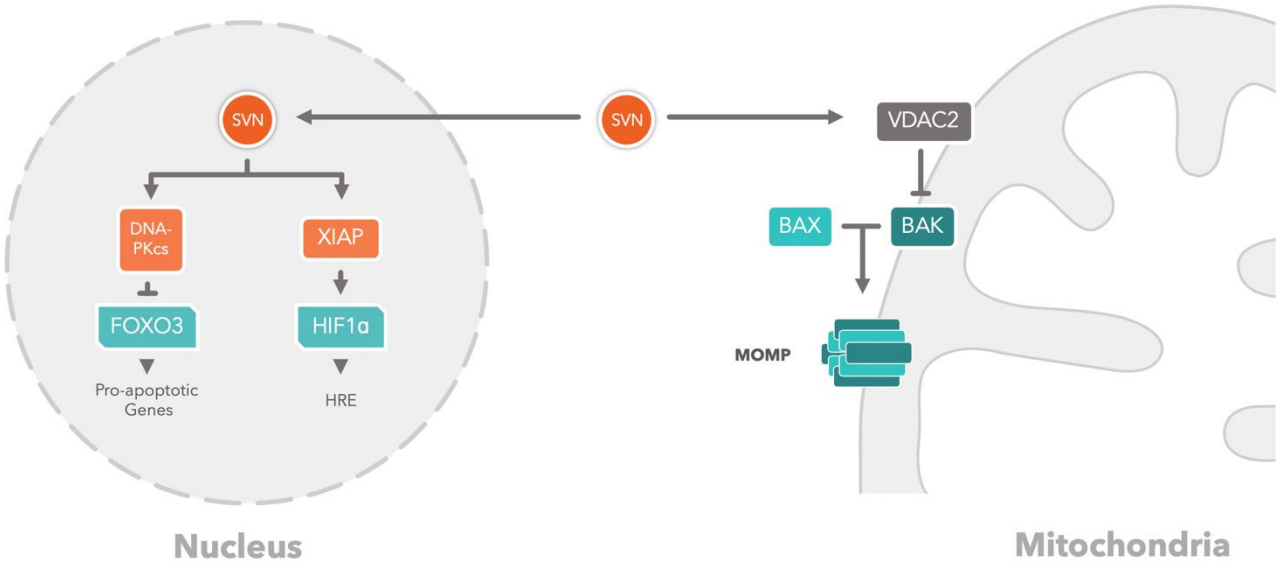


Figure 6.1 – Model of potential survivin pathways mediating apoptosis resistance within the nucleus and mitochondria. Created by author.

6.5 Survivin promotes the Warburg effect

Survivin over-expression correlated with a similar metabolic phenotype to cells exposed to hypoxia: both exhibiting an increased reliance on glycolytic pathways with reduced OXPHOS activity (Summarised in Fig. 6.2). The Warburg effect,

characterised by the predilection of cancer cells for glycolysis under normoxic conditions (Liberti, Locasale 2016), has been partly attributed to the activity of HIF transcription factors (Robey et al. 2005). Elevated glucose consumption was supported by Glut1 and AMPK upregulation under normoxic conditions, facilitating increased glucose import and activity of glycolysis enzymes. P53 was also shown to be downregulated by survivin under normoxia, limiting its inhibitory effects on glycolysis and promotion of OXPHOS activity. In support of the Warburg effect, survivin was shown to decrease mitochondrial OXPHOS, potentially through depolarisation of mitochondrial membrane potential mediated by upregulation of UCP proteins, or decreased mitophagy, preserving dysfunctional depolarised mitochondria. Notably, changes to mitochondrial dynamics were not observed, both in the expression of fission and fusion proteins and mitochondrial morphology, as previously suggested (Hagenbuchner et al. 2013).

A number of putative binding partners were also identified, linking survivin with a range of metabolic pathways. Modulation of these proteins may afford survivin a broad regulatory role in cell metabolism. These interactions may be verified by immunoprecipitation assays using cell extracts. Given the complex and highly interlinked nature of these pathways, how survivin mediates changes to cell metabolism is not clear, however. Previously demonstrated interactions with Src (Dunajová et al. 2016), XIAP (Altieri 2010; Dohi, Okada, et al. 2004) and DNA-PKcs (Güllülü et al. 2021) may enable survivin to influence of range of proteins involved in cell metabolism, in line with its role as an adaptor protein with no intrinsic enzymatic activity. Inhibiting these potential interactions may therefore diminish metabolic alterations, such as increase glucose uptake, associated with survivin expression. Knockdown of these binding partners or targeted modifications of survivin amino acids to alter their binding capacity where known, such phosphoresistant and phosphomimetic substitutions of S20 in the case of XIAP, may be utilised to assess their impact on glycolysis and OXPHOS activity within the cell

together with knockdown/overexpression of survivin and may be measured using the Glucose-Glo and resazurin assays employed in this study respectively.

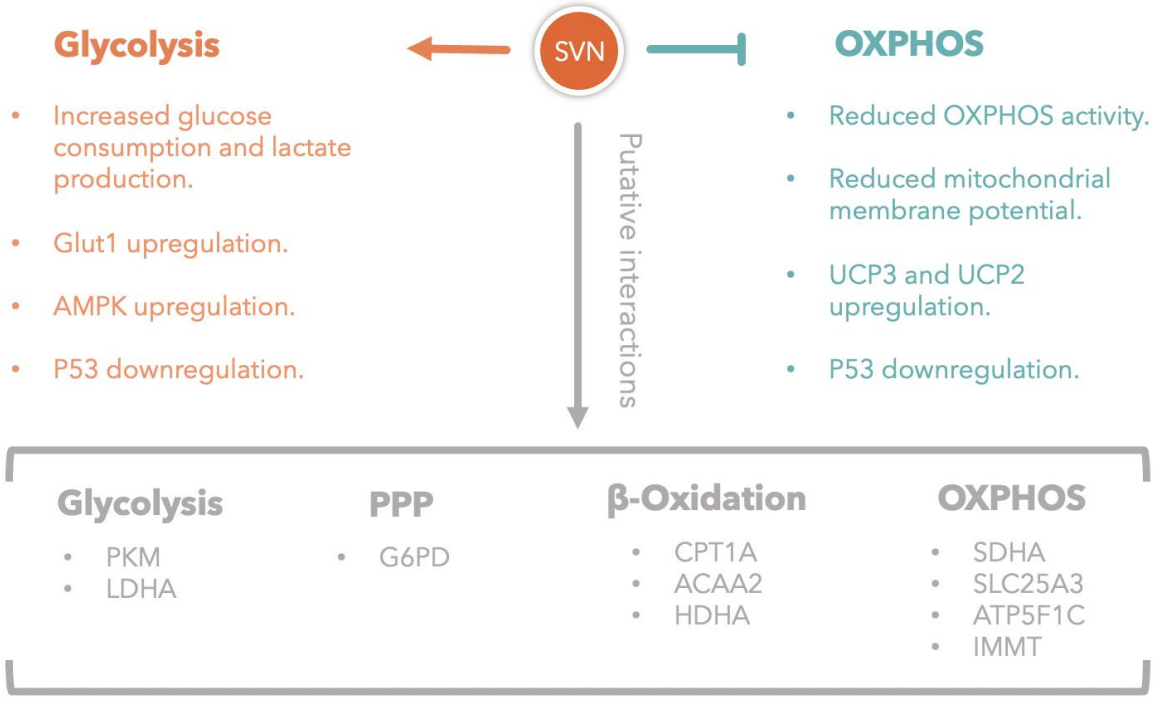


Figure 6.2 – Overview of survivin interactions with metabolic pathways. Created by author.

6.6 Cross-talk in cell survival mechanisms

Apoptotic resistance and altered cell metabolism may additionally function cooperatively, with interplay between anti-apoptotic and metabolic factors (Matsuura et al. 2016). The promotion of aerobic glycolysis has been shown to suppress protein kinase Cδ-dependent p53 activation, promoting cell survival (Mason et al. 2010), while p53 may supress glycolysis through the expression of TIGAR (Bensaad et al. 2006) and downregulation of glycolysis enzymes (Zhang et

al. 2010) and/or glucose transporters (Schwartzenberg-Bar-Yoseph et al. 2004). Growing evidence suggest glycolysis may facilitate DNA repair and protect against DNA damage. Proposed mechanisms include the maintenance of redox balance and nucleotide synthesis through the PPP pathway and lactate-mediated inhibition of HDACs, promoting an open chromatin structure that facilitates the access and transcription of DNA repair proteins (Sobanski et al. 2021). Indeed, a number of novel treatment strategies have aimed to target metabolic pathways to sensitise cancer cells to both chemotherapy and radiotherapy (Turgeon et al. 2018). Moreover, DNA repair proteins, such as ATM and DNA-PKcs, have been implicated in altered cell metabolism following DNA damage, including DNA-PKcs-mediated AMPK upregulation to promote glycolysis (Sobanski et al. 2021), linking similar results observed with survivin expression. Treatment resistance mediated by survivin may therefore be two-pronged, inhibiting apoptotic pathways directly whilst indirectly facilitating cell survival via metabolic rewiring.

These changes may also support cell growth under the adverse conditions of the TME, which experiences reduced oxygen and nutrient availability in addition to signalling molecules, such as growth factors. P53 downregulation by survivin thus circumvents p53-dependent apoptosis induced in the absence of growth factors (Mason et al. 2010). Furthermore, glycolytic pathways support the production of lipids, proteins and nucleic acids required for cell proliferation and tumour development (Graziano et al. 2016) and are associated with increased tumour aggression (Trendowski et al. 2015; Kunkel et al. 2003). The contributions of survivin to the development of cancer are therefore multidimensional, promoting treatment resistance and supporting tumour aggression and growth through metabolic adaptations. This thesis has notably highlighted novel mechanisms underpinning these functions and challenged previously proposed limitations on survivin activity and its interactome in cancer cells

Bibliography

Alavian, K.N. et al., 2011. Bcl-xL regulates metabolic efficiency of neurons through interaction with the mitochondrial F1FO ATP synthase [online]. *Nature cell biology*, 13(10), pp.1224–1233. Available at: https://pubmed.ncbi.nlm.nih.gov/21926988/ [Accessed 28 January 2022].

Alfarouk, K.O. et al., 2014. Glycolysis, tumor metabolism, cancer growth and dissemination. A new pH-based etiopathogenic perspective and therapeutic approach to an old cancer question [online]. *Oncoscience*, 1(12). Available at: www.impactjournals.com/oncoscience [Accessed 6 March 2022].

Alirol, E. et al., 2006. The mitochondrial fission protein hFis1 requires the endoplasmic reticulum gateway to induce apoptosis. *Molecular biology of the cell*, 17(11), pp.4593–4605. 10.1091/MBC.E06-05-0377.

Aljaberi, A.M., Webster, J.R.M., Wheatley, S.P., 2015. Mitotic activity of survivin is regulated by acetylation at K129 [online]. *Cell cycle (Georgetown, Tex.)*, 14(11), pp.1738–1747. Available at: https://pubmed.ncbi.nlm.nih.gov/25928399/ [Accessed 22 March 2022].

Al-Khalaf, H.H., Aboussekhra, A., 2013. Survivin expression increases during aging and enhances the resistance of aged human fibroblasts to genotoxic stress [online]. *Age*, 35(3), pp.549–562. Available at: https://link.springer.com/article/10.1007/s11357-011-9378-2 [Accessed 21 May 2021].

Almeida, K.H., Sobol, R.W., 2007. A unified view of base excision repair: Lesion-dependent protein complexes regulated by post-translational modification. *DNA Repair*, 6(6), pp.695–711. 10.1016/j.dnarep.2007.01.009.

Altieri, D.C., 2010. 10.1042/BJ20100814.

Altmeyer, M., Lukas, J., 2013. To spread or not to spread--chromatin modifications in response to DNA damage [online]. *Current opinion in genetics &*

development, 23(2), pp.156–165. Available at: https://pubmed.ncbi.nlm.nih.gov/23312207/ [Accessed 28 February 2022].

Aluvila, S. et al., 2014. Organization of the mitochondrial apoptotic BAK pore: oligomerization of the BAK homodimers [online]. *The Journal of biological chemistry*, 289(5), pp.2537–2551. Available at: https://pubmed.ncbi.nlm.nih.gov/24337568/ [Accessed 28 January 2022].

Ambrosini, G., Adida, C., Altieri, D.C., 1997. A novel anti-apoptosis gene, survivin, expressed in cancer and lymphoma. *Nature Medicine*, 3(8), pp.917–921. 10.1038/nm0897-917.

Andrabi, S.A. et al., 2014. Poly(ADP-ribose) polymerase-dependent energy depletion occurs through inhibition of glycolysis [online]. *Proceedings of the National Academy of Sciences of the United States of America*, 111(28), pp.10209–10214. Available at: https://pubmed.ncbi.nlm.nih.gov/24987120/ [Accessed 5 February 2022].

Andres, S.N. et al., 2012. A human XRCC4-XLF complex bridges DNA [online]. *Nucleic acids research*, 40(4), pp.1868–1878. Available at: https://pubmed.ncbi.nlm.nih.gov/22287571/ [Accessed 28 February 2022].

Arana, M.E., Kunkel, T.A., 2010. 10.1016/j.semcancer.2010.10.003.

Aravamudhan, P., Goldfarb, A.A., Joglekar, A.P., 2015. The kinetochore encodes a mechanical switch to disrupt spindle assembly checkpoint signalling [online]. *Nature Cell Biology 2014 17:7*, 17(7), pp.868–879. Available at: https://www.nature.com/articles/ncb3179 [Accessed 20 February 2022].

Arganda-Carreras, I. et al., 2010. 3D reconstruction of histological sections: Application to mammary gland tissue [online]. *Microscopy Research and Technique*, 73(11), pp.1019–1029. Available at: https://onlinelibrary.wiley.com/doi/full/10.1002/jemt.20829 [Accessed 25 March 2022].

Arganda-Carreras, I. et al., 2017. Trainable Weka Segmentation: a machine learning tool for microscopy pixel classification [online]. *Bioinformatics*, 33(15),

pp.2424–2426. Available at: https://academic.oup.com/bioinformatics/article/33/15/2424/3092362 [Accessed 25 March 2022].

Aspe, J.R., Wall, N.R., 2010. Survivin-T34A: molecular mechanism and therapeutic potential [online]. *OncoTargets and therapy*, 3, p.247. Available at: /pmc/articles/PMC3024888/ [Accessed 16 March 2022].

Asumen, M.G. et al., 2010. Dynamic changes to survivin subcellular localization are initiated by DNA damage. *OncoTargets and Therapy*, 3, pp.129–137. 10.2147/ott.s11484.

Atala A, 2002. Methods and Compositions for Organ Decellularisation.

Azab, A.K. et al., 2012. Hypoxia promotes dissemination of multiple myeloma through acquisition of epithelial to mesenchymal transition-like features. *Blood*, 119(24), pp.5782–5794. 10.1182/blood-2011-09-380410.

Bader, S.B., Dewhirst, M.W., Hammond, E.M., 2021. Cyclic Hypoxia: An Update on Its Characteristics, Methods to Measure It and Biological Implications in Cancer [online]. *Cancers*, 13(1), pp.1–20. Available at: /pmc/articles/PMC7793090/ [Accessed 21 March 2022].

Bai, H. et al., 2013. Hypoxia inducible factor-1α-mediated activation of survivin in cervical cancer cells [online]. *The journal of obstetrics and gynaecology research*, 39(2), pp.555–563. Available at: https://pubmed.ncbi.nlm.nih.gov/22925504/ [Accessed 30 March 2022].

Baker, B.M., Chen, C.S., 2012. Deconstructing the third dimension – how 3D culture microenvironments alter cellular cues. *Journal of Cell Science*, 125(13), pp.3015–3024. 10.1242/jcs.079509.

Baker, M.J. et al., 2014. Stress-induced OMA1 activation and autocatalytic turnover regulate OPA1-dependent mitochondrial dynamics. *The EMBO journal*, 33(6), pp.578–593. 10.1002/EMBJ.201386474.

Balkwill, F.R., Capasso, M., Hagemann, T., The tumor microenvironment at a glance. *Journal of Cell Science*, 125, pp.5591–5596. 10.1242/jcs.116392.

Banfalvi, G., 2011. Available at: https://link.springer.com/protocol/10.1007/978-1-61779-182-6_1 [Accessed 21 March 2021].

Barnhart, B.C., Alappat, E.C., Peter, M.E., 2003. The CD95 type I/type II model [online]. *Seminars in immunology*, 15(3), pp.185–193. Available at: https://pubmed.ncbi.nlm.nih.gov/14563117/ [Accessed 3 February 2022].

Barrett, R.M.A., Osborne, T.P., Wheatley, S.P., 2009. Phosphorylation of survivin at threonine 34 inhibits its mitotic function and enhances its cytoprotective activity [online]. *Cell cycle (Georgetown, Tex.)*, 8(2), pp.278–283. Available at: https://pubmed.ncbi.nlm.nih.gov/19158485/ [Accessed 22 March 2022].

Bayer, C., Vaupel, P., 2012. Acute versus chronic hypoxia in tumors. *Strahlentherapie und Onkologie*, 188(7), pp.616–627. 10.1007/s00066-012-0085-4.

Beardmore, V.A. et al., 2004. Survivin dynamics increases at centromeres during G2/M phase transition and is regulated by microtubule-attachment and Aurora B kinase activity. *Journal of Cell Science*, 117(18), pp.4033–4042. 10.1242/jcs.01242.

Beghein, E. et al., 2016. A new survivin tracer tracks, delocalizes and captures endogenous survivin at different subcellular locations and in distinct organelles. *Scientific Reports*, 6. 10.1038/srep31177.

Belmokhtar, C.A., Hillion, J., Ségal-Bendirdjian, E., 2001. Staurosporine induces apoptosis through both caspase-dependent and caspase-independent mechanisms. *Oncogene*, 20(26), pp.3354–3362. 10.1038/sj.onc.1204436.

Benjamini, Y., Krieger, A.M., Yekutieli, D., 2006. Adaptive linear step-up procedures that control the false discovery rate. *Biometrika*, 93(3), pp.491–507.

Bensaad, K. et al., 2006. TIGAR, a p53-inducible regulator of glycolysis and apoptosis [online]. *Cell*, 126(1), pp.107–120. Available at: https://pubmed.ncbi.nlm.nih.gov/16839880/ [Accessed 24 April 2022].

Boedtkjer, E., Pedersen, S.F., 2020. The Acidic Tumor Microenvironment as a Driver of Cancer [online]. *Annual review of physiology*, 82, pp.103–126. Available at: https://pubmed.ncbi.nlm.nih.gov/31730395/ [Accessed 8 March 2022].

Boulet, A. et al., 2018. The mammalian phosphate carrier SLC25A3 is a mitochondrial copper transporter required for cytochrome c oxidase biogenesis [online]. *Journal of Biological Chemistry*, 293(6), pp.1887–1896. Available at: http://www.jbc.org/article/S0021925820398379/fulltext [Accessed 13 April 2022].

Boulton, D.P., Caino, M.C., 2022. Mitochondrial Fission and Fusion in Tumor Progression to Metastasis [online]. *Frontiers in Cell and Developmental Biology*, 10. Available at: /pmc/articles/PMC8959575/ [Accessed 30 November 2022].

Bouquet, F. et al., 2011. A DNA-dependent stress response involving DNA-PK occurs in hypoxic cells and contributes to cellular adaptation to hypoxia [online]. *Journal of cell science*, 124(Pt 11), pp.1943–1951. Available at: https://pubmed.ncbi.nlm.nih.gov/21576354/ [Accessed 22 April 2022].

Bradbury, N.A., 2000. Protein kinase-A–mediated secretion of mucin from human colonic epithelial cells - Bradbury - 2000 - Journal of Cellular Physiology - Wiley Online Library [online]. *Journal of Cellular Physiology*, 185(3), pp.408–415. Available at: https://onlinelibrary.wiley.com/doi/10.1002/1097-4652(200012)185:3%3C408::AID-JCP11%3E3.0.CO;2-2 [Accessed 21 March 2022].

Brand, M.D., 2010. The sites and topology of mitochondrial superoxide production. *Experimental Gerontology*, 45(7–8), pp.466–472. 10.1016/J.EXGER.2010.01.003.

Brand, M.D., 2000. Uncoupling to survive? The role of mitochondrial inefficiency in ageing. *Experimental Gerontology*, 35(6–7), pp.811–820. 10.1016/S0531-5565(00)00135-2.

Brandt, J.P., Gerriets, V., 2022. Bleomycin [online]. *xPharm: The Comprehensive Pharmacology Reference*, pp.1–6. Available at: https://www.ncbi.nlm.nih.gov/books/NBK555895/ [Accessed 28 February 2022].

Breiman, L., 2001. Random Forests [online]. *Machine Learning 2001 45:1*, 45(1), pp.5–32. Available at: https://link.springer.com/article/10.1023/A:1010933404324 [Accessed 25 March 2022].

Brennan, D.J. et al., 2008. Altered Cytoplasmic-to-Nuclear Ratio of Survivin Is a Prognostic Indicator in Breast Cancer [online]. *Clinical cancer research : an official journal of the American Association for Cancer Research*, 14(9), p.2681. Available at: /pmc/articles/PMC7295090/ [Accessed 22 March 2022].

Brooks, A.J. et al., 2004. Liver tissue partial pressure of oxygen and carbon dioxide during partial hepatectomy. *British Journal of Anaesthesia*, 92(5), pp.735–737. 10.1093/bja/aeh112.

Brouhard, G.J., Hunt, A.J., 2005. Microtubule movements on the arms of mitotic chromosomes: polar ejection forces quantified in vitro [online]. *Proceedings of the National Academy of Sciences of the United States of America*, 102(39), pp.13903–13908. Available at: https://pubmed.ncbi.nlm.nih.gov/16174726/ [Accessed 21 February 2022].

Bruce Nicklas, R. et al., 1998. Tension-sensitive kinetochore phosphorylation in vitro [online]. *Journal of cell science*, 111 (Pt 21)(21), pp.3189–3196. Available at: https://pubmed.ncbi.nlm.nih.gov/9763513/ [Accessed 18 February 2022].

Burton E. Tropp, 2012. *Molecular Biology: Genes to Proteins - Burton E. Tropp* [eBook] Fourth Edition. Jones & Bartlett Publishers. Available at: https://books.google.co.uk/books?hl=en&lr=&id=CCQYtlufUIAC&oi=fnd&pg=PR3&ots=AB94dDDa1R&sig=90ZulQoehQDEeEjsQlbI2jaKg40&redir_esc=y#v=onepage&q&f=false [Accessed 22 May 2020].

Busti, F. et al., 2018. 10.3390/ph11040094.

Bustin, S.A. et al., 2009. The MIQE Guidelines: Minimum Information for Publication of Quantitative Real-Time PCR Experiments [online]. *Clinical Chemistry*, 55(4), pp.611–622. Available at: https://academic.oup.com/clinchem/article/55/4/611/5631762 [Accessed 30 March 2022].

Büttner, S. et al., 2006. Why yeast cells can undergo apoptosis: death in times of peace, love, and war [online]. *The Journal of cell biology*, 175(4), pp.521–525. Available at: https://pubmed.ncbi.nlm.nih.gov/17101700/ [Accessed 27 January 2022].

Byoung, H.K., Altieri, D.C., 2006. Regulation of survivin stability by the aryl hydrocarbon receptor-interacting protein. *Journal of Biological Chemistry*, 281(34), pp.24721–24727. 10.1074/jbc.M603175200.

Byun, T.S. et al., 2005. Functional uncoupling of MCM helicase and DNA polymerase activities activates the ATR-dependent checkpoint. *Genes and Development*, 19(9), pp.1040–1052. 10.1101/gad.1301205.

Cadenas, E., Davies, K.J.A., 2000. Mitochondrial free radical generation, oxidative stress, and aging. *Free Radical Biology and Medicine*, 29(3–4), pp.222–230. 10.1016/S0891-5849(00)00317-8.

Cairns, R.A., Hill, R.P., 2004. Acute hypoxia enhances spontaneous lymph node metastasis in an orthotopic murine model of human cervical carcinoma. *Cancer research*, 64(6), pp.2054–61.

Cairns, R.A., Kalliomaki, T., Hill, R.P., 2001. Acute (cyclic) hypoxia enhances spontaneous metastasis of KHT murine tumors. *Cancer research*, 61(24), pp.8903–8.

Caldecott, K.W., 2008. 10.1038/nrg2380.

Callegari, A.J. et al., 2010. Postreplication gaps at UV lesions are signals for checkpoint activation. *Proceedings of the National Academy of Sciences of the United States of America*, 107(18), pp.8219–8224. 10.1073/pnas.1003449107.

Campbell-Ritchie, A. et al., 2018. The use of decellularised animal tissue to study disseminating cancer cells. *Journal of Cell Science*, 132(4), p.jcs219907. 10.1242/jcs.219907.

Cantley, L.C., 2002. 10.1126/science.296.5573.1655.

Capalbo, G. et al., 2010. Radiation-Induced Survivin Nuclear Accumulation is Linked to DNA Damage Repair. *International Journal of Radiation Oncology Biology Physics*, 77(1), pp.226–234. 10.1016/j.ijrobp.2009.12.001.

Capra, J., Eskelinen, S., 2017. Correlation between E-cadherin interactions, survivin expression, and apoptosis in MDCK and ts-Src MDCK cell culture models [online]. *Laboratory Investigation 2017 97:12*, 97(12), pp.1453–1470. Available at: https://www.nature.com/articles/labinvest201789 [Accessed 23 April 2022].

Carmena, M. et al., 2012. The Chromosomal Passenger Complex (CPC): From Easy Rider to the Godfather of Mitosis [online]. *Nature reviews. Molecular cell biology*, 13(12), p.789. Available at: /pmc/articles/PMC3729939/ [Accessed 25 February 2022].

Carpenter, P.M. et al., 2009. Motility induction in breast carcinoma by mammary epithelial laminin 332 (laminin 5) [online]. *Molecular cancer research : MCR*, 7(4), pp.462–475. Available at: https://pubmed.ncbi.nlm.nih.gov/19351903/ [Accessed 21 March 2022].

Carreau, A. et al., 2011. Why is the partial oxygen pressure of human tissues a crucial parameter? Small molecules and hypoxia. *Journal of Cellular and Molecular Medicine*, 15(6), pp.1239–1253. 10.1111/j.1582-4934.2011.01258.x.

Cecchini, G., 2003. Function and Structure of Complex II of the Respiratory Chain*. *http://dx.doi.org/10.1146/annurev.biochem.72.121801.161700*, 72, pp.77–109. 10.1146/ANNUREV.BIOCHEM.72.121801.161700.

Cereghetti, G.M. et al., 2008a. Dephosphorylation by calcineurin regulates translocation of Drp1 to mitochondria [online]. *Proceedings of the National Academy of Sciences*, 105(41), pp.15803–15808. Available at: https://www.pnas.org/content/105/41/15803 [Accessed 22 January 2022].

Cereghetti, G.M. et al., 2008b. Dephosphorylation by calcineurin regulates translocation of Drp1 to mitochondria. *Proceedings of the National Academy of Sciences of the United States of America*, 105(41), pp.15803–15808. 10.1073/PNAS.0808249105.

Cervós-Navarro, J., Diemer, N.H., 1991. Selective vulnerability in brain hypoxia. *Critical reviews in neurobiology*, 6(3), pp.149–82.

Chandra, D., Singh, K.K., 2011. Genetic insights into OXPHOS defect and its role in cancer. *Biochimica et Biophysica Acta (BBA) - Bioenergetics*, 1807(6), pp.620–625. 10.1016/J.BBABIO.2010.10.023.

Chang, B.Y., Harte, R.A., Cartwright, C.A., 2002. RACK1: a novel substrate for the Src protein-tyrosine kinase [online]. *Oncogene 2002 21:50*, 21(50), pp.7619–7629. Available at: https://www.nature.com/articles/1206002 [Accessed 23 April 2022].

Chang, T.T., Hughes-Fulford, M., 2009. Monolayer and Spheroid Culture of Human Liver Hepatocellular Carcinoma Cell Line Cells Demonstrate Distinct Global Gene Expression Patterns and Functional Phenotypes. *Tissue Engineering Part A*, 15(3), pp.559–567. 10.1089/ten.tea.2007.0434.

Chapman, J.R., Taylor, M.R.G., Boulton, S.J., 2012. Playing the End Game: DNA Double-Strand Break Repair Pathway Choice [online]. *Molecular Cell*, 47(4), pp.497–510. Available at: http://www.cell.com/article/S1097276512006569/fulltext [Accessed 28 February 2022].

Chatterjee, N., Walker, G.C., 2017a. 10.1002/em.22087.

Chatterjee, N., Walker, G.C., 2017b. Mechanisms of DNA damage, repair and mutagenesis [online]. *Environmental and molecular mutagenesis*, 58(5), p.235. Available at: /pmc/articles/PMC5474181/ [Accessed 28 February 2022].

Chatterjee, N., Walker, G.C., 2017c. Mechanisms of DNA damage, repair and mutagenesis [online]. *Environmental and molecular mutagenesis*, 58(5), p.235. Available at: /pmc/articles/PMC5474181/ [Accessed 26 February 2022].

Cheeseman, I.M., 2014. The kinetochore [online]. *Cold Spring Harbor perspectives in biology*, 6(7). Available at: https://pubmed.ncbi.nlm.nih.gov/24984773/ [Accessed 15 February 2022].

Chen, H., Chomyn, A., Chan, D.C., 2005. Disruption of fusion results in mitochondrial heterogeneity and dysfunction. *Journal of Biological Chemistry*, 280(28), pp.26185–26192. 10.1074/JBC.M503062200/ATTACHMENT/CD6E6D96-EE79-40D2-AB03-44300AB00F0D/MMC1.PDF.

Chen, L. et al., 2008. Cell cycle-dependent complex formation of BRCA1.CtIP.MRN is important for DNA double-strand break repair [online]. *The Journal of biological chemistry*, 283(12), pp.7713–7720. Available at: https://pubmed.ncbi.nlm.nih.gov/18171670/ [Accessed 28 February 2022].

Chen, L. et al., 2012. The enhancement of cancer stem cell properties of MCF-7 cells in 3D collagen scaffolds for modeling of cancer and anti-cancer drugs. 10.1016/j.biomaterials.2011.10.056.

Chen, Z.X., Pervaiz, S., 2007. Bcl-2 induces pro-oxidant state by engaging mitochondrial respiration in tumor cells [online]. *Cell death and differentiation*, 14(9), pp.1617–1627. Available at: https://pubmed.ncbi.nlm.nih.gov/17510660/ [Accessed 28 January 2022].

Cheng, E.H.Y. et al., 2003. VDAC2 inhibits BAK activation and mitochondrial apoptosis [online]. *Science (New York, N.Y.)*, 301(5632), pp.513–517. Available at: https://pubmed.ncbi.nlm.nih.gov/12881569/ [Accessed 23 April 2022].

Cheng, S.M. et al., 2021. YM155 and BIRC5 downregulation induce genomic instability via autophagy-mediated ROS production and inhibition in DNA repair [online]. *Pharmacological Research*, 166. Available at: https://pubmed.ncbi.nlm.nih.gov/33549731/ [Accessed 21 May 2021].

Chernomordik, L. V., Kozlov, M.M., 2008. Mechanics of membrane fusion. *Nature Structural and Molecular Biology*, 15(7), pp.675–683. 10.1038/NSMB.1455.

Chin, H.S. et al., 2018. VDAC2 enables BAX to mediate apoptosis and limit tumor development [online]. *Nature Communications 2018 9:1*, 9(1), pp.1–13. Available at: https://www.nature.com/articles/s41467-018-07309-4 [Accessed 18 April 2022].

Choi, J.Y. et al., 2011. Overexpression of MMP-9 and HIF-1α in Breast Cancer Cells under Hypoxic Conditions. *Journal of Breast Cancer*, 14(2), p.88. 10.4048/jbc.2011.14.2.88.

Chua, Y.L. et al., 2010. Stabilization of hypoxia-inducible factor-1alpha protein in hypoxia occurs independently of mitochondrial reactive oxygen species production [online]. *The Journal of biological chemistry*, 285(41), pp.31277–31284. Available at: https://pubmed.ncbi.nlm.nih.gov/20675386/ [Accessed 23 January 2022].

Cody, N. AL et al., 2008. Influence of monolayer, spheroid, and tumor growth conditions on chromosome 3 gene expression in tumorigenic epithelial ovarian cancer cell lines. *BMC Medical Genomics*, 1(1), p.34. 10.1186/1755-8794-1-34.

Collins, P. et al., 2005. Increased expression of uncoupling protein 2 in HepG2 cells attenuates oxidative damage and apoptosis. *Liver international : official journal of the International Association for the Study of the Liver*, 25(4), pp.880–887. 10.1111/J.1478-3231.2005.01104.X.

Colnaghi, R. et al., 2006. Separating the anti-apoptotic and mitotic roles of survivin [online]. *The Journal of biological chemistry*, 281(44), pp.33450–33456. Available at: https://pubmed.ncbi.nlm.nih.gov/16950794/ [Accessed 13 March 2022].

Compe, E., Egly, J.M., 2012. 10.1038/nrm3350.

Conde, M. et al., 2017a. Chromosomal instability induced by increased BIRC5/Survivin levels affects tumorigenicity of glioma cells. *BMC Cancer*, 17(1), pp.1–17. 10.1186/s12885-017-3932-y.

Conde, M. et al., 2017b. Chromosomal instability induced by increased BIRC5/Survivin levels affects tumorigenicity of glioma cells [online]. *BMC*

Cancer, 17(1), pp.1–17. Available at: https://bmccancer.biomedcentral.com/articles/10.1186/s12885-017-3932-y [Accessed 15 April 2022].

Connell, C.M., Colnaghi, R., Wheatley, S.P., 2008. Nuclear survivin has reduced stability and is not cytoprotective [online]. *Journal of Biological Chemistry*, 283(6), pp.3289–3296. Available at: http://www.jbc.org/article/S0021925820697927/fulltext [Accessed 21 May 2021].

Crampton, N. et al., 2009. Oxidative Stress Inhibits Nuclear Protein Export by Multiple Mechanisms That Target FG Nucleoporins and Crm1 [online]. *Molecular Biology of the Cell*, 20(24), p.5106. Available at: /pmc/articles/PMC2793288/ [Accessed 22 March 2022].

Csermely, P., Schnaider, T., Szántó, I., 1995. Signalling and transport through the nuclear membrane. *Biochimica et Biophysica Acta (BBA) - Reviews on Biomembranes*, 1241(3), pp.425–451. 10.1016/0304-4157(95)00015-1.

Cuvillier, O. et al., 2013. Hypoxia, therapeutic resistance, and sphingosine 1-phosphate [online]. *Advances in cancer research*, 117, pp.117–141. Available at: https://pubmed.ncbi.nlm.nih.gov/23290779/ [Accessed 22 March 2022].

Dalla Pozza, E. et al., 2012. Role of mitochondrial uncoupling protein 2 in cancer cell resistance to gemcitabine. *Biochimica et Biophysica Acta (BBA) - Molecular Cell Research*, 1823(10), pp.1856–1863. 10.1016/J.BBAMCR.2012.06.007.

D'Arcy, M.S., 2019. Cell death: a review of the major forms of apoptosis, necrosis and autophagy [online]. *Cell Biology International*, 43(6), pp.582–592. Available at: https://onlinelibrary.wiley.com/doi/full/10.1002/cbin.11137 [Accessed 27 January 2022].

Davies, R.J.H., 1995. Ultraviolet radiation damage in DNA. In: *Biochemical Society Transactions*. Portland Press Ltd, pp. 407–418. 10.1042/bst0230407.

DeLuca, K.F., Lens, S.M.A., DeLuca, J.G., 2011. Temporal changes in Hec1 phosphorylation control kinetochore-microtubule attachment stability during

mitosis [online]. *Journal of cell science*, 124(Pt 4), pp.622–634. Available at: https://pubmed.ncbi.nlm.nih.gov/21266467/ [Accessed 20 February 2022].

Derdak, Z. et al., 2008. The mitochondrial uncoupling protein-2 promotes chemoresistance in cancer cells. *Cancer research*, 68(8), pp.2813–2819. 10.1158/0008-5472.CAN-08-0053.

Desmoulière, A., Guyot, C., Gabbiani, G., 2004. The stroma reaction myofibroblast: a key player in the control of tumor cell behavior. *The International journal of developmental biology*, 48(5–6), pp.509–17. 10.1387/ijdb.041802ad.

Desouky, O., Ding, N., Zhou, G., 2015. Targeted and non-targeted effects of ionizing radiation. *Journal of Radiation Research and Applied Sciences*, 8(2), pp.247–254. 10.1016/j.jrras.2015.03.003.

Dianov, G.L., Hü Bscher, U., SURVEY AND SUMMARY Mammalian Base Excision Repair: the Forgotten Archangel. 10.1093/nar/gkt076.

Dickens, L.S. et al., 2012. The 'complexities' of life and death: death receptor signalling platforms [online]. *Experimental cell research*, 318(11), pp.1269–1277. Available at: https://pubmed.ncbi.nlm.nih.gov/22542855/ [Accessed 1 February 2022].

Diebold, L., Chandel, N.S., 2016. Mitochondrial ROS regulation of proliferating cells. *Free Radical Biology and Medicine*, 100, pp.86–93. 10.1016/J.FREERADBIOMED.2016.04.198.

Djeungoue-Petga, M.A. et al., 2019. Intramitochondrial Src kinase links mitochondrial dysfunctions and aggressiveness of breast cancer cells [online]. *Cell Death & Disease 2019 10:12*, 10(12), pp.1–15. Available at: https://www.nature.com/articles/s41419-019-2134-8 [Accessed 23 April 2022].

Dohi, T., Okada, K., et al., 2004. An IAP-IAP complex inhibits apoptosis [online]. *Journal of Biological Chemistry*, 279(33), pp.34087–34090. Available at: https://pubmed.ncbi.nlm.nih.gov/15218035/ [Accessed 21 May 2021].

Dohi, T., Beltrami, E., et al., 2004a. Mitochondrial survivin inhibits apoptosis and promotes tumorigenesis [online]. *Journal of Clinical Investigation*, 114(8), pp.1117–1127. Available at: http://www.jci.org [Accessed 21 May 2021].

Dohi, T., Beltrami, E., et al., 2004b. Mitochondrial survivin inhibits apoptosis and promotes tumorigenesis [online]. *The Journal of clinical investigation*, 114(8), pp.1117–1127. Available at: https://pubmed.ncbi.nlm.nih.gov/15489959/ [Accessed 22 March 2022].

Dohi, T., Xia, F., Altieri, D.C., 2007. COMPARTMENTALIZED PHOSPHORYLATION OF IAP BY PROTEIN KINASE A REGULATES CYTOPROTECTION [online]. *Molecular cell*, 27(1), p.17. Available at: /pmc/articles/PMC1986705/ [Accessed 21 March 2022].

Dong, Z. et al., 2003. Apoptosis-resistance of hypoxic cells: multiple factors involved and a role for IAP-2. *The American journal of pathology*, 163(2), pp.663–71. 10.1016/S0002-9440(10)63693-0.

Douglas, R.M., Haddad, G.G., 2003. Invited Review: Effect of oxygen deprivation on cell cycle activity: a profile of delay and arrest. *Journal of Applied Physiology*, 94(5), pp.2068–2083. 10.1152/japplphysiol.01029.2002.

Du, C. et al., 2000. Smac, a mitochondrial protein that promotes cytochrome c-dependent caspase activation by eliminating IAP inhibition [online]. *Cell*, 102(1), pp.33–42. Available at: https://pubmed.ncbi.nlm.nih.gov/10929711/ [Accessed 30 January 2022].

Dunajová, L. et al., 2016. The N-terminus of survivin is a mitochondrial-targeting sequence and Src regulator. *Journal of Cell Science*, 129(14), pp.2707–2712. 10.1242/jcs.183277.

Eckelman, B.P., Salvesen, G.S., Scott, F.L., 2006. Human inhibitor of apoptosis proteins: why XIAP is the black sheep of the family [online]. *EMBO reports*, 7(10), pp.988–994. Available at: https://pubmed.ncbi.nlm.nih.gov/17016456/ [Accessed 30 January 2022].

Efremov, R.G., Sazanov, L.A., 2011. Structure of the membrane domain of respiratory complex I. *Nature 2011 476:7361*, 476(7361), pp.414–420. 10.1038/nature10330.

Elmashhady, H.H. et al., 2017. Decellularized extracellular matrices for tissue engineering applications [online]. Available at: https://doi.org/10.1515/esp-2017-0005 [Accessed 30 August 2018].

Elmore, S., 2007. Apoptosis: a review of programmed cell death [online]. *Toxicologic pathology*, 35(4), pp.495–516. Available at: https://pubmed.ncbi.nlm.nih.gov/17562483/ [Accessed 27 January 2022].

Emerling, B.M. et al., 2009. Hypoxic activation of AMPK is dependent on mitochondrial ROS but independent of an increase in AMP/ATP ratio. *Free Radical Biology and Medicine*, 46(10), pp.1386–1391. 10.1016/J.FREERADBIOMED.2009.02.019.

Engelsma, D. et al., 2007. Homodimerization antagonizes nuclear export of Survivin. *Traffic*, 8(11), pp.1495–1502. 10.1111/J.1600-0854.2007.00629.X.

Falk, S.J., Ward, R., Bleehen, N.M., 1992. The influence of carbogen breathing on tumour tissue oxygenation in man evaluated by computerised p02 histography [online]. *British journal of cancer*, 66(5), pp.919–924. Available at: https://pubmed.ncbi.nlm.nih.gov/1419637/ [Accessed 18 April 2022].

Fatokun, A.A., Dawson, V.L., Dawson, T.M., 2014. Parthanatos: mitochondrial-linked mechanisms and therapeutic opportunities [online]. *British journal of pharmacology*, 171(8), pp.2000–2016. Available at: https://pubmed.ncbi.nlm.nih.gov/24684389/ [Accessed 5 February 2022].

Fink, J. et al., 2011. External forces control mitotic spindle positioning [online]. *Nature cell biology*, 13(7), pp.771–778. Available at: https://pubmed.ncbi.nlm.nih.gov/21666685/ [Accessed 14 February 2022].

Foley, E.A., Kapoor, T.M., 2013. Microtubule attachment and spindle assembly checkpoint signalling at the kinetochore [online]. *Nature reviews. Molecular cell*

biology, 14(1), pp.25–37. Available at: https://pubmed.ncbi.nlm.nih.gov/23258294/ [Accessed 20 February 2022].

Fortugno, P. et al., 2003. Regulation of survivin function by Hsp90 [online]. *Proceedings of the National Academy of Sciences of the United States of America*, 100(SUPPL. 2), pp.13791–13796. Available at: www.pnas.orgcgidoi10.1073pnas.2434345100 [Accessed 18 March 2022].

Fortugno, P. et al., 2002. Survivin exists in immunochemically distinct subcellular pools and is involved in spindle microtubule function. *Journal of Cell Science*, 115(3), pp.575–585. 10.1242/jcs.115.3.575.

Fousteri, M. et al., 2006. Cockayne Syndrome A and B Proteins Differentially Regulate Recruitment of Chromatin Remodeling and Repair Factors to Stalled RNA Polymerase II In Vivo. *Molecular Cell*, 23(4), pp.471–482. 10.1016/j.molcel.2006.06.029.

Fousteri, M., Mullenders, L.H.F., 2008. 10.1038/cr.2008.6.

Friedman, J.R. et al., 2015. MICOS coordinates with respiratory complexes and lipids to establish mitochondrial inner membrane architecture. *eLife*, 4(4), pp.1–61. 10.7554/ELIFE.07739.

Fujita, N. et al., 2002. Involvement of Hsp90 in Signaling and Stability of 3-Phosphoinositide-dependent Kinase-1*. 10.1074/jbc.M106736200.

Gaedtke, L. et al., 2007. Proteomic Analysis Reveals Differences in Protein Expression in Spheroid versus Monolayer Cultures of Low-Passage Colon Carcinoma Cells. *Journal of Proteome Research*, 6(11), pp.4111–4118. 10.1021/pr0700596.

Galluzzi, L. et al., 2015. Essential versus accessory aspects of cell death: recommendations of the NCCD 2015 [online]. *Cell death and differentiation*, 22(1), pp.58–73. Available at: https://pubmed.ncbi.nlm.nih.gov/25236395/ [Accessed 31 January 2022].

Galluzzi, L. et al., 2018a. Molecular mechanisms of cell death: recommendations of the Nomenclature Committee on Cell Death 2018 [online]. *Cell Death &*

Differentiation 2018 25:3, 25(3), pp.486–541. Available at: https://www.nature.com/articles/s41418-017-0012-4 [Accessed 27 January 2022].

Galluzzi, L. et al., 2018b. Molecular mechanisms of cell death: recommendations of the Nomenclature Committee on Cell Death 2018 [online]. *Cell Death & Differentiation 2018 25:3*, 25(3), pp.486–541. Available at: https://www.nature.com/articles/s41418-017-0012-4 [Accessed 27 January 2022].

Ganapathy-Kanniappan, S., Geschwind, J.F.H., 2013. Tumor glycolysis as a target for cancer therapy: progress and prospects [online]. *Molecular Cancer 2013 12:1*, 12(1), pp.1–11. Available at: https://molecular-cancer.biomedcentral.com/articles/10.1186/1476-4598-12-152 [Accessed 8 March 2022].

Garg, H. et al., 2016. 10.1186/s12935-016-0326-1.

Garner, T.P. et al., 2016. An Autoinhibited Dimeric Form of BAX Regulates the BAX Activation Pathway [online]. *Molecular cell*, 63(3), pp.485–497. Available at: https://pubmed.ncbi.nlm.nih.gov/27425408/ [Accessed 28 January 2022].

Geck, P. et al., 2018. Analysis of inflammatory signatures of cancer spheroids in blood and their role in metastasis. *https://doi.org/10.1200/JCO.2018.36.15_suppl.3090*, 36(15_suppl), pp.3090–3090. 10.1200/JCO.2018.36.15_SUPPL.3090.

Giacomello, M. et al., 2020. The cell biology of mitochondrial membrane dynamics [online]. *Nature Reviews Molecular Cell Biology 2020 21:4*, 21(4), pp.204–224. Available at: https://www.nature.com/articles/s41580-020-0210-7 [Accessed 29 December 2021].

Gibert, B., Mehlen, P., 2015. Dependence Receptors and Cancer: Addiction to Trophic Ligands [online]. *Cancer research*, 75(24), pp.5171–5175. Available at: https://pubmed.ncbi.nlm.nih.gov/26627011/ [Accessed 1 February 2022].

Gill, B.J., West, J.L., 2014. Modeling the tumor extracellular matrix: Tissue engineering tools repurposed towards new frontiers in cancer biology. *Journal of Biomechanics*, 47(9), pp.1969–1978. 10.1016/j.jbiomech.2013.09.029.

De Giusti, V.C. et al., 2013. Mitochondrial reactive oxygen species (ROS) as signaling molecules of intracellular pathways triggered by the cardiac renin-angiotensin II-aldosterone system (RAAS). *Frontiers in Physiology*, 4 MAY, p.126. 10.3389/FPHYS.2013.00126/BIBTEX.

Goodson, H. v., Jonasson, E.M., 2018. Microtubules and Microtubule-Associated Proteins [online]. *Cold Spring Harbor perspectives in biology*, 10(6). Available at: https://pubmed.ncbi.nlm.nih.gov/29858272/ [Accessed 15 February 2022].

Gotoh, T. et al., 2004. Hsp70-DnaJ chaperone pair prevents nitric oxide- and CHOP-induced apoptosis by inhibiting translocation of Bax to mitochondria [online]. *Cell death and differentiation*, 11(4), pp.390–402. Available at: https://pubmed.ncbi.nlm.nih.gov/14752510/ [Accessed 18 April 2022].

Grawunder, U. et al., 1997. Activity of DNA ligase IV stimulated by complex formation with XRCC4 protein in mammalian cells [online]. *Nature*, 388(6641), pp.492–495. Available at: https://pubmed.ncbi.nlm.nih.gov/9242410/ [Accessed 28 February 2022].

Graziano, F. et al., 2016. Glycolysis gene expression analysis and selective metabolic advantage in the clinical progression of colorectal cancer [online]. *The Pharmacogenomics Journal 2017 17:3*, 17(3), pp.258–264. Available at: https://www.nature.com/articles/tpj201613 [Accessed 7 March 2022].

Green, D.R., Fitzgerald, P., 2016. Just So Stories about the Evolution of Apoptosis [online]. *Current biology : CB*, 26(13), pp.R620–R627. Available at: https://pubmed.ncbi.nlm.nih.gov/27404257/ [Accessed 27 January 2022].

Griparic, L., Kanazawa, T., Van Der Bliek, A.M., 2007. Regulation of the mitochondrial dynamin-like protein Opa1 by proteolytic cleavage. *The Journal of cell biology*, 178(5), pp.757–764. 10.1083/JCB.200704112.

Güllülü, Ö. et al., 2021. A spatial and functional interaction of a heterotetramer Survivin-DNA-PKcs complex in DNA damage response [online]. *Cancer Research*, 81(9), p.canres.2931.2020. Available at: http://cancerres.aacrjournals.org/ [Accessed 22 May 2021].

Gurbuxani, S. et al., 2005. Differential requirements for survivin in hematopoietic cell development [online]. *Proceedings of the National Academy of Sciences of the United States of America*, 102(32), pp.11480–11485. Available at: https://pubmed.ncbi.nlm.nih.gov/16055565/ [Accessed 14 April 2022].

Güttinger, S., Laurell, E., Kutay, U., 2009. Orchestrating nuclear envelope disassembly and reassembly during mitosis [online]. *Nature reviews. Molecular cell biology*, 10(3), pp.178–191. Available at: https://pubmed.ncbi.nlm.nih.gov/19234477/ [Accessed 23 February 2022].

Hagenbuchner, J. et al., 2013. BIRC5/Survivin enhances aerobic glycolysis and drug resistance by altered regulation of the mitochondrial fusion/fission machinery. *Oncogene*, 32(40), pp.4748–4757. 10.1038/onc.2012.500.

Hall, E.J., Giaccia, A.J., 2011. *Radiobiology for the radiologist* 7th ed. Lippincott Williams and Wilkins.

Hammond, E.M. et al., 2002. Hypoxia Links ATR and p53 through Replication Arrest. *Molecular and Cellular Biology*, 22(6), pp.1834–1843. 10.1128/MCB.22.6.1834-1843.2002.

Han, Y.L. et al., 2019. Lysyl oxidase and hypoxia-inducible factor 1α: biomarkers of gastric cancer [online]. *World Journal of Gastroenterology*, 25(15), p.1828. Available at: /pmc/articles/PMC6478611/ [Accessed 30 March 2022].

Hanahan, D., Weinberg, R.A., 2011. Hallmarks of cancer: the next generation. [online]. *Cell*, 144(5), pp.646–74. Available at: http://www.ncbi.nlm.nih.gov/pubmed/21376230 [Accessed 30 August 2018].

Hanson, K. et al., 2018. The HDAC6 inhibitor trichostatin a acetylates microtubules and protects axons from excitotoxin-induced degeneration in a

compartmented culture model. *Frontiers in Neuroscience*, 12(NOV), p.872. 10.3389/FNINS.2018.00872/BIBTEX.

Harper, M.E. et al., 2002. Decreased mitochondrial proton leak and reduced expression of uncoupling protein 3 in skeletal muscle of obese diet-resistant women. *Diabetes*, 51(8), pp.2459–2466. 10.2337/DIABETES.51.8.2459.

Harris, A.L., 2002. 10.1038/nrc704.

Hassanpour, S.H., Dehghani, M., 2017. Review of cancer from perspective of molecular. *Journal of Cancer Research and Practice*, 4(4), pp.127–129. 10.1016/J.JCRPR.2017.07.001.

Helmlinger, G. et al., 1997. Interstitial pH and pO2 gradients in solid tumors in vivo: High-resolution measurements reveal a lack of correlation. *Nature Medicine*, 3(2), pp.177–182. 10.1038/nm0297-177.

Henle, E.S., Linn, S., 1997. 10.1074/jbc.272.31.19095.

Hernansanz-Agustín, P. et al., 2014. Acute hypoxia produces a superoxide burst in cells [online]. *Free radical biology & medicine*, 71, pp.146–156. Available at: https://pubmed.ncbi.nlm.nih.gov/24637263/ [Accessed 22 March 2022].

Hernansanz-Agustín, P. et al., 2017. Mitochondrial complex I deactivation is related to superoxide production in acute hypoxia. *Redox Biology*, 12, pp.1040–1051. 10.1016/J.REDOX.2017.04.025.

Herzig, S., Shaw, R.J., 2018. AMPK: guardian of metabolism and mitochondrial homeostasis [online]. *Nature reviews. Molecular cell biology*, 19(2), p.121. Available at: /pmc/articles/PMC5780224/ [Accessed 27 March 2022].

Höckel, M., Vaupel, P., 2001. Biological consequences of tumor hypoxia. *Seminars in oncology*, 28(2 Suppl 8), pp.36–41.

Hoeijmakers, J.H.J., 2009. 10.1056/NEJMra0804615.

Hoekstra, A.S., Bayley, J.P., 2013. The role of complex II in disease. *Biochimica et Biophysica Acta (BBA) - Bioenergetics*, 1827(5), pp.543–551. 10.1016/J.BBABIO.2012.11.005.

Honda, R., Körner, R., Nigg, E.A., 2003. Exploring the functional interactions between Aurora B, INCENP, and survivin in mitosis [online]. *Molecular Biology of the Cell*, 14(8), pp.3325–3341. Available at: www.molbiolcell.org/cgi/doi/10.1091/mbc.E02-11-0769. [Accessed 22 May 2021].

Hsu, M. et al., 2000. Cadherin repertoire determines partner-specific gap junctional communication during melanoma progression. *Journal of cell science*, 113 (Pt 9), pp.1535–42.

Hu, S. et al., 2015. The Mechanism of Radiosensitization by YM155, a Novel Small Molecule Inhibitor of Survivin Expression, is Associated with DNA Damage Repair [online]. *Cellular Physiology and Biochemistry*, 37(3), pp.1219–1230. Available at: https://www.karger.com/Article/FullText/430245 [Accessed 30 March 2022].

Hu, W. et al., 2010. Glutaminase 2, a novel p53 target gene regulating energy metabolism and antioxidant function [online]. *Proceedings of the National Academy of Sciences of the United States of America*, 107(16), p.7455. Available at: /pmc/articles/PMC2867677/ [Accessed 24 April 2022].

Hubbi, M.E., Semenza, G.L., 2015. 10.1152/ajpcell.00279.2015.

Hutmacher, D.W., 2010. Biomaterials offer cancer research the third dimension. *Nature Materials*, 9(2), pp.90–93. 10.1038/nmat2619.

Imamura, T. et al., 2009. HIF-1α and HIF-2α have divergent roles in colon cancer. *International Journal of Cancer*, 124(4), pp.763–771. 10.1002/ijc.24032.

Iyer, D.R., Rhind, N., 2017. 10.3390/genes8020074.

James, D.I. et al., 2003. HFis1, a novel component of the mammalian mitochondrial fission machinery. *The Journal of biological chemistry*, 278(38), pp.36373–36379. 10.1074/JBC.M303758200.

Jewell, S.A., Petrov, P.G., Winlove, C.P., 2013. The effect of oxidative stress on the membrane dipole potential of human red blood cells. *Biochimica et Biophysica*

Acta (BBA) - Biomembranes, 1828(4), pp.1250–1258. 10.1016/J.BBAMEM.2012.12.019.

Jeyaprakash, A.A. et al., 2007. Structure of a Survivin-Borealin-INCENP core complex reveals how chromosomal passengers travel together [online]. *Cell*, 131(2), pp.271–285. Available at: https://pubmed.ncbi.nlm.nih.gov/17956729/ [Accessed 16 March 2022].

Ježek, P., Plecitá-Hlavatá, L., 2009. Mitochondrial reticulum network dynamics in relation to oxidative stress, redox regulation, and hypoxia. *The International Journal of Biochemistry & Cell Biology*, 41(10), pp.1790–1804. 10.1016/J.BIOCEL.2009.02.014.

Jin, L. et al., 2017. Phosphorylation-mediated activation of LDHA promotes cancer cell invasion and tumour metastasis [online]. *Oncogene*, 36(27), pp.3797–3806. Available at: https://pubmed.ncbi.nlm.nih.gov/28218905/ [Accessed 23 April 2022].

JM, B., SD, R., 1979. Bleomycin [online]. *Annals of internal medicine*, 90(6), p.945. Available at: https://pubmed.ncbi.nlm.nih.gov/87142/ [Accessed 28 February 2022].

Jonckheere, A.I., Smeitink, J.A.M., Rodenburg, R.J.T., 2012. Mitochondrial ATP synthase: architecture, function and pathology. *Journal of Inherited Metabolic Disease*, 35(2), pp.211–225. 10.1007/S10545-011-9382-9.

Jost, P.J. et al., 2009. XIAP discriminates between type I and type II FAS-induced apoptosis [online]. *Nature*, 460(7258), pp.1035–1039. Available at: https://pubmed.ncbi.nlm.nih.gov/19626005/ [Accessed 3 February 2022].

Julien, O., Wells, J.A., 2017. Caspases and their substrates [online]. *Cell death and differentiation*, 24(8), pp.1380–1389. Available at: https://pubmed.ncbi.nlm.nih.gov/28498362/ [Accessed 30 January 2022].

Kadyrova, L.Y., Kadyrov, F.A., 2016. 10.1016/j.dnarep.2015.11.023.

Kalia, R. et al., 2018. Structural basis of mitochondrial receptor binding and constriction by DRP1. *Nature*, 558(7710), pp.401–405. 10.1038/S41586-018-0211-2.

Kalluri, R., 2016. The biology and function of fibroblasts in cancer. 10.1038/nrc.2016.73.

Kalluri, R., Weinberg, R.A., 2009. The basics of epithelial-mesenchymal transition [online]. *The Journal of Clinical Investigation*, 119(6), p.1420. Available at: /pmc/articles/PMC2689101/ [Accessed 22 March 2022].

Kaminskyy, V.O., Zhivotovsky, B., 2014. Free Radicals in Cross Talk Between Autophagy and Apoptosis. *https://home.liebertpub.com/ars*, 21(1), pp.86–102. 10.1089/ARS.2013.5746.

Kaplon, J. et al., 2013. A key role for mitochondrial gatekeeper pyruvate dehydrogenase in oncogene-induced senescence [online]. *Nature 2013 498:7452*, 498(7452), pp.109–112. Available at: https://www.nature.com/articles/nature12154 [Accessed 11 March 2022].

Karakashev, S. V, Reginato, M.J., 2015. Progress toward overcoming hypoxia-induced resistance to solid tumor therapy. *Cancer management and research*, 7, pp.253–64. 10.2147/CMAR.S58285.

Karimi, D. et al., 2022. FIS1 Overexpression Is Correlated with Tumor Metastasis in Gastric Adenocarcinoma [online]. *Journal of gastrointestinal cancer*, 53(2), pp.466–471. Available at: https://pubmed.ncbi.nlm.nih.gov/33890233/ [Accessed 30 November 2022].

Karkoulis, P.K. et al., 2013. Targeted inhibition of heat shock protein 90 disrupts multiple oncogenic signaling pathways, thus inducing cell cycle arrest and programmed cell death in human urinary bladder cancer cell lines [online]. *Cancer Cell International*, 13(1), pp.1–16. Available at: https://cancerci.biomedcentral.com/articles/10.1186/1475-2867-13-11 [Accessed 22 March 2022].

Karl Pearson, 1896. VII. Mathematical contributions to the theory of evolution.—III. Regression, heredity, and panmixia [online]. *Philosophical Transactions of the Royal Society of London. Series A, Containing Papers of a Mathematical or Physical Character*, 187, pp.253–318. Available at: https://royalsocietypublishing.org/doi/abs/10.1098/rsta.1896.0007 [Accessed 25 March 2022].

Kaur, P. et al., 2011. Human Breast Cancer Histoid. *Journal of Histochemistry & Cytochemistry*, 59(12), pp.1087–1100. 10.1369/0022155411423680.

Ke, F. et al., 2015. Impact of the combined loss of BOK, BAX and BAK on the hematopoietic system is slightly more severe than compound loss of BAX and BAK [online]. *Cell death & disease*, 6(10). Available at: https://pubmed.ncbi.nlm.nih.gov/26492371/ [Accessed 28 January 2022].

Kennedy, F.G., Jones, D.P., 1986. Oxygen dependence of mitochondrial function in isolated rat cardiac myocytes [online]. *The American journal of physiology*, 250(3 Pt 1). Available at: https://pubmed.ncbi.nlm.nih.gov/3953808/ [Accessed 11 March 2022].

Kerr, J.F.R., Wyllie, A.H., Currie, A.R., 1972. Apoptosis: A Basic Biological Phenomenon with Wide-ranging Implications in Tissue Kinetics [online]. *British Journal of Cancer*, 26(4), p.239. Available at: /pmc/articles/PMC2008650/?report=abstract [Accessed 18 April 2022].

Kim, B.M. et al., 2007. Reoxygenation following hypoxia activates DNA-damage checkpoint signaling pathways that suppress cell-cycle progression in cultured human lymphocytes. *FEBS Letters*, 581(16), pp.3005–3012. 10.1016/J.FEBSLET.2007.05.053.

Kim, H. et al., 2009. Stepwise activation of BAX and BAK by tBID, BIM, and PUMA initiates mitochondrial apoptosis [online]. *Molecular cell*, 36(3), pp.487–499. Available at: https://pubmed.ncbi.nlm.nih.gov/19917256/ [Accessed 28 January 2022].

Kim, H.R. et al., 1999. Geldanamycin Induces Cell Cycle Arrest in K562 Erythroleukemic Cells [online]. *IUBMB Life*, 48(4), pp.425–428. Available at: https://onlinelibrary.wiley.com/doi/full/10.1080/713803539 [Accessed 22 March 2022].

Kim, J., McNiff, J.M., 2008. Nuclear expression of survivin portends a poor prognosis in Merkel cell carcinoma [online]. *Modern Pathology 2008 21:6*, 21(6), pp.764–769. Available at: https://www.nature.com/articles/modpathol200861 [Accessed 22 March 2022].

Kim, K., Lu, Z., Hay, E.D., 2002. Direct evidence for a role of beta-catenin/LEF-1 signaling pathway in induction of EMT. *Cell biology international*, 26(5), pp.463–76.

Kim, S.H., Turnbull, J., Guimond, S., 2011. Extracellular matrix and cell signalling: the dynamic cooperation of integrin, proteoglycan and growth factor receptor [online]. *Journal of Endocrinology*, 209(2), pp.139–151. Available at: https://joe.bioscientifica.com/view/journals/joe/209/2/139.xml [Accessed 1 December 2022].

Kimura, H., Sakai, Y., Fujii, T., 2018. Organ/body-on-a-chip based on microfluidic technology for drug discovery. *Drug Metabolism and Pharmacokinetics*, 33(1), pp.43–48. 10.1016/J.DMPK.2017.11.003.

Kirschner, M., Mitchison, T., 1986. Beyond self-assembly: from microtubules to morphogenesis [online]. *Cell*, 45(3), pp.329–342. Available at: https://pubmed.ncbi.nlm.nih.gov/3516413/ [Accessed 16 February 2022].

Kitagawa, M., Lee, S.H., 2015. The chromosomal passenger complex (CPC) as a key orchestrator of orderly mitotic exit and cytokinesis [online]. *Frontiers in Cell and Developmental Biology*, 3(MAR), p.14. Available at: /pmc/articles/PMC4350427/ [Accessed 25 February 2022].

Kleinman, H.K., Martin, G.R., 2005. Matrigel: Basement membrane matrix with biological activity. *Seminars in Cancer Biology*, 15(5), pp.378–386. 10.1016/j.semcancer.2005.05.004.

Knauer, S.K. et al., 2007. Nuclear export is essential for the tumor-promoting activity of survivin [online]. *The FASEB Journal*, 21(1), pp.207–216. Available at: https://faseb.onlinelibrary.wiley.com/doi/full/10.1096/fj.06-5741com [Accessed 21 May 2021].

Knauer, S.K. et al., 2006. The Survivin-Crm1 interaction is essential for chromosomal passenger complex localization and function [online]. *EMBO reports*, 7(12), pp.1259–1265. Available at: https://pubmed.ncbi.nlm.nih.gov/17099693/ [Accessed 16 March 2022].

Korobova, F., Gauvin, T.J., Higgs, H.N., 2014. A role for myosin II in mammalian mitochondrial fission [online]. *Current biology : CB*, 24(4), pp.409–414. Available at: https://pubmed.ncbi.nlm.nih.gov/24485837/ [Accessed 26 April 2022].

Korobova, F., Ramabhadran, V., Higgs, H.N., 2013. An actin-dependent step in mitochondrial fission mediated by the ER-associated formin INF2. *Science (New York, N.Y.)*, 339(6118), pp.464–467. 10.1126/SCIENCE.1228360.

Koukourakis, M.I. et al., 2006. Comparison of Metabolic Pathways between Cancer Cells and Stromal Cells in Colorectal Carcinomas: a Metabolic Survival Role for Tumor-Associated Stroma [online]. *Cancer Research*, 66(2), pp.632–637. Available at: https://aacrjournals.org/cancerres/article/66/2/632/526454/Comparison-of-Metabolic-Pathways-between-Cancer [Accessed 8 March 2022].

Kowaltowski, A.J. et al., 2009. Mitochondria and reactive oxygen species. *Free Radical Biology and Medicine*, 47(4), pp.333–343. 10.1016/J.FREERADBIOMED.2009.05.004.

Krafts, K.P., 2010. 10.4161/org.6.4.12555.

Krauss, S., Zhang, C.Y., Lowell, B.B., 2005. The mitochondrial uncoupling-protein homologues. *Nature reviews. Molecular cell biology*, 6(3), pp.248–261. 10.1038/NRM1592.

Krishnamachary, B. et al., 2003. Regulation of colon carcinoma cell invasion by hypoxia-inducible factor 1. *Cancer research*, 63(5), pp.1138–43.

Kumar, R., 2017. Separase: Function Beyond Cohesion Cleavage and an Emerging Oncogene [online]. *Journal of cellular biochemistry*, 118(6), pp.1283–1299. Available at: https://pubmed.ncbi.nlm.nih.gov/27966791/ [Accessed 21 February 2022].

Kunkel, M. et al., 2003. Overexpression of Glut-1 and increased glucose metabolism in tumors are associated with a poor prognosis in patients with oral squamous cell carcinoma [online]. *Cancer*, 97(4), pp.1015–1024. Available at: https://onlinelibrary.wiley.com/doi/full/10.1002/cncr.11159 [Accessed 11 March 2022].

Kunkel, T.A., 2009. Evolving views of DNA replication (in)fidelity. In: *Cold Spring Harbor Symposia on Quantitative Biology*. Cold Spring Harb Symp Quant Biol, pp. 91–101. 10.1101/sqb.2009.74.027.

de la Puente, P. et al., 2013. Cell Trafficking of Endothelial Progenitor Cells in Tumor Progression. *Clinical Cancer Research*, 19(13), pp.3360–3368. 10.1158/1078-0432.CCR-13-0462.

Lampson, M.A., Cheeseman, I.M., 2011. Sensing centromere tension: Aurora B and the regulation of kinetochore function [online]. *Trends in cell biology*, 21(3), pp.133–140. Available at: https://pubmed.ncbi.nlm.nih.gov/21106376/ [Accessed 20 February 2022].

Le, A. et al., 2010. Inhibition of lactate dehydrogenase A induces oxidative stress and inhibits tumor progression [online]. *Proceedings of the National Academy of Sciences of the United States of America*, 107(5), pp.2037–2042. Available at: www.pnas.org/cgi/doi/10.1073/pnas.0914433107 [Accessed 8 March 2022].

Lee, E.J., 2018. Cancer Chemoprevention Effects of Geldanamycin and 17-AAG in Human Oral Squamous Cell Carcinoma [online]. *Korean Journal of Clinical Laboratory Science*, 50(4), pp.462–469. Available at:

http://www.kjcls.org/journal/view.html?doi=10.15324/kjcls.2018.50.4.462 [Accessed 22 March 2022].

Lee, J.W. et al., 2019. Hypoxia signaling in human diseases and therapeutic targets. *Experimental and Molecular Medicine*, 51(6). 10.1038/S12276-019-0235-1.

Lee, K.Y., Myung, K., 2008. PCNA Modifications for Regulation of Post-Replication Repair Pathways [online]. *Molecules and cells*, 26(1), p.5. Available at: /pmc/articles/PMC3518309/ [Accessed 14 February 2022].

Li, F. et al., 2005. 10.1002/ijc.20768.

Li, F. et al., 1999. Pleiotropic cell-division defects and apoptosis induced by interference with survivin function. *Nature Cell Biology*, 1(8), pp.461–466. 10.1038/70242.

Li, H. et al., 2015. Mic60/Mitofilin determines MICOS assembly essential for mitochondrial dynamics and mtDNA nucleoid organization [online]. *Cell Death & Differentiation 2016 23:3*, 23(3), pp.380–392. Available at: https://www.nature.com/articles/cdd2015102 [Accessed 28 March 2022].

Li, P. et al., 1997. Cytochrome c and dATP-dependent formation of Apaf-1/caspase-9 complex initiates an apoptotic protease cascade [online]. *Cell*, 91(4), pp.479–489. Available at: https://pubmed.ncbi.nlm.nih.gov/9390557/ [Accessed 30 January 2022].

Li, X. et al., 2018. FOXP3 inhibits angiogenesis by downregulating VEGF in breast cancer [online]. *Cell Death & Disease 2018 9:7*, 9(7), pp.1–12. Available at: https://www.nature.com/articles/s41419-018-0790-8 [Accessed 30 March 2022].

Liang, J. et al., 2020. DRP1 upregulation promotes pancreatic cancer growth and metastasis through increased aerobic glycolysis [online]. *Journal of gastroenterology and hepatology*, 35(5), pp.885–895. Available at: https://pubmed.ncbi.nlm.nih.gov/31674061/ [Accessed 30 November 2022].

Liberti, M. v., Locasale, J.W., 2016. The Warburg Effect: How Does it Benefit Cancer Cells? [online]. *Trends in Biochemical Sciences*, 41(3), pp.211–218. Available

at: http://www.cell.com/article/S0968000415002418/fulltext [Accessed 6 March 2022].

Lin, Q., Cong, X., Yun, Z., 2011. Differential hypoxic regulation of hypoxia-inducible factors 1α and 2α [online]. *Molecular cancer research : MCR*, 9(6), p.757. Available at: /pmc/articles/PMC3117969/ [Accessed 30 March 2022].

Lin, T.Y. et al., 2020. BIRC5/Survivin is a novel ATG12–ATG5 conjugate interactor and an autophagy-induced DNA damage suppressor in human cancer and mouse embryonic fibroblast cells. *Autophagy*, 16(7), pp.1296–1313. 10.1080/15548627.2019.1671643.

Lin, W. et al., 2015. The Association of Receptor of Activated Protein Kinase C 1(RACK1) with Infectious Bursal Disease Virus Viral Protein VP5 and Voltage-dependent Anion Channel 2 (VDAC2) Inhibits Apoptosis and Enhances Viral Replication * [online]. *Journal of Biological Chemistry*, 290(13), pp.8500–8510. Available at: http://www.jbc.org/article/S0021925820639904/fulltext [Accessed 23 April 2022].

Lin, X. et al., 2017. BMI1 reduces ATR activation and signalling caused by hydroxyurea. *Oncotarget*, 8(52), pp.89707–89721. 10.18632/oncotarget.21111.

Lindsten, T. et al., 2000. The combined functions of proapoptotic Bcl-2 family members bak and bax are essential for normal development of multiple tissues [online]. *Molecular cell*, 6(6), pp.1389–1399. Available at: https://pubmed.ncbi.nlm.nih.gov/11163212/ [Accessed 28 January 2022].

Liu, C. et al., 2014. A fine-scale dissection of the DNA double-strand break repair machinery and its implications for breast cancer therapy [online]. *Nucleic acids research*, 42(10), pp.6106–6127. Available at: https://pubmed.ncbi.nlm.nih.gov/24792170/ [Accessed 28 February 2022].

Liu, X. et al., 2019. 10.1016/j.bbcan.2018.12.007.

Liu, Z.J. et al., 2003. Relative mRNA expression of the lactate dehydrogenase A and B subunits as determined by simultaneous amplification and single strand

conformation polymorphism. Relation with subunit enzyme activity [online]. *Journal of chromatography. B, Analytical technologies in the biomedical and life sciences*, 793(2), pp.405–412. Available at: https://pubmed.ncbi.nlm.nih.gov/12906915/ [Accessed 30 March 2022].

Llambi, F. et al., 2016. BOK Is a Non-Canonical BCL-2 Family Effector of Apoptosis Regulated by ER-Associated Degradation [online]. *Cell*, 165(2), p.421. Available at: /pmc/articles/PMC5018360/ [Accessed 27 January 2022].

Loboda, A., Jozkowicz, A., Dulak, J., 2010. 10.1007/s10059-010-0067-2.

Locasale, J.W., Cantley, L.C., 2010. Altered metabolism in cancer [online]. *BMC Biology*, 8(1), pp.1–3. Available at: https://bmcbiol.biomedcentral.com/articles/10.1186/1741-7007-8-88 [Accessed 8 March 2022].

London, N., Biggins, S., 2014. Signalling dynamics in the spindle checkpoint response [online]. *Nature Reviews Molecular Cell Biology 2014 15:11*, 15(11), pp.736–748. Available at: https://www.nature.com/articles/nrm3888 [Accessed 20 February 2022].

Loong, J.H.C. et al., 2021. Glucose deprivation-induced aberrant FUT1-mediated fucosylation drives cancer stemness in hepatocellular carcinoma [online]. *The Journal of clinical investigation*, 131(11). Available at: https://pubmed.ncbi.nlm.nih.gov/33878034/ [Accessed 30 March 2022].

Losó n, O.C. et al., 2013. Fis1, Mff, MiD49, and MiD51 mediate Drp1 recruitment in mitochondrial fission. *Molecular biology of the cell*, 24(5), pp.659–667. 10.1091/MBC.E12-10-0721.

Luna-Vargas, M.P.A., Chipuk, J.E., 2016. Physiological and Pharmacological Control of BAK, BAX, and Beyond [online]. *Trends in cell biology*, 26(12), p.906. Available at: /pmc/articles/PMC5118054/ [Accessed 27 January 2022].

Lv, D. et al., 2016. A three-dimensional collagen scaffold cell culture system for screening anti-glioma therapeutics. *Oncotarget*, 7(35), pp.56904–56914. 10.18632/oncotarget.10885.

Lv, D. et al., 2017. Three-dimensional cell culture: A powerful tool in tumor research and drug discovery. *Oncology letters*, 14(6), pp.6999–7010. 10.3892/ol.2017.7134.

Lyons, T.W., Reinhard, C.T., Planavsky, N.J., 2014. The rise of oxygen in Earth's early ocean and atmosphere. *Nature*, 506(7488), pp.307–315. 10.1038/NATURE13068.

Ma, H. et al., 2020. C-Src Promotes Tumorigenesis and Tumor Progression by Activating PFKFB3 [online]. *Cell reports*, 30(12), pp.4235-4249.e6. Available at: https://pubmed.ncbi.nlm.nih.gov/32209481/ [Accessed 23 April 2022].

Ma, H.T., Poon, R.Y.C., 2011. How protein kinases co-ordinate mitosis in animal cells [online]. *The Biochemical journal*, 435(1), pp.17–31. Available at: https://pubmed.ncbi.nlm.nih.gov/21406064/ [Accessed 14 February 2022].

Ma, K. et al., 2020. Mitophagy, Mitochondrial Homeostasis, and Cell Fate. *Frontiers in Cell and Developmental Biology*, 8, p.467. 10.3389/FCELL.2020.00467/BIBTEX.

Ma, S.B. et al., 2014. Bax targets mitochondria by distinct mechanisms before or during apoptotic cell death: a requirement for VDAC2 or Bak for efficient Bax apoptotic function [online]. *Cell death and differentiation*, 21(12), pp.1925–1935. Available at: https://pubmed.ncbi.nlm.nih.gov/25146925/ [Accessed 28 January 2022].

Mackay, D.R., Makise, M., Ullman, K.S., 2010. Defects in nuclear pore assembly lead to activation of an Aurora B-mediated abscission checkpoint [online]. *The Journal of cell biology*, 191(5), pp.923–931. Available at: https://pubmed.ncbi.nlm.nih.gov/21098116/ [Accessed 25 February 2022].

Madhunapantula, S.R. V., Mosca, P.J., Robertson, G.P., 2011. 10.4161/cbt.12.12.18442.

Magidson, V. et al., 2011. The spatial arrangement of chromosomes during prometaphase facilitates spindle assembly [online]. *Cell*, 146(4), pp.555–567.

Available at: https://pubmed.ncbi.nlm.nih.gov/21854981/ [Accessed 16 February 2022].

Mak, P. et al., 2010. ERbeta impedes prostate cancer EMT by destabilizing HIF-1alpha and inhibiting VEGF-mediated snail nuclear localization: implications for Gleason grading [online]. *Cancer cell*, 17(4), pp.319–332. Available at: https://pubmed.ncbi.nlm.nih.gov/20385358/ [Accessed 30 March 2022].

Manders, E.M.M., Verbeek, F.J., Aten, J.A., 1993. Measurement of co-localization of objects in dual-colour confocal images [online]. *Journal of Microscopy*, 169(3), pp.375–382. Available at: https://onlinelibrary.wiley.com/doi/full/10.1111/j.1365-2818.1993.tb03313.x [Accessed 25 March 2022].

Manotham, K. et al., 2004. Transdifferentiation of cultured tubular cells induced by hypoxia. *Kidney International*, 65(3), pp.871–880. 10.1111/j.1523-1755.2004.00461.x.

Martin, S.J. et al., 1996. Phosphatidylserine externalization during CD95-induced apoptosis of cells and cytoplasts requires ICE/CED-3 protease activity [online]. *The Journal of biological chemistry*, 271(46), pp.28753–28756. Available at: https://pubmed.ncbi.nlm.nih.gov/8910516/ [Accessed 31 January 2022].

Martinez-Outschoorn, U.E. et al., 2016. Cancer metabolism: a therapeutic perspective [online]. *Nature Reviews Clinical Oncology 2016 14:1*, 14(1), pp.11–31. Available at: https://www.nature.com/articles/nrclinonc.2016.60 [Accessed 11 March 2022].

Marusawa, H. et al., 2003. HBXIP functions as a cofactor of survivin in apoptosis suppression [online]. *EMBO Journal*, 22(11), pp.2729–2740. Available at: https://www.embopress.org/doi/full/10.1093/emboj/cdg263 [Accessed 22 May 2021].

Mason, E.F. et al., 2010. Aerobic glycolysis suppresses p53 activity to provide selective protection from apoptosis upon loss of growth signals or inhibition of BCR-Abl [online]. *Cancer Research*, 70(20), pp.8066–8076. Available at:

https://aacrjournals.org/cancerres/article/70/20/8066/561009/Aerobic-Glycolysis-Suppresses-p53-Activity-to [Accessed 26 April 2022].

Matoba, S. et al., 2006. P53 regulates mitochondrial respiration [online]. *Science*, 312(5780), pp.1650–1653. Available at: https://www.science.org/doi/abs/10.1126/science.1126863 [Accessed 24 April 2022].

Matos, I. et al., 2009. Synchronizing chromosome segregation by flux-dependent force equalization at kinetochores [online]. *The Journal of cell biology*, 186(1), pp.11–26. Available at: https://pubmed.ncbi.nlm.nih.gov/19581410/ [Accessed 21 February 2022].

Matsuura, K. et al., 2016. Metabolic Regulation of Apoptosis in Cancer [online]. *International review of cell and molecular biology*, 327, p.43. Available at: /pmc/articles/PMC5819894/ [Accessed 23 April 2022].

Mazin, A. v. et al., 2010. Rad54, the motor of homologous recombination [online]. *DNA repair*, 9(3), pp.286–302. Available at: https://pubmed.ncbi.nlm.nih.gov/20089461/ [Accessed 2 March 2022].

McIlwrath, A.J., Brunton, V.G., Brown, R., 1996. Cell-cycle arrest and p53 accumulation induced by geldanamycin in human ovarian tumour cells [online]. *Cancer chemotherapy and pharmacology*, 37(5), pp.423–428. Available at: https://pubmed.ncbi.nlm.nih.gov/8599864/ [Accessed 22 March 2022].

McKeown, S.R., 2014. Defining normoxia, physoxia and hypoxia in tumours—implications for treatment response [online]. *The British Journal of Radiology*, 87(1035). Available at: /pmc/articles/PMC4064601/ [Accessed 18 April 2022].

McKinnon, P.J., Caldecott, K.W., 2007a. DNA Strand Break Repair and Human Genetic Disease. *Annual Review of Genomics and Human Genetics*, 8(1), pp.37–55. 10.1146/annurev.genom.7.080505.115648.

McKinnon, P.J., Caldecott, K.W., 2007b. DNA Strand Break Repair and Human Genetic Disease. *Annual Review of Genomics and Human Genetics*, 8(1), pp.37–55. 10.1146/annurev.genom.7.080505.115648.

Meeusen, S. et al., 2006. Mitochondrial inner-membrane fusion and crista maintenance requires the dynamin-related GTPase Mgm1. *Cell*, 127(2), pp.383–395. 10.1016/J.CELL.2006.09.021.

Mehta, G. et al., 2012. Opportunities and challenges for use of tumor spheroids as models to test drug delivery and efficacy. *Journal of controlled release : official journal of the Controlled Release Society*, 164(2), pp.192–204. 10.1016/j.jconrel.2012.04.045.

Melkonian, E.A., Schury, M.P., 2021. Biochemistry, Anaerobic Glycolysis [online]. *StatPearls*. Available at: https://www.ncbi.nlm.nih.gov/books/NBK546695/ [Accessed 6 March 2022].

Mendonsa, A.M., Na, T.Y., Gumbiner, B.M., 2018. E-cadherin in contact inhibition and cancer [online]. *Oncogene 2018 37:35*, 37(35), pp.4769–4780. Available at: https://www.nature.com/articles/s41388-018-0304-2 [Accessed 22 March 2022].

Meng, J. et al., 2012. The histone deacetylase inhibitor trichostatin A induces cell cycle arrest and apoptosis in colorectal cancer cells via p53-dependent and -independent pathways [online]. *Oncology reports*, 28(1), pp.384–388. Available at: https://pubmed.ncbi.nlm.nih.gov/22552631/ [Accessed 21 March 2022].

Mishra, P., Chan, D.C., 2016. Metabolic regulation of mitochondrial dynamics [online]. *Journal of Cell Biology*, 212(4), pp.379–387. Available at: www.jcb.org/cgi/doi/10.1083/jcb.201511036 [Accessed 24 March 2022].

Mitsushima, M. et al., 2010. Revolving movement of a dynamic cluster of actin filaments during mitosis [online]. *The Journal of cell biology*, 191(3), pp.453–462. Available at: https://pubmed.ncbi.nlm.nih.gov/20974812/ [Accessed 14 February 2022].

Moeller, B.J., Richardson, R.A., Dewhirst, M.W., 2007. Hypoxia and radiotherapy: opportunities for improved outcomes in cancer treatment [online]. *Cancer and Metastasis Reviews 2007 26:2*, 26(2), pp.241–248. Available at:

https://link.springer.com/article/10.1007/s10555-007-9056-0 [Accessed 11 March 2022].

Mohiuddin, I.S., Kang, M.H., 2019. DNA-PK as an Emerging Therapeutic Target in Cancer. *Frontiers in Oncology*, 0, p.635. 10.3389/FONC.2019.00635.

Moldoveanu, T. et al., 2014. Many players in BCL-2 family affairs [online]. *Trends in biochemical sciences*, 39(3), pp.101–111. Available at: https://pubmed.ncbi.nlm.nih.gov/24503222/ [Accessed 28 January 2022].

Mole, D.R. et al., 2009. Genome-wide association of hypoxia-inducible factor (HIF)-1α and HIF-2α DNA binding with expression profiling of hypoxia-inducible transcripts. *Journal of Biological Chemistry*, 284(25), pp.16767–16775. 10.1074/jbc.M901790200.

Morrison, R. et al., 1987. Trophic stimulation of cultured neurons from neonatal rat brain by epidermal growth factor. *Science*, 238(4823), pp.72–75. 10.1126/science.3498986.

Munshi, N.C., Anderson, K.C., 2013. Minimal Residual Disease in Multiple Myeloma. *Journal of Clinical Oncology*, 31(20), pp.2523–2526. 10.1200/JCO.2013.49.2124.

Murray, V., Chen, J.K., Chung, L.H., 2018. The Interaction of the Metallo-Glycopeptide Anti-Tumour Drug Bleomycin with DNA [online]. *International Journal of Molecular Sciences*, 19(5). Available at: /pmc/articles/PMC5983701/ [Accessed 28 February 2022].

Musa, M., Kannan, T.P., Mustafa, S., 2013. *Cell Proliferation Study of Human Osteosarcoma Cell Line (U2OS) using Alamar Blue Assayand Live Cell Imaging* [online]. Available at: www.iosrjournals.org [Accessed 23 May 2021].

Musacchio, A., 2015. The Molecular Biology of Spindle Assembly Checkpoint Signaling Dynamics. *Current Biology*, 25(20), pp.R1002–R1018. 10.1016/J.CUB.2015.08.051.

Musgrove, E.A. et al., 2011. 10.1038/nrc3090.

Muz, B., de la Puente, P., Azab, F., Ghobrial, I.M., et al., 2015. Hypoxia Promotes Dissemination and Colonization in New Bone Marrow Niches in Waldenström Macroglobulinemia. *Molecular Cancer Research*, 13(2), pp.263–272. 10.1158/1541-7786.MCR-14-0150.

Muz, B. et al., 2014. The Role of Hypoxia and Exploitation of the Hypoxic Environment in Hematologic Malignancies. *Molecular Cancer Research*, 12(10), pp.1347–1354. 10.1158/1541-7786.MCR-14-0028.

Muz, B., de la Puente, P., Azab, F., Azab, A.K., 2015. The role of hypoxia in cancer progression, angiogenesis, metastasis, and resistance to therapy. *Hypoxia (Auckland, N.Z.)*, 3, pp.83–92. 10.2147/HP.S93413.

Nagata, S., 2005. DNA degradation in development and programmed cell death [online]. *Annual review of immunology*, 23, pp.853–875. Available at: https://pubmed.ncbi.nlm.nih.gov/15771588/ [Accessed 31 January 2022].

Nardai, G. et al., 1996. Characterization of the 90 kDa heat shock protein (HSP90)-associated ATP/GTPase. *J. Biosci*, 21, pp.179–190.

Nègre-Salvayre, A. et al., 1997. A role for uncoupling protein-2 as a regulator of mitochondrial hydrogen peroxide generation. *The FASEB Journal*, 11(10), pp.809–815. 10.1096/FASEBJ.11.10.9271366.

Nguyen, L.T.S., Robinson, D.N., 2020. The Unusual Suspects in Cytokinesis: Fitting the Pieces Together. *Frontiers in Cell and Developmental Biology*, 8, p.441. 10.3389/FCELL.2020.00441/BIBTEX.

Nicholson, J.M., Cimini, D., 2011. How Mitotic Errors Contribute to Karyotypic Diversity in Cancer. *Advances in Cancer Research*, 112, pp.43–75. 10.1016/B978-0-12-387688-1.00003-X.

Nimonkar, A. v. et al., 2011. BLM-DNA2-RPA-MRN and EXO1-BLM-RPA-MRN constitute two DNA end resection machineries for human DNA break repair [online]. *Genes & development*, 25(4), pp.350–362. Available at: https://pubmed.ncbi.nlm.nih.gov/21325134/ [Accessed 28 February 2022].

Nishi, R. et al., 2005. Centrin 2 Stimulates Nucleotide Excision Repair by Interacting with Xeroderma Pigmentosum Group C Protein. *Molecular and Cellular Biology*, 25(13), pp.5664–5674. 10.1128/mcb.25.13.5664-5674.2005.

Nishitani, H., Lygerou, Z., 2004. 10.2741/1315.

Nitiss, J.L., 2009a. DNA topoisomerase II and its growing repertoire of biological functions [online]. *Nature Reviews Cancer 2009 9:5*, 9(5), pp.327–337. Available at: https://www.nature.com/articles/nrc2608 [Accessed 7 February 2022].

Nitiss, J.L., 2009b. Targeting DNA topoisomerase II in cancer chemotherapy [online]. *Nature reviews. Cancer*, 9(5), p.338. Available at: /pmc/articles/PMC2748742/ [Accessed 7 February 2022].

Nogueira-Ferreira, R. et al., 2013. Exploring the role of post-translational modifications on protein-protein interactions with survivin [online]. *Archives of biochemistry and biophysics*, 538(2), pp.64–70. Available at: https://pubmed.ncbi.nlm.nih.gov/23938875/ [Accessed 16 March 2022].

Norbury, C., Nurse, P., 1992. *ANIMAL CELL CYCLES AND THEIR CONTROL*.

Obexer, P. et al., 2009. Repression of BIRC5/Survivin by FOXO3/FKHRL1 sensitizes human neuroblastoma cells to DNA damage-induced apoptosis [online]. *Molecular Biology of the Cell*, 20(7), pp.2041–2048. Available at: https://www.molbiolcell.org/doi/full/10.1091/mbc.e08-07-0699 [Accessed 30 March 2022].

Odell, I.D., Wallace, S.S., Pederson, D.S., 2013. Rules of engagement for base excision repair in chromatin. *Journal of Cellular Physiology*, 228(2), pp.258–266. 10.1002/jcp.24134.

Ogi, T. et al., 2010. Three DNA Polymerases, Recruited by Different Mechanisms, Carry Out NER Repair Synthesis in Human Cells. *Molecular Cell*, 37(5), pp.714–727. 10.1016/j.molcel.2010.02.009.

Ogura, M. et al., 2012. Mitochondrial c-Src regulates cell survival through phosphorylation of respiratory chain components [online]. *Biochemical*

Journal, 447(Pt 2), p.281. Available at: /pmc/articles/PMC3459221/ [Accessed 23 April 2022].

Okamoto, J. et al., 2008. Inhibition of Hsp90 leads to cell cycle arrest and apoptosis in human malignant pleural mesothelioma [online]. *Journal of thoracic oncology : official publication of the International Association for the Study of Lung Cancer*, 3(10), p.1089. Available at: /pmc/articles/PMC2656438/ [Accessed 21 March 2022].

Olive, P.L., Vikse, C., Trotter, M.J., 1992. Measurement of oxygen diffusion distance in tumor cubes using a fluorescent hypoxia probe. *International journal of radiation oncology, biology, physics*, 22(3), pp.397–402.

Orr, A.W. et al., 2006. Mechanisms of Mechanotransduction. *Developmental Cell*, 10(1), pp.11–20. 10.1016/j.devcel.2005.12.006.

Orrenius, S., Gogvadze, V., Zhivotovsky, B., 2007. Mitochondrial Oxidative Stress: Implications for Cell Death. *http://dx.doi.org/10.1146/annurev.pharmtox.47.120505.105122*, 47, pp.143–183. 10.1146/ANNUREV.PHARMTOX.47.120505.105122.

Ortmann, B., Druker, J., Rocha, S., 2014. Cell cycle progression in response to oxygen levels [online]. *Cellular and Molecular Life Sciences*, 71(18), p.3569. Available at: /pmc/articles/PMC4143607/ [Accessed 18 March 2022].

Otera, H. et al., 2010. Mff is an essential factor for mitochondrial recruitment of Drp1 during mitochondrial fission in mammalian cells. *The Journal of cell biology*, 191(6), pp.1141–1158. 10.1083/JCB.201007152.

Page, E.L. et al., 2008. Hypoxia-inducible factor-1α stabilization in nonhypoxic conditions: Role of oxidation and intracellular ascorbate depletion. *Molecular Biology of the Cell*, 19(1), pp.86–94. 10.1091/MBC.E07-06-0612/ASSET/IMAGES/LARGE/ZMK0010883510007.JPEG.

Pang, B., Qiao, X., Janssen, L., Velds, A., Groothuis, T., Kerkhoven, R., Nieuwland, M., Ovaa, H., Rottenberg, S., van Tellingen, O., et al., 2013. Drug-induced histone eviction from open chromatin contributes to the chemotherapeutic

effects of doxorubicin [online]. *Nature Communications 2013 4:1*, 4(1), pp.1–13. Available at: https://www.nature.com/articles/ncomms2921 [Accessed 7 February 2022].

Pang, B., Qiao, X., Janssen, L., Velds, A., Groothuis, T., Kerkhoven, R., Nieuwland, M., Ovaa, H., Rottenberg, S., Van Tellingen, O., et al., 2013. Drug-induced histone eviction from open chromatin contributes to the chemotherapeutic effects of doxorubicin. *Nature Communications*, 4(1), pp.1–13. 10.1038/ncomms2921.

Panier, S., Boulton, S.J., 2014. Double-strand break repair: 53BP1 comes into focus [online]. *Nature reviews. Molecular cell biology*, 15(1), pp.7–18. Available at: https://pubmed.ncbi.nlm.nih.gov/24326623/ [Accessed 25 February 2022].

Park, C. v., Ivanova, I.G., Kenneth, N.S., 2017. XIAP upregulates expression of HIF target genes by targeting HIF1α for Lys63-linked polyubiquitination [online]. *Nucleic Acids Research*, 45(16), pp.9336–9347. Available at: https://academic.oup.com/nar/article/45/16/9336/3896344 [Accessed 30 March 2022].

Parker, C. et al., 2004. Polarographic electrode study of tumor oxygenation in clinically localized prostate cancer [online]. *International journal of radiation oncology, biology, physics*, 58(3), pp.750–757. Available at: https://pubmed.ncbi.nlm.nih.gov/14967430/ [Accessed 18 April 2022].

Partovian, C., Simons, M., 2004. Regulation of protein kinase B/Akt activity and Ser473 phosphorylation by protein kinase Cα in endothelial cells. *Cellular Signalling*, 16(8), pp.951–957. 10.1016/j.cellsig.2004.01.008.

Perry, S.W. et al., 2011. Mitochondrial membrane potential probes and the proton gradient: a practical usage guide [online]. *BioTechniques*, 50(2), p.98. Available at: /pmc/articles/PMC3115691/ [Accessed 28 March 2022].

Petering, D.H., Byrnes, R.W., Antholine, W.E., 1990. The role of redox-active metals in the mechanism of action of bleomycin [online]. *Chemico-biological*

interactions, 73(2–3), pp.133–182. Available at: https://pubmed.ncbi.nlm.nih.gov/1690086/ [Accessed 28 February 2022].

Peters, J.M., Tedeschi, A., Schmitz, J., 2008. The cohesin complex and its roles in chromosome biology [online]. *Genes & development*, 22(22), pp.3089–3114. Available at: https://pubmed.ncbi.nlm.nih.gov/19056890/ [Accessed 14 February 2022].

Petrova, V. et al., 2018. The hypoxic tumour microenvironment. *Oncogenesis*, 7(1), p.10. 10.1038/s41389-017-0011-9.

Pfaffl, M.W., 2001. A new mathematical model for relative quantification in real-time RT-PCR [online]. *Nucleic acids research*, 29(9), p.E45. Available at: https://pubmed.ncbi.nlm.nih.gov/11328886/ [Accessed 30 March 2022].

Pfeiffer, P., Goedecke, W., Obe, G., 2000. Mechanisms of DNA double-strand break repair and their potential to induce chromosomal aberrations [online]. *Mutagenesis*, 15(4), pp.289–302. Available at: https://academic.oup.com/mutage/article/15/4/289/1143400 [Accessed 28 February 2022].

Phi, L.T.H. et al., 2018. Cancer Stem Cells (CSCs) in Drug Resistance and their Therapeutic Implications in Cancer Treatment [online]. *Stem Cells International*, 2018. Available at: /pmc/articles/PMC5850899/ [Accessed 31 March 2022].

Povirk, L.F., Finley Austin, M.J., 1991. Genotoxicity of bleomycin [online]. *Mutation research*, 257(2), pp.127–143. Available at: https://pubmed.ncbi.nlm.nih.gov/1706477/ [Accessed 28 February 2022].

Prokhorova, E.A. et al., 2018. Apoptosis regulation by subcellular relocation of caspases [online]. *Scientific Reports 2018 8:1*, 8(1), pp.1–11. Available at: https://www.nature.com/articles/s41598-018-30652-x [Accessed 25 April 2022].

Qiao, X. et al., 2020. Uncoupling DNA damage from chromatin damage to detoxify doxorubicin [online]. *Proceedings of the National Academy of Sciences of the*

United States of America, 117(26), pp.15182–15192. Available at: https://www.pnas.org/content/117/26/15182 [Accessed 7 February 2022].

Ramadan, K. et al., 2004. De novo DNA synthesis by human DNA polymerase lambda, DNA polymerase mu and terminal deoxyribonucleotidyl transferase [online]. *Journal of molecular biology*, 339(2), pp.395–404. Available at: https://pubmed.ncbi.nlm.nih.gov/15136041/ [Accessed 28 February 2022].

Ramsden, D.B. et al., 2012. Human neuronal uncoupling proteins 4 and 5 (UCP4 and UCP5): structural properties, regulation, and physiological role in protection against oxidative stress and mitochondrial dysfunction. *Brain and behavior*, 2(4), pp.468–478. 10.1002/BRB3.55.

Ravenna, L. et al., 2014. Distinct phenotypes of human prostate cancer cells associate with different adaptation to hypoxia and pro-inflammatory gene expression [online]. *PloS one*, 9(5). Available at: https://pubmed.ncbi.nlm.nih.gov/24801981/ [Accessed 30 March 2022].

Ray Chaudhuri, A., Nussenzweig, A., 2017. 10.1038/nrm.2017.53.

Reichert, S. et al., 2011. Survivin inhibition and DNA double-strand break repair: A molecular mechanism to overcome radioresistance in glioblastoma [online]. *Radiotherapy and Oncology*, 101(1), pp.51–58. Available at: http://www.thegreenjournal.com/article/S0167814011003768/fulltext [Accessed 15 April 2022].

Renshaw, M.J. et al., 2010. Condensins promote chromosome recoiling during early anaphase to complete sister chromatid separation [online]. *Developmental cell*, 19(2), pp.232–244. Available at: https://pubmed.ncbi.nlm.nih.gov/20708586/ [Accessed 23 February 2022].

Rexhepaj, E. et al., 2010. Validation of cytoplasmic-to-nuclear ratio of survivin as an indicator of improved prognosis in breast cancer [online]. *BMC Cancer*, 10(1), pp.1–12. Available at: https://bmccancer.biomedcentral.com/articles/10.1186/1471-2407-10-639 [Accessed 22 March 2022].

Richard Mcintosh, J., 2016. Mitosis [online]. *Cold Spring Harbor Perspectives in Biology*, 8(9). Available at: /pmc/articles/PMC5008068/ [Accessed 14 February 2022].

Richardson, S.R., O'Malley, G.F., 2021. Glucose 6 Phosphate Dehydrogenase Deficiency [online]. *StatPearls*. Available at: https://www.ncbi.nlm.nih.gov/books/NBK470315/ [Accessed 14 April 2022].

Rijal, G., Li, W., 2017. A versatile 3D tissue matrix scaffold system for tumor modeling and drug screening [online]. *Science Advances*, 3(9). Available at: /pmc/articles/PMC5597314/ [Accessed 1 December 2022].

Riolo, M.T. et al., 2012. Histone Deacetylase 6 (HDAC6) Deacetylates Survivin for Its Nuclear Export in Breast Cancer [online]. *The Journal of Biological Chemistry*, 287(14), p.10885. Available at: /pmc/articles/PMC3322878/ [Accessed 21 March 2022].

Rivadeneira, D.B. et al., 2015. Survivin promotes oxidative phosphorylation, subcellular mitochondrial repositioning, and tumor cell invasion [online]. *Science Signaling*, 8(389), pp.ra80–ra80. Available at: www.SCIENCESIGNALING.org [Accessed 21 May 2021].

Roberts, S.A. et al., 2010. Ku is a 5′-dRP/AP lyase that excises nucleotide damage near broken ends [online]. *Nature*, 464(7292), pp.1214–1217. Available at: https://pubmed.ncbi.nlm.nih.gov/20383123/ [Accessed 28 February 2022].

Robey, I.F. et al., 2005. Hypoxia-Inducible Factor-1α and the Glycolytic Phenotype in Tumors. *Neoplasia*, 7(4), pp.324–330. 10.1593/NEO.04430.

Robin, E. et al., 2007. Oxidant Stress during Simulated Ischemia Primes Cardiomyocytes for Cell Death during Reperfusion *. *Journal of Biological Chemistry*, 282(26), pp.19133–19143. 10.1074/JBC.M701917200.

Rödel, F. et al., 2005. Survivin as a radioresistance factor, and prognostic and therapeutic target for radiotherapy in rectal cancer [online]. *Cancer research*, 65(11), pp.4881–4887. Available at: https://pubmed.ncbi.nlm.nih.gov/15930309/ [Accessed 30 March 2022].

Rodríguez, J.A. et al., 2002. CRM1-mediated nuclear export determines the cytoplasmic localization of the antiapoptotic protein Survivin [online]. *Experimental cell research*, 275(1), pp.44–53. Available at: https://pubmed.ncbi.nlm.nih.gov/11925104/ [Accessed 16 March 2022].

Rohwer, N., Cramer, T., 2011. Hypoxia-mediated drug resistance: Novel insights on the functional interaction of HIFs and cell death pathways. *Drug Resistance Updates*, 14(3), pp.191–201. 10.1016/j.drup.2011.03.001.

Russell, J.C. et al., 2008a. Nuclear translocation of X-linked inhibitor of apoptosis (XIAP) determines cell fate after hypoxia ischemia in neonatal brain [online]. *Journal of neurochemistry*, 106(3), pp.1357–1370. Available at: https://pubmed.ncbi.nlm.nih.gov/18485100/ [Accessed 22 March 2022].

Russell, J.C. et al., 2008b. Nuclear translocation of X-linked inhibitor of apoptosis (XIAP) determines cell fate after hypoxia ischemia in neonatal brain [online]. *Journal of neurochemistry*, 106(3), pp.1357–1370. Available at: https://pubmed.ncbi.nlm.nih.gov/18485100/ [Accessed 30 March 2022].

Russell, J.C. et al., 2008c. Nuclear translocation of X-linked inhibitor of apoptosis (XIAP) determines cell fate after hypoxia ischemia in neonatal brain [online]. *Journal of neurochemistry*, 106(3), pp.1357–1370. Available at: https://pubmed.ncbi.nlm.nih.gov/18485100/ [Accessed 25 April 2022].

Sagan, L., 1967. On the origin of mitosing cells. *Journal of Theoretical Biology*, 14(3), pp.225-IN6. 10.1016/0022-5193(67)90079-3.

Salvador-Gallego, R. et al., 2016. Bax assembly into rings and arcs in apoptotic mitochondria is linked to membrane pores [online]. *The EMBO journal*, 35(4), pp.389–401. Available at: https://pubmed.ncbi.nlm.nih.gov/26783362/ [Accessed 28 January 2022].

Salvesen, G.S., Duckett, C.S., 2002. IAP proteins: blocking the road to death's door [online]. *Nature reviews. Molecular cell biology*, 3(6), pp.401–410. Available at: https://pubmed.ncbi.nlm.nih.gov/12042762/ [Accessed 30 January 2022].

Samudio, I., Fiegl, M., Andreeff, M., 2009. Mitochondrial uncoupling and the Warburg effect: molecular basis for the reprogramming of cancer cell metabolism [online]. *Cancer research*, 69(6), pp.2163–2166. Available at: https://pubmed.ncbi.nlm.nih.gov/19258498/ [Accessed 28 March 2022].

Sancar, A. et al., 2004. Molecular Mechanisms of Mammalian DNA Repair and the DNA Damage Checkpoints. *Annual Review of Biochemistry*, 73(1), pp.39–85. 10.1146/annurev.biochem.73.011303.073723.

Sato, S., Fujita, N., Tsuruo, T., 2000. Modulation of Akt kinase activity by binding to Hsp90. *Proceedings of the National Academy of Sciences of the United States of America*, 97(20), pp.10832–10837. 10.1073/pnas.170276797.

Saxton, W.M. et al., 1984. Tubulin dynamics in cultured mammalian cells [online]. *The Journal of cell biology*, 99(6), pp.2175–2186. Available at: https://pubmed.ncbi.nlm.nih.gov/6501419/ [Accessed 21 February 2022].

Scanlon, S.E., Glazer, P.M., 2015. Multifaceted Control of DNA Repair Pathways by the Hypoxic Tumor Microenvironment [online]. *DNA repair*, 32, p.180. Available at: /pmc/articles/PMC4522377/ [Accessed 18 March 2022].

Schindelin, J. et al., 2012. Fiji: an open-source platform for biological-image analysis [online]. *Nature Methods 2012 9:7*, 9(7), pp.676–682. Available at: https://www.nature.com/articles/nmeth.2019 [Accessed 25 March 2022].

Schoeffler, A.J., Berger, J.M., 2008. DNA topoisomerases: harnessing and constraining energy to govern chromosome topology [online]. *Quarterly Reviews of Biophysics*, 41(1), pp.41–101. Available at: https://www.cambridge.org/core/journals/quarterly-reviews-of-biophysics/article/dna-topoisomerases-harnessing-and-constraining-energy-to-govern-chromosome-topology/C216211DA2C409A8261A3925B46C96BD [Accessed 6 February 2022].

Schwartzenberg-Bar-Yoseph, F., Armoni, M., Karnieli, E., 2004. The tumor suppressor p53 down-regulates glucose transporters GLUT1 and GLUT4 gene

expression [online]. *Cancer research*, 64(7), pp.2627–2633. Available at: https://pubmed.ncbi.nlm.nih.gov/15059920/ [Accessed 24 April 2022].

Scorrano, L. et al., 2002. A distinct pathway remodels mitochondrial cristae and mobilizes cytochrome c during apoptosis [online]. *Developmental cell*, 2(1), pp.55–67. Available at: https://pubmed.ncbi.nlm.nih.gov/11782314/ [Accessed 29 January 2022].

Scrima, A. et al., 2008. Structural Basis of UV DNA-Damage Recognition by the DDB1-DDB2 Complex. *Cell*, 135(7), pp.1213–1223. 10.1016/j.cell.2008.10.045.

Sebbagh, M. et al., 2001. Caspase-3-mediated cleavage of ROCK I induces MLC phosphorylation and apoptotic membrane blebbing [online]. *Nature cell biology*, 3(4), pp.346–352. Available at: https://pubmed.ncbi.nlm.nih.gov/11283607/ [Accessed 31 January 2022].

Semenza, G.L., 2010. HIF-1: upstream and downstream of cancer metabolism. *Current Opinion in Genetics & Development*, 20(1), pp.51–56. 10.1016/J.GDE.2009.10.009.

Seo, J.H. et al., 2019. MFF Regulation of Mitochondrial Cell Death Is a Therapeutic Target in Cancer [online]. *Cancer research*, 79(24), pp.6215–6226. Available at: https://pubmed.ncbi.nlm.nih.gov/31582380/ [Accessed 30 November 2022].

Sermeus, A., Michiels, C., 2011. Reciprocal influence of the p53 and the hypoxic pathways [online]. *Cell Death & Disease*, 2(5), p.e164. Available at: /pmc/articles/PMC3122125/ [Accessed 29 March 2022].

Shabalina, I.G. et al., 2004. Native UCP1 displays simple competitive kinetics between the regulators purine nucleotides and fatty acids. *The Journal of biological chemistry*, 279(37), pp.38236–38248. 10.1074/JBC.M402375200.

Shiloh, Y., 2003. Available at: https://pubmed.ncbi.nlm.nih.gov/12612651/ [Accessed 22 May 2021].

Siefert, J.C., Clowdus, E.A., Sansam, C.L., 2015. 10.1016/j.cbpc.2015.10.003.

Siegel, R.L., Miller, K.D., Jemal, A., 2018. Cancer statistics, 2018. *CA: A Cancer Journal for Clinicians*, 68(1), pp.7–30. 10.3322/caac.21442.

Silke, J., Meier, P., 2013. Inhibitor of apoptosis (IAP) proteins-modulators of cell death and inflammation [online]. *Cold Spring Harbor perspectives in biology*, 5(2). Available at: https://pubmed.ncbi.nlm.nih.gov/23378585/ [Accessed 31 January 2022].

Silva Ramos, E., Larsson, N.G., Mourier, A., 2016. Bioenergetic roles of mitochondrial fusion. *Biochimica et Biophysica Acta (BBA) - Bioenergetics*, 1857(8), pp.1277–1283. 10.1016/J.BBABIO.2016.04.002.

Singh, A., Settleman, J., 2010. EMT, cancer stem cells and drug resistance: an emerging axis of evil in the war on cancer. *Oncogene*, 29(34), pp.4741–4751. 10.1038/onc.2010.215.

Sinkala, M., Mulder, N., Patrick Martin, D., 2019. Metabolic gene alterations impact the clinical aggressiveness and drug responses of 32 human cancers [online]. *Communications Biology 2019 2:1*, 2(1), pp.1–14. Available at: https://www.nature.com/articles/s42003-019-0666-1 [Accessed 28 March 2022].

Smirnova, N.A. et al., 2012. Catalytic mechanism and substrate specificity of HIF prolyl hydroxylases. *Biochemistry (Moscow)*, 77(10), pp.1108–1119. 10.1134/S0006297912100033.

Snell, C.E. et al., 2014. Proline-Hydroxylated Hypoxia-Inducible Factor 1α (HIF-1α) Upregulation in Human Tumours Aziz, S. A., ed. *PLoS ONE*, 9(2), p.e88955. 10.1371/journal.pone.0088955.

Sobanski, T. et al., 2021. Cell Metabolism and DNA Repair Pathways: Implications for Cancer Therapy. *Frontiers in Cell and Developmental Biology*, 9, p.528. 10.3389/FCELL.2021.633305/BIBTEX.

Soengas, M.S. et al., 1999. Apaf-1 and caspase-9 in p53-dependent apoptosis and tumor inhibition [online]. *Science (New York, N.Y.)*, 284(5411), pp.156–159.

Available at: https://pubmed.ncbi.nlm.nih.gov/10102818/ [Accessed 26 January 2022].

Song, P., Zou, M.H., 2015. Roles of Reactive Oxygen Species in Physiology and Pathology. *Atherosclerosis: Risks, Mechanisms, and Therapies*, pp.379–392. 10.1002/9781118828533.CH30.

Stauber, R.H. et al., 2006. Nucleocytoplasmic shuttling and the biological activity of mouse survivin are regulated by an active nuclear export signal [online]. *Traffic*, 7(11), pp.1461–1472. Available at: https://onlinelibrary.wiley.com/doi/full/10.1111/j.1600-0854.2006.00486.x [Accessed 21 May 2021].

Stauber, R.H., Mann, W., Knauer, S.K., 2007. Available at: www.aacrjournals.org [Accessed 21 May 2021].

Stead, B.E. et al., 2012. Mcm2 phosphorylation and the response to replicative stress. *BMC Genetics*, 13, p.36. 10.1186/1471-2156-13-36.

Steger, G., 1998. An unbiased detector of curvilinear structures. *IEEE Transactions on Pattern Analysis and Machine Intelligence*, 20(2), pp.113–125. 10.1109/34.659930.

Steinhardt, R.A., Alderton, J., 1988. Intracellular free calcium rise triggers nuclear envelope breakdown in the sea urchin embryo [online]. *Nature*, 332(6162), pp.364–366. Available at: https://pubmed.ncbi.nlm.nih.gov/3127727/ [Accessed 14 February 2022].

Stokes, M.P. et al., 2002. DNA replication is required for the checkpoint response to damaged DNA in Xenopus egg extracts. *Journal of Cell Biology*, 158(5), pp.863–872. 10.1083/jcb.200204127.

Strauss, M. et al., 2008. Dimer ribbons of ATP synthase shape the inner mitochondrial membrane. *The EMBO journal*, 27(7), pp.1154–1160. 10.1038/EMBOJ.2008.35.

Su, K.C. et al., 2014. An astral simulacrum of the central spindle accounts for normal, spindle-less, and anucleate cytokinesis in echinoderm embryos [online].

Molecular Biology of the Cell, 25(25), pp.4049–4062. Available at: https://www.molbiolcell.org/doi/abs/10.1091/mbc.e14-04-0859 [Accessed 23 February 2022].

Suen, D.F., Norris, K.L., Youle, R.J., 2008. Mitochondrial dynamics and apoptosis [online]. *Genes & Development*, 22(12), p.1577. Available at: /pmc/articles/PMC2732420/ [Accessed 27 March 2022].

Suh, H.N., Han, H.J., 2013. Fibronectin-induced VEGF receptor and calcium channel transactivation stimulate GLUT-1 synthesis and trafficking through PPARγ and TC10 in mouse embryonic stem cells. *Stem Cell Research*, 10(3), pp.371–386. 10.1016/J.SCR.2013.01.008.

Sun, C. et al., 2005. Solution structure of human survivin and its binding interface with Smac/Diablo [online]. *Biochemistry*, 44(1), pp.11–17. Available at: https://pubmed.ncbi.nlm.nih.gov/15628841/ [Accessed 14 March 2022].

Sun, G. et al., 2017. A molecular signature for anastasis, recovery from the brink of apoptotic cell death [online]. *The Journal of cell biology*, 216(10), pp.3355–3368. Available at: https://pubmed.ncbi.nlm.nih.gov/28768686/ [Accessed 31 January 2022].

Sun, X. et al., 2018a. Mitochondrial fission promotes cell migration by Ca2+ /CaMKII/ERK/FAK pathway in hepatocellular carcinoma [online]. *Liver international : official journal of the International Association for the Study of the Liver*, 38(7), pp.1263–1272. Available at: https://pubmed.ncbi.nlm.nih.gov/29210177/ [Accessed 30 November 2022].

Sun, X. et al., 2018b. Mitochondrial fission promotes cell migration by Ca2+ /CaMKII/ERK/FAK pathway in hepatocellular carcinoma [online]. *Liver international : official journal of the International Association for the Study of the Liver*, 38(7), pp.1263–1272. Available at: https://pubmed.ncbi.nlm.nih.gov/29210177/ [Accessed 30 November 2022].

Sun, X. et al., 2020. Role of Proton-Coupled Monocarboxylate Transporters in Cancer: From Metabolic Crosstalk to Therapeutic Potential. *Frontiers in Cell and Developmental Biology*, 8, p.651. 10.3389/FCELL.2020.00651/BIBTEX.

Sung, P., Klein, H., 2006. 10.1038/nrm2008.

Tam, S.Y., Wu, V.W.C., Law, H.K.W., 2020. Hypoxia-Induced Epithelial-Mesenchymal Transition in Cancers: HIF-1α and Beyond [online]. *Frontiers in Oncology*, 10, p.486. Available at: /pmc/articles/PMC7156534/ [Accessed 22 March 2022].

al Tameemi, W. et al., 2019. Hypoxia-Modified Cancer Cell Metabolism. *Frontiers in Cell and Developmental Biology*, 7. 10.3389/fcell.2019.00004.

Tamm I et al., 1998. IAP-family protein survivin inhibits caspase activity and apoptosis induced by Fas (CD95), Bax, caspases, and anticancer drugs. *Cancer Res.* , 58(23), pp.5315–5320.

Tan, C.T. et al., 2016. MOAP-1 Mediates Fas-Induced Apoptosis in Liver by Facilitating tBid Recruitment to Mitochondria [online]. *Cell reports*, 16(1), pp.174–185. Available at: https://pubmed.ncbi.nlm.nih.gov/27320914/ [Accessed 3 February 2022].

Tang, X. et al., 2012. Functional Interaction between Responses to Lactic Acidosis and Hypoxia Regulates Genomic Transcriptional Outputs. *Cancer Research*, 72(2), pp.491–502. 10.1158/0008-5472.CAN-11-2076.

Tercero, J.A., Longhese, M.P., Diffley, J.F.X., 2003. A central role for DNA replication forks in checkpoint activation and response. *Molecular Cell*, 11(5), pp.1323–1336. 10.1016/S1097-2765(03)00169-2.

Thadani, R., Uhlmann, F., Heeger, S., 2012. Condensin, chromatin crossbarring and chromosome condensation [online]. *Current biology : CB*, 22(23). Available at: https://pubmed.ncbi.nlm.nih.gov/23218009/ [Accessed 14 February 2022].

Thery, M., 2010. Micropatterning as a tool to decipher cell morphogenesis and functions. *Journal of Cell Science*, 123(24), pp.4201–4213. 10.1242/jcs.075150.

Timney, B.L. et al., 2016. Simple rules for passive diffusion through the nuclear pore complex. *Journal of Cell Biology*, 215(1), pp.57–76. 10.1083/jcb.201601004.

Tolosa-Díaz, A. et al., 2020. The GDP-Bound State of Mitochondrial Mfn1 Induces Membrane Adhesion of Apposing Lipid Vesicles through a Cooperative Binding Mechanism. *Biomolecules*, 10(7), pp.1–22. 10.3390/BIOM10071085.

Townley, A.R., Wheatley, S.P., 2020. Mitochondrial survivin reduces oxidative phosphorylation in cancer cells by inhibiting mitophagy [online]. *Journal of cell science*, 133(21). Available at: https://pubmed.ncbi.nlm.nih.gov/33077555/ [Accessed 22 March 2022].

Toyoshima, F. et al., 1998. Nuclear export of cyclin B1 and its possible role in the DNA damage-induced G2 checkpoint [online]. *The EMBO Journal*, 17(10), pp.2728–2735. Available at: https://onlinelibrary.wiley.com/doi/full/10.1093/emboj/17.10.2728 [Accessed 21 March 2022].

Trendowski, M. et al., 2015. Chemotherapy with cytochalasin congeners in vitro and in vivo against murine models [online]. *Investigational New Drugs*, 33(2), pp.290–299. Available at: https://link.springer.com/article/10.1007/s10637-014-0203-5 [Accessed 11 March 2022].

Turgeon, M.O., Perry, N.J.S., Poulogiannis, G., 2018. DNA damage, repair, and cancer metabolism. *Frontiers in Oncology*, 8(FEB), p.15. 10.3389/FONC.2018.00015/BIBTEX.

Turrens, J.F., 2003. Mitochondrial formation of reactive oxygen species. *The Journal of Physiology*, 552(2), pp.335–344. 10.1111/J.1469-7793.2003.00335.X.

Twig, G. et al., 2008. Fission and selective fusion govern mitochondrial segregation and elimination by autophagy [online]. *The EMBO journal*, 27(2), pp.433–446. Available at: https://pubmed.ncbi.nlm.nih.gov/18200046/ [Accessed 27 March 2022].

Twig, G., Shirihai, O.S., 2011. The Interplay Between Mitochondrial Dynamics and Mitophagy [online]. *Antioxidants & Redox Signaling*, 14(10), p.1939. Available at: /pmc/articles/PMC3078508/ [Accessed 28 March 2022].

Ünsal-Kaçmaz, K. et al., 2002. Preferential binding of ATR protein to UV-damaged DNA. *Proceedings of the National Academy of Sciences of the United States of America*, 99(10), pp.6673–6678. 10.1073/pnas.102167799.

Uren, A.G. et al., 2000. Survivin and the inner centromere protein INCENP show similar cell-cycle localization and gene knockout phenotype [online]. *Current Biology*, 10(21), pp.1319–1328. Available at: http://www.cell.com/article/S0960982200007697/fulltext [Accessed 18 March 2022].

Valerie, K., Povirk, L.F., 2003. Available at: www.nature.com/onc [Accessed 22 May 2021].

Valle, A., Oliver, J., Roca, P., 2010. Role of Uncoupling Proteins in Cancer [online]. *Cancers*, 2(2), p.567. Available at: /pmc/articles/PMC3835092/ [Accessed 28 March 2022].

Vaupel, P., Harrison, L., 2004. Tumor Hypoxia: Causative Factors, Compensatory Mechanisms, and Cellular Response. *The Oncologist*, 9(S5), pp.4–9. 10.1634/theoncologist.9-90005-4.

Vaupel, P., Höckel, M., Mayer, A., 2007a. Detection and Characterization of Tumor Hypoxia Using pO $_2$ Histography. *Antioxidants & Redox Signaling*, 9(8), pp.1221–1236. 10.1089/ars.2007.1628.

Vaupel, P., Höckel, M., Mayer, A., 2007b. Detection and characterization of tumor hypoxia using pO2 histography [online]. *Antioxidants & redox signaling*, 9(8), pp.1221–1235. Available at: https://pubmed.ncbi.nlm.nih.gov/17536958/ [Accessed 18 April 2022].

Vaupel, P., Höckel, M., Mayer, A., 2007c. Detection and characterization of tumor hypoxia using pO2 histography [online]. *Antioxidants & redox signaling*, 9(8), pp.1221–1235. Available at: https://pubmed.ncbi.nlm.nih.gov/17536958/ [Accessed 21 March 2022].

Vaupel, P., Thews, O., Hoeckel, M., 2001. 10.1385/MO:18:4:243.

Velculescu, V.E. et al., 1999. 10.1038/70487.

Véquaud, E. et al., 2016. Survivin contributes to DNA repair by homologous recombination in breast cancer cells [online]. *Breast Cancer Research and Treatment*, 155(1), pp.53–63. Available at: http://bcgenex.centregauducheau.fr/ [Accessed 22 May 2021].

Verdecia, M.A. et al., 2000. Structure of the human anti-apoptotic protein survivin reveals a dimeric arrangement [online]. *Nature structural biology*, 7(7), pp.602–608. Available at: https://pubmed.ncbi.nlm.nih.gov/10876248/ [Accessed 16 March 2022].

Vermeulen, K., Van Bockstaele, D.R., Berneman, Z.N., 2003. 10.1046/j.1365-2184.2003.00266.x.

Vervliet, T., Parys, J.B., Bultynck, G., 2016. Bcl-2 proteins and calcium signaling: complexity beneath the surface [online]. *Oncogene*, 35(39), pp.5079–5092. Available at: https://pubmed.ncbi.nlm.nih.gov/26973249/ [Accessed 28 January 2022].

Vignard, J., Mirey, G., Salles, B., 2013. 10.1016/j.radonc.2013.06.013.

Villapol, S. et al., 2008. Survivin and heat shock protein 25/27 colocalize with cleaved caspase-3 in surviving reactive astrocytes following excitotoxicity to the immature brain. *Neuroscience*, 153(1), pp.108–119. 10.1016/j.neuroscience.2008.01.054.

Vischioni, B. et al., 2004. Nuclear localization of survivin is a positive prognostic factor for survival in advanced non-small-cell lung cancer. 10.1093/annonc/mdh436.

Vishwanath, V.A., 2016. Fatty Acid Beta-Oxidation Disorders: A Brief Review [online]. *Annals of neurosciences*, 23(1), pp.51–55. Available at: https://pubmed.ncbi.nlm.nih.gov/27536022/ [Accessed 14 April 2022].

Wajant, H., 2002. The Fas signaling pathway: more than a paradigm [online]. *Science (New York, N.Y.)*, 296(5573), pp.1635–1636. Available at: https://pubmed.ncbi.nlm.nih.gov/12040174/ [Accessed 1 February 2022].

Walsh, C.T., Tu, B.P., Tang, Y., 2018. Eight Kinetically Stable but Thermodynamically Activated Molecules that Power Cell Metabolism. *Chemical reviews*, 118(4), pp.1460–1494. 10.1021/ACS.CHEMREV.7B00510.

Wang, H. et al., 2010a. Acetylation directs survivin nuclear localization to repress STAT3 oncogenic activity [online]. *The Journal of biological chemistry*, 285(46), pp.36129–36137. Available at: https://pubmed.ncbi.nlm.nih.gov/20826784/ [Accessed 17 March 2022].

Wang, H. et al., 2010b. Acetylation directs survivin nuclear localization to repress STAT3 oncogenic activity [online]. *The Journal of biological chemistry*, 285(46), pp.36129–36137. Available at: https://pubmed.ncbi.nlm.nih.gov/20826784/ [Accessed 22 March 2022].

Wang, R., Brattain, M.G., 2007. The maximal size of protein to diffuse through the nuclear pore is larger than 60 kDa. *FEBS Letters*, 581(17), pp.3164–3170. 10.1016/j.febslet.2007.05.082.

Wang, Y. et al., 2011. Poly(ADP-ribose) (PAR) binding to apoptosis-inducing factor is critical for PAR polymerase-1-dependent cell death (parthanatos) [online]. *Science signaling*, 4(167). Available at: https://pubmed.ncbi.nlm.nih.gov/21467298/ [Accessed 5 February 2022].

Wang, Z., Fukuda, S., Pelus, L.M., 2004. Survivin regulates the p53 tumor suppressor gene family [online]. *Oncogene 2004 23:49*, 23(49), pp.8146–8153. Available at: https://www.nature.com/articles/1207992 [Accessed 29 March 2022].

Ward, C. et al., 2020. The impact of tumour pH on cancer progression: strategies for clinical intervention [online]. *Exploration of Targeted Anti-tumor Therapy*, 1(2), pp.71–100. Available at: https://www.explorationpub.com/Journals/etat/Article/10025 [Accessed 7 March 2022].

Ward, I.M., Minn, K., Chen, J., 2004. UV-induced Ataxia-telangiectasia-mutated and Rad3-related (ATR) Activation Requires Replication Stress. *Journal of Biological Chemistry*, 279(11), pp.9677–9680. 10.1074/jbc.C300554200.

Ware, M.J. et al., 2016. Generation of homogenous 3D pancreatic cancer cell spheroids using an improved hanging drop technique Chirality in Drug Design and Development View project 3D in vitro cell culture View project Generation of Homogenous Three-Dimensional Pancreatic Cancer Cell Spheroids Using an Improved Hanging Drop Technique. 10.1089/ten.TEC.2015.0280.

Wei, M.C. et al., 2001. Proapoptotic BAX and BAK: a requisite gateway to mitochondrial dysfunction and death [online]. *Science (New York, N.Y.)*, 292(5517), pp.727–730. Available at: https://pubmed.ncbi.nlm.nih.gov/11326099/ [Accessed 28 January 2022].

Weidemann, A., Johnson, R.S., 2008. Biology of HIF-1α [online]. *Cell Death & Differentiation 2008 15:4*, 15(4), pp.621–627. Available at: https://www.nature.com/articles/cdd200812 [Accessed 7 March 2022].

Wenger, R. et al., 2015. Frequently asked questions in hypoxia research. *Hypoxia*, 3, p.35. 10.2147/HP.S92198.

Westermann, B., 2012. Bioenergetic role of mitochondrial fusion and fission [online]. *Biochimica et biophysica acta*, 1817(10), pp.1833–1838. Available at: https://pubmed.ncbi.nlm.nih.gov/22409868/ [Accessed 28 March 2022].

Westermann, B., 2010. Mitochondrial fusion and fission in cell life and death [online]. *Nature Reviews Molecular Cell Biology 2010 11:12*, 11(12), pp.872–884. Available at: https://www.nature.com/articles/nrm3013 [Accessed 13 March 2022].

Weterings, E., Chen, D.J., 2008. The endless tale of non-homologous end-joining [online]. *Cell research*, 18(1), pp.114–124. Available at: https://pubmed.ncbi.nlm.nih.gov/18166980/ [Accessed 28 February 2022].

Wheatley, S.P., Altieri, D.C., 2019a. Survivin at a glance. *Journal of Cell Science*, 132(7). 10.1242/jcs.223826.

Wheatley, S.P., Altieri, D.C., 2019b. Survivin at a glance. *Journal of Cell Science*, 132(7). 10.1242/jcs.223826.

White, E.A., Glotzer, M., 2012. Centralspindlin: at the heart of cytokinesis [online]. *Cytoskeleton (Hoboken, N.J.)*, 69(11), pp.882–892. Available at: /pmc/articles/PMC3821549/ [Accessed 25 February 2022].

White, E.S.Z. et al., 2020. Serum deprivation initiates adaptation and survival to oxidative stress in prostate cancer cells [online]. *Scientific Reports 2020 10:1*, 10(1), pp.1–18. Available at: https://www.nature.com/articles/s41598-020-68668-x [Accessed 18 March 2022].

Williams, A.C., Ford, W.C.L., 2004. Functional significance of the pentose phosphate pathway and glutathione reductase in the antioxidant defenses of human sperm [online]. *Biology of reproduction*, 71(4), pp.1309–1316. Available at: https://pubmed.ncbi.nlm.nih.gov/15189835/ [Accessed 14 April 2022].

Wilson, D.F. et al., 1988. The oxygen dependence of mitochondrial oxidative phosphorylation measured by a new optical method for measuring oxygen concentration - PubMed [online]. *Journal of Biological Chemistry*, pp.2712–2718. Available at: https://pubmed.ncbi.nlm.nih.gov/2830260/ [Accessed 11 March 2022].

Wilson, W.R., Hay, M.P., 2011. Targeting hypoxia in cancer therapy. *Nature Reviews Cancer*, 11(6), pp.393–410. 10.1038/nrc3064.

Winterbourn, C.C., 2008. 10.1038/nchembio.85.

Wozniak, M.A. et al., 2004. Focal adhesion regulation of cell behavior. *Biochimica et Biophysica Acta (BBA) - Molecular Cell Research*, 1692(2–3), pp.103–119. 10.1016/j.bbamcr.2004.04.007.

Wu, D. di et al., 2011. Protein kinase B/Akt may regulate G2/M transition in the fertilized mouse egg by changing the localization of p21Cip1/WAF1 [online]. *Cell Biochemistry and Function*, 29(4), pp.265–271. Available at: https://onlinelibrary.wiley.com/doi/full/10.1002/cbf.1743 [Accessed 22 March 2022].

Xia, C., Liu, J.Z., Xu, Y., 2008. [Effects of GDP on the activity and expression of mitochondrial uncoupling proteins in rat brain in vitro]. *Sheng li xue bao : [Acta physiologica Sinica]*, 60(4), pp.492–496.

Xiong, Z. et al., 2016. Downregulation of AIF by HIF-1 contributes to hypoxia-induced epithelial-mesenchymal transition of colon cancer [online]. *Carcinogenesis*, 37(11), pp.1079–1088. Available at: https://pubmed.ncbi.nlm.nih.gov/27543779/ [Accessed 30 March 2022].

Xu, X. et al., 2014. Enrichment of cancer stem cell-like cells by culture in alginate gel beads. *Journal of Biotechnology*, 177, pp.1–12. 10.1016/j.jbiotec.2014.02.016.

Xu, Y.J., Davenport, M., Kelly, T.J., 2006. Two-stage mechanism for activation of the DNA replication checkpoint kinase Cds1 in fission yeast. *Genes and Development*, 20(8), pp.990–1003. 10.1101/gad.1406706.

Yan, L. et al., 2018. Structural basis for GTP hydrolysis and conformational change of MFN1 in mediating membrane fusion. *Nature structural & molecular biology*, 25(3), pp.233–243. 10.1038/S41594-018-0034-8.

Yang, W. et al., 2012. ERK1/2-dependent phosphorylation and nuclear translocation of PKM2 promotes the Warburg effect [online]. *Nature cell biology*, 14(12), p.1295. Available at: /pmc/articles/PMC3511602/ [Accessed 28 March 2022].

Yang, Y. et al., 2022. HIF-1 Interacts with TRIM28 and DNA-PK to release paused RNA polymerase II and activate target gene transcription in response to hypoxia [online]. *Nature Communications 2022 13:1*, 13(1), pp.1–16. Available at: https://www.nature.com/articles/s41467-021-27944-8 [Accessed 22 April 2022].

Yano, K.I., Chen, D.J., 2008. Live cell imaging of XLF and XRCC4 reveals a novel view of protein assembly in the non-homologous end-joining pathway [online]. *Cell cycle (Georgetown, Tex.)*, 7(10), pp.1321–1325. Available at: https://pubmed.ncbi.nlm.nih.gov/18418068/ [Accessed 27 February 2022].

Ye, J. et al., 2012. Primer-BLAST: a tool to design target-specific primers for polymerase chain reaction. [online]. *BMC bioinformatics*, 13(1), p.134.

Available at: https://bmcbioinformatics.biomedcentral.com/articles/10.1186/1471-2105-13-134 [Accessed 31 March 2022].

Yu, M. et al., 2019. Mitochondrial fusion exploits a therapeutic vulnerability of pancreatic cancer [online]. *JCI insight*, 5(16). Available at: https://pubmed.ncbi.nlm.nih.gov/31335325/ [Accessed 28 March 2022].

Yu, R. et al., 2019. Human Fis1 regulates mitochondrial dynamics through inhibition of the fusion machinery. *The EMBO journal*, 38(8). 10.15252/EMBJ.201899748.

Yu, T., Tang, B., Sun, X., 2017. Development of Inhibitors Targeting Hypoxia-Inducible Factor 1 and 2 for Cancer Therapy. *Yonsei medical journal*, 58(3), pp.489–496. 10.3349/ymj.2017.58.3.489.

Yu, X. et al., 2006. BRCA1 ubiquitinates its phosphorylation-dependent binding partner CtIP [online]. *Genes & development*, 20(13), pp.1721–1726. Available at: https://pubmed.ncbi.nlm.nih.gov/16818604/ [Accessed 28 February 2022].

Yuan, S. et al., 2014. Methylation by NSun2 Represses the Levels and Function of MicroRNA 125b [online]. *Molecular and Cellular Biology*, 34(19), p.3630. Available at: /pmc/articles/PMC4187725/ [Accessed 30 March 2022].

Yuan, Y. et al., 2016. Role of the tumor microenvironment in tumor progression and the clinical applications (Review) [online]. *Oncology Reports*, 35(5), pp.2499–2515. Available at: https://www.spandidos-publications.com/10.3892/or.2016.4660 [Accessed 30 August 2018].

Yuhas, J.M. et al., 1977. A simplified method for production and growth of multicellular tumor spheroids. *Cancer research*, 37(10), pp.3639–43.

Zakeri, Z.F., Ahuja, H.S., 1997. Cell death/apoptosis: normal, chemically induced, and teratogenic effect. *Mutation Research/Fundamental and Molecular Mechanisms of Mutagenesis*, 396(1–2), pp.149–161. 10.1016/S0027-5107(97)00181-4.

Zhang, B. et al., 2014. Upregulation of HIF-1α by hypoxia protect neuroblastoma cells from apoptosis by promoting survivin expression. *Asian Pacific journal of cancer prevention : APJCP*, 15(19), pp.8251–7.

Zhang, H., Burrows, F., 2004. 10.1007/s00109-004-0549-9.

Zhang, J. et al., 2012. Measuring energy metabolism in cultured cells, including human pluripotent stem cells and differentiated cells. *Nature protocols*, 7(6), pp.1068–85. 10.1038/nprot.2012.048.

Zhang, X.D., Qin, Z.H., Wang, J., 2010. The role of p53 in cell metabolism [online]. *Acta Pharmacologica Sinica*, 31(9), p.1208. Available at: /pmc/articles/PMC4002322/ [Accessed 23 April 2022].

Zhang, Xulang et al., 2008. Development of an in Vitro Multicellular Tumor Spheroid Model Using Microencapsulation and Its Application in Anticancer Drug Screening and Testing. *Biotechnology Progress*, 21(4), pp.1289–1296. 10.1021/bp050003l.

Zhang, Y. et al., 2019. Downregulation of microRNA-425-5p suppresses cervical cancer tumorigenesis by targeting AIFM1 [online]. *Experimental and Therapeutic Medicine*, 17(5), pp.4032–4038. Available at: http://www.spandidos-publications.com/10.3892/etm.2019.7408/abstract [Accessed 30 March 2022].

Zhang, Z. et al., 2018. PI3K/Akt and HIF-1 signaling pathway in hypoxia-ischemia (Review) [online]. *Molecular Medicine Reports*, 18(4), pp.3547–3554. Available at: http://www.spandidos-publications.com/10.3892/mmr.2018.9375/abstract [Accessed 21 March 2022].

Zhao, H., Piwnica-Worms, H., 2001. ATR-Mediated Checkpoint Pathways Regulate Phosphorylation and Activation of Human Chk1. *Molecular and Cellular Biology*, 21(13), pp.4129–4139. 10.1128/mcb.21.13.4129-4139.2001.

Zhao, J. et al., 2013. Mitochondrial dynamics regulates migration and invasion of breast cancer cells [online]. *Oncogene*, 32(40), p.4814. Available at: /pmc/articles/PMC3911914/ [Accessed 30 November 2022].

Zhao, R.Z., Jiang, S., Zhang, L., Yu, Z. Bin, 2019. Mitochondrial electron transport chain, ROS generation and uncoupling (Review). *International Journal of Molecular Medicine*, 44(1), pp.3–15. 10.3892/IJMM.2019.4188/HTML.

Zhao, R.Z., Jiang, S., Zhang, L., Yu, Z. bin, 2019. Mitochondrial electron transport chain, ROS generation and uncoupling (Review) [online]. *International Journal of Molecular Medicine*, 44(1), pp.3–15. Available at: http://www.spandidos-publications.com/10.3892/ijmm.2019.4188/abstract [Accessed 28 March 2022].

Zhao, Y. et al., 2019. Nuclear E-Cadherin Acetylation Promotes Colorectal Tumorigenesis via Enhancing β-Catenin Activity [online]. *Molecular cancer research : MCR*, 17(2), pp.655–665. Available at: https://pubmed.ncbi.nlm.nih.gov/30401720/ [Accessed 22 March 2022].

Zheng, J., 2012. Energy metabolism of cancer: Glycolysis versus oxidative phosphorylation (review) [online]. *Oncology Letters*, 4(6), pp.1151–1157. Available at: http://www.spandidos-publications.com/10.3892/ol.2012.928/abstract [Accessed 8 March 2022].

Zhou, J. et al., 2016. Comparison of clinical outcomes of squamous cell carcinoma, adenocarcinoma, and adenosquamous carcinoma of the uterine cervix after definitive radiotherapy: a population-based analysis [online]. *Journal of Cancer Research and Clinical Oncology 2016 143:1*, 143(1), pp.115–122. Available at: https://link.springer.com/article/10.1007/s00432-016-2246-9 [Accessed 11 March 2022].

Zou, J. et al., 2013. Notch1 is required for hypoxia-induced proliferation, invasion and chemoresistance of T-cell acute lymphoblastic leukemia cells [online]. *Journal of Hematology and Oncology*, 6(1), pp.1–13. Available at: https://jhoonline.biomedcentral.com/articles/10.1186/1756-8722-6-3 [Accessed 11 March 2022].

Zou, L., Elledge, S.J., 2003. Sensing DNA damage through ATRIP recognition of RPA-ssDNA complexes. *Science*, 300(5625), pp.1542–1548. 10.1126/science.1083430.

Zumbrägel, F.K. et al., 2017. Survivin does not influence the anti-apoptotic action of XIAP on caspase-9. *Biochemical and Biophysical Research Communications*, 482(4), pp.530–535. 10.1016/j.bbrc.2016.11.094.

Appendix

Image Analysis Macro Link and WEKA Segmentation Model File Folder Link

https://1drv.ms/f/s!AvrxOHQ61ZTHgQb35HT30i4DID0A